ASSESSING THE VARIABILITY OF LONG-TERM MEXICAN INSTRUMENTAL RECORDS AND THE ENSO MODULATING FORCE.

Marco Antonio Salas Flores

A thesis submitted in fulfilment of the requirements for the degree of Doctor of Philosophy at the University of East Anglia

Climatic Research Unit (CRU)

School of Environmental Sciences

June 2008

ASSESSING THE VARIABILITY OF LONG-TERM MEXICAN INSTRUMENTAL RECORDS AND THE ENSO MODULATING FORCE.

Marco Antonio Salas Flores

2008

ABSTRACT

Undisputable evidence of climate change is accumulating from direct observations. Unfortunately, for some unanalysed regions of the world, the data coverage is still sparse (IPCC, 2007). This study aims to assess the changing patterns of precipitation and temperature across Mexico and the direct influence of El Niño-Southern Oscillation.

A network of 175 stations with precipitation and 52 with temperature of monthly data were built for the Principal Component Analysis (PCA) and the ENSO modulation assessments. A set of 35 stations with daily data for weather extremes analyses was also developed. Oblique-rotated solutions have been applied to the monthly datasets to regionalise groups of stations that are varying coherently. Extreme indices are calculated using the RClimDex in the daily time-series of rainfall and temperature. Finally, linear (Kendall's tau-b) and lag correlations have been applied to establish relationships between three different ENSO indices, the precipitation regional averages (resulting from PCA) and also with the weather extreme indices.

A clear latitudinal transition is observed when the annual and rainy (May-Oct) seasons of regional precipitation averages and extreme rainfall indices are correlated with the ENSO indices: wetter conditions are observed north of the tropic of cancer and below normal precipitation is dominant in the southern part of the country. Meanwhile, a national climatic picture of wetter conditions is observed when the standardised versions of the

dry (Nov-Apr) season of the regional precipitation averages and the extreme precipitation indices are correlated with the ENSO indices; precipitation responds mainly close to the peak of El Niño-like conditions. Warmer temperatures are observed when the extreme temperature indices are correlated with the ENSO indices. Nevertheless, the most significant results are seen in the minimum temperatures, although timing of response to the ENSO modulation is not as clear as in the case of precipitation.

ACKNOWLEDGEMENTS

I like to express my thankfulness for all the people who have made this thesis possible. I owe a great deal of gratitude to the members of my supervisory committee at the University of East Anglia (UEA): Prof. Phil Jones, Dr. Mick Kelly and Dr. Chris Vincent. I would like to recognise especially to my main supervisor, Prof. Jones, for his dedication, patience and understanding during the last stages of this thesis.

I would also like to show a profound gratitude to all the Climatic Research Unit (CRU) people who have contributed to the present research. Special mention deserves David Lister who has provided the information necessary to complete the meteorological database used in this study. I am also pleased with all the help that Dimitrios kindly offered me for the understanding of some of the analyses applied in this thesis. Definitive for the completion was also the friendly atmosphere of my office-mates (Stephen, Mansour, David, Cyrille, Matt, and Sally) and all the friends in CRU in general. Special thanks to Mike that always kept my PC running.

It must also be acknowledged all the people in Mexico who has provided useful information for this study. My debt to Isabel Quintas and Jorge Sánchez-Sesma of the Mexican Institute for Water Technology (IMTA) in Cuernavaca; Adriel González and Luis Antonio Cabrera of the Mexican Meteorological Office in Mexico City; and the researchers of the Institute of Geography of the National University of Mexico. I would like to thank to the Science and Technology Council of Mexico (Consejo Nacional de Ciencia y Tecnología, CONACYT) that has sponsored this research, and all the people there that helped me with all my academic and financial issues.

I was also sustained by the love of the Christian fellowship in Norwich. Memories of generosity and kindness of those very special persons: Angela, Paulina, Tony, John, Ruth, Howard, Mary, and Martin. I am extremely grateful to my fellows Judith, Abdullah, Lukman, Gyung-Yung, Yvonne, Heidi, Yi-Yin, Hiroko, and Serah. I also appreciate the company of all the Mexican friends in Norwich. Finally, I cannot express in full all the love to my family, their support and faith in me that made me feel confident in the completion of this thesis.

CONTENTS

LIST OF FIGURES

Page

CHAPTER 2:

CHAPTER 3:

CHAPTER 4:

CHAPTER 5:

CHAPTER 6:

CHAPTER 7:

LIST OF TABLES

Page

CHAPTER 5:

CHAPTER 6:

CHAPTER 7:

calculated using the Pearson function. Lags (leads) are expressed in months and related to the maximum correlation found after trying several lags and leads.
218

CHAPTER 1: INTRODUCTION

There is now unequivocal evidence from direct observations of a warming of the climate system (IPCC, 2007). Despite remaining uncertainties, it is now clear that the upward trend on global averaged temperatures during the 20th century is very likely due to anthropogenic origin; especially changes in the greenhouse gas concentrations (IPCC, 2007). These climatic changes have been recorded in observations of air and ocean temperatures, ice cores, glaciers, and increasing sea levels. With some geographical variations, all their average conditions testify to globally increasing temperatures.

Certainly, one of the arguments of the sceptics against global warming is the spatial inhomogeneity of the changes of the parameters that measure climate change across the world, like temperature (Soon et al., 2003). The largest percentage of the meteorological data, for example, comes from mid-latitude developed countries (Vose et al., 2005). There is a real necessity to gather information from developing countries to complete the picture of the global climate. It is only recently that more extensive climatic information from these regions has been added to the global databases. Among these developing countries, some of them are of great interest for climatologists: countries, for example, that lie at the transition between tropical and extra-tropical climatic conditions. Mexico is one of those countries that encompass a rich variety of climatic regions within its territory.

Mexico is a bridge between tropical and temperature latitudes that reflects a broad distribution of climatic regimes. For instance, are the climatic change patterns similar or they are strongly differing in the southern or northern part of the country? These questions need to be addressed in the climate change context in order to increase our understanding of the variables involved in the climate system. Although rapidly increasing, there is still a lack of studies on climate change in Mexico (Jauregui, 1997). A proper network of stations in terms of data coverage and length is necessary to analyse the climate of these regions. A pre-requisite for reliable results within these climatic studies are long-term and high-quality databases. Fortunately, it has been only recently

that several digital databases of climatological data have become available and suitable for different scientific and social studies including climatic research.

Several efforts have been made in Mexico to build a large network of climatological stations across the country. The oldest set of stations to measure meteorological variables began in 1921, just after the end of the Mexican Revolution. In that year the Servicio Meteorológico de México (Mexican Meteorological Service) was created with 600 stations distributed across the country (Metcalfe, 1987). The latest digital datasets contain daily records of the main meteorological parameters. Several mathematical and statistical processes have been applied to different spatial and temporal resolutions in this thesis and the consistency of the results compared.

In this context, the aims of this thesis are:

1. A national appraisal of climatic patterns in México using instrumental data. In particular, daily and monthly (land surface) precipitation and air temperature will be used.
2. Climatic regionalisation of seasonal rainfall and temperature according to their secular variations using Principal Component Analysis (PCA).
3. An assessment of spatial and secular changes of rainfall and temperature extremes during the twentieth century, with special focus on finding the climatic patterns of the last few decades and consistency between local and regional scales. For this purpose, digital instrumental data and up_to_date software to calculate the weather extreme indices have been used.
4. Finally, an exploration of one of the large-scale atmospheric controls which modulate the long-term trends of Mexican climate at both regional and local scales is made, especially those associated with El Niño Southern Oscillation (ENSO) phenomenon.

The main characteristics of the climate of Mexico are addressed in Chapter two. Geographical features are explained in section 2.2. As mentioned above, Mexico is located in the transition between tropical and temperate climates. Therefore, latitude

plays a key role in the rich variety of its climatic regimes, and that is fully explained in section 2.2.1. With two large mountain ranges along both coasts and a high central plateau, altitude has a great influence in many regions of Mexico, especially those in the northern part of the country that are affected during the winter by polar fronts, or the line of high-altitude sites within the neovolcanic belt in central Mexico. The orographic influence on climate is found in section 2.2.2. Two great bodies of waters also exert their influence on Mexican climate. Along the east coast, the Gulf of Mexico is a relatively closed basin that modulates the weather. The greatest variations in precipitation here are seen during the Hurricane season (approximately May-Nov). This is most apparent in the peninsula of Yucatan, and its rainfall patterns completely differ from the neighbouring regions. Because of its length and the vast extent the Pacific has larger influence than the Atlantic Ocean; and an enclosed body of water, the Gulf of California acts like a physical barrier to the cold marine currents at those latitudes to regulate what otherwise could be a more varying climatic region in north-western Mexico. Oceanic and continental influences are both addressed in section 2.2.3. Large-scale phenomena are considered in section 2.3. Northern Hemisphere General Circulation, Trade Winds and Subtropical High Pressure Belt are important, but probably the most extensive studied large-atmospheric control is the El Niño Southern Oscillation (ENSO) phenomenon with the key research on ENSO found in this section. Other important resources to understand the climate are: documentary and proxy data; these records aim to extend, back in time, the picture of the climate of Mexico. The different efforts to develop meteorological instrumental measurements are studied in section 2.4. The development of recent digital databases and their limitations are also seen in this section. Documentary and proxy data like historical records are addressed in section 2.5. Finally, some of the most important studies that have been explored about the climate of Mexico are shown in section 2.6. Conclusions are discussed in the last section (2.7) of the Chapter.

A rich variety of climates occur across Mexico (García, 1988). In order to understand and unveil these (sometimes contrasting) conditions of climate, different mathematical and statistical methods were applied. The best possible data quality is an essential condition for reliable results in climatology. For this reason, the extraction of the data was one of the most important stages in the present study. The whole process of gathering and analysing climatological time-series is reviewed in section 3.2. Only long records of digital instrumental data were used in this thesis. The different databases of daily temperature and precipitation are explained in section 3.2.1. For a station to be selected, its time-series needed to comply with several conditions such as: daily data, at least 30 years of information, less than ten percent of missing values, etc. This selection is explained in detail in section 3.2.2. Amongst the several natural causes that modulate the climate of Mexico, El Niño Southern Oscillation (ENSO) is probably the most extensively studied. In order to test the stability of the relations between the climate and ENSO, three different indices will be used: the Southern Oscillation Index (SOI), El Niño 3.4 and the Multivariate ENSO Index (MEI). The different sources, time-series lengths, characteristics, and other limitations are explained in section 3.2.3.

The selection of the different methods to be applied in the meteorological databases is crucial for the interpretation of the results. These are divided into the consideration of homogeneity, Principal Component Analysis (PCA), extreme weather analysis and regional averages within section 3.3. It has been already mentioned that one of the most important processes in the analysis of climate is the quality of the data. For instance, a few typing errors can severely alter the results. Considerations on homogeneity and urbanisation are found in section 3.3.1. For Mexico, a territory of complex climatic conditions; Principal Component Analysis (PCA) was chosen as an effective method to identify sets of stations (regionalisation) that vary coherently. The general characteristics and limitations of this technique will be discussed in section 3.3.2. Based on the results of PCA, the method used to obtain averages of the different regions is shown in section 3.3.3. For their extraordinary characteristics, and direct impact on society extreme weather indices are an important part of climatic studies. The consideration of these extraordinary events and their definitions for temperature and precipitation are explained

in section 3.3.4. Because the analysis of extremes needs high-quality daily data a further refined selection among the rainfall and temperature stations was made in the same section. For different purposes linear and lag-cross correlations are used in the present research and these methods are explained in section 3.3.5. Non-parametric correlation, in particular kendall tau-b is preferred to the Pearson correlation coefficient and its advantages and limitations are described here. Because frequently, local meteorological parameters reflect a delayed response to large-atmospheric controls like ENSO, lag-cross correlations will be used in the present study. The main characteristics of this method are shown in the same section 3.3.5.

Chapter 4 outlines the search for coherent patterns of climatic variations in the networks of the main meteorological variables. PCA is the method selected to unveil these spatially coherent variations. Rotated PCA methods are preferred for their ability to deal with large networks of meteorological variables. The mean temperature and precipitation data have been processed into seasonal periods, i.e., annual, wet (May to October) and dry (November to April). PCA on the precipitation data is studied in section 4.2. Annual totals are analysed in section 4.2.1. A large percentage of the annual precipitation total occurs during the wet season (section 4.2.2); therefore, quite similar PCA regionalisations are expected for annual and wet season rainfalls. A different climatic picture is observed during the dry season in which most of the precipitation falls in winter, especially in the northwestern part of the country. The regionalisation of the dry season is found in section 4.2.3.

The variability of mean temperature increases from the narrow south to the wide territory of northern Mexico. The same PCA orthogonal (varimax) and oblique rotation techniques (promax) that were applied to precipitation are used for seasonal mean temperature. The temperature network (52 stations) is data-sparse when compared with the rainfall database (175 stations), and the time-series length is also shorter (1941-2001). The details of the analysis of annual mean temperature are found in section 4.3.1. Wet season analysis of mean temperature is presented in section 4.3.2. Due to their poor results in regionalisation, an additional analysis was performed using the standard three-monthly

periods (DJF, MAM, JJA, and SON). The results of the application of PCA to these periods are shown in section 4.3.3. Because the division of the time-series into three monthly periods does not improve the results; a final attempt (seeking better results) was made applying K-means cluster analysis to the annual totals and wet season and these are discussed in section 4.3.4. The conclusions to chapter 4 are given in detail in section 4.4.

Another important aspect of studies on climate change is extreme events. In the case of precipitation, the network of monthly and daily data allows a comparison at both spatial and temporal scales. Non-parametric correlations using Kendall tau-b are applied to precipitation extreme indices at regional and local scales. In addition, results are divided in two parts using the Tropic of Cancer as a geographical limit in order to test a latitudinal transition of the changes on precipitation extremes.

The introduction to Chapter 5 and general considerations on precipitation extremes are detailed in section 5.1. In order to simplify the evaluation of the results, the precipitation indices have been divided in two different groups: one that measures depth (mm) or intensity (mm/day) and the other that calculates the frequency (number of cases). All these indices are evaluated separately, beginning with a classification according to the level of statistical significance (i.e., at 1% or 5%). Finally, how these climatic changes are occurring geographically, i.e., are they basically occurring in the southern part of Mexico or they are more drastic in the north of the country? All these details are explained in section 5.2.1. In order to check the consistency in the precipitation patterns, a linear trend is applied among the stations with the most important results (correlations) in section 5.2.2. General conclusions on precipitation extreme indices are evaluated in section 5.3.

According to instrumental records, the year 2005 (with 1998) had the warmest global average surface temperature (Osborn and Briffa, 2006). Mean temperatures have been studied extensively but less research has been made on extreme temperatures at a global scale. This situation is changing rapidly, see the recent study of Alexander et al. (2006). Nevertheless, there is a lack of studies on extreme temperatures in developing countries.

Chapter 6 aims to deal with this necessity in Mexico calculating the extreme temperature indices using a network of 26 stations that contain daily data from 1941 to 2001.

Based on daily data, extreme temperature indices (defined in section 3.3.4) are calculated for each station. Linear correlations are estimated for these indices using Kendall tau-b. In order to facilitate their evaluation, the extreme temperature indices have been classified into three different groups: one group deals with those indices expressed in absolute temperature; the indices that count the frequency a temperature exceeds a set limit in °C and the final groups measure the frequency with which the temperature surpasses a limit based on a percentile measure. The trend correlations are separated according to their levels of statistical significance (at 5% or 1% level), and also their tendency towards warming or cooling conditions. In addition, these correlations are evaluated geographically as to whether they are located south or north of the Tropic of Cancer in order to find any spatial pattern in these climatic changes. All these analyses are detailed in section 6.2.1. An analysis of linear trends on the temperature stations of with the most important correlations is applied in section 6.2.2. Conclusions and general remarks related to the analyses performed in this chapter are addressed in section 6.3.

Although, as mentioned earlier anthropogenic causes are increasing their influence on climate, natural variability is, however, still the greatest force on the climate system. Among the most important of the large-scale atmospheric controls, the El Niño-Southern Oscillation (ENSO) phenomenon plays a key role in the climate of Mexico. Its impact on rainfall has been extensively studied at both regional (Magaña et al., 2003; Englehart and Douglas, 2002; Giannini et al., 2001; Cavazos, 1999; Magaña et al., 1997; Cavazos and Hastenrath, 1990) and local scales (Alexander et al., 2006; Aguilar et al., 2005). Fewer studies have been made on temperature (Alexander et al., 2006; Aguilar et al., 2005; Englehart and Douglas, 2004). The relationships between three different ENSO indices and the regional monthly precipitation averages and daily data of rainfall and temperature are explored using non-parametric and lag cross correlations. The results of these correlations will allow a comparison of the results at different spatial and temporal scales.

A general introduction to the databases of rainfall and temperature and the ENSO indices, and also the methods applied in chapter 7 is detailed in section 7.1. The next three sections of the chapter 7 address the results of correlating the three different ENSO indices with regional precipitation averages and daily rainfall and temperature data: the Southern Oscillation Index (SOI) is used in section 7.2, El Niño 3.4 index in section 7.3, and the Multivariate El Niño Index (MEI) in section 7.4. Non-parametric correlations for SOI are applied in section 7.2.1. Regional precipitation averages are correlated with SOI and with daily data in the form of extreme rainfall and temperature indices. Regional and local relationships of the results are established at the final of this section. In order to test delayed responses of the meteorological variables to the ENSO modulation, lag cross-correlations are analysed in section 7.2.2. The time-series of regional precipitation averages are correlated with the SOI index. The lag correlations of SOI and extreme rainfall and temperature indices are detailed also in this section. The same structure is applied in sections 7.3 and 7.4. For instance linear correlations of El Niño 3.4 with the regional precipitation averages and the extreme weather indices are explained in section 7.3.1, and lag cross-correlations of El Niño 3.4 index with the same variables are addressed in section 7.3.2. The same distribution of the MEI results is presented in section 7.4. Contrasting results at local and regional scales using the different ENSO indices are detailed in section 7.5. General conclusions and remarks of the modulation of the ENSO to the climate of Mexico are addressed in this last section of chapter 7.

Chapter 8 summarises the final conclusions of this thesis. The main topics addressed in this thesis are: the construction of a high-quality and long-term network of precipitation and temperature data, the regionalisation of meteorological stations varying coherently, the analysis of extreme weather indices and the ENSO modulation. The main findings of the thesis are presented in section 8.1. The most important goals per topic are presented in detail; and also general remarks and additional considerations of these research areas of climate change in Mexico are discussed in this section. Finally, further study on the topics evaluated in this thesis and new questions posed by the present research are addressed in section 8.2.

CHAPTER 2: THE MEXICAN CLIMATOLOGY

2.1 INTRODUCTION

With increasing evidence indicating that global warming is being partly caused by human activities, it is important to study regional climatic change especially in developing countries. Of particular interest are those areas, lying between tropical and extra-tropical climatological conditions, which have been generally less studied than mid and higher latitudes. Hence, Mexico because of its particular geographical position is a good opportunity to explore such changing regional climates.

There are only a few studies of climate change/impacts in Mexico (Jauregui, 1997). The limited length and quality of the climatological records (Jauregui, 1992; Metcalfe, 1987), as well as the sparsity of the meteorological observations network (Englehart and Douglas, 2002; O'Hara and Metcalfe, 1995) are some of the reasons for the few published papers. However, since the mid 1980s, some projects have developed a small number digitised meteorological databases; a fact that has increased the possibilities to evaluate the climatic patterns and trends in the country as a whole using instrumental data.

An essential necessity in México for both societal and economic reasons is to further develop an up_to_date database of high-quality climatological data. This should be the starting point for any assessment of the climate in this country, and will enhance the usefulness of the results. This will also lead to the next step, which is to analyse the variability of the Mexican climate from the daily records of the national meteorological network with recent statistical and mathematical techniques. This will allow the possibility to explore the complexity of the climate of Mexico using instrumental data.

General geographic characteristics such as: latitude, altitude, orography, ocean influence and continentality, that make the climate of Mexico particularly interesting, are presented in the first part of the chapter. The analysis of the development of the network of

(meteorological) instrumental data is reviewed before considering the efforts to construct a reliable archive of proxy (historical) data. The most influential papers dealing with the climate of Mexico are considered at the end of this chapter.

2.2 GEOGRAPHICAL CHARACTERISTICS.

2.2.1 LATITUDE.

The Mexican Republic lies between the latitudes of 14°30´N and 32°42´N. An interesting feature, that has been noted by several authors like Cavazos and Hastenrath (1990), is that it represents a latitudinal band encompassing the transition from the tropics to temperate latitudes, being highly sensitive to climatic fluctuations of the large-scale atmospheric circulation (Metcalfe, 1987). For instance, the Tropic of Cancer is roughly considered as the southern limit of the unimodal annual temperature cycle; south of this tropic two maxima of the annual temperature cycle are observed (Mosiño and García, 1974). This sort of gradual change can also be noted in total annual precipitation. Wet regions are mainly concentrated south of the Tropic of Cancer, particularly in the southern states of Veracruz, Tabasco and Chiapas where totals rainfalls reach between 3000 and 4000 mm; while much drier conditions prevail in northern areas, especially within the semiarid part of Baja California (near the Mexico-USA border) where the total precipitation is usually around 200 mm per year (Wallen, 1955. see Fig. 2.1).

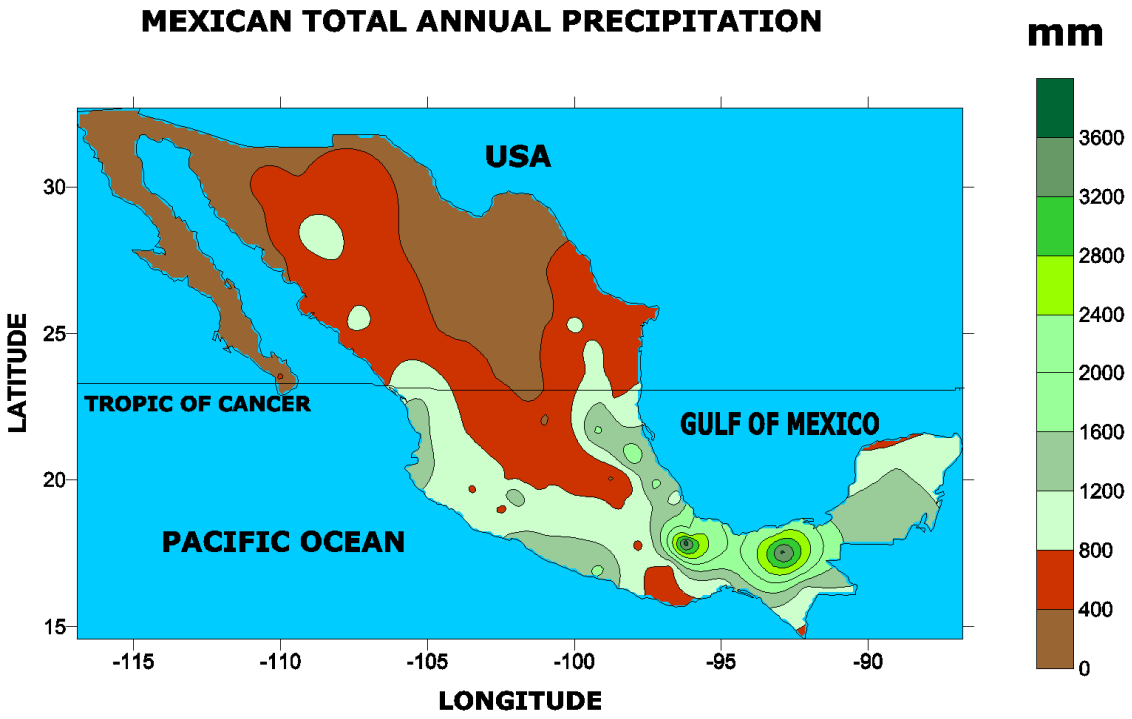

Fig. 2.1. Distribution of the total annual precipitation [mm] in Mexico. Map based in the 175 stations network of monthly rainfall (see section 3.2).

There is a national widespread dominant characteristic in the precipitation annual cycle: the convective activity and rainfall are concentrated during the boreal summer months (Cavazos and Hastenrath, 1990). The largest amount of precipitation occurs between the months of May and October (Mosiño and García, 1974, Hastenrath, 1967); the only exception in the country is the northern part of the peninsula of Baja California near the border with the United States of America (USA), when most of the rainfall falls between November and April. Ortega and Velázquez (1995) point out two months of transition: May when climatic conditions change from extratropical to tropical regimes, and October when the opposite occurs. Therefore, for the purposes of the present research, the wet season is considered as the period between May and October, and the dry period is defined between the months of November and April.

2.2.2. OROGRAPHY

Orography is another key factor affecting the climate of Mexico. Latitudinal differences and large-scale atmospheric circulation are not sufficient to explain all the variability of climatic conditions. Two great mountain ranges on both coasts, one well-defined nearly parallel to the Pacific Coast and the other partly along the Atlantic Coast, influence the weather especially during the rainy season. Large amounts of moisture from the eastern tropical Pacific enters the country during the North American Monsoon System (NAMS) (Mechoso et al., 2004; Hu and Feng, 2002), that is a response to the heat gradient between the land and the neighbouring oceans (Higgins et al., 1997). The greatest quantities of annual precipitation in the NAMS area falling along the slopes of the mountain region called the Sierra Madre Occidental near Mazatlán (Douglas et al., 1993), and moves northwards reaching the south-western USA in early July (Castro et al., 2001), clearly showing the importance of the orographic influence.

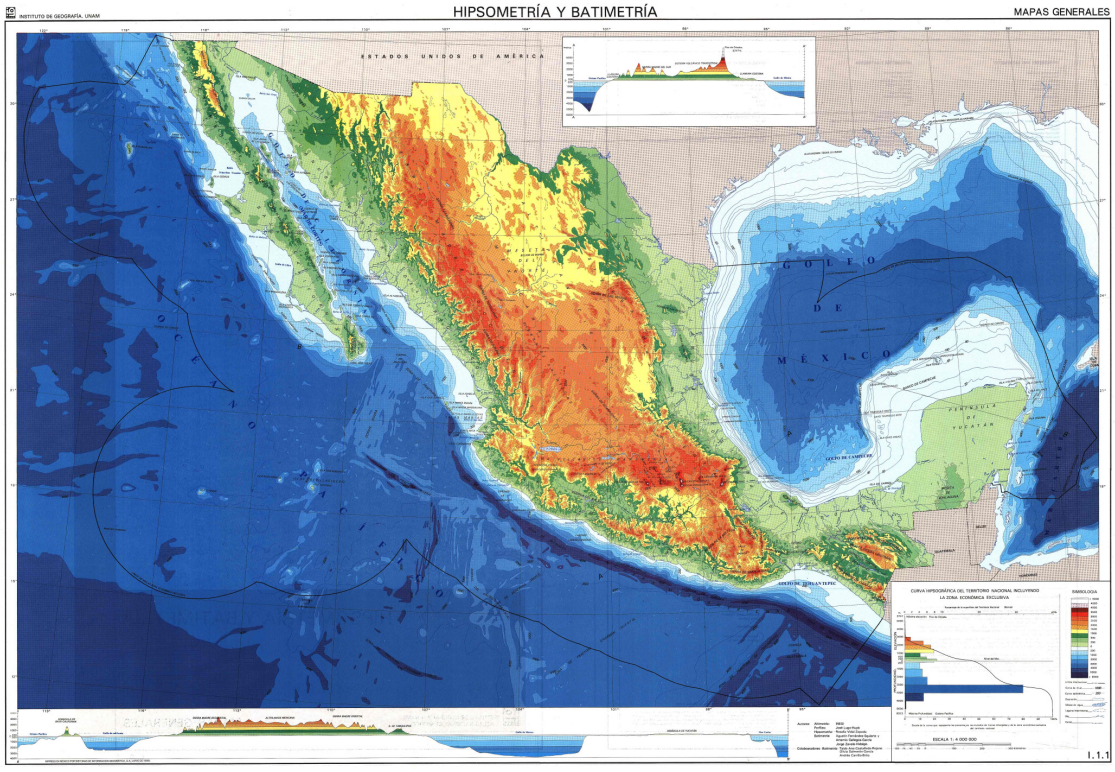

Fig. 2.2. Map of Mexican hypsometry and bathymetry. Atlas Nacional de México. Instituto de Geografía. UNAM (Accesed on July, 30, 2008).

However, the most remarkable topographic feature is the High Plateau. Locations at relatively high altitudes are sometimes affected by the upper level circulation, especially during the boreal winter. The elevation-climate relationship in Mexico is still an area that needs to be more fully investigated before reaching reliable conclusions.

2.2.3. OCEAN AND CONTINENTAL INFLUENCE.

A particular continental shape stretching from north to south makes the climate of Mexico contrasting. Southern parts of the country inside the narrow land mass enjoy milder and wetter climates than in the much broader northern regions. The adjacent expanses of the oceans exert their influence as a big thermostat smoothing otherwise larger changes in the meteorological parameters; but these great water volumes are also the source of moisture and heat: during the summer season air flow (Trade Winds), coming from the Caribbean sea enters the Gulf of Mexico, and carry the moisture and heat inland contributing to the more humid and warmer climatic conditions across most of the entire country (Mosiño and García, 1974). In the north of the country, the peninsula of Baja California in the north-western side of the Pacific Coast introduces another factor to the complex picture of Mexican climate. It is only in this part of the country where the effects of the ocean currents can really be appreciated; north of the Baja Californian Gulf, the cold streams (the Californian current) and shallow waters exert a regional influence on the temperature modulating process. In contrast, between the continent and the peninsula, the Gulf of California (Sea of Cortez) warm waters act as a barrier to the cold currents. Wetter conditions in the Mexican Monsoon (Douglas et al., 1993) region are correlated to sea surface temperatures below averages in the east Pacific basin (Castro et al., 2001). Land-sea interactions have played an important role in the evolution of the climate in Mexico; nevertheless some large-scale features sometimes override these more regional and geographic controlling forces.

2.3 LARGE-SCALE ATMOSPHERIC CONTROLS.

Large-scale atmospheric phenomena are important components that must be considered when trying to explain the processes that influence the climate in the country.

Northwards/southwards displacements of the Northern Hemisphere General Circulation are considered to be one of the main controlling factors of the nature and variability of the Mexican climate (Jauregui, 1997). For instance, precipitation in the southeast area responds to the large-scale circulation, the latter controlling the wetday frequency, relative magnitude and wet season length (Hewitson and Crane, 1992). In the Northern Hemisphere summer, two mid-latitude circulation phenomena have a great influence on national weather conditions: the Trade Winds and the Subtropical High Pressure Belt. In contrast, only the northern part of the country is affected, during the boreal winter, by a third major circulation feature: the Westerlies (O'Hara and Metcalfe, 1995). Interestingly, a shift in the middle (and upper) troposphere from Westerlies (winter) to Easterlies (summer) is linked to the Mexican Monsoon in the north-western part of the country (Castro et al., 2001; Higgins et al., 1997). It is relatively recent that another phenomenon, the El Niño Southern Oscillation (ENSO) phenomenon has been considered as one of the most important causes affecting the Mexican climate.

The relationships between ENSO and the Mexican climate are not yet well understood. The Southern Oscillation tends to exert a modulating influence on the precipitation throughout the year with two contrasting responses; extra-tropical conditions for the Northern Hemisphere dry season and a tropical response in the boreal summer rainy period (Cavazos and Hastenrath, 1990). Wetter conditions are observed in the northern part of Mexico, while drier conditions prevail in the southern half of the country during El Niño years (Magaña et al., 2003). Although, as in the 1997-1998 ENSO event, precipitation could vary considerably in comparison to established patterns from previous events (Magaña et al., 1999).

One of the most consistent El Niño-like climatic responses is observed during the winter season (DJF). Above normal precipitation has been experienced in the United States Gulf coast, northern Mexico, Texas and the Caribbean Islands (Díaz and Kiladis, 1992); meanwhile during the same season decreasing rainfall occurs in the Isthmus of Tehuantepec. A larger geographical modulation can be perceived during the summer season. Precipitation deficits (relative to the normals) occur nationwide during the June,

July and August (JJA) period (Trenberth and Caron, 2000). Cooler temperatures prevail during El Niño years in the south-eastern USA and eastern North America (Dettinger et al., 2001). In contrast, during the opposite phase of the ENSO phenomenon La Niña, widespread wetter conditions are dominant throughout the tropical regions; for these same ocean-atmospheric conditions, summer precipitation returns to their normals or even exceeds this threshold. Overall, El Niño is the most important factor that modulates the precipitation in Mexico (Magaña et al., 2003).

Among the atmospheric conditions observed during El Niño years are: southward displacement of the Inter Tropical Convergence Zone (ITCZ), strengthening of subsidence over the north of Mexico, a reinforcing process of the subtropical jet, and the same process also occurs with the midlatitude westerlies (Magaña et al., 2003). Other characteristics seen during the warm phase of the SOI include: southward displacement of low pressure systems, below normal storminess in the northwestern United States and more stormy weather conditions for the southwestern USA (Dettinger et al., 2001), including the North American Monsoon Region (NAMR).

Although nowadays there is increasing evidence of global warming, less clear is the link between this sort of climatic change and the fluctuations of the hurricane activity. The intense hurricane season of 2004 lead some scientists to suggest that it was partly caused by global warming (Pielke Jr et al., 2005). However, the historical and observational data of hurricanes do not show any clear relationship with the changing climatic trends: 2004 and 2005 hurricane seasons were not extraordinary when compared with the seasons of 1958, 1969, 1980, 1995 and 1998 (Virmani and Weiberg, 2006). In the same context, simulations of General Circulation Models (GCMs) show only small changes in tropical cyclone patterns and numbers in anthropogenic climate change experiments (Trenberth, 2005).

There is great variability in hurricane activity across Central America and the Caribbean Basins. In the north Caribbean region, high interannual and decadal variability is observed. This sort of decadal variation is also true for the southern Caribbean, but

smaller fluctuations are observed in Central America. The long-term (annual average) frequency of hurricane strikes is 1.0 and 0.4 for the northern and southern Caribbean respectively. During La Niña years a net increase in hurricane activity is observed in Central America and the Caribbean, meanwhile fewer tropical cyclones are seen during El Niño years (Pielke Jr. et al., 2003).

Closely replicating the rainy period in Mexico, the hurricane season goes from May to November; tropical cyclones occur mainly in August, September and October (García-Oliva et al., 1991). Along the Mexican Atlantic coast, the interannual anomalies of hurricane activity are mainly associated with the El Niño Southern Oscillation (ENSO) phenomenon. In contrast, the number of hurricanes near the Pacific coast is principally modulated by the Quasibiennial Oscillation (QBO) and solar sunspot activity (Reyes and Troncoso, 1999). There is a clear differentiation between the patterns of hurricane activity on both coasts: along the Pacific Ocean there are more tropical cyclones (16 per year); while in the Atlantic coast -because of its warmer sea surface temperatures- the hurricanes are more intense and last longer than in the Pacific. The frequency of hurricanes in the Mexican Caribbean Sea and the Gulf of Mexico is nine per year (Pielke Jr. et al., 2003). Along the Pacific coast, the rainfall probability has a very well defined regional distribution; the cold California stream and the tropical cyclonic trajectories are important factors that dominate the regional precipitation patterns. In the central Pacific coast, tropical cyclone precipitation is the most important influence in the total annual rainfall (García-Oliva et al., 1991).

The hurricanes have impacts that can completely separate them climatically from the neighbouring regions (Englehart and Douglas, 2002). Extreme events associated to hurricanes can disrupt the normal precipitation patterns along the Mexican coasts, especially over the north-eastern Atlantic coast in Tamaulipas state (Magaña et al., 2003). The 2005 hurricane season showed both the strength of the tropical cyclones like Wilma, the strongest Atlantic hurricane on record (Schrope, 2005) that hit the Mexican Caribbean especially at Cancún, and the vulnerabilities of some areas along the coasts of developing countries as Hurricane Stan has demonstrated (Aubry, 2005).

This physical and geographical knowledge can be expanded using different sources, especially those that have been recording the climate indirectly.

2.4 INSTRUMENTAL DATA.

In México, long-term records of meteorological variables are scarce, so there are only a few studies on climate change in the country (Jauregui, 1997). Several socioeconomic factors since the beginning of its independent life in 1821 did not allow continuous records to be collected until the beginning of the 20th century after the revolutionary period. During the Porfirio Díaz regime (1877-1911) the first meteorological network was established in 1877 at three different sites: Tacubaya (Mexico City), Guadalajara and Chihuahua; but it was only in 1921 when the Servicio Meteorológico de México (Meteorological Office) was created when 600 stations spread throughout the country (Metcalfe, 1987), that systematic observations really started. Since then, the records have been kept almost consistently (generally for the major Mexican cities) only interrupted during periods of economic crisis such as the 1980s, large catastrophic events or the 1985 earthquake in Mexico City. These events have affected the continuity of these time-series making them of reduced length and potentially reduced quality (Jauregui, 1992).

The advent of new computing technologies opened a number of opportunities in almost every research area; enabling the bulk of the instrumental data (meteorological variables) in Mexico to be digitised. These efforts really started in 1985 when the CLImat COMputing (CLICOM) initiative was established, as one more of the projects of the World Climate Programme (WCP); its objective is the maintenance and upgrading of automated Climate Database Management Systems (CDMSs) among the members of the World Meteorological Organisation (WMO). Since then several projects to gather and digitise much of these data have been made. Some of the data have been released by the Mexican Institute of Water Technology (Instituto Mexicano de Tecnología del Agua, IMTA) as software with interfaces to get the raw data or compute basic statistics (Quintas, 2001; Gonzalez, 1998).

Several reasons, however, have impeded a full use of the potential of the digital databases of climatic variables in Mexico. Since the first efforts of García (1988) introducing a digital database covering the entire country, several datasets have been released (Quintas, 2001; González, 1998). Nevertheless, until today the revised databases to construct the network of stations (used in this thesis) share, among others, three main limitations: little extensive quality control (QC) analyses, poor spatial coverage for some regions, and largest cities generally not included in the networks. Some authors have noted several systematic errors in the databases that need some mathematical and statistical treatment before being utilised in their climatic studies (Giddins et al., 2005; Englehart and Douglas, 2004; Englehart and Douglas, 2003). Sparsity of the climatological network within some of the most geographically inaccessible regions (northern and mountainous areas) in Mexico is another of the unwanted features of the digital datasets (Englehart and Douglas, 2002; O'Hara and Metcalfe, 1995). Finally, one disadvantage found in this study while extracting the stations, is that some of the oldest and largest cities and presumably with long-term records (like Tacubaya station in Mexico City) were not included in the digital databases (see section 3.2).

2.5 DOCUMENTARY AND PROXY DATA.

Documentary and proxy climatic (pre-instrumental) data have started to be used as surrogate sources due to the lack of long-term series of meteorological (instrumental) data to reconstruct past climates. Although there is increasing research on climate change from historical records in Europe and North America less has been done in the rest of the world (Bradley and Jones, 1992). O'Hara and Metcalfe (1995) refer to several studies that have been made to reconstruct the climate of Mexico based on historical archives.

During prehispanic, colonial times and to the present day, agriculture has played a key role in the history of México, so many of the historical documents refer to periods of drought or floods. A recent study of tree-ring data for central and northern Mexico is linked to drought cycles as described in Aztec codices (Therrell et al., 2004) finding a good match with what Mexicas (the way the Aztecs liked to call themselves) called the

One Rabbit year curse in the chronologies (Cook, 1946). But this is only one of the many aspects of the Mexican culture that can be used in climatic reconstructions from historical files.

Religion is another important facet of the life in México relating history and climate. Droughts in the basin of the México City Valley have been rigorously archived (because of the importance of the social and economic aspects involved) by registered rogation ceremonies (Garza, 2002). The intensity and duration of the dry periods are measured by the ceremonial levels being the maximum (level V) the Transfer of the Virgen de los Remedios (Virgin of the remedies) from the port of Veracruz to México City and the carrying from Parroquia de la Santa Veracruz (Santa Veracruz Parish) to the Cathedral in the historical city centre. It is interesting to note that the highest level of rogation was reached several times during the independence war in México (1810-1821). Nevertheless, historical data are of limited value on climatic reconstructions because of their intrinsically indirect nature. That is why meteorological records have to be used to improve our understanding of the climate of México.

2.6. KEY STUDIES ON THE CLIMATE OF MEXICO.

With the objective of finding the impact of atmospheric circulation on the economy of Mexico, Wallén (1955) applies several statistical tests, and successfully established some of the most important large-atmospheric controls that modulate the precipitation regimes in Mexico. Mosiño and García (1974) extended the statistical analyses of large-scale atmospheric controls to include the most important geographical characteristics, providing a more complete climatic picture (includes precipitation and also temperature) of the whole country and its main controlling physical mechanisms. The main findings of this assessment is the establishment of the length of la canícula, that is a drastic depletion of rainfall during the wet season over the Atlantic and the south Pacific coasts, and the orographic factor as two important characteristics on the determination of the main climatic regions of Mexico. Probably, the first national evaluation of the climate of México using digitised data is the study undertaken by García (1988). In this research, the

complex picture of climatic conditions described above made it necessary to modify the traditional Köppen climatic system that defines climatic regions based on latitudinal changes, the classification establishing the limits between the different types of vegetation utilising primarily precipitation and temperature (Burroughs, 2003), which when applied to México, apparently enables large homogeneous areas to emerge. However, inside those areas non-trivial climatic differences are evident. So, the main result of Garcia's research contribution has been to alter the Köppen classification and then adapt it to the great diversity of the climate of México.

Using statistical techniques like PCA (Principal Component Analysis) and the recent digital databases a few studies have been made to regionalise Mexico into climatic zones using precipitation and temperature. Using northern Mexico and southern USA precipitation monthly totals for 1961-1990, Comrie and Glenn (1998) applied PCA with oblique rotation (direct oblimin) to obtain large-homogeneous regions; they found that amongst monsoon sub-regions rainfall variability closely responded to 500 mb pressure heights. In a similar study but using the first quality-revised long-term (1927-1997) Mexican digitised database, Englehart and Douglas (2002) published an analysis on summer (June through September) rainfall time-series and their connectivity with the Pacific Decadal Oscillation (PDO). They found a tendency for teleconnections, to be more intense and affecting larger areas of the country during positive phases of the PDO. Following an analogous design they (Englehart and Douglas, 2004) have also evaluated a network of Surface Air Temperature (SAT) monthly (1941-2001) time-series, using PCA (oblique-rotated solution) that showed that four climatically coherent regions appeared across Mexico. They assessed month-to-month persistency and observed that the largest occurs during the warm season. They also evaluated SAT-ENSO relationships, but did not find clear links except for the far southern area. These three studies show the potential of using the recent databases of digitised meteorological information and up to date techniques for climatic studies.

One of the greatest Mexican contributions to the study of climate change has been made by Julián Adem. A summary account of his works and collaborations can be found in

Garduño (1999). The most important contribution, the Hemispheric Thermodynamic Climate Model (HTCM) is reviewed in Adem (1991). The basic aims of the HTCM are: a simulation of the climatic conditions of the northern hemisphere (NH) during the last deglaciation; the prediction of the variations of monthly temperature anomalies in the NH, with a verification of the results over the USA; simulation of the sea surface temperatures (SSTs) in the Atlantic and Pacific oceans; simulation of the cycle of SSTs in the Gulf of Mexico; the evaluation of the changing conditions of the climate under a scenario of doubling CO_2 emissions. An application of a revised version of the HTCM to the case of Mexico can be found in Adem et al. (1995).

General Circulation Models (GCMs) are capable of performing computer simulations of the global atmospheric conditions upon which most climate change projections are based (Liverman and O'Brien, 1991). Since their early development, the limitations of GCMs have, until recently, not allowed then to adequately simulate the climate at regional scales (Crowley, 2000). Among the technical obstacles are those related to the oceanic circulation and the atmospheric convection including the role of the water vapour in feedback processes (Prinn et al., 1999).

Nevertheless, a few simulations have been made to evaluate current and future climate scenarios and their impacts in México. Using two different GCMs: the Geophysical Fluids Dynamics Laboratory (GFDL-R30) and the Canadian Climate Center (CCC) models, Magaña et al. (1997) show that, according to all simulations, increasing temperature is evident under the doubled atmospheric carbon dioxide concentrations ($2xCO_2$), however a marked difference is evident for precipitation patterns between the models. Perhaps the most important conclusion of this study is the importance of an alternative method downscaling for regionalization, in which the correlation of mesoscale variables with large-scale circulation patterns seems more convenient than direct interpolation for the GCMs outputs. Downscaling (Magaña, 1994) can establish relationships between large-scale circulation patterns and regional climatic variables. Regressions are calculated using sea surface temperatures, 500 or 700mb geopotential heights or sea level pressure (large-scale variables) and instrumental records of rainfall

or temperature (regional-scale variables). In the use of future climate scenarios, only a few studies have been made of the potential impacts under $2xCO_2$ conditions. Forests and natural protected areas have been considered (Villers-Ruiz and Trejo-Vazquez, 1998) where the results show a national reduction of those spaces. Basins and watersheds have been assessed by Mendoza et al. (1997) who show that responses vary from negative to positive in a non-homogeneous and complex picture. One weak point found in many of these assessments is the use of old climatic databases. Most of them use a definition of current climate scenario taking into account a database of precipitation and temperature for the period of 1951-1980. Since the release of new digital databases of Meteorological variables in the 1990s (see section 2.4); the spatial coverage for climatic studies has been expanded, allowing a better understanding of the Climate of Mexico. This makes the early studies pioneering and conceptual, but of relatively limited value today.

According to the last report of the Intergovernmental Panel of Climate Change (IPCC, 2007), increasing conditions of atmospheric moisture transport and convergence, besides the amplification and northward movement of the subtropical anticyclone would produce warmer conditions in North America this century. The annual mean warming in North America could be greater than the global mean warming. A generalised pattern of increasing annual precipitation for North America with the exception of the south and south-western part of the USA and over Mexico.

Regional Climate Models (RCMs) are also successful in simulating present climate conditions in North America, particularly cold-season temperature and precipitation. In this region temperatures are expected to increase linearly with time. Athough modest, precipitation changes are predicted to vary seasonally. Increasing rainfall during winter and precipitation below normal is caused, according to the RCMs, by an enhanced subsidence, drier air masses flowing southwest USA and northern Mexico, and also by an amplification of the subtropical anticyclone along the west coast.

In Central and South America temperatures are also expected to increase during this century according to the last report of the IPCC (2007). Annual mean warming in these

regions are predicted to be above the global mean warming. In most of Central America the simulations predict a reduction in the amount of annual precipitation, especially drier (boreal) springs. Nevertheless, these scenarios are still uncertain because of the limitations (of the models) to properly simulate among other physical phenomena: El Niño and the seasonal evolution of the rainy season.

The ability of the coupled Atmospheric and Oceanic General Circulation Models (AOGCMs) to predict the present climate, is still limited by their inability to simulate the annual cycle, for example, the mid-summer drought. There are also a few simulations for the regions of Central and South America utilising RCMs. Overall, a generalised pattern of warming is expected over Central and South America, with the largest changes in the continental areas, like the inner Amazonia and northern Mexico. In Central America a trend of decreasing precipitation is expected across the region. But these future scenarios are still not completely reliable because of the large variability of the projections among the RCMs.

All these uncertainties have been slowly overcome with the most recent generation of AOGCMs that through higher horizontal resolutions and improved parametrizations are contributing towards a better understanding of the climate system and their possible future scenarios under the global warming context (IPCC, 2007).

2.7. CONCLUSIONS.

Although the climate of Mexico has been widely studied using different sources, the conclusions reached are limited mainly due to the instrumental data being spatially scarce and the short length of the time series. This is not a minor issue if we consider the complexity of the country's climatic conditions. In the last two decades with the arrival of new computing technologies, several efforts have slowly dealt with the obstacle of having even less information in digital formats. Still most of the studies are based on assessments of monthly data of well-known meteorological parameters, impeding the full use (daily records) of the available digital information.

The complex picture of the Mexican climate can clearly be appreciated by the geographical features of the country. The difficult orography (two large mountain ranges and the Central High Plateau as remarkable examples) introduces another factor to the otherwise simplistic view of the climate being affected only by latitudinal differences. In the same sense the particular shape (much broader in the north compared to the south of the country) and the large expanses of ocean on both coasts add contrasting responses. There is a rough north–south climatic transition, generally milder conditions in the south, due partly to the ocean temperature-smoothing process, and more fluctuating climatic conditions in the northern part of Mexico. Well-known large-atmospheric controls like the Trade Winds, the Subtropical High Pressure Belt or the mid-latitude Westerlies are contrasting factors that affect the climate of the country. The El Niño Southern Oscillation (ENSO) phenomenon has emerged as a new factor, in the last 30 years, and it is a scientific challenge to find and explain connections with the climate of Mexico, although there are an increasing number of studies on this topic, even if most results are not yet very clear.

In order to clarify the varied climatic conditions of Mexico, and also to contribute for the knowledge, the instrumental data are not able to unveil. More recently, historical data have started being used for climatic studies. Historical sources are utilised within the context of climatic studies for two main reasons: their close relationship with Mexican culture and in order to expand the time-series lengths. Strict accounting of events in important aspects of everyday life like agriculture or religion have been recorded, from which sometimes quasi-cyclic wet or dry periods could be extracted: the curse of the one rabbit year for the Aztecs (the 260-day religious calendar years were counted as a combination of a number 1 to 13 and 1 to 20 “day signs”) or the Mexican Independence and Revolution wars during drought periods are just two of many examples. It is relatively recent that some studies combining historical and instrumental data in Mexico have started to emerge in response to the lack of research in this area.

CHAPTER 3: METHODS AND ANALYSES APPLIED.

3.1. INTRODUCTION.

This chapter deals with the extraction of the meteorological variables to be used in the analyses and the description of different mathematical and statistical tools to explore the patterns and variability of the climatic change in Mexico.

The construction of a large network of long-term high-quality databases of daily precipitation and temperature is addressed in the first part of the chapter. The extraction procedure for these meteorological time-series and the process of data quality control are both explained here. Because one of the purposes of the thesis is to link climate change patterns in Mexico during instrumental periods with the El Niño-Southern Oscillation (ENSO) phenomenon, the extraction of the three different indices (SOI, Niño 3.4 and MEI) used in these thesis are also considered in the first half of this chapter.

Three main mathematical methods are discussed in the second half of this chapter. The first is the application of Principal Component Analysis as a tool to find groups of stations that vary coherently, together with their use in calculating weighted regional averages. The second topic deals with the changes of the climatic variables at the fringes of their probability distributions, usually called weather extremes. The last method describes the two different approaches to estimate correlations between meteorological variables. Non-parametric correlations are obtained using Kendall's tau, as an alternative (to measure the association between the time-series) to the extensively used linear correlation is shown first. Lag-cross correlations are finally presented as a tool to find the lag that maximises the coherence (linear correlation) between a pair of variables.

3.2. DATA EXTRACTION.

In México the longest meteorological time series are those of (land surface) precipitation and air temperature, especially the former. This is true for either daily or monthly data. As several studies have been made using monthly values, daily figures were the first objective of the extraction, in order to explore the possibility of having a database of relatively long climatic records with high temporal resolution.

3.2.1. PRECIPITATION AND TEMPERATURE DAILY DATA.

Among the digitized data considered (because of their digital accessibility and length) are:

DAT322©

This software was prepared by the Mexican Institute of Water Technology (Instituto Mexicano de Tecnología del Agua, IMTA) to manage the 322 meteorological stations with the longest time series. The selection of the stations included was made by the Mexican Meteorological Office (Servicio Meteorológico Nacional, SMN). The documentation of this software states that climatological analyses were performed according to the Manual of the CLImat COMputing (CLICOM) project of the World Meteorological Organization (WMO) to identify outliers in the information. Strangely, it does not contain several of the largest cities (presumably with the longest data files) in Mexico, failing to present a complete national picture of the potential instrumental records. Another problem found is that missing values are defined with a zero value instead of the other options conventionally accepted.

ERIC©

This software was also prepared by IMTA with the latest version released in 2000, and contains daily precipitation and temperature data among other variables. Most of the stations have information from 1960 to 1995. No data quality analyses were performed in this database, and being typed manually this is not a minor issue. For instance, for certain months at several stations, temperature data was typed instead of precipitation in

the rainfall time series. That is why, careful attention and reserved use was given to this source.

CLICOM

Another source of data is the already mentioned CLImat COMputing Project (CLICOM) of the World Meteorological Organization (WMO). It incorporates digital daily data for almost all the stations considered by DAT322 and ERIC, but some of them have been updated until 2002 inclusive. Like DAT 322 this database does not include sufficient information for the largest - and most of the times oldest - cities in Mexico.

GASIR

GASIR (Gerencia de Aguas Superficiales e Ingeniería de Ríos) was developed by the office of Dams operation and river engineering of the National Water Commission (Comisión Nacional del Agua, CNA). They received daily precipitation data from many stations located across the country. Unfortunately, they only have digital information available from 1989 to 2001, so this database was used mainly to complete many recent gaps. Because this source is used mainly for reservoir purposes, its format is slightly different (the date is one day ahead) from the other databases, a program in fortran was needed to adapt the precipitation values to the WMO general rules. An important aspect of GASIR data, on the other hand, is that it has good quality as a whole and is almost free of errors.

3.2.2. STATIONS SELECTED.

Having all those daily digital databases available, it was necessary to choose the most appropriate stations for the subsequent analyses. Because, according to its documentation, DAT322 claimed to have the longest records selected by SMN, it was selected as the first reference or the start of the extraction for every station to be processed. The first condition defined – for climatological reasons - was that every station to be considered should have at least thirty years of information. Less than ten per cent of missing values was considered as a second limitation to extract a time series. So,

every other source already mentioned with time series fulfilling both conditions was included initially.

DATA EXTRACTION PROCEDURE.

Having enough information is not a sufficient condition for climatic studies. It is essential to assure the quality of the data extracted. That is why a procedure was designed to compare and complete the data for every station to be processed. Basically, it could be described as follows: every station in DAT322 having thirty or more years of information was compared with the other different sources and the missing values filled when possible. Then, with the daily data ready, a process to compute monthly values (mean temperatures or accumulated precipitation) and basic statistics was performed. The maximum number of missing values allowed for a month was set to four, otherwise the month was considered as missing. With these statistics it was also possible to identify (for instance, in comparison with known climatological normals) suspicious values (see fig. 3.1). An example in which data from ERIC substitute missing values (tagged as -1 in fig. 3.2) in the CLICLOM database. Another case in which the values in the CLICOM database has been multiply by a factor of ten are replaced with the ERIC data (see fig. 3.3).

After all this information was processed, only a limited number (93 stations, see table 3.1 and fig. 3.4) of daily data stations were considered as being long enough, resulting - already pointed out by several authors - in the sparsity of the meteorological observations network (O' Hara and Metcalfe, 1995; Englehart and Douglas, 2003). So, another source was used. Such a database is a monthly precipitation collection from 1931 to 1989; it was prepared by Carlos Espinosa Cruishank (specialist in Hydraulics) in the SMN. Hence, a triple checking process was made with every time series: among Espinosa's monthly data, climatological monthly figures by García (1988), and the data processed (DAT322, CLICOM, ERIC, and GASIR) from the stations reporting daily. Finally, a plot of every annual time series was made in order to find any inconsistency among of them.

Fig. 3.1. DAILY DATA EXTRACTION PROCEDURE

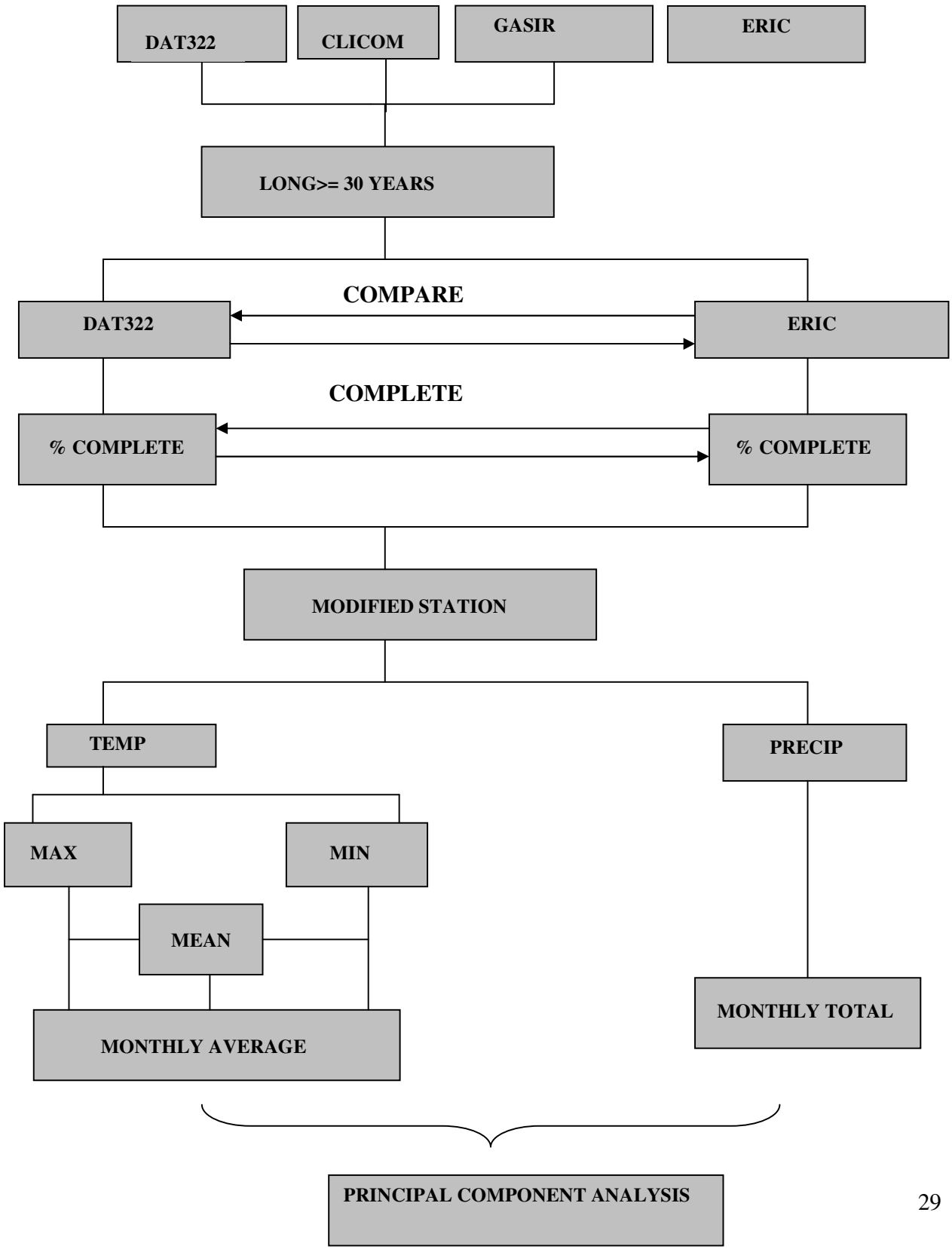

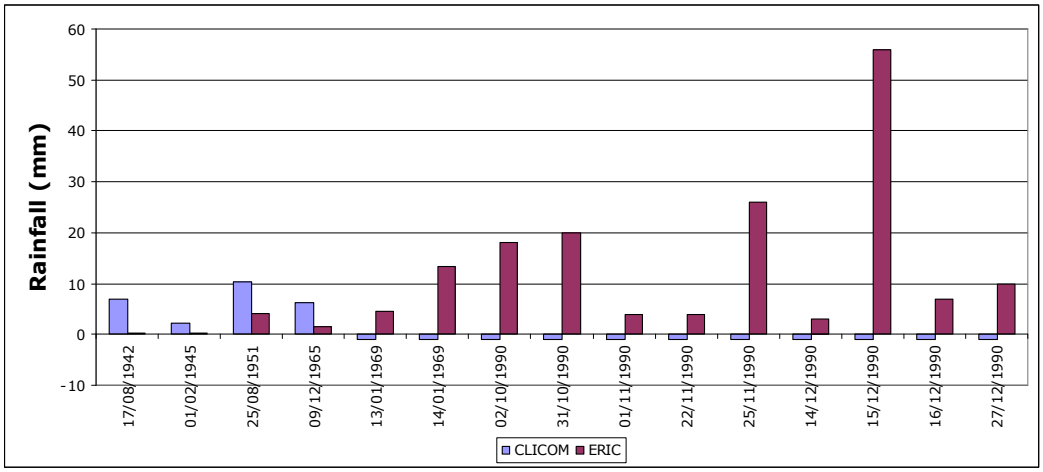

Fig. 3.2. Example of daily precipitation data being corrected. Two different databases are compared. In this case, missing values (-1) in one time-series (CLICOM) are corrected with the second dataset (ERIC).

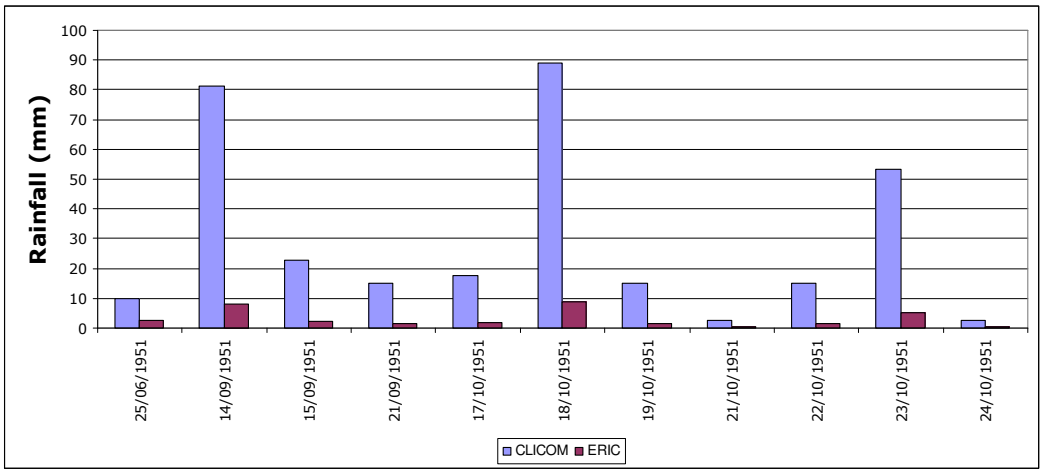

Fig. 3.3. Example of daily precipitation data being corrected. Two different databases are compared. In this case, a systematic error (values are multiplied by a factor of 10) in the first time-series (CLICOM) are substituted by the corrected values in the second dataset (ERIC).

	STATION NAME	STATE	SMN ID	LONGITUDE	LATITUDE	ALTITUDE*
1	PABELLON DE ARTEAGA	AGS	01014	-102.33	22.18	1920
2	PRESA CALLES	AGS	01018	-102.43	22.13	2025
3	PRESA RODRIGUEZ	BCN	02038	-116.90	32.45	100
4	EL PASO DE IRITU	BCS	03012	-111.12	24.77	140
5	LA PURíSIMA	BCS	03029	-112.08	26.18	95
6	LORETO	BCS	03035	-111.33	26.00	15
7	SAN JOSE DEL CABO	BCS	03056	-109.67	23.05	7
8	SANTA ROSALíA	BCS	03061	-112.28	27.30	17
9	SANTIAGO	BCS	03062	-109.73	23.47	125
10	TODOS SANTOS (DGE)	BCS	03066	-110.22	23.43	18
11	CHAMPOTON	CAMP	04008	-90.72	19.35	2
12	HECELCHAKAN	CAMP	04011	-90.13	20.18	13
13	SABANCUY	CAMP	04029	-91.11	18.97	2
14	RAMOS ARIZPE	COAH	05032	-100.98	25.53	1399
15	SALTILLO	COAH	05048	-101.00	25.42	645
16	COLIMA	COL	06040	-103.73	19.23	495
17	OCOZOCUAUTLA	CHIAP	07123	-93.38	16.70	864
17	CIUDAD GUERRERO	CHIH	08028	-108.52	28.52	2000
18	CD CUAUHTEMOC	CHIH	08026	-106.85	28.42	2050
19	CIUDAD DELICIAS	CHIH	08044	-105.43	28.20	1170
20	HIDALGO DEL PARRAL	CHIH	08078	-105.67	26.93	1950
21	LA JUNTA	CHIH	08090	-107.97	28.75	1900
22	BATOPILAS	CHIH	08161	-107.75	27.02	556
23	EL PALMITO	DUR	10021	-104.78	25.52	1540
24	FCO. I MADERO	DUR	10027	-104.30	24.47	1960
25	GUANACEVI	DUR	10029	-105.97	25.93	2200
26	RODEO	DUR	10060	-104.53	25.18	1340
27	SAN MARCOS	DUR	10070	-103.50	24.27	
28	SANTIAGO PAPASQUIARO	DUR	10100	-105.42	25.05	1740
29	IRAPUATO	GTO	11028	-101.35	20.68	1725
30	SAN DIEGO DE LA UNION	GTO	11064	-100.87	21.47	2080
31	SAN JOSE ITURBIDE	GTO	11066	-100.40	21.00	2100
32	AYUTLA (CFE)	GRO	12012	-99.10	16.95	
33	CHILAPA	GRO	12110	-99.18	17.60	1450
34	HUICHAPAN	HGO	13012	-99.65	20.38	1102
35	MIXQUIHUALA	HGO	13018	-99.20	20.23	2050
36	CHAPALA	JAL	14040	-103.20	20.30	1523
37	MASCOTA	JAL	14096	-104.82	20.52	1240
38	SAN FRANCISCO	MEX	15089	-99.97	19.30	2630
39	LA PIEDAD CABADAS (DGE)	MICH	16065	-102.03	20.37	1700
40	TACAMBARO	MICH	16123	-101.47	19.23	1820
41	YURECUARO	MICH	16141	-102.28	20.35	1537
42	ZAMORA	MICH	16144	-102.28	20.00	1540
43	CUERNAVACA	MOR	17004	-99.25	18.92	1529
44	ACAPONETA	NAY	18001	-105.37	22.50	22
45	CADEREYTA	NL	19008	-100.00	25.60	350
46	EL CUCHILLO	NL	19016	-99.25	25.73	145

	STATION NAME	STATE	SMN ID	LONGITUDE	LATITUDE	ALTITUDE*
47	LOS RAMONES	NL	19042	-99.63	25.70	210
48	MONTEMORELOS	NL	19048	-99.83	25.20	425
49	MONTERREY	NL	19052	-100.30	25.68	540
50	JUCHITAN	OAX	20048	-95.03	16.43	46
51	MATIAS ROMERO	OAX	20068	-95.03	16.88	201
52	SANTO DOMINGO TEHUANTEPEC	OAX	20149	-95.23	16.33	95
53	PIAXTLA	PUE	21063	-98.25	18.20	1155
54	TEZIUTLAN	PUE	21091	-97.35	19.82	2050
55	HUAUCHINANGO	PUE	21118	-98.05	20.18	1575
56	JALPAN	QRO	22008	-99.47	21.22	860
57	PRESA CENTENARIO	QRO	22025	-99.90	20.52	1880
58	ALVARO OBREGON	QROO	23001	-88.62	18.30	
59	CHETUMAL	QROO	23032	-88.30	18.50	6
60	CHARCAS	SLP	24010	-101.12	23.13	2020
61	MATEHUALA	SLP	24040	-100.63	23.65	1575
62	MEXQUITIC	SLP	24042	-101.12	22.27	2030
63	SAN LUIS POTOSI (DGE)	SLP	24069	-100.97	22.15	1870
64	CIUDAD DEL MAIZ	SLP	24116	-99.60	22.40	1245
65	BADIRAGUATO	SIN	25110	-107.55	25.37	230
66	QUIRIEGO	SON	26075	-109.25	27.52	521
67	TRES HERMANOS	SON	26102	-109.20	27.20	100
68	YECORA	SON	26109	-108.95	28.37	
69	SAN FERNANDO	TAM	28086	-98.15	24.85	43
70	TAMPICO (DGE)	TAM	28111	-97.87	22.22	12
71	VILLAGRAN	TAM	28118	-99.48	24.48	380
72	APIZACO	TLX	29002	-98.13	19.42	2404
73	TLAXCALA	TLX	29030	-98.23	19.32	2552
74	TLAXCO	TLX	29032	-98.13	19.63	2444
75	CATEMACO	VER	30022	-95.10	18.42	338
76	CHICONTEPEC	VER	30041	-98.17	20.98	595
77	IXHUATLAN	VER	30072	-98.00	20.70	306
78	JALTIPAN	VER	30077	-94.43	17.97	46
79	PAPANTLA	VER	30125	-97.32	20.45	298
80	RINCONADA	VER	30141	-96.55	19.35	313
81	SOLEDAD DOBLADO	VER	30163	-96.42	19.05	183
82	VERACRUZ	VER	30192	-96.13	19.20	16
83	JALAPA	VER	30228	-96.92	19.53	1999
84	TUXPAN	VER	30229	-97.40	20.95	4
85	PANUCO	VER	30285	-98.17	22.05	60
86	PROGRESO	YUC	31023	-89.65	21.28	8
87	SOTUTA	YUC	31030	-89.02	20.60	11
88	MERIDA (DGE)	YUC	31044	-89.62	20.98	9
89	EL SAUZ	ZAC	32018	-103.23	23.18	2100
90	SOMBRERETE	ZAC	32054	-103.63	23.63	2300
91	JUCHIPILA	ZAC	32067	-103.13	21.42	1240
92	TEUL DE GLEZ. ORTEGA	ZAC	32070	-103.47	21.47	1900
93	ZACATECAS	ZAC	32086	-102.57	22.77	2450

Table 3.1. Spatially incomplete network of daily data stations for precipitation. The period of records for all the stations is from 1931 to 2001. * meters above sea level.

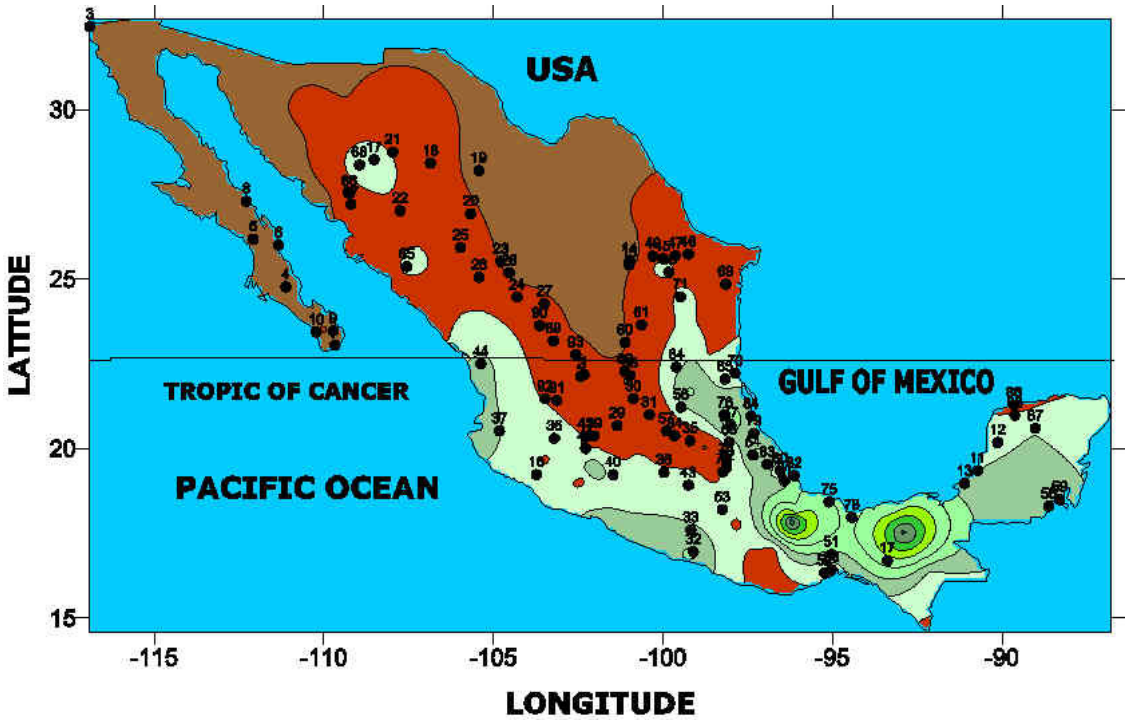

Fig. 3.4. Resulting network of 93 stations after the first stage of extraction of daily rainfall data.

The final network consists of a set of 175 stations having monthly precipitation, 168 are Mexican and 7 are southern USA stations, with good spatial coverage (Table 3.2, and Fig. 3.5). The length of every time series is of 71 years, starting in 1931 and ending in 2001. The maximum percentage of missing values was restricted to 10%.

It is possible that some information has been left out of the extraction efforts as there are some records still on paper in SMN, but this is unlikely to happen in terms of digital databases. All the currently known Mexican climatological digitised sources were considered. That is why an acceptable spatial coverage is expected, markedly better than all the few former studies aiming at a national appraisal of the Mexican climate using the longest time series available. For extraction purposes of precipitation and temperature data, the definitions of wet and dry seasons established in section 2.2.1 are applied in this chapter.

	STATION NAME	STATE	SMN ID	LONGITUDE	LATITUDE*	ALTITUDE+
1	AGUASCALIENTES	AGS	01001	-102.30	21.88	1870
2	PABELLON DE ARTEAGA	AGS	01014	-102.33	22.18	1920
3	PRESA CALLES	AGS	01018	-102.43	22.13	2025
4	PRESA RODRIGUEZ	BCN	02038	-116.90	32.45	100
5	ENSENADA	BCN	02072	-116.60	31.88	24
6	BUENAVISTA	BCS	03004	-111.80	25.10	30
7	EL PASO DE IRITU	BCS	03012	-111.12	24.77	140
8	LA PURíSIMA	BCS	03029	-112.08	26.18	95
9	LORETO	BCS	03035	-111.33	26.00	15
10	MULEGE	BCS	03038	-111.98	26.88	35
11	SAN BARTOLO	BCS	03050	-109.85	23.73	395
12	SAN JOSE DEL CABO	BCS	03056	-109.67	23.05	7
13	SANTA GERTRUDIS	BCS	03060	-110.10	23.48	350
14	SANTA ROSALíA	BCS	03061	-112.28	27.30	17
15	SANTIAGO	BCS	03062	-109.73	23.47	125
16	TODOS SANTOS (DGE)	BCS	03066	-110.22	23.43	18
17	LA PAZ	BCS	03074	-110.37	24.15	10
18	SABANCUY	CAMP	04029	-91.11	18.97	2
19	CAMPECHE	CAMP	04038	-90.53	19.85	8
20	CHAMPOTON	CAMP	04041	-90.72	19.37	2
21	PRESA VENUSTIANO CARRANZA	COAH	05030	-100.60	27.52	270
22	RAMOS ARIZPE	COAH	05032	-100.98	25.53	1399
23	MONCLOVA	COAH	05047	-101.42	26.90	645
24	SALTILLO	COAH	05048	-101.00	25.42	1520
25	MANZANILLO	COL	06018	-104.32	19.05	3
26	COLIMA	COL	06040	-103.73	19.23	495
27	COMITAN	CHIAP	07025	-92.13	16.25	1530
28	MOTOZINTLA	CHIAP	07119	-92.25	15.37	1455
29	CIUDAD DELICIAS	CHIH	08044	-105.43	28.20	1170
30	HIDALGO DEL PARRAL	CHIH	08078	-105.67	26.93	1950
31	CHINIPAS	CHIH	08167	-108.53	27.40	700
32	CAÑON FERNANDEZ	DUR	10004	-103.75	25.28	1300
33	LERDO	DUR	10009	-103.52	25.53	1135
34	CUENCAME	DUR	10012	-103.67	24.78	1580
35	EL SALTO	DUR	10025	-105.37	23.78	2538
36	FCO. I MADERO	DUR	10027	-104.30	24.47	1960
37	GUANACEVI	DUR	10029	-105.97	25.93	2200
38	NAZAS	DUR	10049	-104.12	25.23	1245
39	RODEO	DUR	10060	-104.53	25.18	1340
40	CELAYA	GTO	11009	-100.82	20.53	1754
41	DOLORES HIDALGO	GTO	11017	-100.93	21.15	1920
42	IRAPUATO	GTO	11028	-101.35	20.68	1725
43	OCAMPO	GTO	11050	-101.48	21.65	2250
44	SALVATIERRA	GTO	11060	-100.87	20.22	1760
45	SAN DIEGO DE LA UNION	GTO	11064	-100.87	21.47	2080
46	SAN JOSE ITURBIDE	GTO	11066	-100.40	21.00	2100
47	SANTA MARíA YURIRíA	GTO	11071	-101.15	20.22	1751

	STATION NAME	STATE	SMN ID	LONGITUDE	LATITUDE*	ALTITUDE+
48	PRESA VILLA VICTORIA	GTO	11082	-100.22	21.22	1740
49	SAN MIGUEL DE ALLENDE	GTO	11093	-100.75	20.92	1900
50	GUANAJUATO	GTO	11094	-101.25	21.02	2037
51	LEON (LA CALZADA, DGE)	GTO	11095	-101.68	21.08	1809
52	AYUTLA (CFE)	GRO	12012	-99.10	16.95	
53	IGUALA	GRO	12116	-99.53	18.35	635
54	HUICHAPAN	HGO	13012	-99.65	20.38	1102
55	SANTIAGO TULANTEPEC	HGO	13031	-98.37	20.08	2180
56	PACHUCA	HGO	13056	-98.73	20.12	2435
57	PRESA REQUENA	HGO	13084	-99.32	19.97	2109
58	ATEQUIZA (CHAPALA)	JAL	14016	-103.13	20.40	1520
59	CHAPALA	JAL	14040	-103.20	20.30	1523
60	EL FUERTE, OCOTLáN	JAL	14047	-102.77	20.30	1527
61	GUADALAJARA	JAL	14066	-103.42	20.72	1583
62	MAZAMITLA	JAL	14099	-103.02	19.92	2800
63	TEPALPA	JAL	14142	-103.77	19.95	2060
64	CD. GUZMAN	JAL	14500	-103.47	19.70	1535
65	APATZINGAN	MICH	16007	-102.35	19.08	682
66	PRESA COINTZIO	MICH	16022	-101.27	19.62	1997
67	CUITZEO DEL PORVENIR	MICH	16027	-101.15	19.97	1831
68	HUINGO	MICH	16052	-100.83	19.92	1832
69	JESUS DEL MONTE (MORELIA)	MICH	16055	-101.15	19.65	1950
70	LA CAIMANERA	MICH	16059	-100.90	18.47	287
71	PRESA LA VILLITA	MICH	16070	-102.18	18.05	
72	MORELIA (DGE)	MICH	16081	-101.18	19.70	1941
73	YURECUARO	MICH	16141	-102.28	20.35	1537
74	ZAMORA	MICH	16144	-102.28	20.00	1540
75	ZINAPECUARO	MICH	16145	-100.82	19.87	1840
76	ARTEAGA	MICH	16151	-102.28	18.35	860
77	CIUDAD HIDALGO	MICH	16152	-100.57	19.70	2000
78	URUAPAN	MICH	16164	-102.07	19.42	1610
79	ZACAPU	MICH	16171	-101.78	19.82	1986
80	ATLATLAHUACáN	MOR	17001	-98.90	18.93	1630
81	CUERNAVACA	MOR	17004	-99.25	18.92	1529
82	CUAUTLA	MOR	17005	-98.95	18.82	1291
83	PRESA EL RODEO	MOR	17006	-99.32	18.78	1100
84	ACAPONETA	NAY	18001	-105.37	22.50	22
85	AHUACATLAN	NAY	18002	-104.48	21.05	990
86	IXTLAN DEL RIO	NAY	18016	-104.37	21.03	1035
87	LAS GAVIOTAS	NAY	18021	-105.15	20.88	43
88	TEPIC	NAY	18038	-104.88	21.50	920
89	ALLENDE	NL	19003	-100.03	25.28	457
90	CERRALVO	NL	19010	-99.62	26.08	345
91	EL CUCHILLO	NL	19016	-99.25	25.73	145
92	HIGUERAS	NL	19025	-100.02	25.95	
93	ITURBIDE	NL	19027	-99.92	24.73	1480
94	LAMPAZOS	NL	19028	-100.52	27.03	320

	STATION NAME	STATE	SMN ID	LONGITUDE	LATITUDE*	ALTITUDE+
95	LOS RAMONES	NL	19042	-99.63	25.70	210
96	MIMBRES, GALEANA	NL	19047	-100.25	24.97	
97	MONTEMORELOS	NL	19048	-99.83	25.20	425
98	MONTERREY	NL	19052	-100.30	25.68	540
99	HUAJUAPAN DE LEON	OAX	20035	-97.78	17.80	1650
100	SANTA MARíA JACATEPEC	OAX	20042	-96.20	17.85	
101	JUCHITAN	OAX	20048	-95.03	16.43	46
102	MATIAS ROMERO	OAX	20068	-95.03	16.88	201
103	OAXACA DE JUAREZ	OAX	20079	-96.72	17.03	1550
104	SANTO DOMINGO TEHUANTEPEC	OAX	20149	-95.23	16.33	95
105	PIAXTLA	PUE	21063	-98.25	18.20	1155
106	PUEBLA	PUE	21065	-98.18	19.03	2209
107	TEZIUTLAN	PUE	21091	-97.35	19.82	2050
108	ZOQUITLAN	PUE	21114	-97.02	18.35	2140
109	PRESA CENTENARIO	QRO	22025	-99.90	20.52	1880
110	ALVARO OBREGON	QROO	23001	-88.62	18.30	
111	CHETUMAL	QROO	23032	-88.30	18.50	6
112	BALLESMI	SLP	24005	-98.93	21.75	30
113	CERRITOS	SLP	24008	-100.28	22.43	1150
114	CHARCAS	SLP	24010	-101.12	23.13	2020
115	MATEHUALA	SLP	24040	-100.63	23.65	1575
116	MEXQUITIC	SLP	24042	-101.12	22.27	2030
117	SAN LUIS POTOSI (DGE)	SLP	24069	-100.97	22.15	1870
118	TANZABACA	SLP	24090	-99.22	21.67	120
119	BOCATOMA SUFRAGIO	SIN	25009	-108.78	26.08	152
120	CULIACAN	SIN	25015	-107.40	24.82	62
121	CHOIX (DGE)	SIN	25019	-108.33	26.73	350
122	EL FUERTE	SIN	25023	-108.62	26.42	84
123	GUAMUCHIL	SIN	25037	-108.08	25.47	45
124	BADIRAGUATO	SIN	25110	-107.55	25.37	230
125	MAZATLAN	SIN	25135	-106.38	23.22	3
126	CIUDAD OBREGON	SON	26018	-109.97	27.50	35
127	PRESA LA ANGOSTURA	SON	26069	-109.37	30.43	50
128	TRES HERMANOS	SON	26102	-109.20	27.20	100
129	YECORA	SON	26109	-108.95	28.37	
130	HERMOSILLO	SON	26138	-110.97	29.07	200
131	(PRESA) PLUTARCO ELIAS CALLES	SON	26191	-110.63	29.93	
132	COLMACALCO	TAB	27009	-93.22	18.27	10
133	TAPIJULAPA	TAB	27042	-92.77	17.45	60
134	TEAPA	TAB	27044	-92.95	17.55	72
135	ABASOLO	TAM	28001	-98.37	24.05	61
136	MANTE (CAMPO EXPERIMENTAL INGENIO)	TAM	28012	-98.98	22.73	100
137	ANTIGUO MORELOS (EL REFUGIO)	TAM	28032	-99.08	22.55	242
138	MIGUEL HIDALGO	TAM	28038	-99.43	24.25	
139	MAGISCATZIN	TAM	28058	-98.70	22.80	90
140	SAN FERNANDO	TAM	28086	-98.15	24.85	43
141	TAMPICO (DGE)	TAM	28111	-97.87	22.22	12
142	VILLAGRAN	TAM	28118	-99.48	24.48	380

	STATION NAME	STATE	SMN ID	LONGITUDE	LATITUDE*	ALTITUDE+
143	SOTO LA MARINA	TAM	28152	-98.20	23.77	25
144	APIZACO	TLX	29002	-98.13	19.42	2404
145	TLAXCALA	TLX	29030	-98.23	19.32	2552
146	TLAXCO	TLX	29032	-98.13	19.63	2444
147	ANGEL R. CABADAS	VER	30011	-95.45	18.60	19
148	ATZALAN	VER	30012	-97.25	19.80	1842
149	CATEMACO	VER	30022	-95.10	18.42	338
150	CD. ALEMáN	VER	30025	-96.08	18.18	29
151	CHICONTEPEC	VER	30041	-98.17	20.98	595
152	IXHUATLAN	VER	30072	-98.00	20.70	306
153	JALTIPAN	VER	30077	-94.43	17.97	46
154	PAPANTLA	VER	30125	-97.32	20.45	298
155	RINCONADA	VER	30141	-96.55	19.35	313
156	VERACRUZ	VER	30192	-96.13	19.20	16
157	LAS VIGAS	VER	30211	-97.10	19.65	37
158	JALAPA	VER	30228	-96.92	19.53	1999
159	TUXPAN	VER	30229	-97.40	20.95	4
160	PANUCO	VER	30285	-98.17	22.05	60
161	PROGRESO	YUC	31023	-89.65	21.28	8
162	SOTUTA	YUC	31030	-89.02	20.60	11
163	MERIDA (DGE)	YUC	31044	-89.62	20.98	9
164	EL SAUZ	ZAC	32018	-103.23	23.18	2100
165	SOMBRERETE	ZAC	32054	-103.63	23.63	2300
166	JUCHIPILA	ZAC	32067	-103.13	21.42	1240
167	TEUL DE GLEZ. ORTEGA	ZAC	32070	-103.47	21.47	1900
168	ZACATECAS	ZAC	32086	-102.57	22.77	2450
169	ABILENE	TX	ABITX	-99.70	32.40	
170	EL PASO	TX	ELPTX	-106.50	31.80	
171	ELEPHANT BUTTE DAM	NM	EPBNM	-107.18	33.15	
172	PHOENIX	AZ	PHXAZ	-112.00	33.50	
173	SAN DIEGO	CA	SANCA	-117.20	32.70	
174	SAN ANTONIO	TX	SATTX	-98.47	29.53	
175	TUCSON	AZ	TUSAZ	-110.95	32.23	

Table 3.2. Spatially incomplete network of daily data stations for precipitation. The period of records for all the stations is from 1931 to 2001. * meters above sea level.

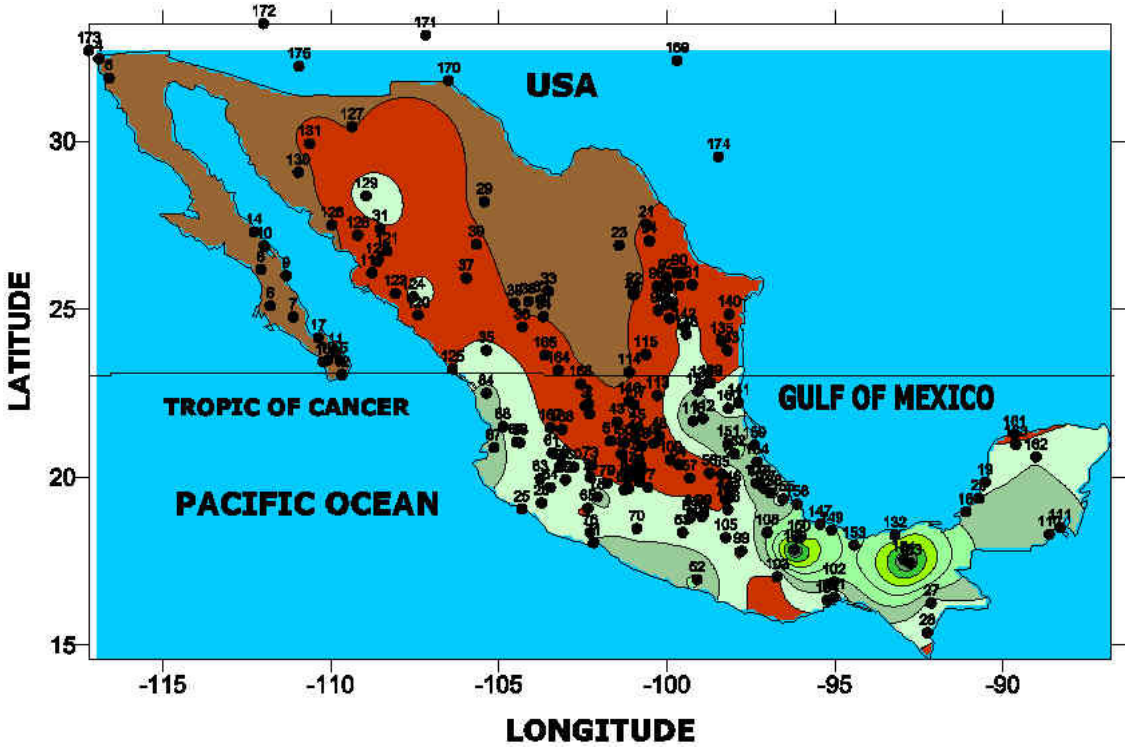

Fig. 3.5. Meteorological network of 175 with monthly precipitation data from 1931 to 2001 as used in the analysis of Principal Components (PC).

3.2.3 ENSO INDICES.

The Southern Oscillation Index (SOI).

One of the most typical measures utilised to explore the impacts of ENSO, is the Southern Oscillation Index (SOI). Since the 1800s this phenomenon had been observed as a difference in the sea-level pressures in the South Pacific, but its characteristics, extent and linked impacts in temperature and precipitation were not fully established by Walker and Bliss in the 1930s (Trenberth and Caron, 2000). Nowadays, it is widely accepted that the Southern Oscillation (SO) is a planetary-scale phenomenon, which involves an atmospheric mass of air in a standing wave shape, with a coherent exchange between the Eastern and Western hemispheres. The SO has its centre over Indonesia and the south tropical area of the Pacific Ocean. The SO is strongly associated with El Niño (EN), in this sense the cold phase is now called La Niña, while the warm phase is

frequently termed as El Niño, although their association is not always present. Nevertheless, the phenomenon is now universally referred as El Niño Southern Oscillation or ENSO (Ropelewski and Halpert, 1996).

The most extensively SO index recently used, because its correlation consistency, is the difference in sea level pressures between Tahiti and Darwin. In this research we are going to use the index defined by Ropelewski and Jones (1987). The index is calculated using five-month running means of the SOI that lie below the threshold of -0.5 standard deviations for more than five consecutive months; these cases considered "warm" episodes, and "cold" episodes are referred to the contrary conditions. Ropelewski and Jones (1987) state the post 1935 is a reliable source for ENSO related studies, and this condition makes it suitable with the purposes of the analysis.

Niño 3.4 Index

The high intensity of the ENSO events of the 1990s showed the necessity to extend the definitions of the four regions established in the 1980s. In this sense, Niño 3.4 (5° N - 5° S, 120°- 170° W) is today identified through Sea Surface Temperature (SST) anomalies centred approximately in the eastern half of the equatorial Pacific towards the west near the date line (fig. 3.6). up to date this index has proved to have the strongest link with ENSO-related impacts during the last decades (Barnston and Chelliah, 1997). Since April 1996 the measure also has allowed an improved scientific insight of the SSTs within the vital area between ENSO regions 3 and 4 (fig. 3.6). For the purposes of this research the standardised version of the Niño 3.4 index has been selected and extracted from the Climate Diagnostics Center (CDC) website: http://www.cdc.noaa.gov/ClimateIndices/.

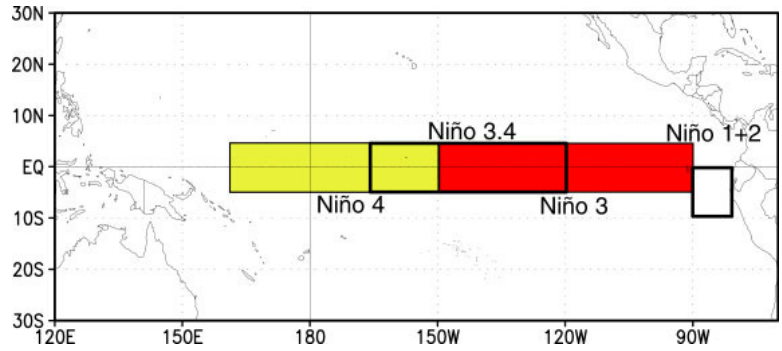

Fig 3.6. Current defined ENSO regions extracted from the Climate Diagnostics Center (CDC) website: http://www.cdc.noaa.gov/ClimateIndices/.

MULTIVARIATE ENSO INDEX (MEI)

Another option to explore the ENSO influence in a broader way (in the Mexican climate change context) is the Multivariate ENSO Index (MEI). The MEI is a more complete climatic measure when compared with the other ENSO indices available. The ocean and atmospheric variations are better considered by it, while it is also less vulnerable to the infrequent data errors of the monthly updating process. The index is computed as a weighted average of six different variables over the tropical Pacific, these parameters are: sea-level pressure (P), zonal (U) and meridional (V) surface winds, sea surface temperature (S), surface air temperature (A), and total cloudiness fraction of the sky (C). The MEI values are calculated for twelve sliding bi-monthly seasons (Dec/Jan, Jan/Feb, ... , Nov/Dec) based on the first unrotated Principal Component of the six combined fields of observation using the covariance matrix for the extraction, then standardised with respect to each season and considering 1950-93 as the reference period. More details about the index calculations can be found in Wolter (1987) and Wolter and Timlin (1993). Positive MEI values are linked to warm ENSO periods (El Niño), while negative values to cold periods of ENSO (La Niña). As this index is said to perform better at large-scale correlations (http://www.cdc.noaa.gov/people/klaus.wolter/MEI/table.html) and not necessarily at regional scales, It is expected that MEI can reflect better the relationships of the ENSO phenomenon with the meteorological variables chosen for this study, despite MEI incorporates more ocean and atmospheric parameters than the other indices,. In any case, MEI has been selected to check consistency in the results with those of the SOI and El Niño 3.4 indices.

3.3. MATHEMATICAL AND STATISTICAL METHODS APPLIED.

3.3.1. CONSIDERING DATA HOMOGENEITY.

It is well documented that small spatial and temporal variations or observational practices such as a slight change in the elevation of the station or the type of instrument could affect the consistency of records of a meteorological variable (Easterling et al., 1999). These changes could be reflected in the short or long term variation of the time series, and consequently influence the analysis of climate extremes variability, and their influence on the results can be significant, for Principal Component Analysis (see section 3.3.2) as well. For this reason, it is desirable to test the homogeneity of the stations selected before applying any analysis.

A time series is said to be homogeneous if all its fluctuations are caused by natural variability. In this sense, when an inhomogeneous time series is adjusted we are reducing the uncertainties of the results, and improving our understanding of the climate accordingly. The necessity of a precise scientific knowledge in this topic has recently increased its importance within the context of the study of climate change. Therefore, in applying the process of homogenisation to the data, utilising different techniques, we are searching for factors other than climate and weather. Although there is no single best technique, the approaches currently recommended to homogenise a time series are discussed in the following four steps (Aguilar et al., 2003):

1) Metadata analysis and quality control.
2) Creation of a reference time series.
3) Breakpoint detection.
4) Data adjustment.

For the analysis of homogeneity a detailed documentation of the history of the station is desired. For meteorological purposes the information about the data is called metadata. Knowledge of the station's history plays an essential part when preparing a high-quality dataset. Consequently, the reliability of the results is increased when the documentation

for the stations is available.

Metadata can help to identify changes in the conditions of the station. Among the changes that can be mentioned are: relocation, replacement of the instrument, exposure modifications, and changes in the recording procedures. Greater or lesser, all of them have a direct impact on the parameter values of the station. That is why a complete history of the station relates actual changes in the station with (gradual or sudden) observed changing patterns in the time series.

For the present study only digital instrumental data were used, in such a way that the objective was to extract the largest number of stations. Having this sort of digital information the available metadata was restricted to the most basic characteristics like station identifier, location, elevation and climatological normals. Other sources of metadata like changes in location, instruments, and observational practices were inaccessible to this research, making it extremely difficult to determine the artificial nature of some of the identified inhomogeneities.

Data quality control was addressed in section 3.2 of this chapter, as part of the process of detection of inhomogeneities. Daily comparisons, among the different digital databases were applied in order to find inconsistencies.

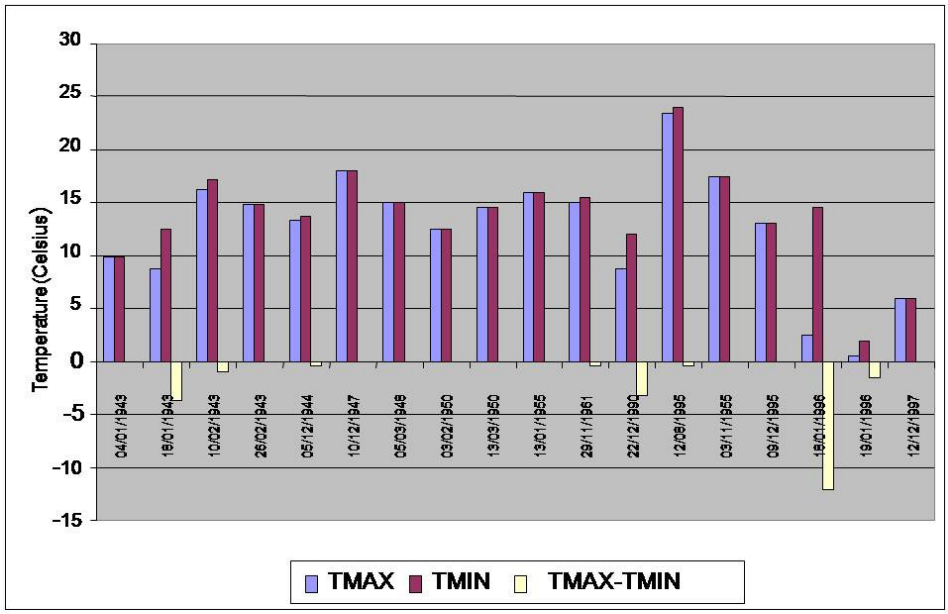

Fig. 3.7. Station with daily temperature errors before being corrected. In this case Tmin values are greater than Tmax.

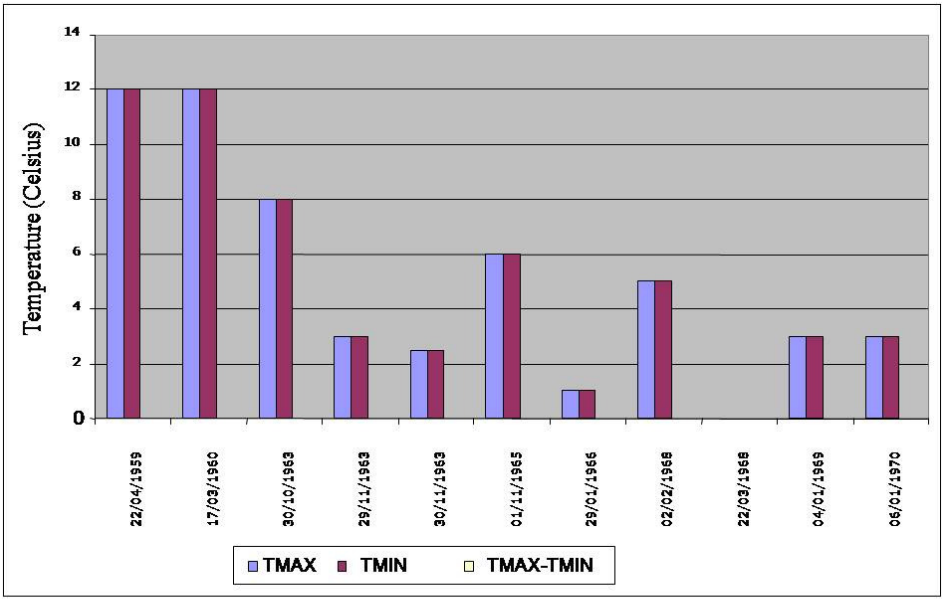

Fig. 3.8. Station with daily temperature errors before being corrected. In this case Tmin and Tmax have the same values.

Once the time series was ready, a set of basic statistics were computed like: mean, standard deviation, maximum and minimum to compare with other climatic studies in Mexico; these statistics were also used to easily identify outliers. Finally, annual precipitation, mean temperature and double-mass plots were prepared in this quality control process for every single time series to spot sudden changes in the climatic patterns. The Double-Mass plot is a technique utilised to find inconsistencies in a climatogical time-series. The underlying assumption is that the plotting of the accumulation of one quantity (a meteorological parameter at one station) against another during the same period will produce a straight line (45° slope) as far as the data are proportional. So, when a break is found that means a change in the constant of proportionality, or that the constant of proportionality is not the same at all rates of accumulation. Double-mass plots can be used to identify one or more inhomogeneities, and to correct them if the errors are clear enough (Cluis, 1983). An example of a plot after the application of this technique is seen in figures 3.9 and 3.10.

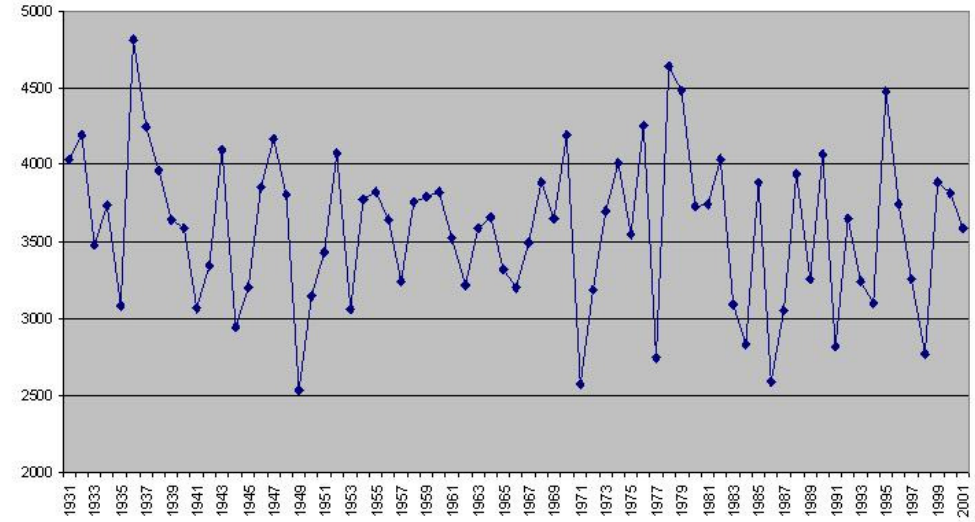

Fig. 3.9. Annual total precipitation (in mm) for station 27042; Tapijulapa, Tabasco.

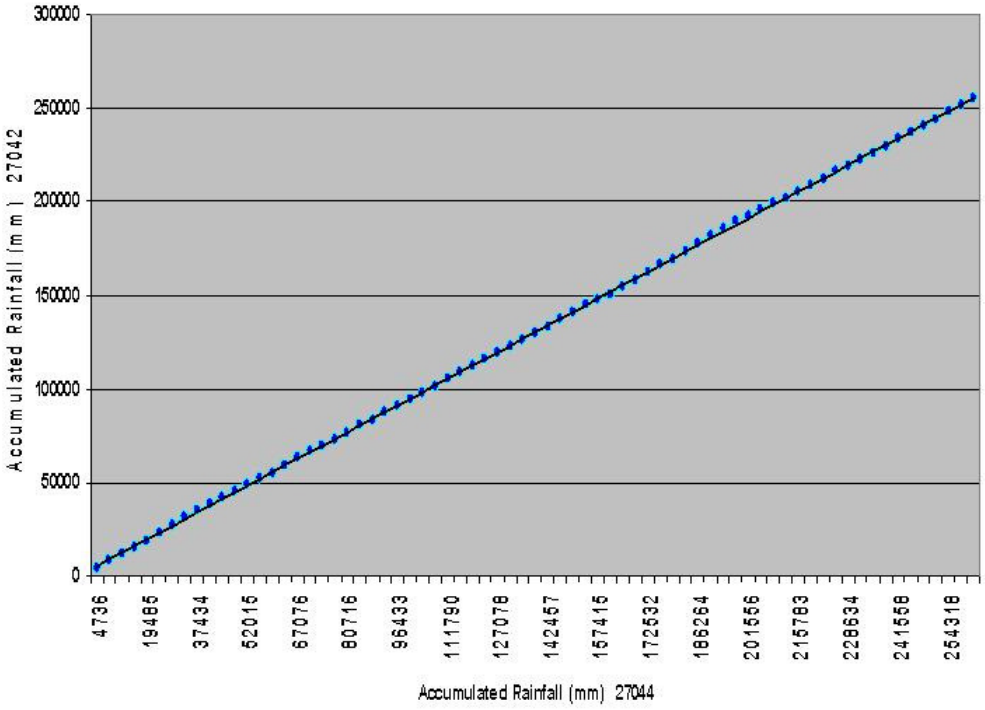

Fig. 3.10. Double Mass Plot for the station 27042; Tapijulapa, Tabasco.

No sudden jumps appear in Fig. 3.9 for station 27042 (Tapijulapa, Tabasco) after the quality control process described in section 3.2. After this analysis and "filtering out" evident errors like mistyped values, no major changes seem to have occurred in this location. The nearly "perfect" slope of the double mass plot of fig. 3.10 shows that the time-series of 27042 (against the data for station 27044) can be considered as a reliable source for the climatic analyses to be applied.

Another stage of *quality control of the data* was performed using the interactive program called RClimdex as an initial step to the extremes indices calculation. The main objective here was to identify possible mistyped errors that could affect the analysis. For instance, all precipitation values lower than 0 were considered as missing data; the same treatment was applied to the case in which daily minimum temperature was greater or equal than daily maximum temperature. Fig. 3.7 shows examples in which Tmin are equal or exceed the values of Tmax. Meanwhile the fig. 3.8 show examples in which Tmin values systematically are equal than Tmax, both set of data errors were corrected before applying subsequent analyses. The software is also able to identify outliers for a user-defined threshold, for the values of temperature (daily maximum and minimum temperature) the lower limit was set to the mean minus three standard deviations (mean - 3σ) and the mean plus three standard deviations (mean + 3σ) as the upper limit. All values beyond these thresholds were marked as suspicious and checked, then corrected accordingly when undisputable errors were present.

Due to the inherent characteristics of inhomogeneities -sometimes their variations are equal or even smaller than real natural climatic fluctuations- the process of detection is frequently difficult. To overcome this complexity it is recommended to create a reference time series. The most frequent way to construct them is to compute a weighted average using data from neighbouring stations or to select a section of surrounding stations whose data are considered homogeneous.

A clear regionalisation of the rainfall stations network made using PCA (see chapter 4) has facilitated the analysis of homogenisation. Having a group of stations that coherently varied across time made the comparisons easier. A weighted regional and individual time-series were prepared using the approach proposed by Jones and Hulme (1996). Using different indices like the Percentage Anomaly Index (PAI) and Standardised Anomaly Index (SAI) all the stations were plotted (See one example in fig. 3.11) searching for inhomogeneities.

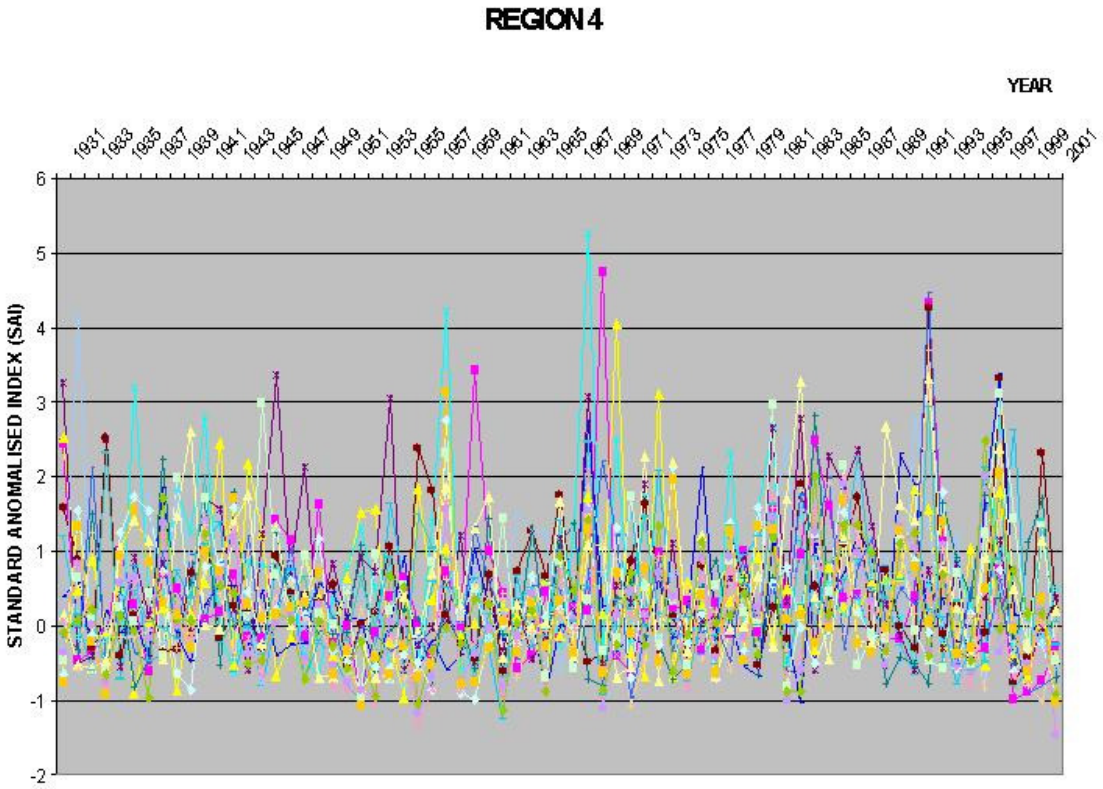

Fig. 3.11. Standard Anomalised Index (SAI) for the annual precipitation of all the stations of the resulting Region 4 after the Principal Component Analysis (PCA, see section 4.1).

In the process of calculation of the regional PAIs or SAIs, similarities include the possibility that the indices of the regions can generally avoid local effects. They share the same order of magnitude, are also designed to smooth sudden jumps in the series, and can identify the quasi-periodicity or modulation effect of large-atmospheric controls as can be fully observed in the very wet years of the late 1950s or the prolonged droughts of the 1990s. Among several differences, regional indices can preserve particularities inherent only to some regions like those along both coasts that are strongly impacted by hurricanes (as is the case of the north-eastern region hit by Hurricane Gilbert on 1988) or some areas by ENSO (like the north-western part of Mexico during the strong El Niño of 1982-83). Fig. 3.12 shows the calculated SAIs for the eleven regions extracted (of total annual precipitation) using Principal Component Analysis (see section 4.2).

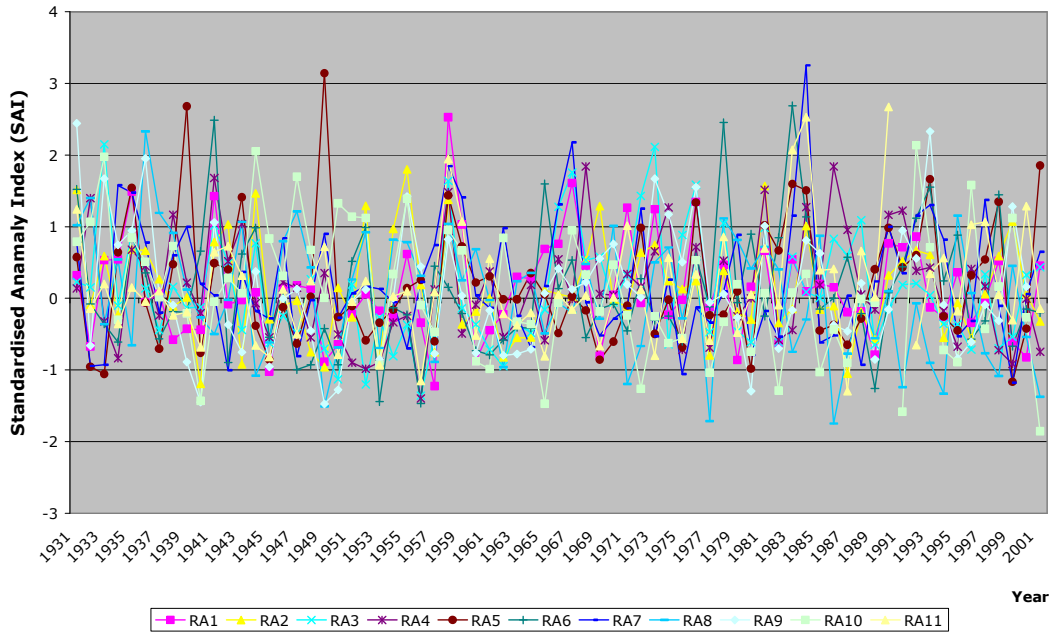

Fig. 3.12. Standard Anomalised Index (SAI) for the different regions (with total annual precipitation) after the Principal Component Analysis (PCA, see table 4.1).

Unfortunately, the detection of these inconsistencies for temperature using reference time-series was not feasible, as no clear results, i.e., coherent regions, were obtained with PCA (see section 4.3). So the construction of the weighted regional average was impossible. Another reason that impeded the comparisons among the stations for temperature was the sparsity of the network; neighbouring stations were not available for comparison of the dubious time-series. Finally, few homogeneous neighbouring temperature stations were ready to be used in this process.

Other indirect methods have been explored to identify undocumented inhomogeneities. If, it is not possible to build a reference time series, for reasons such as the sparsity of the network, there are alternative methods to identify the sorts of inhomegeneities within the data. In order to identify a sudden jump in a time series, common statistical methods like t-test are able to deal with the problem very well. If gradual artificial trends are involved like those caused by urbanisation, then regression analysis can perform better. For this study, the R-based program called RHtest was used to identify breakpoints. The approach of the program is the one outlined in Wang (2003). The objective of the two-phase regression model is to find a sudden changepoint (c) in the time-series. This undocumented breakpoint is found when:

$$F_{max} = \max_{1 \le c \le n} F_c$$

in which the changepoint c maximises F_c. For multiple changepoints c $\in$ {2,..., n-1} the F_c is computed as:

$$F_c = \frac{(SSE_{red} - SSE_{Full})}{SSE_{Full}/(n-3)}$$

under the null hypothesis of no changepoints and Gaussian errors ϵ_t, SSE_{Full} (the "full model" sum of squared errors) and SSE_{Red} (the "reduced model" of squared errors) are

defined as:

$$SSE_{Full} = \sum_{t=1}^{c}(X_t - \hat{\mu}_1 - \hat{\alpha}t)^2 + \sum_{t=c+1}^{n}(X_t - \hat{\mu}_2 - \hat{\alpha}t)^2$$

$$SSE_{Red} = \sum_{t=1}^{n}(X_t - \hat{\mu}_{Red} - \hat{\alpha}_{Red}t)^2$$

For this technique the case of a two-phase regression model with a common trend α ($\alpha = \alpha_1 = \alpha_2$) is considered, so the time-series is defined as:

$$X_t = \begin{cases} \mu_1 + \alpha t + \varepsilon_t, & 1 \le t \le c \\ \mu_2 + \alpha t + \varepsilon_t, & c < t \le n \end{cases}$$

In the context of climatology, extremes are singular events, within the limits of the dataset distributions having special weather conditions associated, that makes them of high interest for climatic studies. In order to assess these weather extremes daily data are essential. Until today there are only a few methods to correct sub-monthly inhomogeneities, Aguilar et al. (2003) give a good account of these techniques, although no recommendations are made to deal with extremes at these scales. Nevertheless, as it has been addressed in this section, several processes have been applied to identify the most obvious inconsistencies in the data, in order to avoid misleading results.

Finally, rapid urban growth is a possible factor for the increasing trend in temperatures across the globe. If we take the definition of urban as those places with a population greater than 50,000 (Easterling et al., 1997), we have that 8 stations for precipitation and 9 for temperature in Mexico fall under this condition. The urban heat island has been explored locally in tropical cities particularly in Mexico City by Jauregui (1995), or at regional and subregional scales by Englehart and Douglas (2003). Several procedures have been suggested by Karl et al. (1988) to correct this urbanisation temperature bias.

But when compared with the global average rise in mean temperatures, heat urban biases are relatively small (Karl et al., 1991). However, with the geographically widespread and accumulating evidence towards warming in temperatures, it is unlikely that urbanisation plays a key role in the upward trend (Karl et al., 1993). Principally because the SST average of the world is warming at a similar rate to the land average (IPCC, 2007). Urbanisation influences cannot be ignored at local scales, and care will be taken when evaluating the results on climate extreme indices for stations within urban areas.

Recent social and economic impacts of extreme events have highlighted the necessity of having more than a global network of average monthly climatic conditions. Extraordinary weather events require by definition long-term, and high-quality daily data. Although there are a few attempts to have a global set of daily data (Alexander et al., 2006; Vose et al., 2005; Easterling et al., 1999), there is a lack of a worldwide dataset that impedes the evaluation of climatic changes during the twentieth century (Karl and Easterling, 1999; Jones et al., 1999). This data deficiency is especially observed in tropical regions across the world (Easterling et al., 1997). Until the goal of a global database of daily data of the most important meteorological variables is reached, a set of widely accepted climatic extreme indices is being used instead (Alexander et al., 2006; Easterling et al., 2000). The development in this research of a set of Mexican climatological stations with spatial and temporal improved resolution permits the application of up-to-date methods to assess the secular behaviour of weather extremes in this country. This evaluation will contribute to a better understanding and comparison of the past climatic conditions, in a region encompassing tropical to subtropical regions within the context of a global changing climate.

3.3.2 PRINCIPAL COMPONENT ANALYSIS (PCA).

No matter what statistics and climatological normals could show us, non-linear behaviour and multi-dimensionality are still intrinsic, and even more important, frequently dominate the climate (Hannachi, 2004). In this context of complexity, how to extract the most important information behind a large set of meteorological stations with time discrete observations, and then make the data simpler to describe, is one of the basic questions within atmospheric sciences, and particularly in climatology. Principal Component Analysis (PCA) is the main technique to reduce the dimensionality.

Principal Component Analysis is a powerful multivariate analysis tool that reduces the high dimensionality of a dataset preserving as much as possible of the original variability of the data. In order to achieve these purposes PCA transforms the original set of observations to a new smaller group of pairwise uncorrelated variables (Principal Components, PCs) capturing the largest parts of the total variance. In that sense, the first member of the group or First PC is able to extract the highest fraction of the data variance, then the second Principal Component can obtain from the remaining variance the second highest part of the variability, and so on (Fig. 4.2).

The first PC ($\boldsymbol{\alpha}_1'\mathbf{x}$) is a linear function of the elements x (for p variables) with the largest maximum variance, $\boldsymbol{\alpha}_1$ is a vector of constants $\alpha_{11}, \alpha_{12}, \ldots, \alpha_{1p}$, and ′ meaning transpose (Joliffe, 2002), so the formula could be expressed as:

$$\boldsymbol{\alpha}_1'\mathbf{x} = \alpha_{11}x_1 + \alpha_{12}x_2 + \ldots + \alpha_{1p}x_p = \sum_{j=1}^{p} \alpha_{1j}x_j$$

In the same manner, k uncorrelated PCs ($\boldsymbol{\alpha}_1'\mathbf{x}, \boldsymbol{\alpha}_2'\mathbf{x}, \ldots, \boldsymbol{\alpha}_k'\mathbf{x}$) with the maximum variances in descending order can be extracted. A relatively small number (m<<p) of PCs containing most of the variance of the data is generally the result.

How are these PCs developed? Let Σ be the covariance (or correlation) matrix of the vector of random variables (or S for the variance of a sample), for each k=1, 2, …, p. The

k^{th} PC is defined by $z_k = \boldsymbol{\alpha}_k' \mathbf{x}$ in which $\boldsymbol{\alpha}_k$ is an eigenvector of Σ that corresponds to the k^{th} largest eigenvalue λ_k. If $\boldsymbol{\alpha}_k$ (sometimes called loading or coefficient) is conveniently chosen having unit length ($\boldsymbol{\alpha}_k' \boldsymbol{\alpha}_k = 1$, or normalisation constraint), then var $(z_k) = \lambda_k$ is the variance of z_k. The searching of the largest eigenvalue that maximises the variance of each k^{th} PC ($\boldsymbol{\alpha}_k' \mathbf{x}$) could then be expressed in general with the formula:

$$\text{Var}[\boldsymbol{\alpha}_k' \mathbf{x}] = \lambda_k \qquad \text{for } k=1,2,\ldots p.$$

In the early developments of PCA, unrotated techniques were the only option possible; this condition has gradually changed to the current wide spectrum of orthogonal and oblique rotated solutions which today allow better results to be produced. Unrotated solution techniques, as pointed by Richman (1986) are only suitable for application to those cases when weak simple structures are present and the PCs extracted have both positive and negative correlations throughout all the field of study. For this reason, although explored, unrotated techniques were explicitly disregarded in the present research as being useful for the final interpretations.

The resulting orthogonal PCs often allow easier interpretation than the original variables by reducing their dimensionality but conserving the highest possible variance, and therefore their most important characteristics. Indeed, simple structure is one of the most important characteristics of PCA. Its objective is to decrease the dimensions (p) of the original matrix in such a way than a linear composite of the m PCs found permits a concise scientific description of every variable (Richman, 1986).

It is precisely targeting simplicity in the physical interpretation that a technique for rotating PCs is used. Orthogonal solutions were first developed to overcome most of the unrotated techniques limitations, in particular VARIMAX has been extensively used in climatological studies; the special characteristic for orthogonal solutions in which each axis has to be normal to the rest has been frequently pointed out as artificial. In (rotated) orthogonal solutions like VARIMAX, QUARTIMAX and EQUAMAX the axes are

selected in such a manner that maximum variation along each axis is found, and also another condition is that any axis must be perpendicular to the others. Therefore, all these rotation methods try to define "important" components as those with the maximum absolute loadings, and are separated from the lowest ones. Loadings with moderate values (not easy for interpretation) are explicitly avoided.

Orthogonality is sometimes considered as a non-natural approach constraining the solution. Ignoring the orthogonal condition led to a new generation of techniques in which the restriction of perpendicularity was not present. For this reason, oblique (non-orthogonal) rotated solutions represented an alternative answer to unrotated and orthogonal solutions in PCA. Oblique methods like OBLIMIN or PROMAX try to define clusters and associate them precisely to only one component. This characteristic is frequently linked to the process of clarifying the interpretation when compared with orthogonal rotated solutions. In atmospheric sciences, oblique rotations are sometimes preferred to orthogonal solutions for their advantages in the interpretation of the results (Englehart and Douglas, 2002). DIRECT OBLIMIN has been frequently used amongst oblique rotations. Nevertheless, PROMAX permits clearer results in meteorology when a network with a large number of stations and high grade of complexity are found. So, one orthogonal (VARIMAX) and one oblique solution (PROMAX with kappa=2) were selected as suitable options to explore the complex climatic variability conditions of México.

It is known within PCA, and to be more specific in the simple structure rotation theory, that S-mode helps in regionalisation purposes. S-mode is only one of six different matrix configurations, in which the stations are the columns versus time that is the rows in the array.

In order to cope with contrasting climatic conditions in México: wet regimes in some south-eastern areas (total annual precipitation ≈ 4000 mm) and desert conditions in some regions of the north (total annual precipitation is sometimes less than 300 mm), the correlation instead of the covariance matrix has been used. Even, when we have variables

with the same units (mm) as for precipitation, large variance differences would dominate the low-order PCs; so the correlation matrices are preferred to covariance matrices for the PCA. Another reason to prefer correlation matrices is that covariance matrices are often chosen because of their easier interpretation for statistical inference, but given that the purpose of this regionalisation is purely descriptive as a preparation for further analyses, that advantage is not a factor for this study.

As this research has both an aim of regionalization of México but in contrasting climatic conditions, an obvious question arises: How many regions are sufficient to precisely describe Mexican climate? This discussion leads to the determination of the number of components to be retained.

Several studies have assessed the performance of single methods, or contrast the competence of a number of different techniques, but there is no consensus about the best method for determing the most significant number of principal components (Peres-Neto et al., 2005; Al-Kandari et al., 2005). Because of the size and complexities of the datasets, a PCA graphical tool called the Scree Test is used in this thesis. The component numbers are the abscissa in the plot and their corresponding eigenvalues the ordinates. The plot is seen as a mountain in which the slope is formed by the "true number" of factors containing most of the variance, and the foot by the random components. Therefore, the foot of the mountain or scree straightens closely matching a line at the end of the plot. The aim is to find the last evident break before the variance between components becomes negligible (Cattell, 1966). The low-order PCs before this point of inflexion are then considered as the most relevant and meaningful for the study.

The determination of the number of PCs and therefore of climatic regions in Mexico has also required a careful classification, i.e., to assign each one of the stations to only one of the resulting regions. To comply with this requirement a strict rule was set of only accepting absolute loadings greater than 0.4. (White et al., 1991). So, according to this, the largest value in the loadings (or primary pattern) matrix clearly defines its corresponding component and consequently the region to which the station belongs. With

the same classification purpose in mind, the 'eigenvalue one' criterion was applied (Mather, 1976), i.e. only eigenvalues greater than 1.0 were considered for the extraction. The reason behind this is that, when is normalised each variable has a intrinsic variance equal to unity, every eigenvalue less than one should then be discriminated, and not worthy to be considered in the analysis. Finally, recalling that the missing values total was restricted to less than ten per cent for every station in the network and replaced with the long-term mean, the election of pairwise or listwise deletion has no influence on the final results.

All methods of rotation overcome the disadvantages of unrotated solutions. Among the drawbacks of these non-rotated solutions we can list the following:

Geographically dependent results. It is a well known phenomenon that sometimes topography has a strong influence on the delineation of contours. For some meteorological variables like precipitation, altitude exerts a linear response. This characteristic is frequently observed in the loading patterns of the PCs across an area using unrotated solutions.

No stability. In order to prove the consistency of the results, sometimes the data are divided into subdomains of the original variables. For example, a group of stations could be classified geographically taking into account their coordinates, in which a latitudinal or longitudinal line could represent a boundary. Regardless of any subdivisions, PCA patterns should be in accordance to the results when the whole domain is considered (Comrie and Glenn, 1998).

Closed Eigenvalues. When extracted eigenvalues are so closely spaced, most of the time, unrotated methods are unable to precisely separate PCs. Even worse, sometimes this problem becomes so difficult that eigenvalues could be mixed among them.

Artificial Results. Unrotated solutions could produce patterns that don't have a physical basis, i.e. *Buell patterns*. This is particularly true when from a previous insight to the data

a well known configuration is expected. Richman and Lamb (1985) shows an example in which PCs two to 10 are not completely in accordance with the observed patterns before the analysis.

Regardless of orthogonal or oblique solution ease of interpretability classifies the degrees of simple structure as strong, moderate or weak. The amount of simple structure is best explored through pairwise plots of the resulting coefficients. In theory a strong simple structure unveils a hidden order in the data.

Among the applications of PCA that can be mentioned are:

- Identification of groups of variables that vary coherently in a dataset.
- Reduction of the original dimension of the dataset, resulting in a smaller and independent set.
- PCA is able to eliminate redundancy in the original variables.
- It could be considered as a preliminary step of cluster analysis. PCA clarifies the clustering by eliminating the eigenvectors with the lowest-valued eigenvalues.
- PCA is an alternative to the construction of a set of linear functions of the original variables; as opposed to a process based solely on *a priori* judgements.
- The possibility to spot a new group of individuals varying coherently, that other method cannot successfully achieve.
- Principal Component Analysis could help to easily identify “outliers”, i.e. individuals that are behaving clearly different to the other variables in a group.

- PCA could be considered as a preliminary tool to multiple regression analysis. The resulting components could be used as an approach of a set of regressor variables.

3.3.3. REGIONAL AVERAGES.

In performing PCA across the network, the objective was to find different groups of stations that are varying coherently across time. The amplitude of a particular PC will incorporate all the stations. Here we want to calculate a regional average, based on PCA, but just with the stations in a region. When calculating regional averages we want the dominant time-series features of the sites to remain. Also, we are trying to avoid local factors like topography. We use the approach suggested by Jones and Hulme (1996) to compute regional averages. Among the different indices proposed, the Standardised Anomaly Index (SAI) has been selected, to be consistent with the extracted ENSO indices (See section 3.2.3). Standardised anomalies are first calculated for each station as:

$$\Delta\hat{P}_{ik} = \frac{P_{ik} - \overline{P}i}{\sigma_i}$$

where $\Delta\hat{P}_{ik}$ is the standardised anomaly for year k at station i from a group of N stations, in accordance with the resulting regions of PCA (section 4.3.1). $\overline{P}i$ and σ_i are mean and standard deviation of the station i respectively (based on a common period which is the total length of the time-series).

The weighted regional SAI is computed as follows:

$$\left\langle \Delta\hat{P}_k \right\rangle = \sum_{i=1}^{N} w_i \Delta\hat{P}_{ik}$$

In this equation $\left\langle \Delta\hat{P}_k \right\rangle$ is the regional standardised anomaly for year (month) k. The

weights are obtained as the long-term ratio of the local ($\overline{P_i}$) to regional $\langle \overline{P} \rangle$ means:

$$w_i = \frac{\overline{P_i}}{\left\langle \overline{P} \right\rangle}$$

where the long-term mean (of the total N years) for a single station (i) is defined as:

$$\overline{P_i} = \frac{1}{N} \sum_{k=1}^{N} P_k$$

and the mean (of all the N stations) of a region as:

$$\left\langle \overline{P} \right\rangle = \frac{1}{N} \sum_{i=1}^{N} \overline{P_i}$$

In order to test the stability of the regional values a different weight was utilised

$$w_{ik} = \frac{P_{ik}}{P_{k(total)}}$$

in which

$$P_{k(total)} = \sum_{i=1}^{N} P_{ik}$$

is the sum of the precipitations of all the stations in a region, for a given year (month) k.

The two different results were compared year by year, finding very similar results. Therefore, the first approach was used in the subsequent analyses.

It is important to notice here that, for the regional averages the same seasonal definitions

established in section 2.2.1 were applied here, i.e. total annual precipitation, wet (May-Oct) and dry (Nov-Apr) seasons. These time series would also be used in our ENSO-related research. But monthly time-series are also available, especially for lag correlation analyses.

3.3.4. EXTREME WEATHER ANALYSIS.

During the 2005 hurricane season in Mexico, tropical cyclone Stan struck the south-eastern part of Chiapas State, and later Hurricane Wilma hit the Mexican Atlantic coast around the tourist city of Cancún. There was a perception with the public, influenced by the media that extraordinary events were occurring. The question for the scientific community, however, is: Are the intensity and frequency of extreme events increasing and if so is this related to anthropogenic influences on the climate system? To scientifically evaluate these sorts of climatic questions is very difficult. What is important first is to be sure that the climatic series are of good quality.

Average climatic conditions and their variability have been extensively explored recently; this is especially true in the case of anthropogenic climate change (Easterling et al., 1999). Mean conditions of the climate do not give a complete picture; they just tell us part of the history of the changing regional climates of the world. Other aspects of these meteorological parameters need to be explored if we are to understand the underlying processes of the climate system. Amongst the important characteristics that can be assessed are the weather extremes, because they are a good measure of the rapid change of climate, and also they generally have a great impact on society in general. Greater trends in extremes compared to the mean temperature trends were found in an analysis applied to long time series from Europe and China (Yan et al., 2002). Unfortunately, studies on climate extremes using daily data are still relatively scarce, but improvements and extension into unanalysed areas are gradually being made.

Time series of monthly data are sufficient to explain changes in the climatological normals and their variability on similar or longer time scales (Jones et al., 1999). These

databases are satisfactory for documenting the climatic history of the recent warming at hemispheric and global scales. But, as recent years have shown in different regions of the world, there appear to be more extremes occurring (Alexander et al., 2006). Nevertheless, unequivocal proofs of these fluctuations in weather extremes are necessary to support the accumulating evidence.

Even in developed countries with potential for large climatic databases like the USA and Canada, there is still a deficiency of homogeneous climatological time-series to evaluate the recent secular behaviour of the extremes in this region (Easterling et al., 1999). Ironically the analysis of extremes can also help to highlight that monthly-based homogeneity analyses are inadequate (Yan et al., 2002). Fewer studies exist dealing with extreme weather in developing countries. This situation is being rectified and a recent study by Alexander et al. (2006) analyses extensive datasets. This work stems from developed datasets in specific regions: Africa (New et al., 2006), South America (Haylock et al., 2006), South East Asia and the South Pacific (Manton et al., 2001), Central America and northern South America (Aguilar et al., 2005), and Central and South Asia (Klein Tank et al., 2006).

As a country, Mexico is not not well represented or definitively absent in the climatic extreme analyses. The very few assessments of the changing climate in the country were made as part of a global evaluation or the North American region (e.g. Alexander et al., 2006; Vose et al., 2005; Easterling et al., 1999). When dealing with climatological monthly data as well as for evaluating extremes, part of the problem is the geographical sparsity of the set of stations with suitable long-term time-series of daily data. In Mexico, the Servicio Meteorológico Nacional (Mexican Meteorological Service) maintain a network that has remained unchanged assuring relatively long records with minor variations (Easterling et al., 1999); but these data have only generally been kept in manuscript form. A key factor that contributed to the development in this field of science was the needs of the Intergovernmental Panel on Climate Change (IPCC) to monitor firstly the mean climatic state of the world and secondly to evaluate the trends in extreme weather at national, regional and global scales.

There still is not a single way to define an extreme in climate. Up to today climatologists continue dealing with the problem of isolating changes due to sampling, station location, and indisputable changes in extremes (Frich et al., 2002). For these reasons, several attempts have been made to build a scientific consensus in the analysis of weather extremes. Unfortunately, it is very frequent that these extraordinary events also have socio-economic impacts, deeply affecting the way they are perceived. Therefore, not only scientific but sometimes socio-economic considerations have played an important role in the process of defining climatic extremes.

The lack of climate extremes definitions has gradually been overcome. For studying weather extremes across the USA, Karl et al. (1996) defined an index which was termed the Climate Extremes Index based not only on the exceedence of thresholds for meteorological variables (such as temperature or precipitation), but also the percentage of the country affected by severe drought. Following on from this, Beniston and Stephenson (2004) developed a set of characteristics (not mutually exclusive) that can measure extremes. These are listed in there study as follows:

- how rare they are, which involves notions of frequency of occurrence;
- how intense they are, which involves notions of threshold exceedence; and
- the impacts they exert on environmental or economic sectors in terms of costs or damages.

They also point out the way in which weather extremes have been defined in the Third Assessment Report of the IPCC (2001) in terms of frequency, as several meteorological variables (precipitation, wind velocity or temperature) exceed the 10% or 90% quantiles of their distribution. But it really was when the IPCC 2nd Assessment report identified the deficiency of studies on trends of daily data and climate extremes that these efforts significantly increased in scale: locally, regionally and globally (Alexander et al., 2006; New et al., 2006; Haylock et al., 2006). Since then a group of climatologists, The Expert Team (ET) on Climate Change Detection and Indices (ETCCDI) have been conducting an international effort to develop, calculate and analyse a set of indices to standardise and compare the results globally (http://cccma.seos.uvic.ca/ETCCDMI/index.shtml). Data

For Precipitation

PRCPTOT	**Wet-day precipitation**	**Annual total precipitation from wet days**	**mm**
SDII	Simple daily intensity index	Average precipitation on wet days	mm/day
CDD	Consecutive dry days	Maximum number of consecutive dry days	days
CWD	Consecutive wet days	Maximum number of consecutive wet days	days
R10mm	Heavy precipitation days	Annual count of days when RR>=10mm	days
R20mm	Very heavy precipitation days	Annual count of days when RR>=20mm	days
R95p	Very day wet precipitation	Annual total precipitation when RR>=95th percentile of 1961-1990	mm
R99p	Extremely wet day precipitation	Annual total precipitation when RR>=99th percentile of 1961-1990	mm
RX1day	Max 1-day precipitation	Annual maximum 1-day precipitation	mm
RX5day	Max 5-day precipitation	Annual maximum 5-day precipitation	mm

For Temperature

FD	**Frost days**	**Annual count when TN(daily minimum)<0˚C**	**days**
SU	Hot days	Annual count when TX(daily maximum)>25˚C	days
ID	Cold days	Annual count when TX(daily maximum)< 0˚C	days
TR20	Warm nights	Annual count when TN(daily minimum)> 20˚C	days
GSL	Growing season length	Annual count between first span of at least 6 days with TG>5˚C after winter and first span after summer of 6 days with TG<5˚C	days
TXx	Hottest day	Monthly highest TX	˚C
TNx	Hottest night	Monthly highest TN	˚C
TXn	Coolest day	Monthly lowest TX	˚C
TNn	Coolest night	Monthly lowest TN	˚C
TN10p	Cool night frequency	Percentage of days when TN<10th percentile of 1961-1990	%
TX10p	Cool day frequency	Percentage of days when TX<10th percentile of 1961-1990	%
TN90p	Hot night frequency	Percentage of days when TN>90th percentile of 1961-1990	%
TX90p	Hot day frequency	Percentage of days when TX>90th percentile of 1961-1990	%
WSDI	Warm spell day index	Annual count of days with at least 6 consecutive days when TX>90th percentile of 1961-1990	days
CSDI	Cold spell day index	Annual count of days with at least 6 consecutive days when TN<10th percentile of 1961-1990	ysda
DTR	Diurnal temperature range	Monthly mean difference between TX and TN	˚C

Table. 3.3. Weather Extreme Indices as defined by the Expert Team (ET) on Climate Detection and Indices (ETCCDI) and tabulated in New et al. (2006).

quality and calculations can be performed using the free statistical package "R" (http://www.r-project.org) through a graphical-interfaced program called "RClimDex". The current core indices - as defined by the ET and tabulated in New et al. (2006) - are:

REFINING THE DATA SELECTION FOR EXTREME ANALYSIS

Although the selection of stations nearly replicates the process of the Data Extraction (see section 3.2.); a few additional characteristics needed to be introduced in order to comply with the slightly more particular conditions necessary for the analysis of weather extremes. As mentioned, meteorological daily records are practically indispensable in the analysis of extremes. *Originally, daily temporal resolution was targeted for the data extraction*. However, during the process of reviewing and choosing the suitable stations to be analysed many of them were incomplete with some missing data. These data were filled with their corresponding monthly averages of the same stations whenever it was available (see section 3.3.2). This means that only a relatively small number of time-series are free of unfilled data.

Daily data with low percentages of unfilled data were preferred when selecting the stations to calculate the extreme indices. Given that good spatial coverage was obtained for the Principal Component Analysis (PCA) (section 4.1) for the network of monthly precipitation, rainfall was used as the reference database for the determination of both: the best daily records of temperature and precipitation. In order to compare the extreme analysis with the PCA results, at least one station was desirable to be selected per (precipitation) region. A contrasting assessment could then be made between regional and local scales. The main objective is to obtain for daily data the same database as that set of monthly rainfall data used in the analysis of PC. A comparison will then be possible between the regional time series –constructed from the results of PCA- and the single station data, and hopefully find inconsistencies or differences between their climatic patterns. The resulting set of stations for both meteorological variables is listed in Table 3.2.

	station name		longitude° W	latitude° N	precip	temp	altitude*	pop+
1	PABELLON DE ARTEAGA	AGUASCALIENTES	-102.33	22.18		X	1920	34.296
2	PRESA RODRIGUEZ	BAJA CALIFORNIA	-116.9	32.45	X	X	100	1210.82
3	COMONDú	BAJA CALIFORNIA SUR	-111.85	26.08		X	260	63.864
4	EL PASO DE IRITU	BAJA CALIFORNIA SUR	-111.12	24.77		X	140	196.907
5	LA PURíSIMA	BAJA CALIFORNIA SUR	-112.08	26.18		X	95	11.812
6	SAN BARTOLO	BAJA CALIFORNIA SUR	-109.85	23.73		X	395	
7	SAN JOSE DEL CABO	BAJA CALIFORNIA SUR	-109.67	23.05	X		7	105.469
8	SANTA GERTRUDIS	BAJA CALIFORNIA SUR	-110.1	23.48		X	350	
9	SANTIAGO	BAJA CALIFORNIA SUR	-109.73	23.47		X	125	
10	CHAMPOTON	CAMPECHE	-90.72	19.35	X		2	70.554
11	OJINAGA	CHIHUAHUA	-104.42	29.57	X		841	24.307
12	FCO. I MADERO	DURANGO	-104.30	24.47	X		1960	
13	GUANACEVI	DURANGO	-105.97	25.93	X		2200	10.794
14	EL PALMITO	DURANGO	-104.78	25.52		X	1630	6.011
15	SANTIAGO PAPASQUIARO	DURANGO	-105.42	25.05		X	1740	43.517
16	CELAYA	GUANAJUATO	-100.82	20.53	X		1754	382.958
17	IRAPUATO	GUANAJUATO	-101.35	20.68	X	X	1725	440.134
18	PERICOS	GUANAJUATO	-101.1	20.52		X	1772	226.654
19	SALAMANCA	GUANAJUATO	-101.18	20.57		X	1722	226.654
20	APATZINGAN	MICHOACAN	-102.35	19.08	X		682	117.949
21	CUITZEO DEL PORVENIR	MICHOACAN	-101.15	19.97		X	1831	26.269
22	HUINGO	MICHOACAN	-100.83	19.92		X	1832	48.917
23	CIUDAD HIDALGO	MICHOACAN	-100.57	19.7		X	2000	106.421
24	ZACAPU	MICHOACAN	-101.78	19.82		X	1986	69.7
25	AHUACATLAN	NAYARIT	-104.48	21.05		X	990	15.371
26	LAMPAZOS	NUEVO LEON	-100.52	27.03		X	320	5.305
27	JUCHITAN	OAXACA	-95.03	16.43	X		46	325.295
28	MATIAS ROMERO	OAXACA	-95.03	16.88		X	201	75.095
29	SANTO DOMINGO TEHUANTEPEC	OAXACA	-95.23	16.33		X	95	217.624
30	MATEHUALA	SAN LUIS POTOSI	-100.63	23.65		X	1575	78.187
31	BADIRAGUATO	SINALOA	-107.55	25.37	X	X	230	37.757
32	YECORA	SONORA	-108.95	28.37	X		1500	6.069
33	SAN FERNANDO	TAMAULIPAS	-98.15	24.85	X	X	43	57.412
34	ATZALAN	VERACRUZ	-97.25	19.80	X	X	1842	48.179
35	LAS VIGAS	VERACRUZ	-97.10	19.65	X	X	37	14.161

Table 3.2. Daily data stations for temperature and precipitation for extreme analysis. The period of records for all the stations is from 1941 to 2001. * meters above sea level. + Population in thousands.

Thirty five stations were selected for the extreme analysis: 15 of those time-series have daily precipitation and 26 temperature data. Unfortunately for comparison purposes, only six climatological stations have good enough data for both meteorological variables. The period of the records for the analysis starts in 1941 and ends in 2001. The lengths of records for precipitation have been reduced for this study to begin in 1941 instead of 1931 as for the monthly records. The reason behind this decision is that there should be at least one climatic representative station containing daily data per PCA region (see chapter 4). This is true for all regions except those from region 7 to 11. Climatic regionalisation using PCA had clear results for annual rainfall; that is why, a time-series per PCA resulting region was computed utilising weighted averages, besides selecting one climatic representative station per region. This permits comparison between regional and local scales for rainfall. However, no clear results (no clear PCA regions) were obtained for temperature; this means no PCA regions could be used. For this reason, the 175 station network with monthly precipitation (see section 4.2.1.) was then considered as a reference for the extraction of the largest number of temperature stations. Despite the limitations, only some north and south-eastern areas of the country were not covered for the extreme analysis. The spatial coverage of both networks is displayed in figure 3.6 a) for precipitation, and 3.6 b) for temperature.

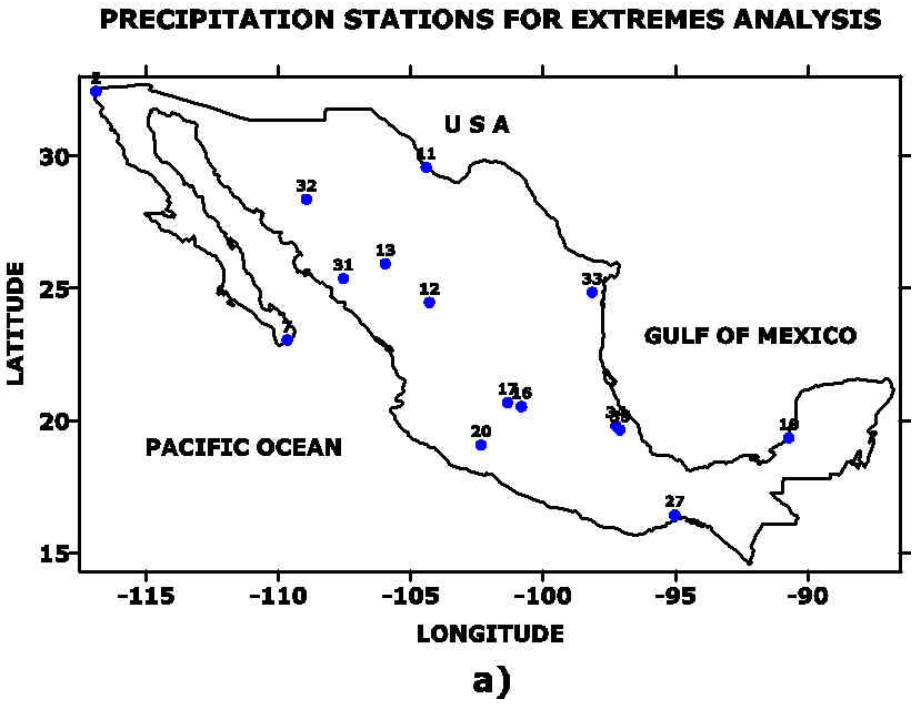

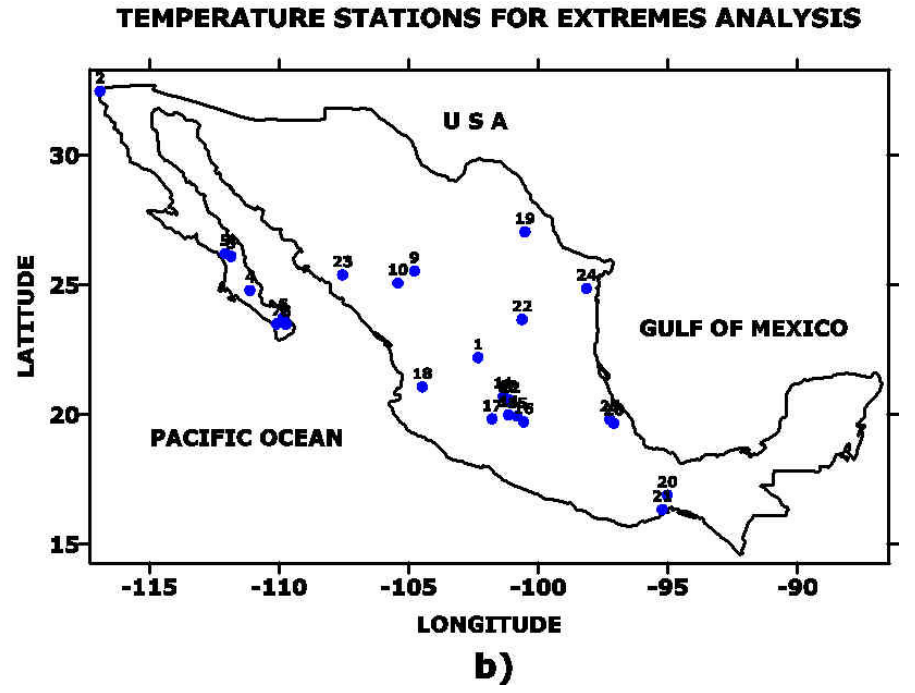

Fig 3.13. Network of a) precipitation and b) temperature stations with daily data for the analysis of extremes (in accordance with table 3.2). The period of the records is from 1941 to 2001.

Three main factors dominated the selection process of the time-series for the extreme analysis: daily data, the length of the records and the completeness (low numbers of missing values). However additional characteristics considered were the possible influence on extremes from: altitude, homogeneity and urbanisation. As discussed in section 4.2, even though the altitude effect is explicitly avoided (using the ratio of the precipitation of each station to its long-term mean) for the PCA on precipitation, high elevation could still exert its force in the atmospheric phenomena. It is interesting to note that 6 rainfall and 10 temperature stations exceed the 1000 m.a.s.l. threshold.

3.3.5 CORRELATION ANALYSES.

Non-parametric Correlations.

Frequently, the task of scientists is to establish relationships between two or more variables. A correlation measures the linear relationship between variables (Field, 2005). The most widely used method (for the complexity of their calculations, non-parametric were more complicated than linear correlations, it is not until recently that computers have overcome with this limitation) to evaluate linear correlations is the Pearson product-moment correlation coefficient. Although a linear correlation coefficient can often give an approximate idea of the strength of the relation between the variables under study, it has a limited resistance and robustness, and also lacks reliability in the determination of the level of significance (Haylock, 2005). Rank (or Non-parametric) correlation coefficients can overcome these limitations; normally distributed data is also not a condition for these techniques.

In contrast to the linear correlation, a non-parametric correlation coefficient measures association, i.e. a monotonic relationship between variables. Very well known measures of association are the Spearman rank-order and Kendall's tau correlation coefficients. Because Kendall's tau deals better (than Spearman's) with small datasets and a large number of tied ranks (Haylock, 2005), this is the non-parametric correlation coefficient that will be used to test the strength of the relationships and level of significance between two variables in this thesis.

Kendall's tau-b (τ) is a non-parametric correlation that measures the association of the number of concordant and discordant pairs of observations. A pair of values is said to be concordant if the vary together, and discordant if the vary differently. The coefficient ranges between -1 (ranks increasing separately) and +1 (ranks increasing together). The formula for Kendall's tau-b is:

$$\tau = \frac{\sum_{i<j} \operatorname{sgn}(x_i - x_j)\operatorname{sgn}(y_i - y_j)}{\sqrt{(T_0 - T_1)(T_0 - T_2)}}$$

where

$$T_0 = \frac{n(n-1)}{2}$$

$$T_1 = \sum \frac{t_i(t_i - 1)}{2}$$

$$T_2 = \sum \frac{u_i(u_i - 1)}{2}$$

t_i is the number of tied x values in the i_{th} group of tied x values, u_i is the number of tied y values in the j_{th} group of tied y values, n is the number of observations and sgn(z) is defined as:

$$\operatorname{sgn}(z) = \begin{cases} 1 \, if \; z > 0 \\ 0 \, if \; z = 0 \\ -1 \, if \; z < 0 \end{cases}$$

The main advantages of Kendall's tau-b are that the distribution has slightly better statistical properties and also being defined in terms of probability of concordant and discordant pairs of observation, this non-parametric correlation coefficient leads to a direct interpretation of the results (Chrichton, 2001).

Lag Correlation.

Responses in meteorological parameters (e.g. rainfall) to changes in large-scale phenomena are not immediate. It sometimes takes a time period the scale of months to seasons for an ocean-atmospheric process, like ENSO (El Niño Southern Oscillation), to be fully developed. Then, for its scientific understanding, it is crucial to address these delayed modulations when evaluating these atmospheric relationships.

The Cross-Correlation function (or lag cross-correlation) is a suitable technique to measure the time shifts between the continuum and lag variations (Chatfield, 1991). Its main purpose is to find the lag that maximises the coherence (linear correlation) between two time series. When this tool is only applied to the same variable is called AutoCorrelation Function. Lag Cross-Correlations must be compiled for all lags (positive or negative), in such a way that a significant maximum correlation is found for a specific time shift (τ_k). The formula that explains these relations between the variables is:

$$CCF(\tau_k) = \frac{(1/N)\sum_{i=1}^{N-k}(x_i - \bar{x})(y_{i+k} - \bar{y})}{\sqrt{(1/N)\sum_{i=1}^{N}(x_i - \bar{x})^2}\sqrt{(1/N)\sum_{i=1}^{N}(y_i - \bar{y})^2}}$$

where the lag τ_k is the size of the time shift: $\tau_k = k\Delta t$, k=0,1,…,N-1 and $\bar{x}$ y $\bar{y}$ are the means of y_i and x_i.

This definition implicitly assumes that both time-series are stationary in their means and variances in a sample of N pairs of values. A direct dependency expressed in the linear correlation between the variables is also expected; nevertheless, this relationship could be substituted by a non-parametric correlation (e.g. Spearman's rho). Although CCF is probably not the best estimator (Welsh, 1999), it is mainly utilised because of its efficiency and consistency.

CCF has among other limitations, the following:

- It is defined in terms of linear dependency. This restriction is really artificial; a non-linear approach could lead to better results.
- Because of its lack of robustness, non-parametric tests can be more useful than the linear correlation technique used in the formula.

3.4. CONCLUSIONS.

Studies on climate change using daily data are scarce in developing countries. The research in this area needs reliable information, especially long-term time-series. In Mexico there have been several efforts to develop a national digital database of climatological data. Unfortunately, those databases still lack sufficient geographical coverage and analysis of data quality. Therefore, in order to contribute to the understanding of the climatic patterns of Mexico within the context of global warming, it was necessary to construct a national high-quality database of rainfall and temperature at monthly and daily time-scales.

A network of 175 rainfall and 52 temperature stations with monthly data, with good spatial coverage has been prepared to study climate change patterns in Mexico. The meteorological time-series have been extracted from six different digital sources, and a process of inter-comparison has been applied among them. Monthly data for precipitation has 71 years of information from 1931 to 2001; meanwhile the length of the daily data (rainfall and temperature) series is ten years shorter, spanning 1941 to 2001. The maximum fraction of missing values was restricted to ten per cent. Climatically speaking, in most of the country the precipitation is concentrated during the months of May to October, this period was considered as the wet season, while the interval from November to April was called the dry season. These definitions and the computing of annual figures were also applied to temperature. In addition, basic statistical properties

like: mean, standard deviation, maximum and minimum values were calculated to assure the reliability of the results of the analyses in this research.

Three different ENSO-related indices of this phenomenon have been selected in order to test their relationships with the rainfall and temperature across the country. They are the Southern Oscillation Index (SOI), Niño 3.4 and the Multivariate El Niño index (MEI), all of them are expressed in a standardised form in order to avoid external influences. The decades of 1980s and 1990s have seen a period of increasing intensity and frequency of ENSOs, with accumulating evidence of global warming. Therefore, the extracted ENSO indices are expected to be strongly linked to the rainfall and temperature in Mexico at regional and local scales.

The meteorological variables extracted are expressed at both monthly and daily time scales. These temporal scales have had direct influence in the methods selected and applied for this research. For instance, PCA is able to unveil a hidden order among a set of variables. Climatically speaking, one of the most important properties is that this method can find groups of stations varying coherently. Technically, rotated are more efficient than the unrotated solutions, in separating clusters of stations with similar climatic patterns. Furthermore, in order to avoid the impact of any other external influence like altitude, anomalies were used in the analysis for both temperature and rainfall.

Based on the results of PCA (see chapter 4), different methods to calculate seasonal time-series of weighted regional averages of precipitation were explained. Two versions of weights are considered to estimate the regional series to compare the stability of the results. Standardised anomalies were also described; they smooth sudden fluctuations, while basically preserving the original climatic patterns.

Weather extreme indices are defined using the guidelines of the Expert Team (ET) on Climate Change Detection and Indices (ETCCDI). These indices are going to be calculated using the long-term and high-quality databases of rainfall and temperature

described in section 3.2. The main objective is to increase the understanding of weather extremes in Mexico; as the few studies of climate extremes were part of global or regional assessments.

Kendall's tau was selected as an alternative to the usual Pearson correlation coefficient due to its possibility of dealing with small datasets and a great number of tied ranks. This non-parametric correlation technique has better statistical properties. Because meteorological responses to large-atmospheric controls are sometimes delayed, lag cross correlations try to find the lag that maximises the coherence between two variables. In this thesis lag correlation is a method that is going to be applied to find the optimum relationships between regional precipitation averages or weather extreme indices and El Niño. This technique is preferred for its efficiency and consistent results, but is also sometimes limited to linear correlations so lacking robustness.

CHAPTER 4: REGIONAL MODES OF VARIABILITY.

4.1. INTRODUCTION.

Using the climatological network, the development and construction which is explained in the previous chapter; our objective is now to investigate the spatial coherence in the climatic variations at the station level. The determination of these regional coherencies is just a preliminary step to find the relationships between their climatic fluctuations and a large-scale atmospheric control like El Niño–Southern Oscillation (ENSO) phenomenon. In this context, Principal Component Analysis (PCA) provides two important features that can help to achieve this objective: 1) it is the technique most commonly used for regionalisation and 2) its results can generally be easily interpreted in a physical way. The method was selected, therefore, as a suitable tool to be applied to the digital Mexican climatological databases.

Principal Component Analysis has been used in a wide range of scientific and social areas since its development in the early 1900s. But it was not until the discovery in atmospheric sciences around the 1980s of the advantages of rotated versus unrotated solutions that an increasing number of scientific studies have been undertaken (Richman, 1986; Richman and Lamb, 1985; Tabony, 1981). The previous chapter stated that the main purpose of PCA is to reduce the high dimensionality of the data, conserving the highest possible amount of the original variance in a few components, but lately has moved to deal as well with individual modes of variability such as El Niño Southern Oscillation (ENSO) (e.g., Gershunov, 1998) often referred as to teleconnections (Gershunov and Barnett, 1998). Climatology is one of the fields in which PCA has been applied extensively (Dyer, 1975).

4.2. PRINCIPAL COMPONENT ANALYSIS (PCA) ON PRECIPITATION.

There are only a few studies in which PCA has been applied to the climate of México. Amongst the many meteorological variables, precipitation has been more consistently explored using Principal Components (Comrie and Glenn, 1998; Englehart and Douglas, 2002) than temperature (Englehart and Douglas, 2004). This condition has been slowly changing for both parameters since the release of digital databases in the early 1990s. Still, for rainfall the studies lack the best possible (in terms of completeness and homogeneity) coverage at both the temporal or spatial scale. One of the main thrusts of this research has been to obtain the best network of climatological stations, defining precisely at the same time the wet and dry seasons.

In order to help with improving studies of Mexican climate, it was necessary to comply with two essential characteristics: the use of the largest possible set of stations across the nation and also a careful determination of the dry and wet seasons (see section 2.2.1).

4.2.1 ANNUAL RAINFALL.

Considering the total annual precipitation (mm) in Mexico (Fig. 2.1), a climatic bridge can clearly be seen between wet conditions in the southern part of the country and drier northern conditions. The tropic of Cancer can be roughly considered as the limit of such a transition. In the southern region, tropical climatic conditions prevail all year around, and precipitation is mostly convective in nature during the boreal summer, while in the north convection partly accounts moderately for the total amount of precipitation, while monsoon conditions prevail in the north-western part of the country during July, August and September (Higgins et al., 1997, Douglas et al., 1993). Several factors other than convective activity have an influence on Mexican precipitation, including hurricanes, orography, polar fronts, etc. Despite this, total annual rainfall was also considered as one of the temporal resolutions to be studied using PCA along with the wet and dry seasons (see sections 2.2 and 2.3). When fluctuations in climate are considered in the north-

eastern Pacific, the warm related to the Inter Tropical Convergence Zone (ITCZ) triggers intense convective activity (Magaña et al., 2003).

In order to observe and clarify some the geographical factors that affect the climate of México and also obtain coherently varying regions, a network of 175 stations has been gathered (see section 3.2.1), and the precise definition of annual, wet and dry seasons has been established in section 2.2.1. The PCA methods applied at the annual time-scale are also valid for the wet and dry season time-series.

Replacing monthly missing values with long-term means for every station should not significantly affect the following results. This is why a database of 175 time series of total annual precipitation was used, in which months not reported were filled with their means and expressed as the ratio of the precipitation of each station to its long-term mean (the average for the base period), for purposes of regionalisation when applying PCA.

Mexico lies in a regional climatic transition between tropical and subtropical conditions, therefore, is useful for the identification -among the network of climatological stations- of the differences and/or similarities in the climatic patterns across the country. But here, this question could be expanded: are the changes occurring in only one geographical region or are they of a particular distinctive nature across regions? If the latter is so, we could also ask: are the changes occurring gradually or abruptly? Therefore, the objective is to determine different sets of stations that vary coherently through time. To reach this target PCA was used.

ORTHOGONAL AND OBLIQUE ROTATED SOLUTIONS.

The scree test plot is used to determine the number of components above the noise level. Ranking the components in the X axis against the eigenvalues in the Y axis, the plot has the objective to find the scree in which the contribution of the components to the total variance is nearly negligible (see section 3.3.2). Eigenvalues for components between 10 and 11 in Fig. 4.1 are showing a small decrease, after the 11th component the ratio of variation with the next component becomes almost imperceptible. A nearly flat slope can be observed in the graph, so their contributions are not more important to the communality of the variables. The first 11 components contribute with 58.2% of the total variance. Therefore, there was no reason to consider more modes of variation and 11 is the selected number of components analysed for the annual total precipitation.

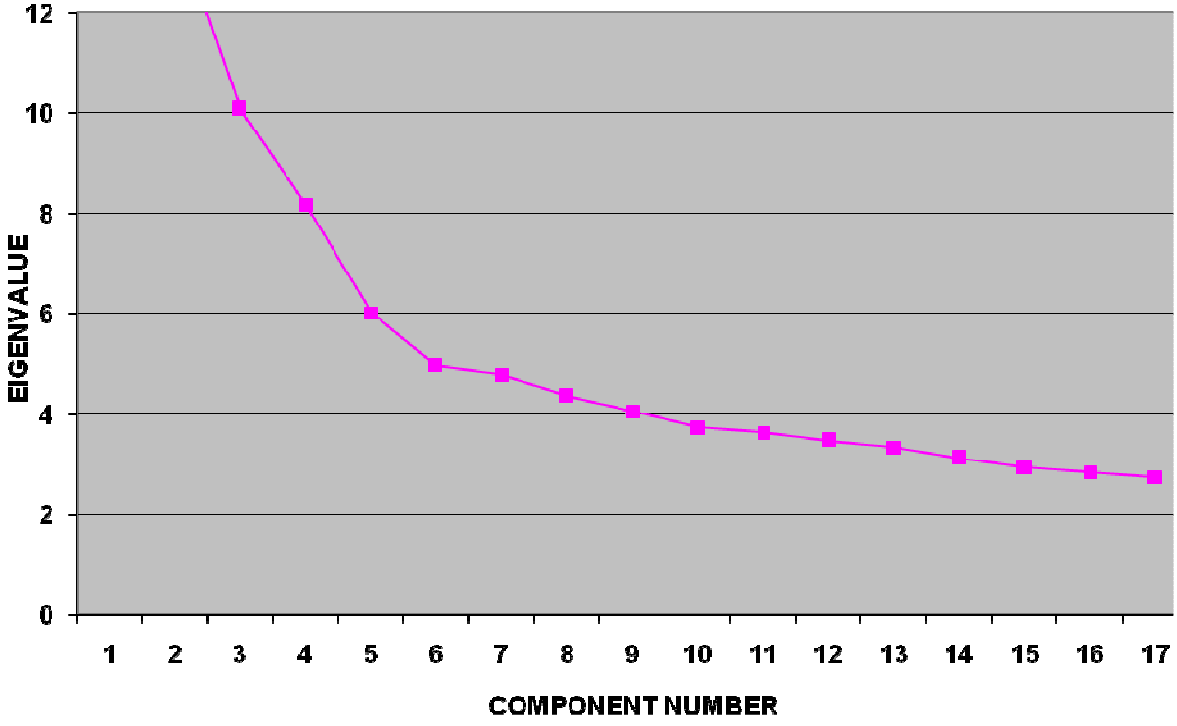

Fig. 4.1. Determination of the number of regions (components) considered in the analysis of the annual precipitation using the cliff analogy (Wuensch, 2005).

It has been suggested that the Scree Test method leads to an overestimation of the components (Horn and Engstrom, 1979), or that the way it distinguishes eigenvalues is somehow arbitrary (Jackson, 1993). Nevertheless, because the purpose of using PCA in this chapter is the identification of a spatial pattern (regionalisation) rather than a data compression, the possibility of an overdetermination of the components must not greatly affect the interpretation of the results.

The mode in which each station is assigned to one corresponding region is explained in section 3.3.2. Briefly, for the extraction of the components only eigenvalues larger than 1.0 are considered, also as missing data were replaced by the long-term mean pairwise or listwise deletion does not affect the final results; and only absolute loading values greater than 0.4 are accepted. The largest loading for each station was then related to one corresponding region. This selection process is repeated for all the precipitation and temperature stations.

When analysing climatological data with PCA for regionalisation purposes, the results from different rotation techniques have subtle differences. For total annual precipitation, the resulting regions show (Fig. 4.2) great consistency between varimax (orthogonal) and promax (oblique) solutions, and also strongly correspond with known Mexican climatic regions (García et al., 1990, García, 1988). Promax (kappa=2) yields clearer results than varimax, as can be observed in the Mexican Monsoon Region (RA11 in table 4.1), where the oblique solution leads to a better grouping of the stations, omitting two stations near the Pacific coast identified by the orthogonal solution. This is also clear in some parts of northeast México (Northeast, RA3 in table 4.1) where again promax has delineated more efficiently the clusters across the region, like in the north-eastern part of the country north of the Tropic of Cancer.

Overall, apart from slight differences, a clear regionalisation of the annual precipitation emerges as a product of the Principal Component Analysis, regardless of the rotation technique applied. The regions developed for annual precipitation totals are listed in table 4.1 and will be discussed according to known features of Mexican climates.

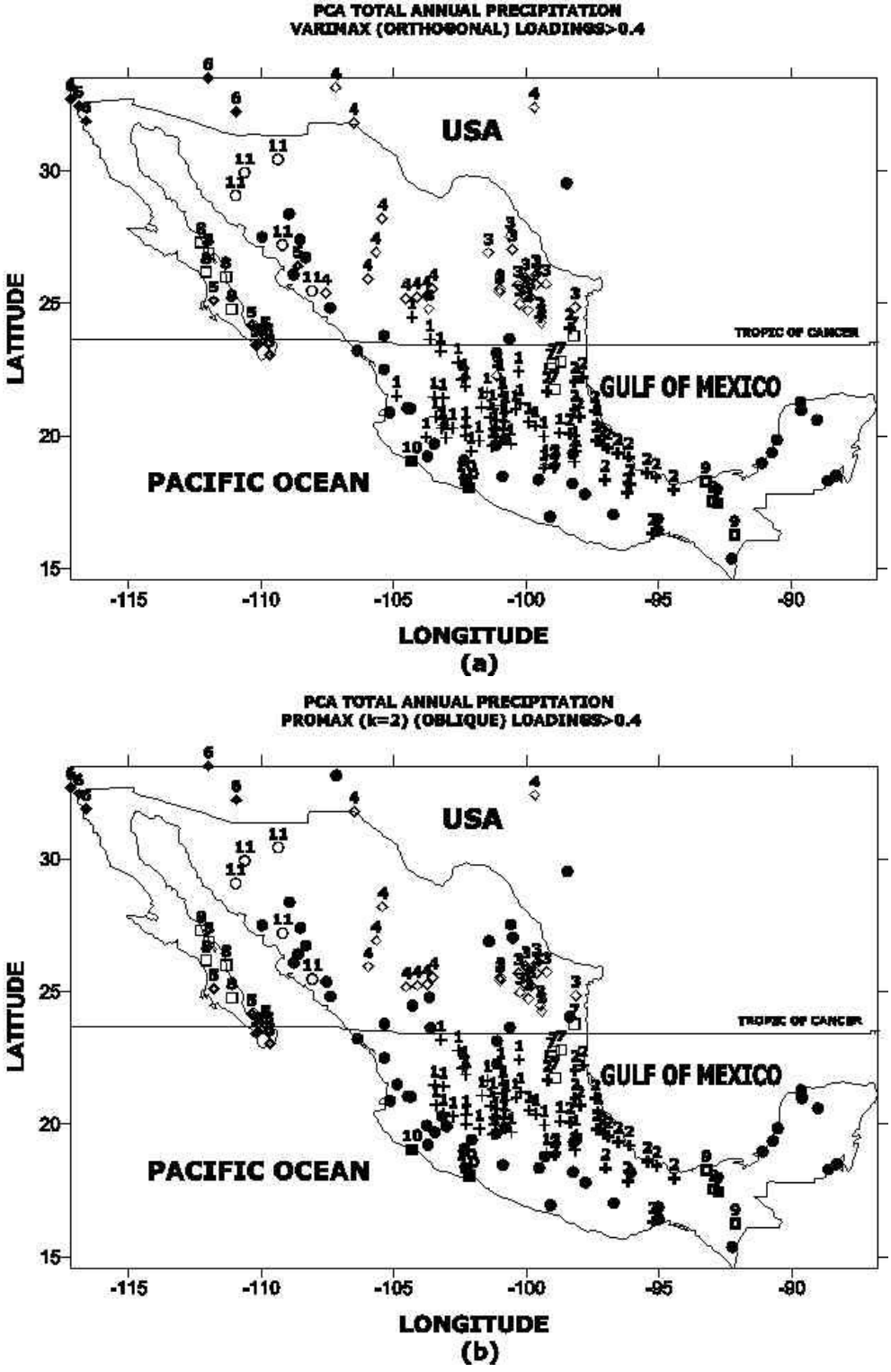

Figure 4.2. Principal component analysis (regionalisation) of a network of 175 stations with annual precipitation totals (1931-2001) using two different solutions: varimax (a) and promax with kappa=2 (b).

Component	Associated region	Climatic characteristics
Region one (RA1)	Central Mexican Highlands	Trends in summer, monsoon from the Pacific, summer rainfall, two temperature maxima
Region two (RA2)	Gulf of Mexico coast	Trends in summer, hurricanes in summer and autumn, polar fronts in winter, two temperature maxima.
Region three (RA3)	Northeast	Trends in summer, polar fronts in winter, hurricanes in summer and autumn, one temperature maximum.
Region four (RA4)	Desertic north, New Mexico and Texas	Little moisture sources, arid regions, one temperature maximum
Region one (RA5)	Humid south Baja California	Summer monsoon, hurricanes y summer and autumn.
Region six (RA6)	North Baja California	Westerlies, winter precipitation, one temperature maximum.
Region seven (RA7)	La Huasteca	Summer precipitation, hurricanes in summer and autumn, polar fronts.
Region eight (RA8)	Desertic south Baja California	Westerlies, one temperature maximum
Region nine (RA9)	Southeast rainforest	InterTropical Convergence Zone (ITCZ), southeastern trades, hurricanes in summer and autumn, two temperature maxima.
Region ten (RA10)	South Pacific coast	InterTropical Convergence Zone (ITCZ), southeastern trades, hurricanes in summer and autumn, low winter precipitation, two temperature maxima.
Region eleven (RA11)	Mexican Monsoon	Summer rainfalll, westerlies, hurricanes in summer and autumn, one temperature maximum.

Table 4.1. Total annual precipitation PCA resulting regions identified according to the known Mexican climatology (García, 1988).

The eleven groups depict a congruent picture of how the stations have been varying coherently across time, and could be clearly differentiated from each other accordingly. Therefore, each group can be identified with one specific climatic region and their main geographic characteristics in terms of precipitation variations (see Table 4.1).

Central Mexican Highlands includes (RA1 in table 4.1) sites like Mexico City -that is one of the capital cities with highest altitude in the world- and its surroundings. High elevations sometimes permit large scale high-altitude atmospheric circulations features to have influence on the local weather, which are often limited by mountain barriers.

The second region (RA2) can be roughly related to the gulf (of México) coast where summer convective precipitation has great influence on annual precipitation totals, but

the winter precipitation is also deeply affected by polar fronts (Cavazos, 1997; Jauregui, 1997).

The northeast part of México is the third region (RA3) of the analysis; this set of stations is a good example of the climatic transition in México from tropical to extratropical conditions: the amount of annual precipitation across the stations shows significant decreases in comparison with the stations south of the tropic of Cancer, for instance RA2.

The dry northern region (RA4) is represented by the stations labelled 4 in fig. 4.2; this part of the country is geographically isolated by two mountain ranges that act as barriers for the moisture sources that facilitate the rainfall processes in other regions. The lack of precipitation could easily be observed as some stations only reach 300 mm per year (see fig. 2.1 in chapter 2).

Again, south of the Baja Californian peninsula, a climatic division can be clearly seen for contrasting climatic conditions (tropical to extra-tropical), the southern tip yields wetter conditions (RA5 in table 4.1) when compared with the low precipitation area of the desertic south Baja California (RA8 in table 4.1). Here it can be clearly seen that the Tropic of Cancer is a geographic limit.

The driest climatic regimes of the country are experienced in the most north-western part of México, north of the Baja Californian peninsula and south Arizona in the USA (RA6); this is the only region of all in which the percentage of November-April totals (dry season) exceeds those of the wet season (May-October). More than fifty per-cent of the annual totals occurs during the low rain period in the other regions. Autumn-winter precipitation has a greater influence than spring-summer rainfall in this area.

RA7 can also be considered as a geographical transition, but this time from drier to wetter climatic conditions. This region has been called La Huasteca (humid areas of Tamaulipas, Veracruz, San Luis Potosí and Hidalgo states) and includes mainly stations of the Pánuco

River Basin characterised by dense vegetation and higher precipitation than their surrounding stations in RA2 and RA3.

México's wettest region (RA9) is located in the southeast of the country; here rainfall totals can be as high as 4000mm per year, but one of the remarkable features is the balance between the seasons with the dry season accounting for around 30-40% of the annual totals (see fig. 2.1; García, 1988); not surprisingly it is here that Mexican tropical rainforest areas can be found.

One of the most geographically concentrated PCA resulting groups is RA10, the Michoacán coasts are represented here. Drier conditions are prevalent in RA10 when they are compared with the stations near the mountain ranges (Sierra Madre Occidental) within the southern fringes of what is called the Mexican Monsoon Region (RA11) along the Nayarit and Sinaloa states (coasts bordering the Pacific Ocean).

The last group (RA11) has recently been studied extensively (see chapter 2); precipitation in the Mexican Monsoon Region is characterized by its concentration during the boreal summer season in the lowlands of western side of the North Pacific mountain range (Sierra Madre Occidental). It is important to point out here that, for total annual precipitation, this region does not extend far north beyond the México-USA border but is restricted to only the Mexican side and therefore has been called The Mexican Monsoon region (Douglas et al., 1993).

As can be seen, regions can be clearly related to specific regional precipitation patterns across the country; it is then presumed that rotated PCA solutions, especially oblique methods have succeed in regionalising the Mexican climatic conditions for annual precipitation totals.

4.2.2 SEASONAL PRECIPITATION.

WET SEASON.

It has been shown in section 2.2.1 that most of the precipitation occurs during what has been termed the wet season (May-Oct), for this reason it is expected that PCA results for total annual precipitation will agree closely to those of the rainy season. Conditions for the Principal Component Analysis differ only in that rainfall totals for wet season are only accumulated from May to October. We begin with PCA defining the number of components for regionalisation. For this purpose, we have applied the scree test plot (see section 3.3.2), we observe a small variation between the eigenvalues of the 11th and 12th components (-0.05); these first 11 components contribute with 57.9% of the total variance (fig. 4.4). A nearly flat slope is seen after this point. Therefore, we will consider 11 modes of variation (regions) to study the spatial pattern of the wet season (May-Oct) precipitation.

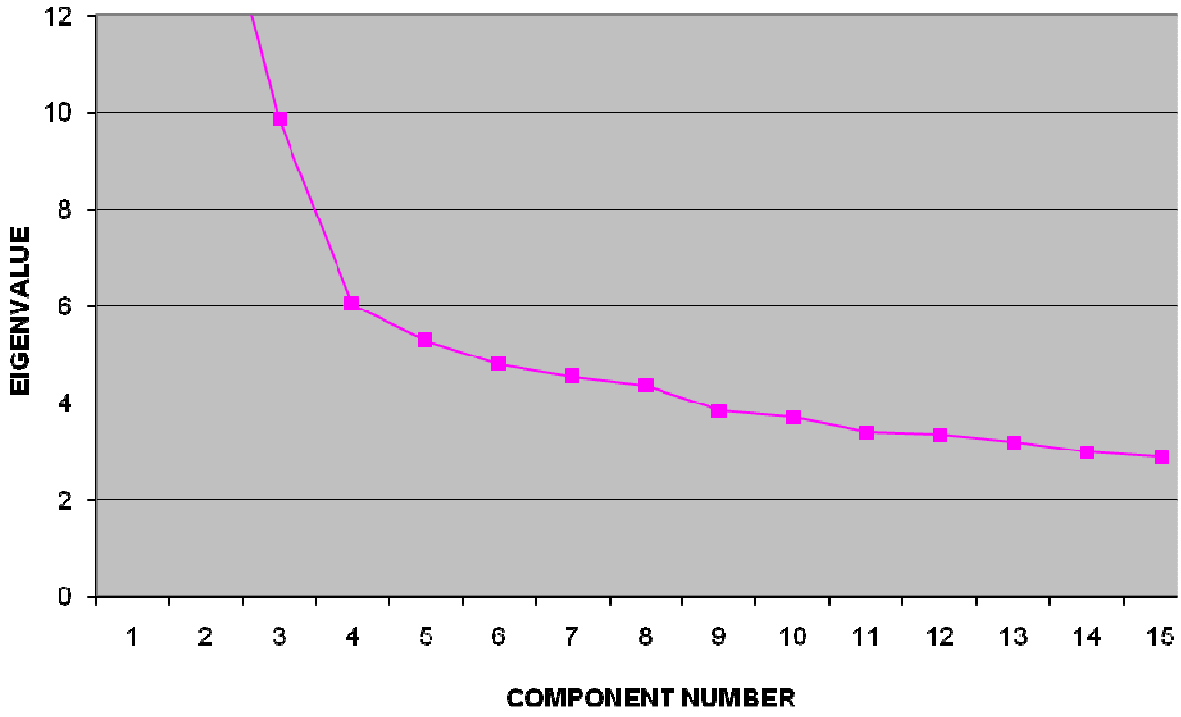

Fig. 4.3. Determination of the number of regions (components) considered in the analysis of the May to October (Wet Season) precipitation using the scree plot technique.

ORTHOGONAL AND OBLIQUE ROTATED SOLUTIONS.

A strong agreement can be observed between wet season and annual precipitation results (see figs 4.2 and 4.4). The distribution is geographically coincident but a bit different in the order of the components. The Mexican Monsoon Region has disappeared with the rainy season analysis. In the same sense, groups not observed when the PCA was applied on the annual precipitation, the Nayarit State region (stations close to the Pacific coast) has emerged here [some studies (Mitchell et al., 2002; Higgins et al., 1997; Douglas et al., 1993) have pointed this region out as the most southern fringe of the Mexican Monsoon Region]. Some stations classified during the PCA with annual rainfall (like the couple appearing in Arizona State RA9, or those in RA11) have not been grouped here.

The strong coincidence found when annual total precipitation and wet season solutions of PCA are compared can also be seen between the orthogonal and oblique rotated results. Nevertheless, as has been noticed for annual rainfall, the promax (k=2) technique is in general more efficient in showing clearer clusters than varimax (see section 3.3.2). The different resulting regions of applying PCA to the wet season are shown in table 4.2. Promax has better delineated RW2, RW3 and RW5 when contrasted with the orthogonal solution. The Gulf of Mexico climatic group (RW2 in table 4.2) in the case of promax (k=2) is less extended geographically to Central Mexico. In terms of clarity of the clusters, the Northeast (RW3) and humid Baja California (RW5) regions share one characteristic: both have one odd station when analysed with the varimax rotation. In the former group the odd station is located in the state of Coahuila [in which according to the García et al. (1990) regionalisation is a climatic transition from arid to semiarid conditions] while in the latter the additional station was placed in the Mexican Monsoon Region instead of the Baja California peninsula as is the case for promax (k=2).

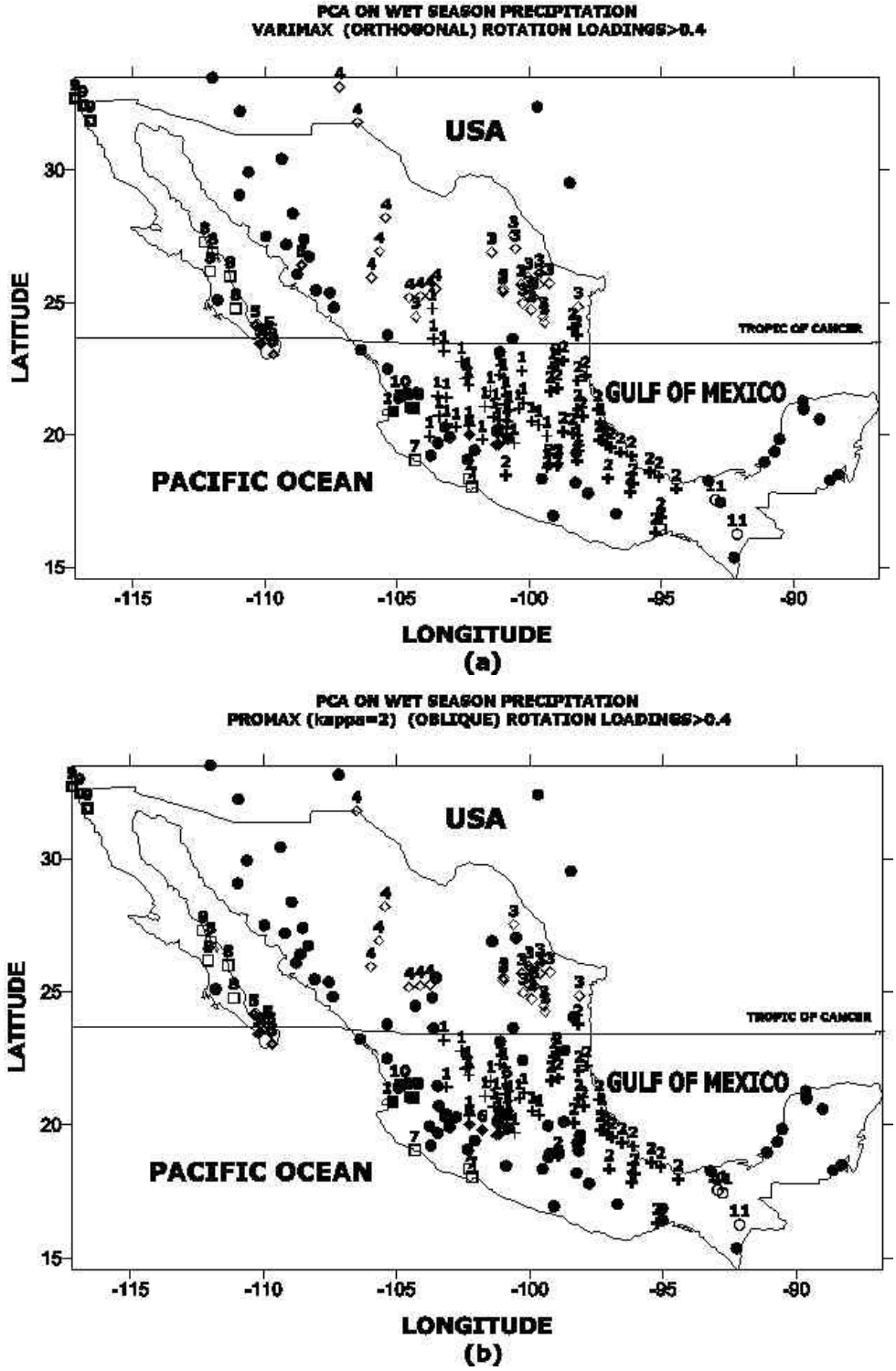

Figure 4.4. Principal component analysis (regionalisation) on a network of 175 stations with wet season (May-Oct) precipitation (1931-2001) using two different solutions: varimax (a) and promax with kappa=2 (b).

RW1 (Central Mexican Highlands, see table 4.2) is smaller and better defined, less geographically extended in the promax solution and concentrated more in central Mexico (probably better avoiding the influence of altitude among the stations). RW2 (Gulf of Mexico coast), RW3 (Northeast) and RW4 (Desertic North, New Mexico and Texas) are basically the same clusters either comparing annual total precipitation versus wet season or the orthogonal against the oblique solutions. Two regions not observed [RW6 (Transverse Neovolcanic Belt) and RW10 (Nayarit state)] when the PCA was applied to the annual total precipitation have produced the same results in the wet season for the varimax and promax solutions; for the oblique solution RW6 is clearer delineated, this cluster could be associated to what is called the transmexican volcanic axis (Eje volcánico Trans-mexicano, Demant and Robin, 1975), the stations in this region are mainly situated in Michoacán State, all of them part of the Transverse neovolcanic belt. Altitudes of these stations easily exceed 1500 metres above sea level (m.a.s.l.) that can be considered as a proof of the influence of altitude on the climate of the region, a variable that it has been frequently disregarded in the studies of the Mexican climatology (see chapter 2). Region ten (RW10) is the most geographically concentrated of the regions, only covering an area of Nayarit State near to the Pacific Coast, the southern tip of the Mexican Monsoon Region in which only one station has an elevation above 1000 m.a.s.l, a topographic factor that is described in section 2.2.2. Finally, region RW11 (Southeast rainforest) can be related to the wettest area of the country, the south-eastern tropical rainforest, and again it is better delineated using promax (k=2) than varimax. Overall, wet season (May-Oct) precipitation clusters extracted with PCA are in accordance with the Mexican climatology (see Table 4.2).

Component	Associated region	Climatic characteristics
Region one (RW1)	Central Mexican Highlands	Trades in summer, monsoon from the Pacific, summer rainfall, two temperature maxima
Region two (RW2)	Gulf of Mexico coast	Trades in summer, hurricanes in summer and autumn, polar fronts in winter, two temperature maxima.
Region three (RW3)	Northeast	Trades in summer, polar fronts in winter, hurricanes in summer and autumn, one temperature maximum.
Region four (RW4)	Desertic north, New Mexico and Texas	Few moisture sources, arid regions, one temperature maximum
Region five (RW5)	Humid south Baja California	Summer monsoon, hurricanes y summer and autumn.
Region six (RW6)	Transverse Neovolcanic Belt	Summer precipitation, Pacific monsoon, high altitude sites, two temperature maxima.
Region seven (RW7)	South Pacific coast	InterTropical Convergence Zone (ITCZ), southeastern trades, hurricanes in summer and autumn, low winter precipitation, two temperature maxima.
Region eight (RW8)	Desertic south Baja California	Westerlies, one temperature maximum
Region nine (RW9)	North Baja California	Westerlies, winter precipitation, one temperature maximum.
Region ten (RW10)	Nayarit state	Summer rainfall, Pacific monsoon, hurricanes in summer and autumn.
Region eleven (RW11)	Southeast rainforest	InterTropical Convergence Zone (ITCZ), southeastern trades, hurricanes in summer and autumn, two temperature maxima.

Table 4.2. Wet season precipitation PCA resulting regions identified according to the known Mexican climatology (García, 1988).

The few former PCA regionalisations in Mexico have mainly been made for the summer season (Englehart and Douglas, 2001; Comrie and Glenn, 1998). The results of the present research, however, are closer to the regionalisation made by Giddins et al. (2005) in terms of the seasonality defined as wet and dry seasons for the May to October and November to April periods. Our resulting regions are also closer to those delineated in García et al. (1990), and also with the clusters proposed by Comrie and Glenn (1998), but unfortunately the latter study does not consider the whole country, as only the northern part of the country was used to define regions based on PCA. Because of the effort dedicated to developing the network, our research can only be compared with the

research of Englehart and Douglas (2002) who use a dataset of long-term time-series of approximately 70 years covering practically the entire country.

The regionalisation performed in this chapter for the annual and the wet season has helped us to determine some key features such as highlighting the importance of altitude, for instance the Transverse Neo-Volcanic Belt (RW6 in table 4.2) during the May to October (wet) season regionalisation. The importance of some large-scale atmospheric controls in some regions of the north of the country, such as the Mexican Monsoon Region (Douglas et al., 1993), that only appears in the annual season and not during the wet season that could be the effect of winter precipitation in the region. In the same north-western region but in the Baja Californian peninsula, three very well defined regions (from the southern tip to the northern border) are extracted that are not delineated because of the lack of sufficient stations in this area for the other studies (Englehart and Douglas, 2004; Englehart and Douglas, 2002); and probably because of the hurricane influence no PCA region is found in the Yucatán peninsula for the annual and wet seasons. So far, Promax (k=2) has proved to be the most suitable technique to extract the best results across Mexico using PCA.

DRY SEASON.

As a natural consequence of having defined the period May to October as the wet season, the rest of the year (climatologically speaking), i.e., the months from November to April are considered the dry season. Most of the country then experiences *relatively* scarce rainfall totals through this time-interval. Only in the region north of the Peninsula of Baja California do precipitation totals exceed fifty per cent of the rainfall annual totals during this season. For some regions, the small amounts of precipitation (in the arid areas) have a larger impact than during the wet season even if the ratios of the precipitation with respect to their long-term means are used. Despite these potential problems, we utilised the same methods and approaches to regionalise the dry season.

The number of components selected is a key feature of the PCA, and this is especially true when this technique is used for regionalisation. A nearly horizontal line is seen after the 11th component when the scree test is applied (section 3.3.2). These first 11 components account for 69.2% of the total variance, the change on eigenvalues with respect to the 12th component is approximately -0.134 (Fig. 4.5). Based on this small variation, eleven different regions are considered to study the spatial pattern of the dry season (Nov-Apr) precipitation.

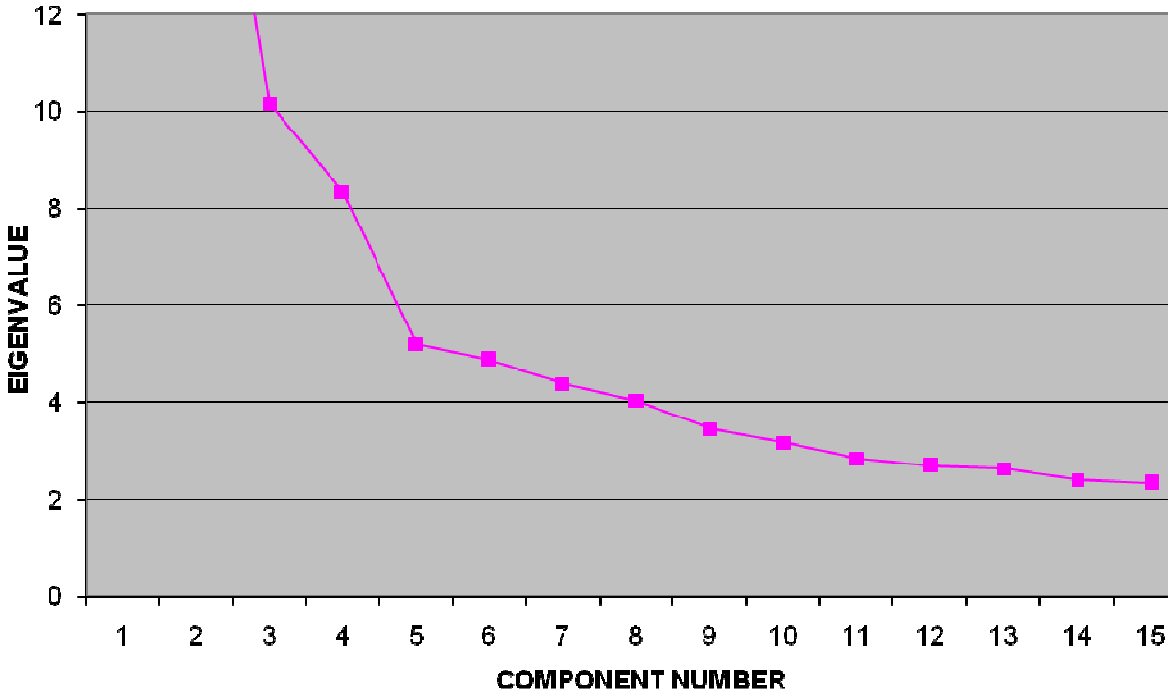

Fig. 4.5. Determination of the number of regions (components) considered in the analysis of the Nov-Apr (Dry Season) precipitation using the the cliff analogy (Wuensch, 2005).

ORTHOGONAL AND OBLIQUE ROTATED SOLUTIONS.

Regions for the dry season in Table 4.3 show an evident different spatial structure (fig. 4.6) when compared with the annual and wet season analyses. First of all, components reflect a larger spatial coverage for the dry season.

The area named the Mexican Central Highlands region (RD1) in the annual and wet season PCA results has now being geographically extended towards the Pacific Coast. Probably larger scale (than during the annual and wet seasons) dry season phenomena, like polar fronts, penetrate far south in the country despite its orographic barriers (the two mountainous ranges along both coasts). Nevertheless, the tropic of cancer remains as a climatic threshold to delineate the region.

RD2 (Northwest, Arizona and Texas) covers now not only the Mexican Monsoon, but also some stations south of the Baja Californian Peninsula that had been split in the annual and wet season results, and now appears as a single cluster in the peninsula. It can be appreciated that, when compared with varimax, promax (k=2) has better delineated RD2. The spatial coverage in the latter case does not reach any station far East (the state of Texas in the USA) as in the case of varimax. Both techniques are coincident in showing clusters of RD2 on both sides of the Sea of Cortez; it would be worth investigating the role of the thermal inertia of the Gulf of California (Sea of Cortez) in relation with the climate during the dry season in this region.

RD3 (Northeast) extends geographically eastwards just north of the central highlands covering sites that were RA4 and RW4 (Desert north, New Mexico, Texas) in the previous sections.

The Gulf of Mexico Coast Region (RD4) is smaller in extension than its counterparts of the annual and wet seasons, covering now only the south of the Gulf of México, probably because polar fronts generally do not penetrate far south into this area during the cold season, as is the case in northern Gulf of Mexico.

One of the only two coincident resulting regions is not surprisingly the area of North Baja California (RD5). Only in this part of the country the dry season precipitation exceed fifty percent of the annual totals. The cluster replicates identically the annual rainfall one, but when compared with the wet season it spreads westwards covering some parts of Arizona, separating them from part of the RD2 that is related to the Mexican Monsoon

region (RA11 in table 4.1) in the PCA regionalisation of the annual rainfall. Therefore, we can say that these stations in Arizona are not affected by the same physical controls of the Mexican Monsoon during the dry season.

Although, RD6 can be still be related to the Transverse Neovolcanic Belt, the stations within it are not the same when compared with the ones of the rainy season results, yet all the sites in the group are above 1000 m.a.s.l., three of them having altitudes greater than 2000 m.a.s.l., reinforcing what has been pointed out before, that altitude should be considered as one of the most important factors in the study of the climate of México (Mosiño and García, 1974).

Probably the PCA's most striking feature for the dry season analysis is the cluster in the Yucatán peninsula (RD7). This area is under the influence of Hurricanes during the rainy season like Hurricane Gilberto in 1988 (one of the strongest of the last century, see section 5.1), and it is likely that the variable nature of hurricane tracks and their associated sudden changes in precipitation impede simultaneous impacts in the stations throughout the entire region during the wet season and therefore the annual totals. Nevertheless, as November to April is a Hurricane-free period, the rainfall patterns are now easier to identify within RD7 and its surroundings.

La Huasteca region can still be linked to RD8 covering the area north of Veracruz and south of Tamaulipas states, in which winter atmospheric controls like polar fronts could penetrate far south directly affecting the precipitation patterns during the dry season.

The humid South Pacific coast is represented as RD9. It has not been classified either for the annual or the wet season analyses, but it is possible (as in the case of the Yucatán Peninsula, RD7 in table 4.3) that tropical-cyclone precipitation have affected the PCA results during those periods, so only allowing its classification for the dry season.

Closely replicating results in the previous sections, RD10 shows the wettest Mexican rainforest area. This is the only region that could be observed in the three different

regionalisation analyses using Principal Components. This supports what has already been mentioned above. In this region precipitation amounts are roughly balanced between wet and dry seasons.

Finally, R11 is the least clear region of all; this could be either an artificial effect of PCA or product of the decision of using more components in order to compare with the annual and wet seasons.

Clear regionalisation can be observed either for orthogonal (varimax) or oblique (promax k=2) solutions, when we apply PCA to the dry season. Nevertheless, because of the complexity of the database that has been analysed, clearer results are obtained with promax (see section 3.3.2), in terms of the clusters of stations for the different groups. Reduced regions and omission of the odd classified stations (like in the first PCs: regions RD1, RD2, RD3 and RD4) are two discernible characteristics of using promax (k=2). Overall, dry season regions depict a markedly different structure when compared with the annual and wet season PCA results. These resulting regions support the conclusion that wet season is the most important period for the annual precipitation in most of the country (see section 2.2). However, PCA results on the dry season suggest that precipitation totals during this period are not ignorable, and should be take into account for future studies of the Mexican climatic patterns.

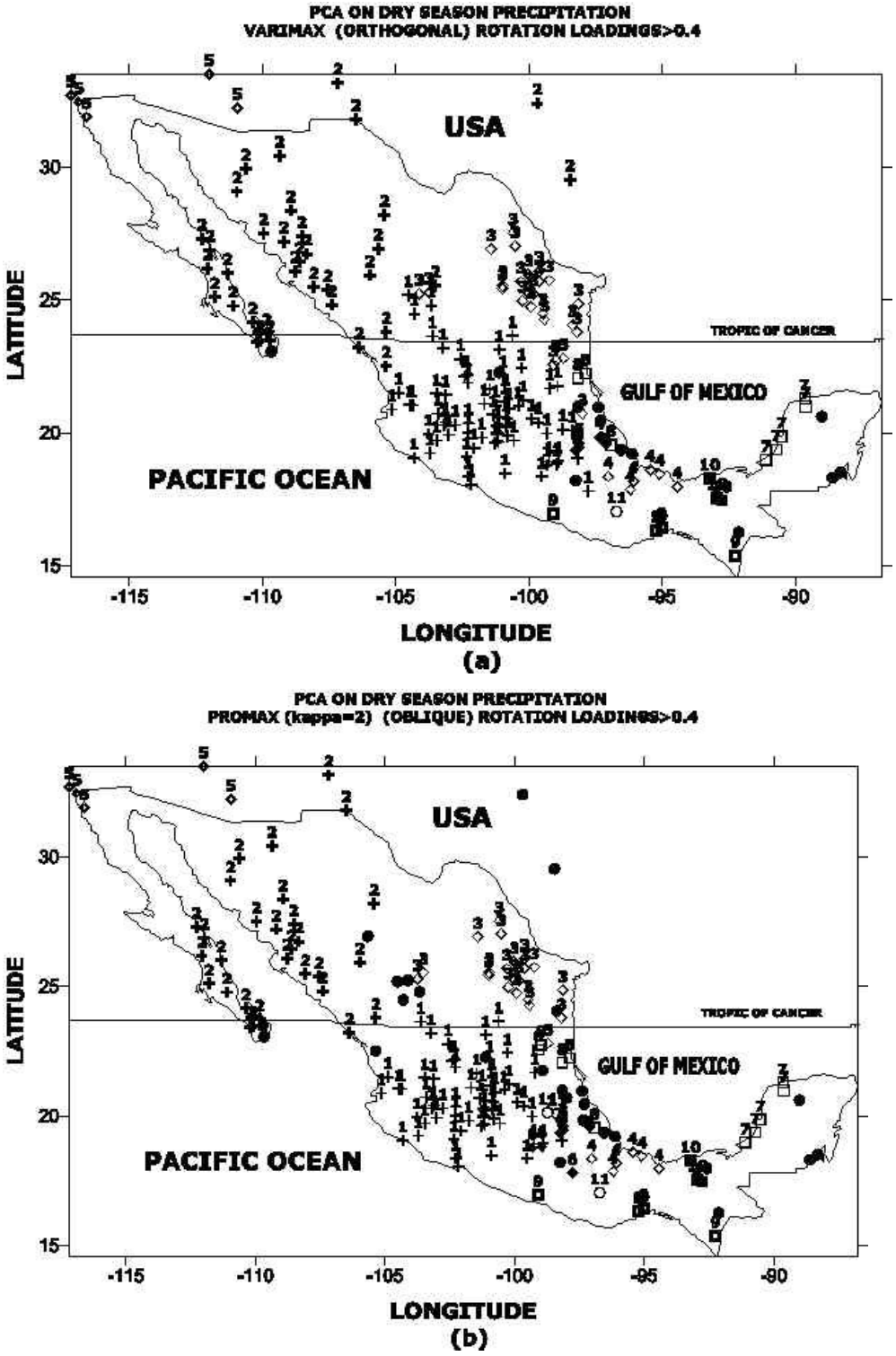

Figure 4.6. Principal component analysis (regionalisation) of a network of 175 stations with dry season (Nov-Apr) precipitation (1931-2001) using two different solutions: varimax (a) and promax with kappa=2 (b).

Component	Associated region	Climatic characteristics
Region one (RD1)	Central Mexican Highlands	Trades in summer, monsoon from the Pacific, summer rainfall, two temperature maxima
Region two (RD2)	Northwest, Arizona and Texas	Subtropical high pressures, westerlies, one temperature maximum.
Region three (RD3)	Northeast	Trades in summer, polar fronts in winter, hurricanes in summer and autumn, one temperature maximum.
Region four (RD4)	Gulf of Mexico coast	Trades in summer, hurricanes in summer and autumn, polar fronts in winter, two temperature maxima.
Region nine (RD5)	North Baja California	Westerlies, winter precipitation, one temperature maximum.
Region six (RD6)	Transverse Neovolcanic Belt	Summer precipitation, Pacific monsoon, high altitude sites, two temperature maxima.
Region seven (RD7)	Yucatán peninsula	East and Northeast trades, hurricanes during summer and autumn, polar fronts in winter, summer rainfall with considerables percetages of winter precipitation, two temperature maxima.
Region eight (RD8)	La Huasteca	Summer precipitation, hurricanes in summer and autumn, polar fronts.
Region nine (RD9)	Humid South Pacific	Westerlies, winter precipitation, one temperature maximum.
Region ten (RD10)	Southeast rainforest	InterTropical Convergence Zone (ITCZ), southeastern trades, hurricanes in summer and autumn, two temperature maxima.

Table 4.3. Dry season precipitation PCA resulting regions identified according to the known Mexican climatology (García, 1988).

4.3. PRINCIPAL COMPONENT ANALYSIS (PCA) ON MEAN TEMPERATURE.

In order to expand the understanding of the climate of México, and also to complete the picture depicted by the PCA on precipitation, it was decided to apply the same sort of analysis to mean temperature. Only a few have been made applying PCA to Mexican temperatures (see section 4.2). As has been pointed out in previous chapters this is not surprising, as it is only relatively recently (late 1990s, see section 3.2) that extended digital databases prepared from instrumental data have been released. Still, the number and spatial coverage of temperature stations is smaller when compared with that of precipitation. This can be explained as the Mexican post-revolutionary economic era before the 1980s being partially linked to agriculture (Liverman and O'Brien, 1991), and therefore the precipitation pattern changes were more important than those for temperature. The meteorological network developed more towards rainfall measurements during the early instrumental periods, instead of developing simultaneously with other climatological variables like temperature. The temperature data network to be used follows the same conditions established for precipitation, i.e., to have as many stations as possible across the nation together with a precise definition of the seasons under study. The smaller number of Surface Air Temperature (SAT) stations than those for precipitation, does not permit a good spatial coverage throughout the country (Fig. 4.7). A database of fifty-two stations containing monthly mean temperature was prepared. Except for those located in the USA, all of them were processed from daily data. Following the same conditions for the PCA on precipitation, the maximum percentage of missing values was restricted to 10%, and missing months were replaced with their respective means. In contrast, the length of the time series is only 61 years, starting in 1941 and ending in 2001; ten years shorter than the rainfall network (see section 3.2.2). Anomalies with respect to their long-term means were also calculated, in order to avoid as much as possible sudden changes in the time-series and well-known direct "external" influences such as altitude (Comrie and Glenn, 1998). Other factors play important roles in the annual temperature cycle, among them latitude is crucial for the determination of the seasonality of the dynamics of temperature (see section 2.2.1).

	STATION NAME	STATE	SMN ID	LONGITUDE	LATITUDE*	ALTITUDE+
1	PABELLON DE ARTEAGA	AGS	01014	-102.33	22.18	1920
2	PRESA CALLES	AGS	01018	-102.43	22.13	2025
3	PRESA RODRIGUEZ	BCN	02038	-116.90	32.45	100
4	ENSENADA	BCN	02072	-116.60	31.88	24
5	COMONDú	BCS	03008	-111.85	26.08	260
6	EL PASO DE IRITU	BCS	03012	-111.12	24.77	140
7	LA PURíSIMA	BCS	03029	-112.08	26.18	95
8	SAN BARTOLO	BCS	03050	-109.85	23.73	395
9	SANTA GERTRUDIS	BCS	03060	-110.10	23.48	350
10	SANTA ROSALíA	BCS	03061	-112.28	27.30	17
11	SANTIAGO	BCS	03062	-109.73	23.47	125
12	LA PAZ	BCS	03074	-110.37	24.15	10
13	MANZANILLO	COL	06018	-104.32	19.05	3
14	MOTOZINTLA	CHIAP	07119	-92.25	15.37	1455
15	EL PALMITO	DUR	10021	-104.78	25.52	1540
16	EL SALTO	DUR	10025	-105.37	23.78	2538
17	GUANACEVI	DUR	10029	-105.97	25.93	2200
18	RODEO	DUR	10060	-104.53	25.18	1340
19	SANTIAGO PAPASQUIARO	DUR	10100	-105.42	25.05	1740
20	IRAPUATO	GTO	11028	-101.35	20.68	1725
21	OCAMPO	GTO	11050	-101.48	21.65	2250
22	PERICOS	GTO	11052	-101.10	20.52	1720
23	SALVATIERRA	GTO	11060	-100.87	20.22	1760
24	SALAMANCA	GTO	11096	-101.18	20.57	1723
25	CUITZEO DEL PORVENIR	MICH	16027	-101.15	19.97	1831
26	HUINGO	MICH	16052	-100.83	19.92	1832
27	CIUDAD HIDALGO	MICH	16152	-100.57	19.70	2000
28	ZACAPU	MICH	16171	-101.78	19.82	1986
29	AHUACATLAN	NAY	18002	-104.48	21.05	990
30	EL CUCHILLO	NL	19016	-99.25	25.73	145
31	LAMPAZOS	NL	19028	-100.52	27.03	320
32	MATIAS ROMERO	OAX	20068	-95.03	16.88	201
33	SANTO DOMINGO TEHUANTEPEC	OAX	20149	-95.23	16.33	95
34	TEZIUTLAN	PUE	21091	-97.35	19.82	2050
35	MATEHUALA	SLP	24040	-100.63	23.65	1575
36	BADIRAGUATO	SIN	25110	-107.55	25.37	230
37	TRES HERMANOS	SON	26102	-109.20	27.20	100
38	SAN FERNANDO	TAM	28086	-98.15	24.85	43
39	ATZALAN	VER	30012	-97.25	19.80	1842
40	RINCONADA	VER	30141	-96.55	19.35	313
41	LAS VIGAS	VER	30211	-97.10	19.65	37
42	EL SAUZ	ZAC	32018	-103.23	23.18	2100
43	BROWNSVILLE	TX	BWVTX	-97.40	25.80	6
44	SAN ANTONIO	TX	SATTX	-98.50	29.50	223
45	MIDLAND	TX	MAFTX	-102.20	32.00	846
46	EL PASO	TX	ELPTX	-106.40	31.80	1150
47	TOMBSTONE	US	TSTUS	-110.10	31.70	1405
48	TUCSON	AZ	TUSAZ	-110.90	32.10	780
49	PHOENIX	AZ	PHXAZ	-112.00	33.40	335
50	SAN DIEGO	CA	SANCA	-117.20	32.70	5
51	CUYAMACA	CA	CYCCA	-116.60	33.00	1414
52	LOS ANGELES	CA	LAXCA	-118.20	34.10	4

Table 4.4. List of stations with monthly mean temperature. The period of records for all the stations is from 1941 to 2001. * meters above sea level.

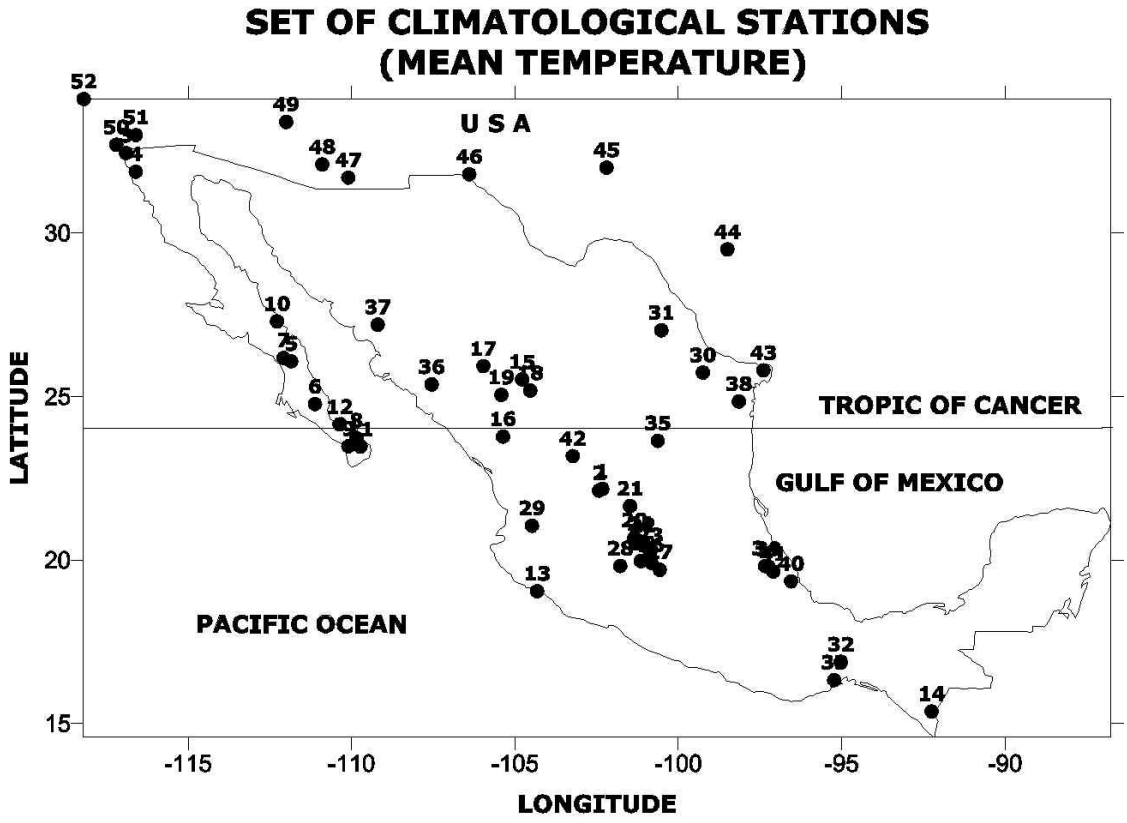

Fig.4.7. Locations of the 52 climatological stations with monthly mean temperature during the period 1941-2001 used in the Principal Component Analysis (PCA).

Much of the annual rainfall is concentrated in Mexico in the summer months; and closely agrees with the procession of the seasons modulated by temperature (Mosiño and García, 1974). The progression of the temperature maxima shows a northwards movement starting in May, with exceptions observed along both Mexican coasts. For these reasons, it was decided to define the same three seasons as for precipitation: May to October, November to April and the annual period, and to analyse them applying PCA with S-mode for regionalisation purposes, using the correlation matrix for contrasting climatic conditions (see section 3.3.2). Rotated (orthogonal and oblique) solutions techniques were applied to the databases to obtain the regionalisation.

4.3.1 ANNUAL MEAN TEMPERATURE.

The contrasting conditions for precipitation explained in Chapter two are closely replicated by mean annual temperature. The smallest differences are experienced in the south Pacific coast, whilst the most dissimilar conditions are observed over the north to north-western regions of the country, in a gradual increasing tendency from south to north. Apart of this evident characteristic, to identify different regions that are coherently

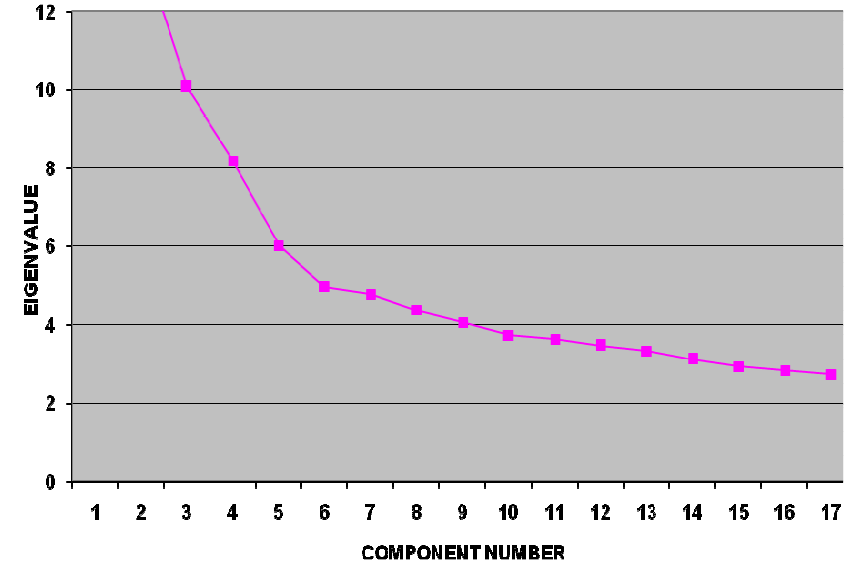

a)

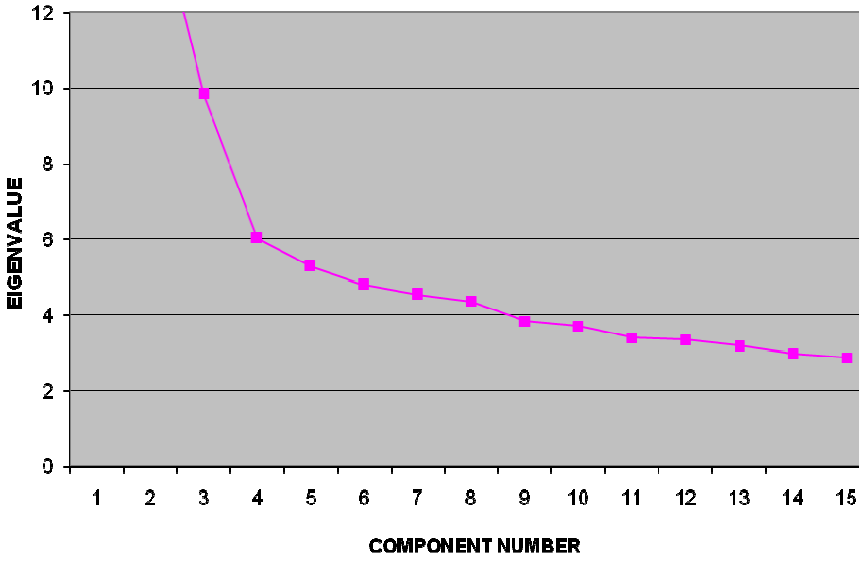

b)

Figure 4.8. Scree Test Plot on a) Annual and b) wet season (May-Oct) Mean Temperature.

varying, it was necessary to define how many components were going to be used. For this purpose the scree test and the same separation method of the previous sections was applied. Based on the scree test (see section 3.3.2) of Fig. 4.8 a), we can select the number of components using two different criteria. Firstly, after the 12th component, the variation with respect to the next components is negligible and these first 12 components account for 80.1% of the total variance, and secondly the eigenvalue of the 12th component is close to the unity (1.0), i.e. the Kaiser-Guttman rule (Peres-Neto et al., 2005). Therefore, the number of components is set to 12.

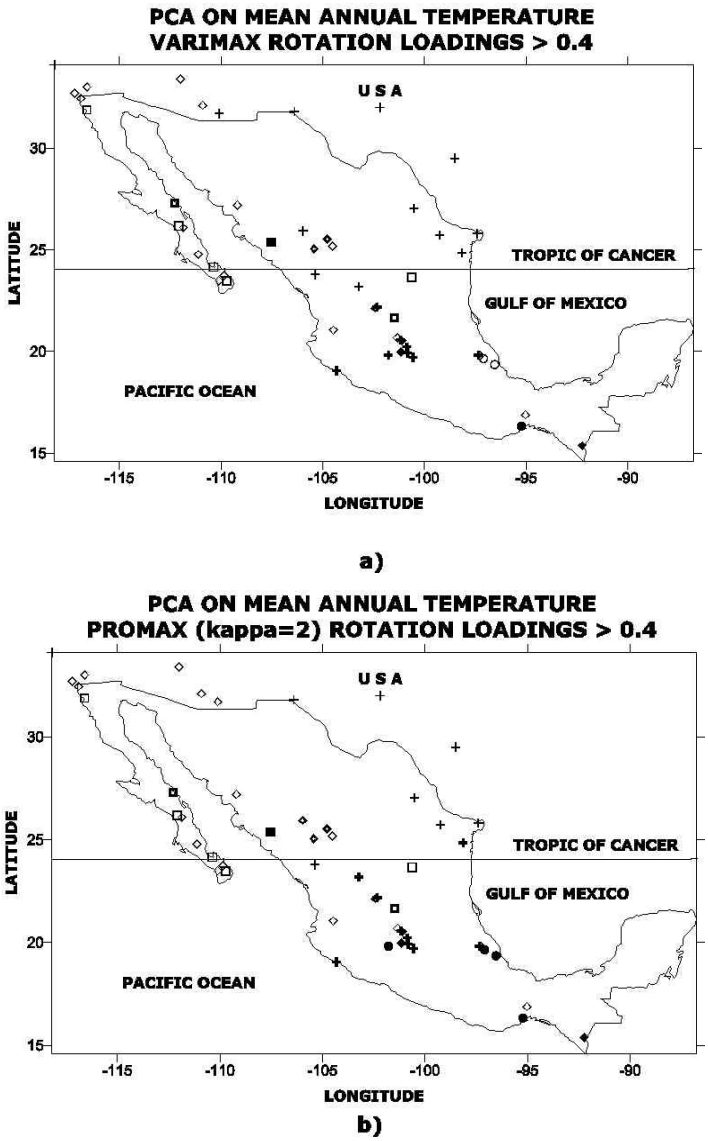

Figure 4.9. Principal Component Analysis (PCA regionalisation) of a network of 52 stations with annual mean temperature (1941-2001) using two different solutions: a) varimax and b) promax with kappa=2.

In contrast to the precipitation results, a lack of clarity in regions can be easily observed (see Fig. 4.9). Probably the only regions reasonably well delineated are located in the north of the country near the border with the USA. One is centred in the north and northeast of México related to the Río Bravo Basin, whilst the other is in North Baja California – California region near to the Pacific coast. No other region can be easily defined and linked to any known climatic features in the country.

4.3.2. MAY TO OCTOBER MEAN TEMPERATURE.

The scree test (see section 3.3.2) on the May to October period reveals that 12 components would be sufficient to explain the climatology of this period. The curve becomes close to a line after the 12^{th} component, the rest of modes of variation are practically not contributing to the communalities (Fig. 4.8). As in the case of annual mean temperature, the regions are not clearly defined except for what seems to be the Río Bravo Basin. None of the rotated solutions improved the results when contrasted with the annual mean temperature regions (Fig. 4.10). These results appear to closely replicate what has been seen in the previous section (annual mean temperature). It is possible that, the smaller fluctuations in mean temperature (in comparison with the larger and easy detectable changes in precipitation) have influenced the unsuccessful regionalisation of the annual and May to October mean temperatures. The only clear regions extracted applying PCA to mean temperature are observed in Northern Mexico where sudden changes in temperature can occur especially during winter, in contrast with the less variable temperatures in Southern Mexico. A latitudinal transition (defined by the tropic of Cancer) can be pointed out in this analysis. PCA is then, going to be applied to the three-monthly periods Dec-Jan-Feb (DJF), Mar-Apr-May (MAM), Jun-Jul-Aug (JJA), Sep-Oct-Nov (SON), in order to explore alternatives for improving the results.

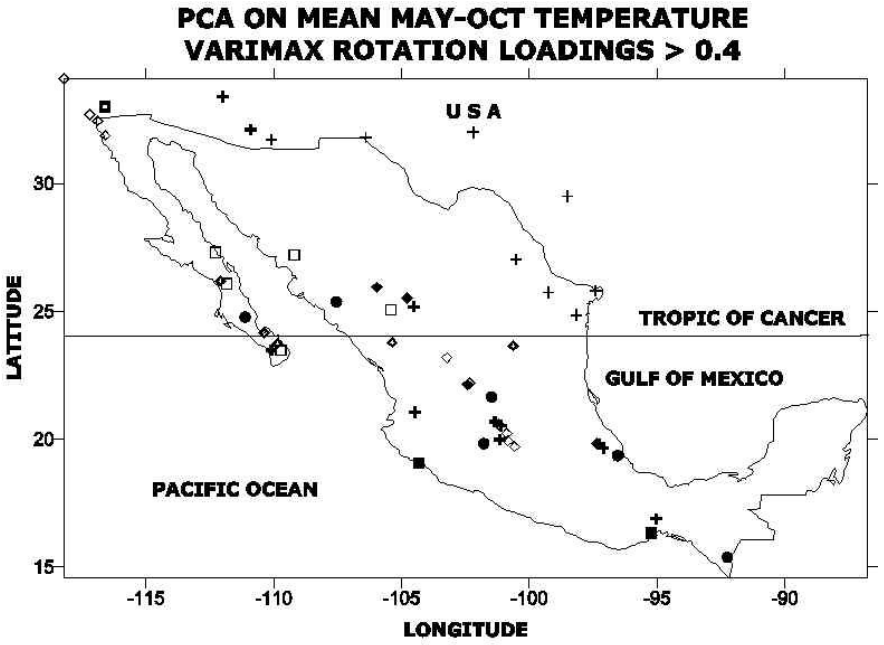

a)

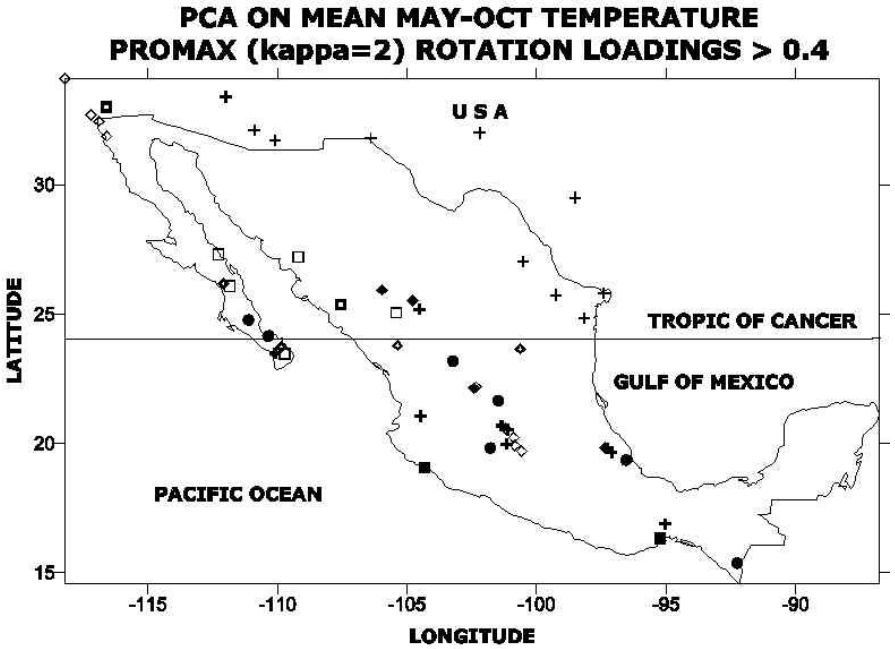

b)

Figure 4.10. Principal Component Analysis (PCA regionalisation) of a network of 52 stations with May-Oct mean temperature (1941-2001) using two different solutions: a) varimax and b) promax with kappa=2.

4.3.3. SEASONAL MEAN TEMPERATURE.

It is clear observing the Figure 4.12 that no regions can be extracted for the mean temperature (as was the case for precipitation), that make sense with the Mexican climatology. These poor results obtained for the cases of annual and May to October (wet season for rainfall) mean temperature enforced the decision to split the periods on a traditional seasonal basis (DJF, MAM, JJA, SON), and analyse them using PCA. Dividing seasonally the mean temperature, we will explore the possibility of improving the PCA regionalisation. The scree tests (see Fig. 4.11) for seasonal mean temperature show an agreement after the 11th component. The rest eigenvalues associated to their modes of variation are no more contributing to the total variance, and not helping in the interpretation of the spatial patterns.

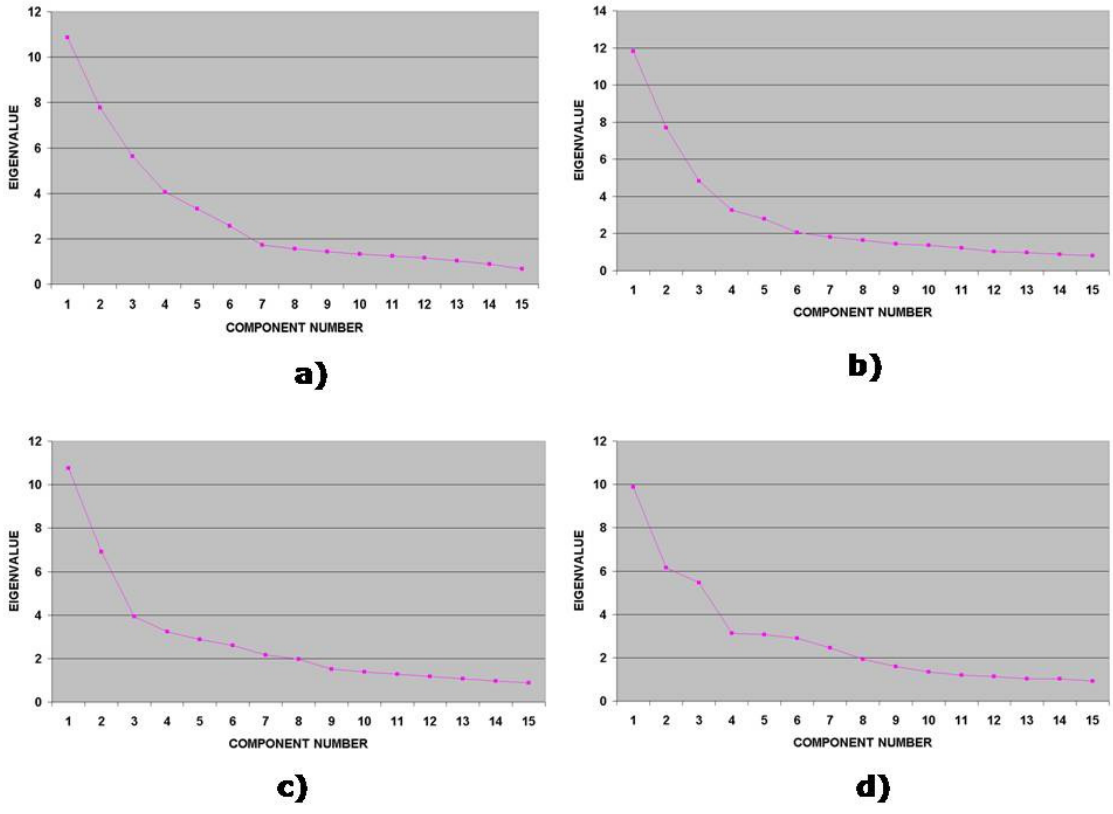

Figure 4.11. Scree Test Plot on a) DJF b) MAM c) JJA and d) SON periods for the selection of number of components.

The resulting distribution of regions (Fig 4.12) of the analysis of PC using an orthogonal rotated solution (Varimax) does not show a clear pattern in any of the (three monthly) periods. The only consistent region across all the periods is the northeast region that we have linked to the Río Bravo Basin in the previous section. Less clear but present is the north-western North Baja California – California region, however, only during the DJF period is this well defined. None of the other results have apparently any relation with those of rainfall.

No improvement in the results (Fig 4.13) is observed when using the rotated oblique solution (Promax), in contrast with the precipitation regionalisation applying PCA (see section 4.2.1). Here, the northern areas of the country, near the USA border are the only regions delineated by the analysis, repeating the clusters linked to the Río Bravo Basin and the north Baja California area. The latter extends eastwards to cover Arizona and New México in the USA during the DJF and MAM periods. These are seasons when polar fronts affect both rainfall and temperature, especially in northern Mexico. The results closely mirrored those of the orthogonal solution; but overall, as in the case of the varimax (orthogonal) solution, the regions do not show a spatial consistency through all the seasons.

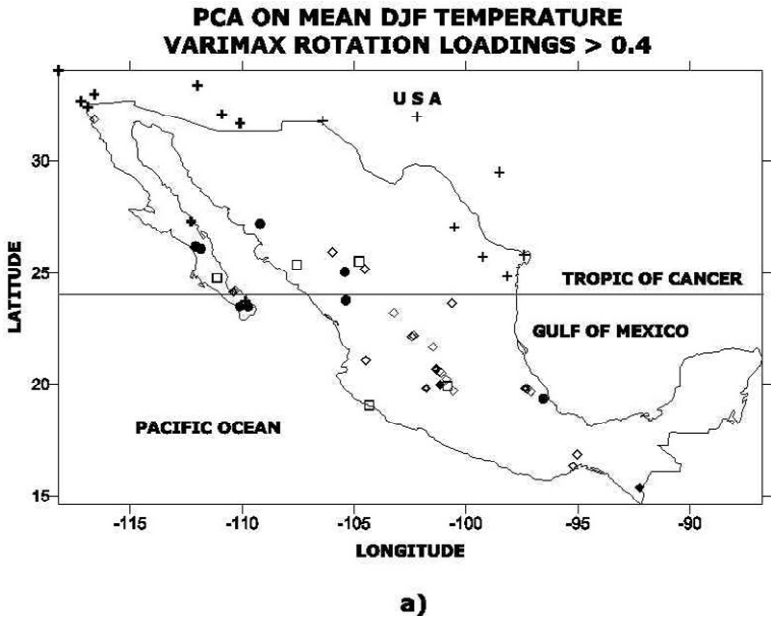

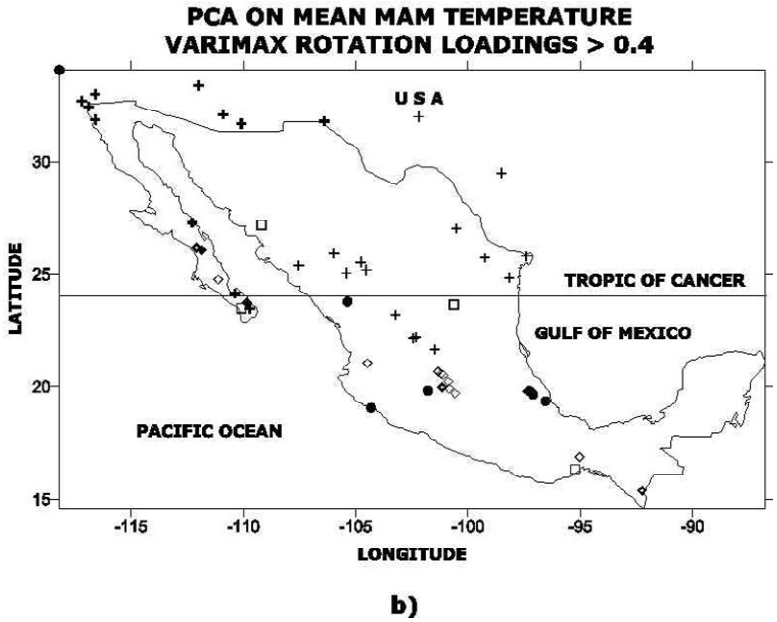

Figure 4.12. Principal Component Analysis (PCA regionalisation) applying an orthogonal rotated solution (Varimax) of a network of 52 stations with a) DJF b) MAM mean temperature (1941-2001).

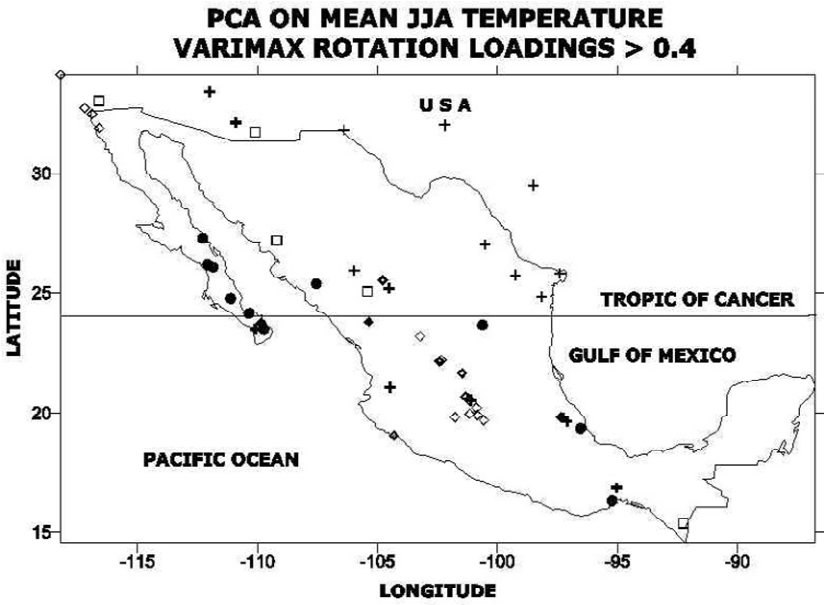

c)

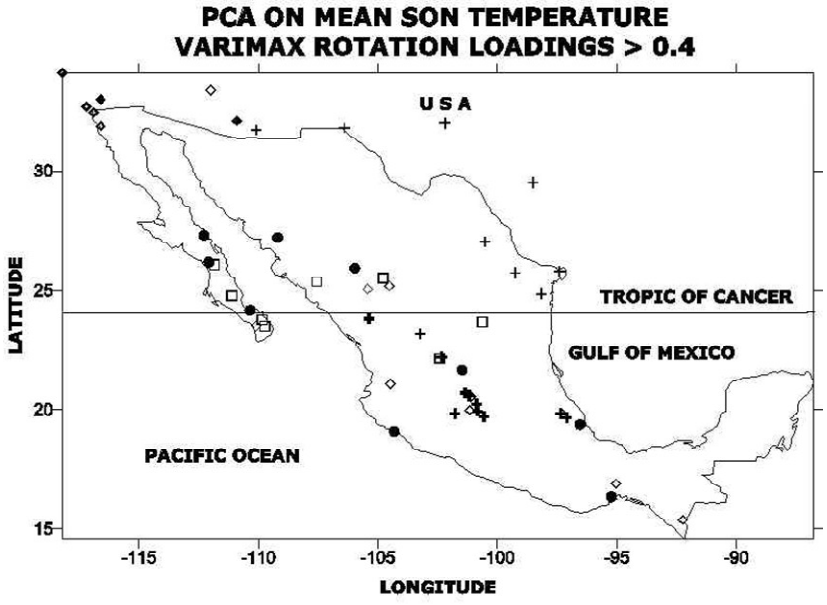

d)

Figure 4.12. Principal Component Analysis (PCAregionalisation) applying an orthogonal rotated solution (Varimax) of a network of 52 stations with c) JJA and d) SON mean temperature (1941-2001).

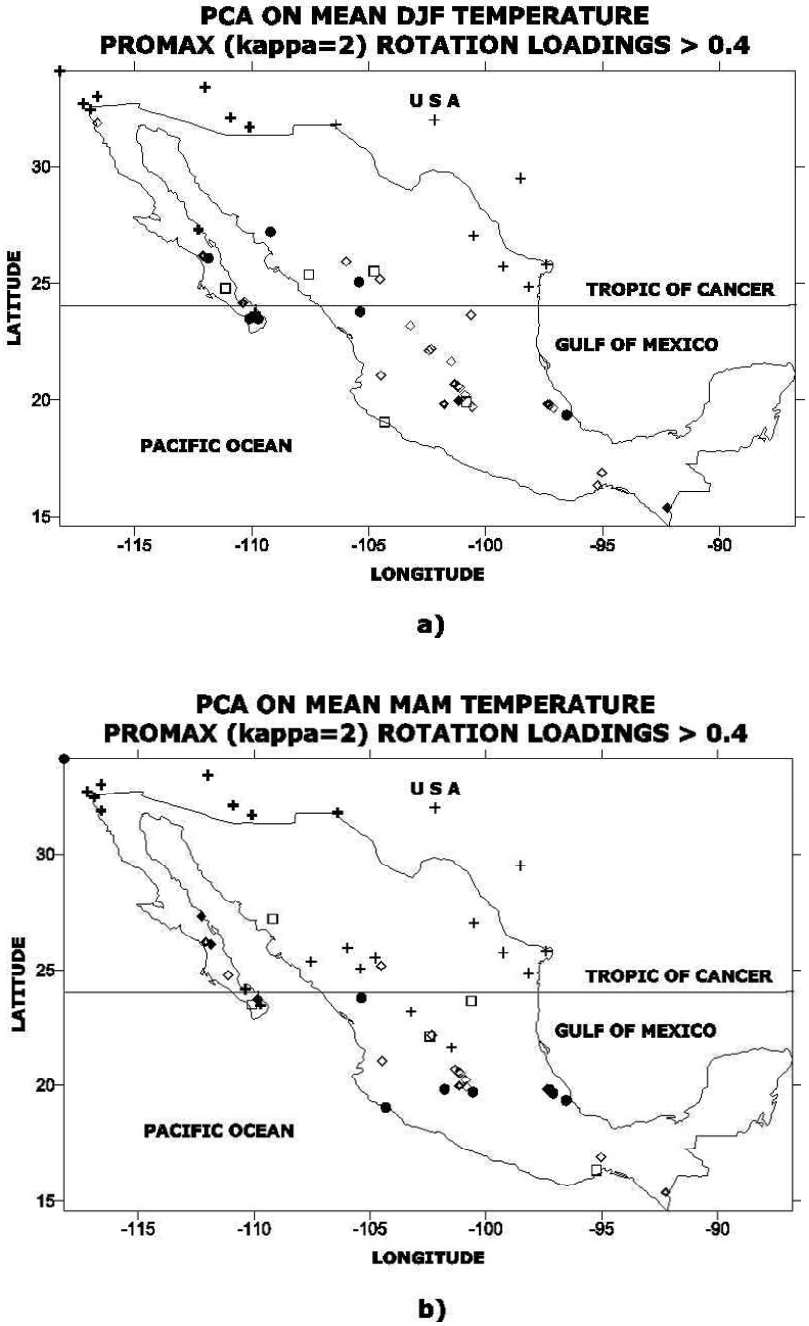

Figure 4.13. Principal Component Analysis (PCA regionalisation) applying an oblique rotated solution (Promax) of a network of 52 stations with a) DJF b) MAM mean temperature (1941-2001).

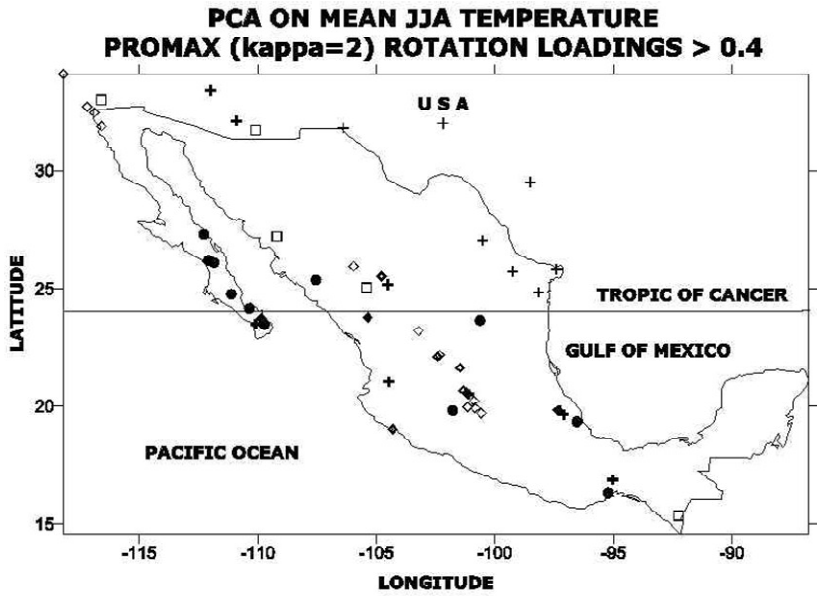

c)

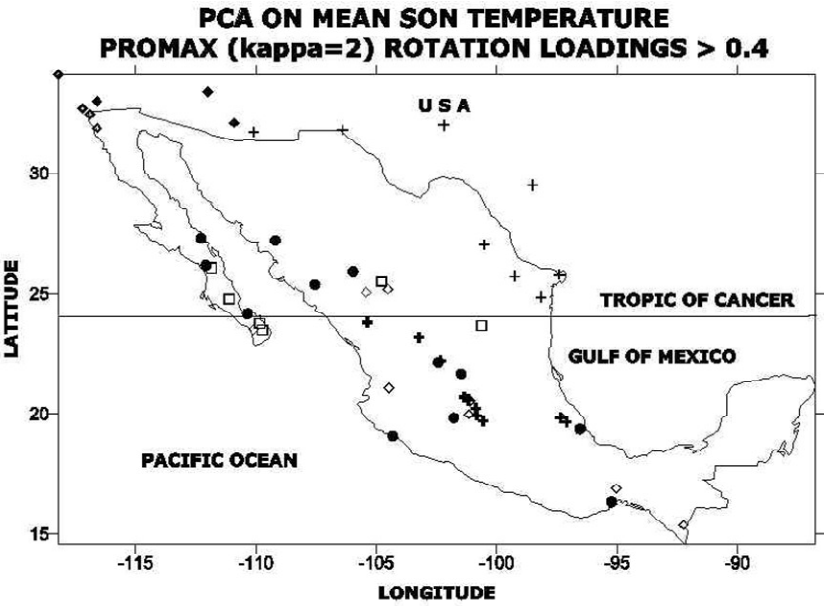

d)

Figure 4.13. Principal Component Analysis (PCA regionalisation) applying an oblique rotated solution (Promax) on a network of 52 stations with c) JJA and d) SON mean temperature (1941-2001).

4.3.4. K-Means Cluster Analysis.

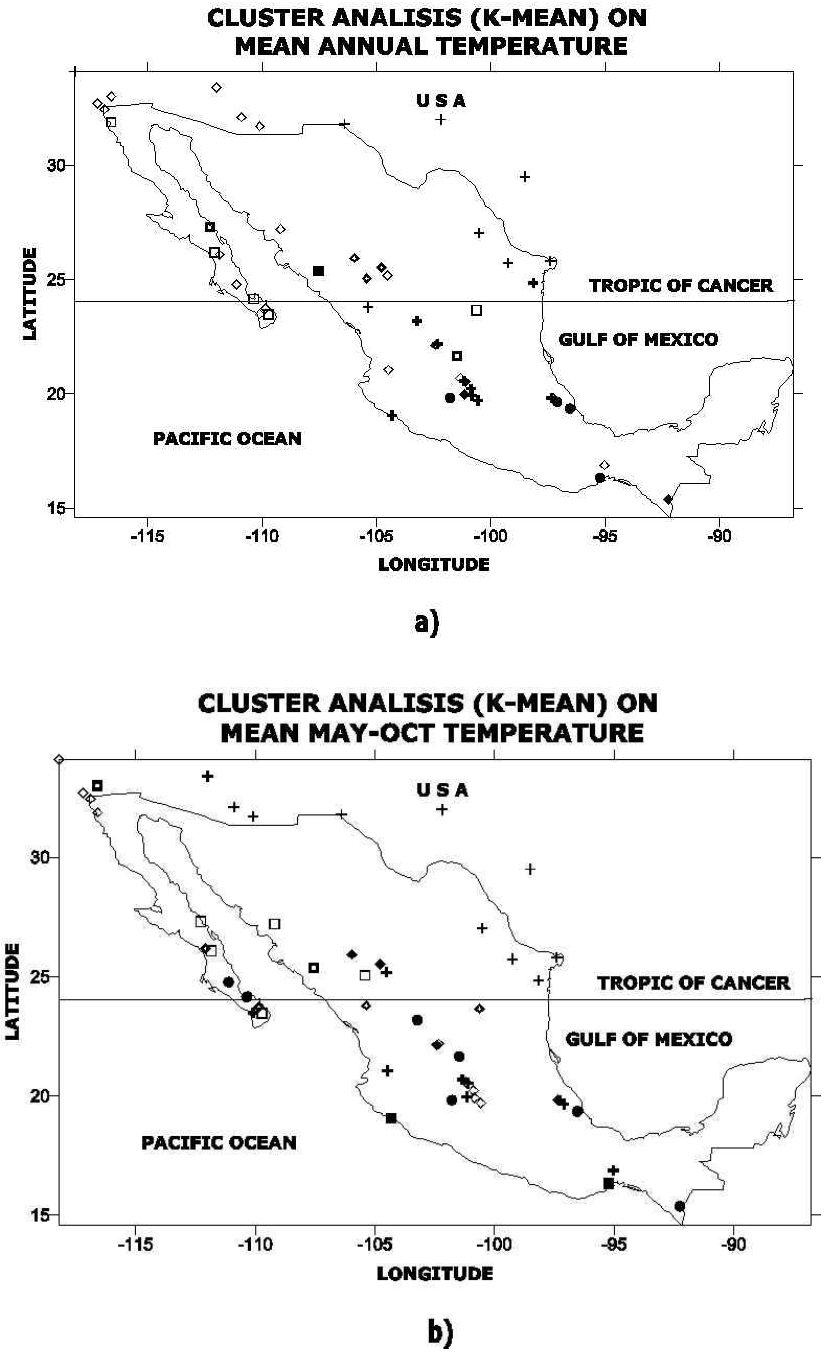

Figure 4.14. Cluster Analysis (K-mean) of a network of 52 stations with a) annual b) wet season mean temperature (1941-2001).

A final option for the purpose of regionalisation of the mean temperature data was to apply what is termed K-means cluster analysis. The resulting regions are shown in Fig. 4.14., but no improvement can really be observed when compared with those obtained by rotated PCA. In fact, what the cluster analysis shows is an agreement with the mean temperature PCA regionalisation, replicating the distribution already observed using that technique. It can be concluded, therefore that the type of analysis has no influence on the final results, but it is very likely that primarily the small number of stations and the length of the time series utilised have impeded a clear outcome in comparison with those obtained in the case of precipitation.

4.4. CONCLUSIONS TO THE CHAPTER.

A process of regionalisation using Principal Component Analysis (PCA) has been applied to two different networks of monthly precipitation and temperature data. Amongst other reasons, because of its better temporal and spatial coverage; successful results have been obtained with precipitation, and poor results for mean temperature. Clearer results are also evident for oblique rotated [in particular (promax, k=2)] solutions than those of orthogonal rotated (varimax) solutions.

The analyses were divided into three main seasons for precipitation: annual, wet (May to October) and dry (November to April) seasons. Annual and wet season results are quite similar. They share most of the PCA regions, but also have slight differences. The North American Monsoon and La Huasteca are regions that only appear during the analysis of annual total precipitation. These regions are sometimes strongly affected by winter rainfall influencing the annual precipitation.

In contrast, Nayarit state and the transverse neovolcanic belt are regions that can only be extracted during the wet season. In the case of the neovolcanic belt region, altitude certainly exerts a large influence on the results. This is an area that needs to be explored in much detail in future research. The great amounts of moisture entering the continent

seem to be affecting the Nayarit (Pacific) coast during the wet season. This is the reason the region does not appear during the dry season or the annual totals. Finally, during the rainfall dry season there is a markedly latitudinal transition. The Mexican monsoon and North Baja Californian are regions in which winter precipitation is an important percentage of the annual totals; these two regions are located in the north-western part of the country. November to April is basically a hurricane-free period; therefore, those regions that are deeply affected by these phenomena during the wet season, have now appeared in the dry season results. The Yucatán peninsula and the South Pacific regions clearly show that the heavy precipitation caused by hurricanes can strongly affect their rainfall patterns completely separating them from their (PCA) neighbouring regions during the wet season and the annual totals.

Mean temperature was the other variable analysed using PCA. This method was applied using the rotation techniques to the annual mean temperatures and wet season; nevertheless, no clear results were obtained for these seasons. An alternative approach was used defining three-monthly periods that aimed at obtaining better results. However, no improvement was observed in comparison with the previous analysis. A final attempt was made using K-means cluster analysis but poor results were also evident. Only the northern regions within the border of Mexico-USA appear consistently across all these analyses.

CHAPTER FIVE: EXTREME PRECIPITATION INDICES.

5.1. INTRODUCTION.

On September 14 1988, Hurricane Gilbert hit Cancún on the east coast of the Yucatan Peninsula, and a few days later (on September 17) caused severe damage in Monterrey in north-eastern Mexico. Gilbert is considered the storm of the twentieth century with records for size, straightness of track, lowest atmospheric pressure and total energy (Meyer-Arendt, 1991). At the centre of Gilbert the pressure reached an outstanding low of 888 mb. The beginning of the twentieth-first century has also shown in Mexico one of the most dangerous faces of anthropogenic climate change: weather extremes. In the Atlantic Ocean Basin, 2005 was the most active hurricane season in history (Lawrimore et al., 2005). Several southern Mexican states (Yucatan, Chiapas, Oaxaca, Puebla and Veracruz) were hit by Stan from October 1 to 5 (Hernández-Unzón and Bravo, 2005a), and it was not long (October 22) before Wilma, the strongest hurricane on record, struck the Yucatan Peninsula. This storm set the lowest atmospheric pressure (882 mb) ever recorded, and the highest 24 hrs accumulated precipitation in Mexico (1576 mm at Isla Mujeres), seriously damaging the touristic infrastructure of Cancún (Hernández-Unzón and Bravo, 2005b). These sorts of events illustrate the delicate balance of the climate system between extremes and average weather. Extreme weather events fall within the "probability distribution" fringes of meteorological variables; most of the time revealing an "unexpected" aspect of the known distributional patterns for a location or region.

Seeking simplicity in the description of rainfall extreme indices for 15 stations with daily precipitation (Table 5.1; see also Table 3.2 and Fig. 3.6), we partition the data into two different aspects: one dealing with depth or intensity (amount and rate) and the other with frequency (number of occurrences). We will then examine both sets of indices using linear correlation (with time) involving Kendall's tau (see section 4.5.1). For some of the most important statistically significant correlations (as Kendall's tau does not compute the trend magnitude), additionally we plot the least-squares linear trends. Natural mechanisms that partially control their patterns are discussed in relation to all these

extreme parameters. The study seeks to find coherent spatial patterns of change among the indices of precipitation extremes, especially when comparing local against regional scales as in the case of the PRCPTOT index (see Table 3.1), or within the resulting regions of the Principal Component Analysis (Section 4.2.1). Therefore, one of the main targets of this chapter (of the indices of rainfall extremes) is the identification of consistencies among several statistically significant correlations, of one single station or a group of stations.

In the second part of the chapter, the hypothesis of a climatic transition between different parts of Mexico is explored further. The Tropic of Cancer has been defined as a geographical threshold for this purpose. Statistically significant correlations of the precipitation extreme indices with time are contrasted either side of this imaginary line for both positive/negative correlations and wet/dry conditions.

5.2. DISCUSSION.

For the purposes of this chapter, the rainfall extreme indices (defined in Table 3.1 of Section 3.3.4) can be classified into two groups: one group measures the precipitation depth (mm) or intensity (mm/day) (PRCPTOT, SDII, R95P, R99P, RX1day and RX5day) and the other calculates the frequency (number of cases) of the index exceeding or not exceeding its defined threshold (CDD, CWD, R10mm, R20mm). It is expected that this separation of magnitude and frequency can give an additional insight into the often subtle differences of the climatic regions across Mexico (Table 5.1).

5.2.1. PRECIPITATION EXTREME INDICES.

As PRCPTOT is probably the most important index reflecting rainfall variations over the entire year, the discussion of extremes will start with the changes of this parameter at local and regional levels. At regional scales (recall the methods to calculate regional series see Section 3.3.3), the most striking characteristic in this index [Fig 5.1. d)] is that significant negative correlations are observed in two different southern regions. The fist is decreasing regional precipitation [Fig 5.1. d)] over the Michoacán coastal

Number*	STATION	STATE	Statist. signif +5%	Statist. signif +1%	Statist. signif -5%	Statist. signif -1%
2	PRESA RODRIGUEZ	BCN	PRCPTOT, R20mm, R95P,SDII			
7	SAN JOSE DEL CABO	BCS	R10mm, R20mm	R25mm		
10	CHAMPOTON	CMP	RX1day,R95P	CWD, PRCPTOT		CDD, SDII
11	OJINAGA	CHIH	CWD			SDII
12	FCO. I. MADERO	DUR				
13	GUANACEVI	DUR	SDII			
16	CELAYA	GTO				
17	IRAPUATO	GTO				
20	APATZINGAN	MICH	R20mm, R25mm, SDII			
27	JUCHITAN	MICH				
31	BADIRAGUATO	SIN				
32	YECORA	SON			R95P	CWD, RX5day
33	SAN FERNANDO	TAM				
34	ATZALAN	VER			CWD	
35	LAS VIGAS	VER	CDD		R99P	R25mm, R95P, RX1day, RX5day

Table 5.1. List of temperature stations (with data from 1941 to 2001) show correlations (Kendall's tau) between the precipitation extreme indices with time, that are statistically significant at the 5 and 1% level. * Stations numbers are in correspondence with Table 3.2 and Fig. 3.6.

Number*	STATION	STATE	Non Significant Correlations
2	PRESA RODRIGUEZ	BCN	R99P, RX1day, RX5day, CDD, CWD, R10mm, R25mm
7	SAN JOSE DEL CABO	BCS	PRCPTOT, SDII, R95P, R99P, RX1day, RX5day, CDD, CWD, R25mm
10	CHAMPOTON	CMP	R99P, RX5day, R10mm, R20mm, R25mm
11	OJINAGA	CHIH	PRCPTOT, R95P, R99P, RX5day, R10mm, R20mm, R25mm
12	FCO. I. MADERO	DUR	PRCPTOT, SDII, R95P, R99P, RX1day, RX5day, CDD, CWD, R10mm, R20mm, R25mm
13	GUANACEVI	DUR	PRCPTOT, R95P, R99P, RX1day, RX5day, CDD, CWD, R10mm, R20mm, R25mm
16	CELAYA	GTO	PRCPTOT, SDII, R95P, R99P, RX1day, RX5day, CDD, CWD, R10mm, R20mm, R25mm
17	IRAPUATO	GTO	PRCPTOT, SDII, R95P, R99P, RX1day, RX5day, CDD, CWD, R10mm, R20mm, R25mm
20	APATZINGAN	MICH	PRCPTOT, R95P, R99P, RX1day, RX5day, CDD, CWD, R10mm, R25mm
27	JUCHITAN	MICH	PRCPTOT, SDII, R95P, R99P, RX1day, RX5day, CDD, CWD, R10mm, R20mm, R25mm
31	BADIRAGUATO	SIN	PRCPTOT, SDII, R95P, R99P, RX1day, RX5day, CDD, CWD, R10mm, R20mm, R25mm
32	YECORA	SON	PRCPTOT, SDII, R95P, R99P, RX1day, RX5day, CDD, CWD, R10mm, R20mm, R25mm
33	SAN FERNANDO	TAM	PRCPTOT, SDII, R95P, R99P, RX1day, RX5day, CDD, CWD, R10mm, R20mm, R25mm
34	ATZALAN	VER	PRCPTOT, SDII, R95P, R99P, RX1day, RX5day, CDD, R10mm, R20mm, R25mm
35	LAS VIGAS	VER	PRCPTOT, SDII, R95P, R99P, RX1day, RX5day, CDD, CWD, R10mm, R20mm, R25mm

Table 5.2. List of temperature stations (with data from 1941 to 2001) for which weather extreme indices show correlations (Kendall's tau) between the precipitation extreme indices with time that are no statistically significant. * Stations numbers are in correspondence with Table 3.2 and Fig. 3.6.

area (Region 10 in table 4.1) which is statistically significant at the 1% level. There are two geographical features of this region: the first is that it is located on the Mexican Southern Pacific Coast, so the Pacific Ocean certainly acts as one of the modulators of climatic variations in the area (Mitchell et al., 2002). The second characteristic is that the area is a well known forest zone (Villers-Ruiz and Trejo-Vazquez, 1998). The second is the Southeast rainforest region (Region 9 in table 4.1) which also has a negative correlation and it is statistical significant at the 5% level. This is an area of dense vegetation (García, 1988), within one of the wettest parts of the country. The effects of deforestation are a research topic that could be explored, as both regions are clearly reflecting that the precipitation is decreasing (Masera et al., 1997) that can be caused by the loss of vegetation. But, as will be addressed in Chapter 7, the El Niño Southern Oscillation (ENSO) phenomenon is another atmospheric modulator, complicating the understanding of the causes which control these climatic regions.

At the local level [(Fig 5.1. c)], in opposition to what has been observed with the regional PRCPTOT averages [(Fig 5.1. d)], a positive and significant correlation (with time) is evident for a number of stations. For Champotón, in Campeche State (station number 10 in Table 5.1, see Section 3.3.4.1) the correlation is significant at the 1% level and for Presa Rodríguez in Tijuana at 5% (station number 5 in Table 5.1). It is interesting that both rainfall stations are located at the heads of Peninsulas: Champotón within the Yucatan and Tijuana for the Baja California Peninsula respectively. The rainfall station at Champotón has been added for this analysis of extremes; it was not considered during the Principal Component Analysis (PCA) due to completeness and minimum time-series length conditions not being fulfilled. In Chapter 4, we saw that only during the dry season (November to April) could a climatic-related region be isolated here, as a result of the Principal Components Analysis (PCA). For this coastal area in the Gulf of Mexico Hurricanes during the wet season affect the annual totals (Englehart and Douglas, 2002), often leading to a completely different rainfall pattern when compared with the remaining stations across the country (see section 4.2). For Yecora station (number 32 in Table 5.1) within the North American Monsoon Region (NAMR) or Mexican Monsoon Region (see

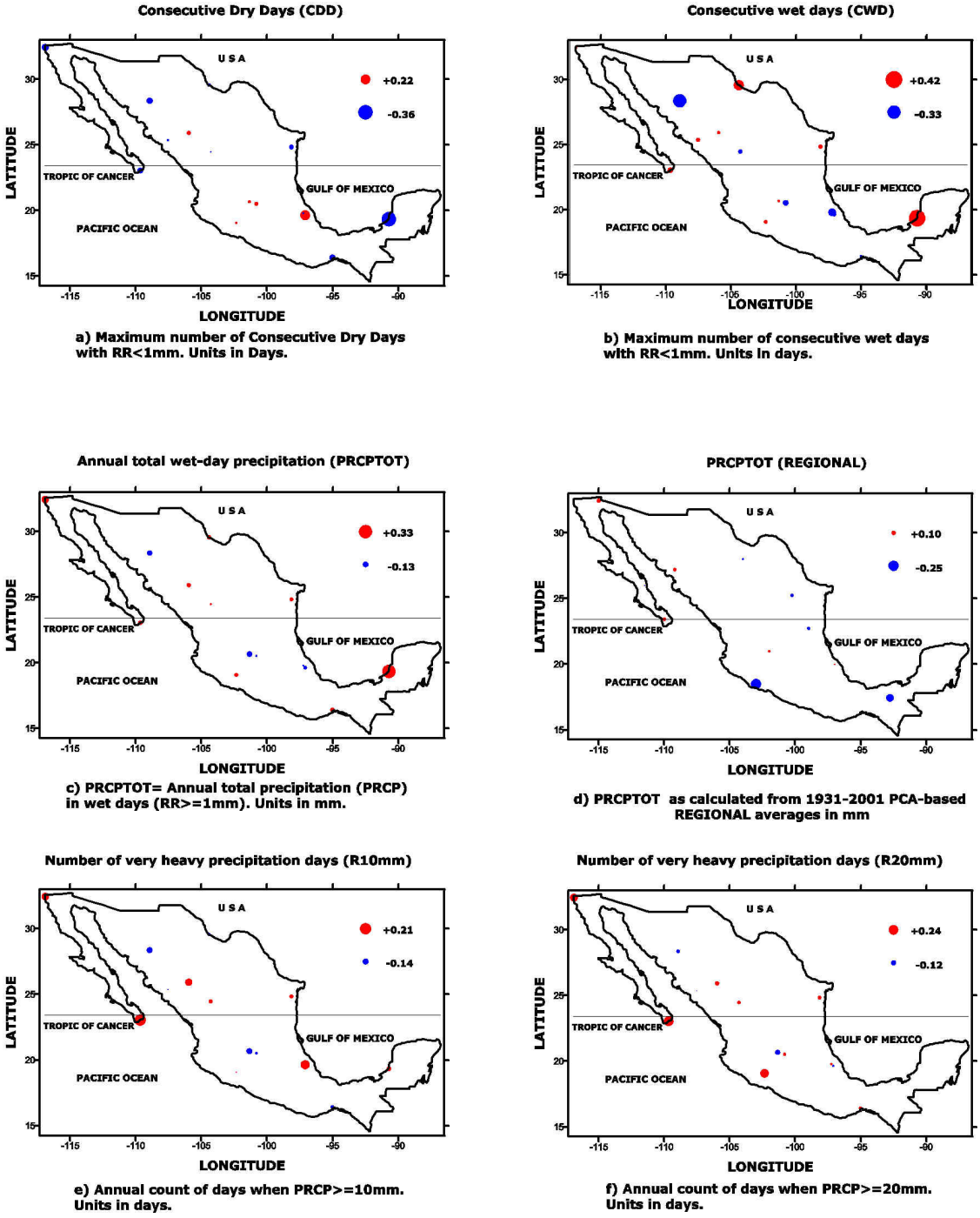

Fig. 5.1. Extreme precipitation indices maps. A Kendall's tau-b (linear) correlation analysis has been applied between the precipitation extreme indices and time. Circles red represent a positive and in blue negative correlations.

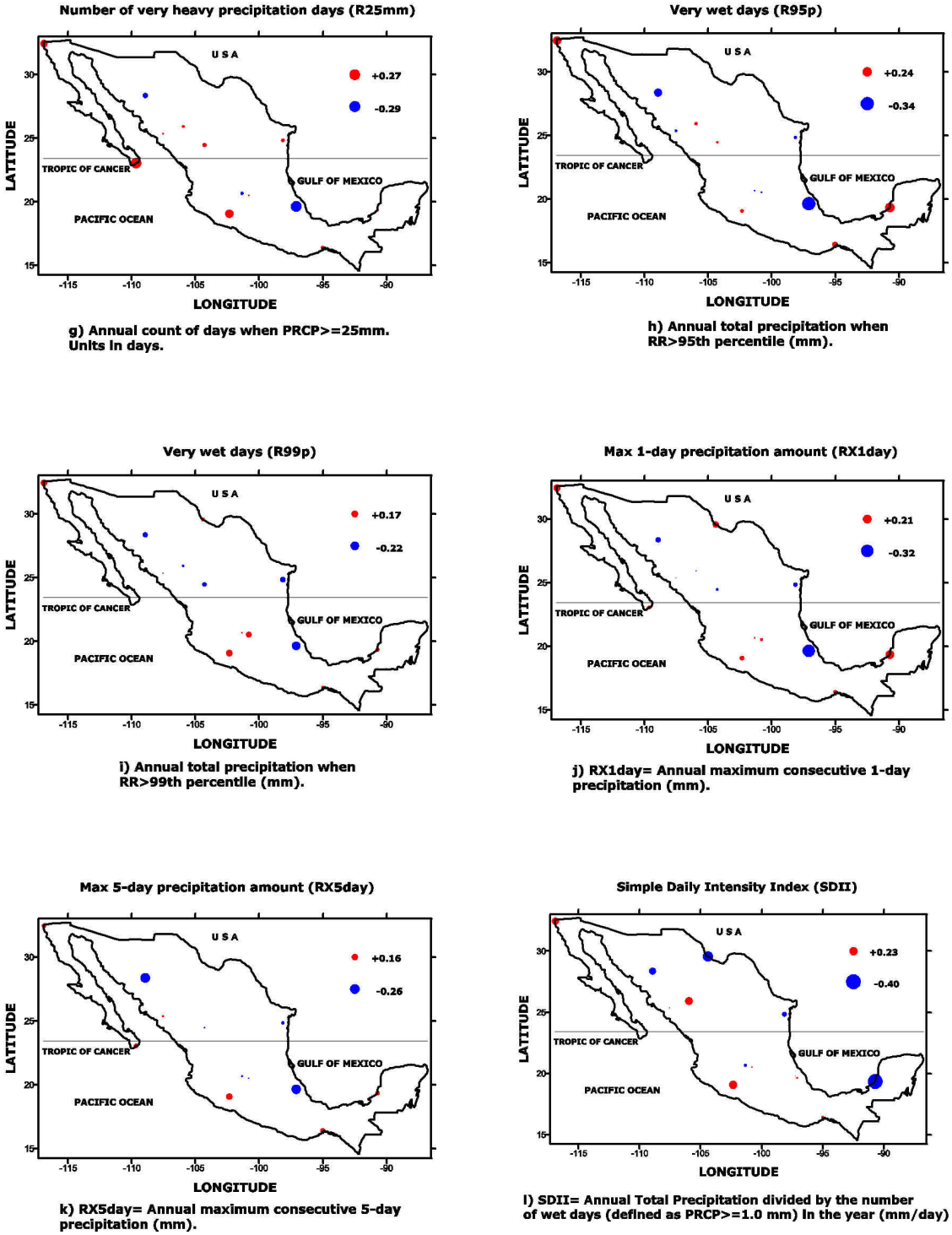

Fig. 5.1. Extreme precipitation indices maps. A Kendall's tau-b (linear) correlation analysis has been applied between the precipitation extreme indices and time. Circles red represent a positive and in blue negative correlations.

section 4.2), a positive correlation can be observed as well but this time it is not statistically significant.

One index that takes into account not only the total amount of precipitation throughout the year but also reflects changes in daily rainfall is the Simple Daily Intensity Index (SDII). SDII [(Fig 5.1 l)] combines the total amount of annual precipitation and the number of days when rainfall (greater than 0.1 mm) actually occurs (see Table 3.1 in Section 3.3.4). A roughly longitudinal transition can be observed in the results, with an east-west differentiation relatively clear. Positive correlations along the Pacific Coast are evident, suggesting that the ocean can be partly modulating the spatial pattern of SDII. For all the stations along the western side of the country the statistical significance remains below the 5% level. Contrasting negative correlations are observed along the eastern side, the partial connection with the Gulf of Mexico is weaker when compared with the former results along the Pacific Ocean. One pair of stations, Champotón and Ojinaga (station number 10 and 11 in Table 5.1) is below the 1% statistical level of significance for the SDII index. Champotón lies within an area frequently affected by the passing of hurricanes along the Atlantic coast (Jauregui, 2003).

The R95P and R99P [Fig 5.1. h) and i)] indices are used to measure heavy precipitation that exceeds the 95 and 99 percentile thresholds. Statistically significant negative correlations (with time) are found at Las Vigas (station number 35 in Table 5.1) for both indices: at 1% level of significance for R95P and 5% for R99P. As observed for local PRCPTOT [(Fig 5.1. c)], there is a marked positive correlation for the stations located at the head of the Peninsulas (Champotón and Tijuana, see Table 5.1 and Fig. 3.6) when R95P is considered. It can be stated that positive correlations are observed at the Peninsulas and negative correlations for those stations which are more continental.

Very heavy or intense rainfall is measured using the RX1day and RX5day [(Fig 5.1. j) and k)] indices, respectively. Clear negative correlations are observed for Las Vigas (number 35 in table 3.2), which is part of a large rainforest region. Although both extreme indices for this station are statistically significant, it is the RX1day index that lies

below the 1% of significant level. Less drastic is the change for the RX5day, for which we can observe only two correlations below the 5% of level of significance. Nevertheless, both correlations show a consistent pattern when compared with the results of R95p and R99p that leads to clear decreasing precipitation at Las Vigas. Although, the Max 5-day precipitation (RX5day index) map does not show any clear geographical pattern, reduced precipitation is also observed in the North American Monsoon or Mexican Monsoon Region (Region 11 in Table 4.1 of Section 4.2) for the RX5day index, lying below the 5% statistical significant level. The only positive correlation leading to increasing rainfall is found at the Champotón station in the Yucatan peninsula. This is possibly linked to enhanced hurricane activity in the region (Pielke et al., 2005).

Amongst the indices that can measure a change to drier conditions is the Consecutive Dry Days (CDD) Index. On the whole, statistically significant results are geographically concentrated in the southern part of the country [Fig 5.1 a)]. Central and Northern areas do not show clear (statistically significant) patterns of changing rainfall. However, contrasting correlations (between the CDD with time) are observed, in the South: an increasing pattern for Las Vigas (station number 35 in Table 3.2) and a negative correlation for Champotón (station number 10 in table 3.2); they are statistically significant at the 5 and 1% level respectively.

If CDD is a measure of dryness; then the Consecutive Wet Days (CWD) index [(Fig 5.1. b)], on the contrary, reflects time-series variations that can lead to wetter conditions. There is little of a geographical pattern to the map for CWD across Mexico. Nevertheless, there is some consistency for the stations Las Vigas and Champotón (station number 35 and 10 in Table 3.2) in comparison with those of CDD: this time a positive correlation (below the 5% of statistical level of significance) is seen for Las Vigas station and a negative correlation for Champoton (below the 1% statistical level of significance). Thus, these two indices both point to wetter conditions for Champotón, Campeche and drier patterns for Las Vigas. Additionally, for the first time in the discussion of rainfall extreme indices one of the stations within the NAMR (Region 11 in Table 4.1) shows a

level of statistical significance below the 1% for CWD. This is evident in the negative correlation for the Yecora Station (see table 3.2 in chapter 3) in Sonora. In contrast, though, none of the surrounding stations in the North Pacific area, including the Baja California Peninsula; show similar results. Finally, the border (Mexico-USA) station at Ojinaga (station number 11 in Table 3.2) shows an increasing trend in CWD significant at the 5% level of significance.

Lastly, the persistence of intense precipitation can be measured by the number of cases of daily rainfall exceeding the 10mm, 20mm and 25mm limits, defined as the R10mm, R20mm and R25mm indices. A longitudinal transition can be observed in the maps [(Fig 5.1. e) f) and g)]: positive correlations (increasing precipitation) for the western part of Mexico and negative correlations (reducing precipitation) of these precipitation extreme indices tith time for the eastern part of the country. More stations with statistical significant results, leading to coherent and more easily interpretable regions are found for the R20mm and R25mm indices. Stations with consistent results across the indices are San José del Cabo and Apatzingán (station numbers 7 and 20 in Table 5.1). Coincidently, both stations are located within the western part of Mexico, probably being partly modulated by the Pacific Ocean (Magaña et al., 1999). The most significant result for San José del Cabo is the increase for the R25mm index, being below the 1% of statistical significance level, in addition R10mm and R20mm are significant at 5% statistical level. Positive correlations are also seen for the Apatzingán, where the number of cases surpassing the 20 and 25mm thresholds (R20mm and R25mm) are significant at the 5% level. Negative correlations (with time) are present for Irapuato (station number 17 in Table 5.1) and Las Vigas (both significant at 1%) for the R10mm and R25mm indices respectively. Finally, positive correlation is found at Tijuana (5% statistical significant) for the R20mm index.

In Mexico, rainfall patterns are generally well defined by taking into account total annual precipitation: wet conditions south of the Tropic of Cancer and dry conditions to the north of this geographic limit (see section 2.1). As in the case of regional PRCPTOT, this

characteristic opens the possibility of exploring this climatic transition for weather extreme indices as well.

Is there also a latitudinal transition when we study the rainfall extreme indices? Do they preserve the contrasting picture observed for the total annual precipitation (regional PRCPTOT)? Are these patterns following what has been shown for PCA regions (see section 4.2.1)? Table 5.1 shows the distribution of positive and negative Kendall's tau correlations, when levels are statistically significant at 5 or 1%. The patterns of positive/negative correlations with time show the (defined) climatic transition. This can be clearly perceived with statistically significant positive correlations at 1%, in which the number of cases clearly changes from South to North (3 to 0). Champotón (station number 10 in table 5.1) has two statistically significant indices: CWD and PRCPTOT; and R25mm is the statistically significant index for San José del Cabo (station number 7 in Table 5.1). The same contrasting pattern is true when values with negative correlations statistically significant at the 1% level (9 cases) are greater compared to their counterparts at 5% (2 cases). In general, positive correlations that are statistically significant at 5% are more frequent than those at 1% (14 versus 3). In fact, about one half of the numbers of total cases (29 statistically significant correlations) are concentrated in the positive correlations at 5% (14), and around one third with negative correlations significant at 1% (9). Therefore, together they account for about 75% of the cases in total.

South to North contrasting conditions are also evident when statistically significant levels are studied (Table 5.2). The climatic transition is better observed when positive correlations at 5% (8 to 6) are compared to those at 1% (3 to 0), the difference is more drastic for the latter. The eight statistically significant positive correlations at the 5% level in the South are distributed as follows: San José del Cabo (R10mm, and R20mm), Champotón (R95P, RX1day), Apatzingán (R20mm, R25mm, and SDII) and Las Vigas (CDD). Values are greater in the South for both 5 and 1% significant levels regardless of whether positive/negative correlations (of the precipitation extreme indices with time) are considered.

	North	South	Total
Pos. Corr. (5%)	6	8	14
Pos. Corr. (1%)	0	3	3
Neg. Corr. (5%)	1	2	3
Neg. Corr. (1%)	3	6	9
Total	10	19	29

Table. 5.3. Geographical patterns of positive/negative correlations (rainfall extreme indices with time using Kendall's tau) with statistical significant levels at 5 and 1%. The numbers of cases are classified defining the Tropic of Cancer as the divide to separate the northern/southern regions.

Positive and negative significant correlations of the rainfall extreme indices with time can also give us valuable information about wet and dry conditions. These relations are expressed in Table 5.3. Stations with correlations pointing to more precipitation (wet conditions) account for around two thirds (18) of the cases (29), with the southern part of the country reflecting changes in 19 of the totals. The latitudinal climatic transition is better observed during dry than wet conditions, as the northern half of the country has only 4 cases, while the southern part accounts for 7 statistically significant correlations of the total of 11 significant results, showing a change in the rainfall extreme indices to drier conditions.

At local level, the stations Champotón (RX1day, CWD, PRCPTOT, R95P, CDD and SDII) and Las Vigas (CDD, R99P, R25mm, R95P, RX1day, and RX5day) account for nearly 63% of the cases of statistically significant results (using the extreme indices) in the southern part of the country. Likewise, for the northern part, the stations at Presa Rodríguez in Tijuana (PRCPTOT, R20mm, R95P, SDII) and Yecora (CWD, R95P,

RX5day) together have around 64% of the totals of statistical significant results. Therefore, for both the north and south, only two stations have about two thirds of the indices with significant correlations.

	North	South	Total
Wet	6	12	18
Dry	4	7	11
Total	10	19	29

Table. 5.4. Geographical patterns of positive/negative correlations (rainfall extreme indices with time using Kendall's tau) with statistical significant levels at 5 and 1%. The number of cases are classified defining the Tropic of Cancer as the divide to separate northern/southern results.

5.2.2. LINEAR TREND ANALYSIS.

Until now, for non-parametric correlations applied in this chapter on rainfall extreme indices, statistically significant results and spatial analyses have shown us a geographical (north-south) transition in the results. Giving the impossibility of the Kendall-tau test (see section 3.3.5) to calculate the magnitude of the trends, we are now going to study the trends and plots computed by the R software (section 3.3.4) utilizing least-squares fittings. A positive autocorrelation can affect severely the detection of a significant trend, leaving the calculation unreliable (Zhang et al., 2005). In order to test this possibility, serial correlation magnitudes were computed using SPSS 14.0 before the estimation of significant trends, and none of them show a considerable positive autocorrelation able to influence the results.

There is one characteristic that both halves of Mexico (defining the tropic of Cancer as the geographic divide) share: two stations concentrate about two thirds of the total of the statistically significant correlations (Table 5.1). Champotón and Las Vigas in the southern half and Presa Rodríguez and Yecora in the northern half of the country were chosen to evaluate the trends for several rainfall extreme indices. The most prevalent indices among the stations were selected for this assessment. For instance, R95P has statistically significant results in all the stations evaluated, and two of the most important indices PRCPTOT and SDII (see table 3.1) in three of the four stations considered.

The selected indices also give different insights about the secular changes of precipitation in Mexico, like changes in totals (PRCPTOT) or in percentiles as is the case for the R95P and R20mm indices. In this sense, it is expected that the chosen indices will be sufficient to get information on the rainfall indices variations across Mexico, and also to test the hypothesis of (north-south) climatic transition in the country.

The first rainfall extreme index to be analysed is the annual total precipitation (PRCPTOT see Table 5.1). This is one of the most extensively analysed indices in climatology, in which we can clearly observe the differences in the rainfall amounts across the year among the stations considered. A downward trend is found at Las Vigas (station number 35 in table 5.1) pointing towards drier conditions. The magnitude of the trend calculated by least-squares is about -42.7 mm/decade for a climatological mean of 1152.1 mm per year, with a clear decrease in total rainfall since the 1960s [Fig. 5.2 b)]. Wetter conditions are also observed at Champotón, the other southern station assessed [Fig. 5.2 a)]. In fact its positive trend is larger than the observed trend for Las Vigas (+65.1 mm/decade with an annual mean of 1261.7 mm per year). The slight positive trend in hurricane activity during recent decades is likely to be affecting this increased precipitation (IPCC, 2007; Jauregui, 2003). Contrasting trends are also observed in the northern part of the country. Although having several missing years, Yecora station shows a clear decreasing trend (-71.7 mm/decade, and a long-term mean of 1117.6 mm per year) [Fig. 5.2 c)]. Meanwhile a modest positive slope is found for the Presa Rodríguez station in Tijuana with a changing pattern to wetter conditions, its trend shows

an increase of 9.9 mm/decade (the long-term mean of the station is 232.9 mm per year). The recent increase in ENSO activity could be affecting the annual total rainfall of this station [Fig. 5.2 d)]. This aspect will be discussed later in Chapter 7.

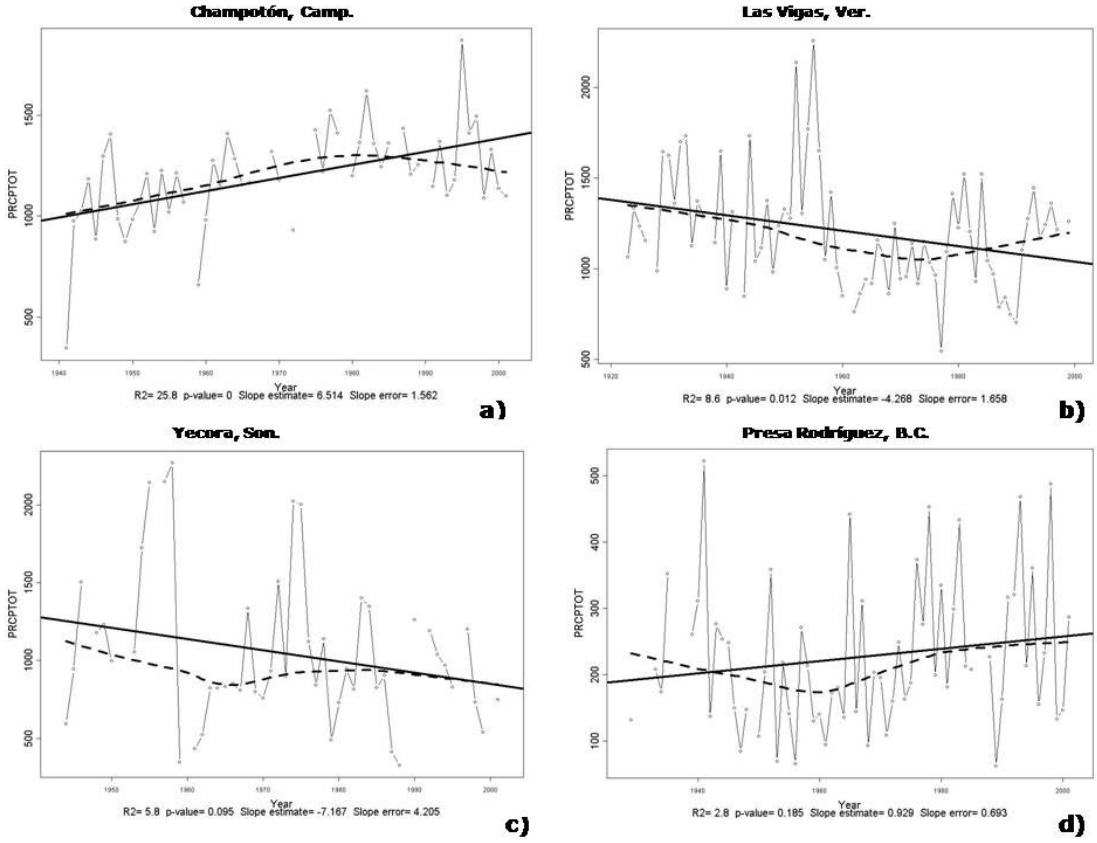

Fig. 5.2. Linear trends calculated using a least-squares fitting on the annual total precipitation (PRCPTOT) of the stations with the largest number of statistically significant results (see Table 5.1).

Contrasting trends are also observed for the R20mm index. As pointed out in Section 3.3.4 (see table 3.1), R20mm counts the number of days per year when daily precipitation exceeds a pre-defined 20 mm threshold. In the northern part of the country, a clear trend of decreasing rainfall is observed at Yecora station (about -1 day/decade) [Fig. 5.3 c)].

Wetter conditions are observed at Tijuana (Presa Rodríguez station), its positive trend (+0.14 days/decade), is, though, almost imperceptible [Fig. 5.3 d)]. The Mexican Monsoon and the ENSO phenomenon are the possible physical mechanisms that partially modulate the R20mm index at Yecora and the Presa Rodríguez stations. Gradual changes in R20mm are also observed in the southern half of the country. A slight positive trend (+0.19 days/decade) is observed at Champotón (station number 10 in Table 5.1), in which sudden jumps occur in a quasi-cyclic mode according to the plot [Fig 5.3 a)], likely being partially modulated regularly by hurricane activity. A modest change towards drier conditions (negative trend of -0.32/decade) is observed at Las Vigas near to the Gulf of Mexico [Fig 5.3 b)]. Therefore, we can say that contrasting conditions are observed in both the northern and the southern part of Mexico. Positive trends are observed in those stations located in the Peninsulas (Presa Rodríguez and Champotón), while negative trends are found in the more continental stations (Yecora and Las Vigas).

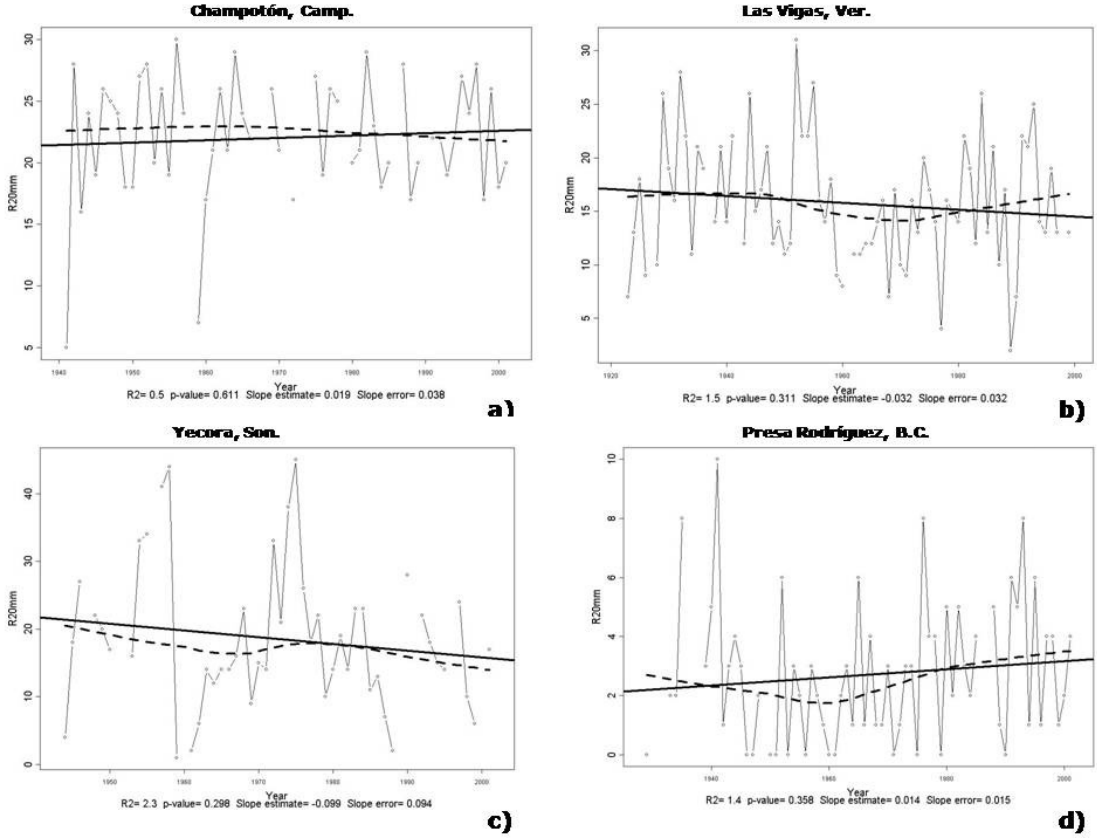

Fig. 5.3. Linear trends calculated using a least-square fitting on the Very Heavy Precipitation Days (R20mm) index of the stations with the largest number of statistically significant results (see Table 5.1).

Contrasting patterns can be appreciated between the stations in both the northern and southern part of Mexico for the R95P index. For instance, in the northern part of Mexico a clear downward trend (-52.7 mm/decade) is observed at Yecora within the Mexican Monsoon (North American Monsoon) Region (see section 4.2.1). A clear decrease in magnitude (amounts) of the peaks is evident for the most recent years. An upward slope is seen for Presa Rodríguez, it has a less pronounced trend than Yecora with a change of about +6.8 mm/decade, and the most important peaks of the indices are found in the 1990s. It is important here to point out that this upward trend in recent peaks is coincident with a period of long "El Niños" during the same decade (Allan and D'Arrigo, 1999). In the South of Mexico, Las Vigas shows an important downward trend (-46.8 mm/decade), leading to drier conditions. As mentioned above for the PRCPTOT index, deforestation (along with El Niño influence discussed in Chapter 7) may be playing an important role in modulating the climate at this location. Meanwhile a recent increasing hurricane activity (Jauregui, 2003) seems to be affecting the R95P index pattern at Champotón (station number 10 in Table 5.1 and Fig. 3.6). A trend of +26.0 mm/decade is found at this station. Overall, for the R95P index, upward trends are found for the stations in the peninsulas (Champotón in the Yucatán peninsula, and Presa Rodríguez in the peninsula of Baja California), and downward trends for the stations within the main continental land (Las Vigas and Yecora).

In the northern part of the country, we can observe consistency with the former indices evaluated when the trends of SDII are considered. An upward trend (+0.2 mm/day/decade) is found at Presa Rodríguez station in Tijuana. A marked increase in the precipitation intensity is especially observed during the last two decades of the records that is apparently in phase with a period of longer El Niños (Allan and D'Arrigo, 1999), and is also linked to an increase in the amount of annual total rainfall [Fig. 5.2 d)] for this station. Slightly larger in magnitude is the negative slope (when compared with Presa Rodríguez station in Tijuana) at Yecora station (-0.7 mm/day/decade). This pattern leading towards drier conditions seems to be directly linked to a decrease in the annual total precipitation [as in Fig. 5.2 d)] rather than the number of wet days [Fig. 5.1 b)]. The

southern half of Mexico also shows contrasting patterns between the analysed stations when the SDII is assessed. An almost imperceptible positive trend (+0.16 mm/day/decade) is found at Las Vigas. This is an interesting case, because as we

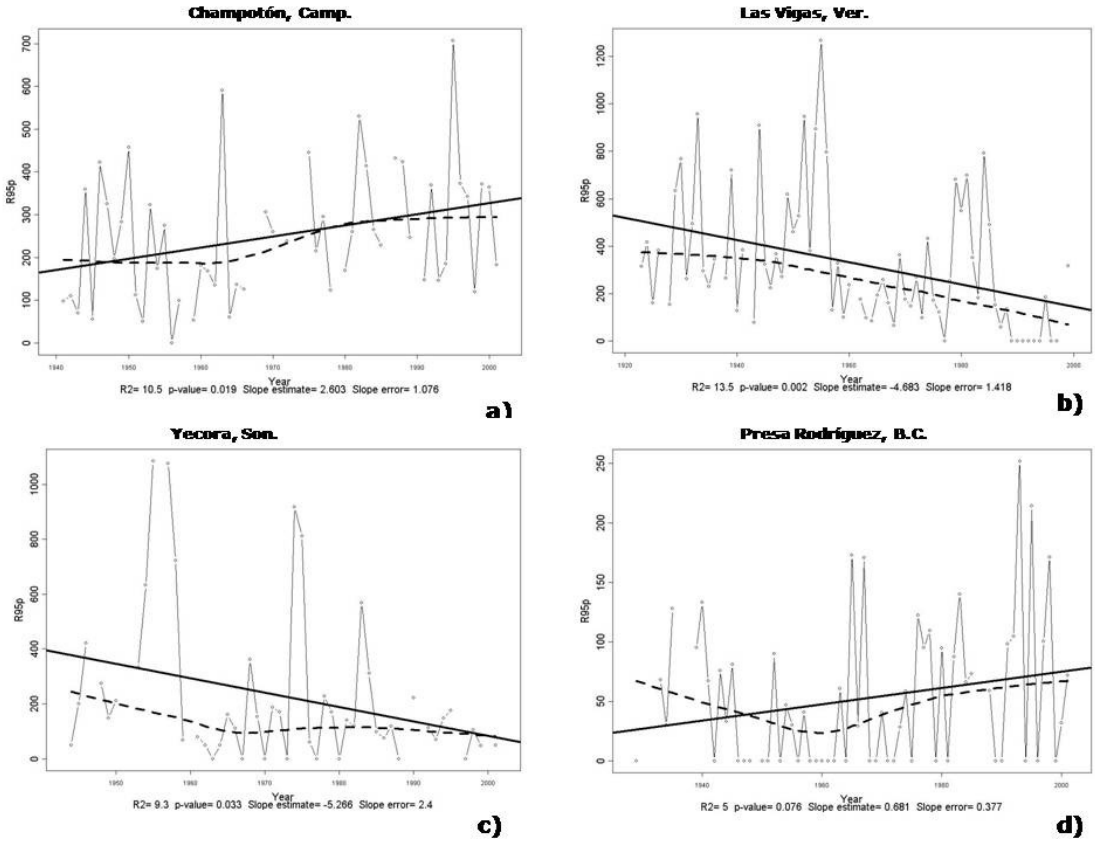

Fig. 5.4. Linear trends calculated using a least-square fitting on the Very Wet Day Precipitation (R95P) index of the stations with the largest number of statistically significant results (see Table 5.1).

have seen the PRCPTOT index [as in Fig. 5.2 b)] pointing towards drier conditions; it seems that the number of wet days has a greater influence on the SDII index [Fig. 5.1 b)]. It is clear that the annual total precipitation is decreasing at a slower rate than the number of days when rains occurs. Finally the clearest trend on SDII is found at Champotón within the Yucatán peninsula. The downward trend (-1.4 mm/day/decade) is directly affected by an increase in the number of wet days [Fig. 5.1 b)] rather than the annual total precipitation (PRCPTOT) that shows a pattern towards wetter conditions. It can be said that this region (Yucatán peninsula) has been recently affected by increasing hurricane

activity (IPCC, 2007), but in also more rainy days have been observed during the year, leading to a decrease in the daily intensity index (SDII) at Champotón.

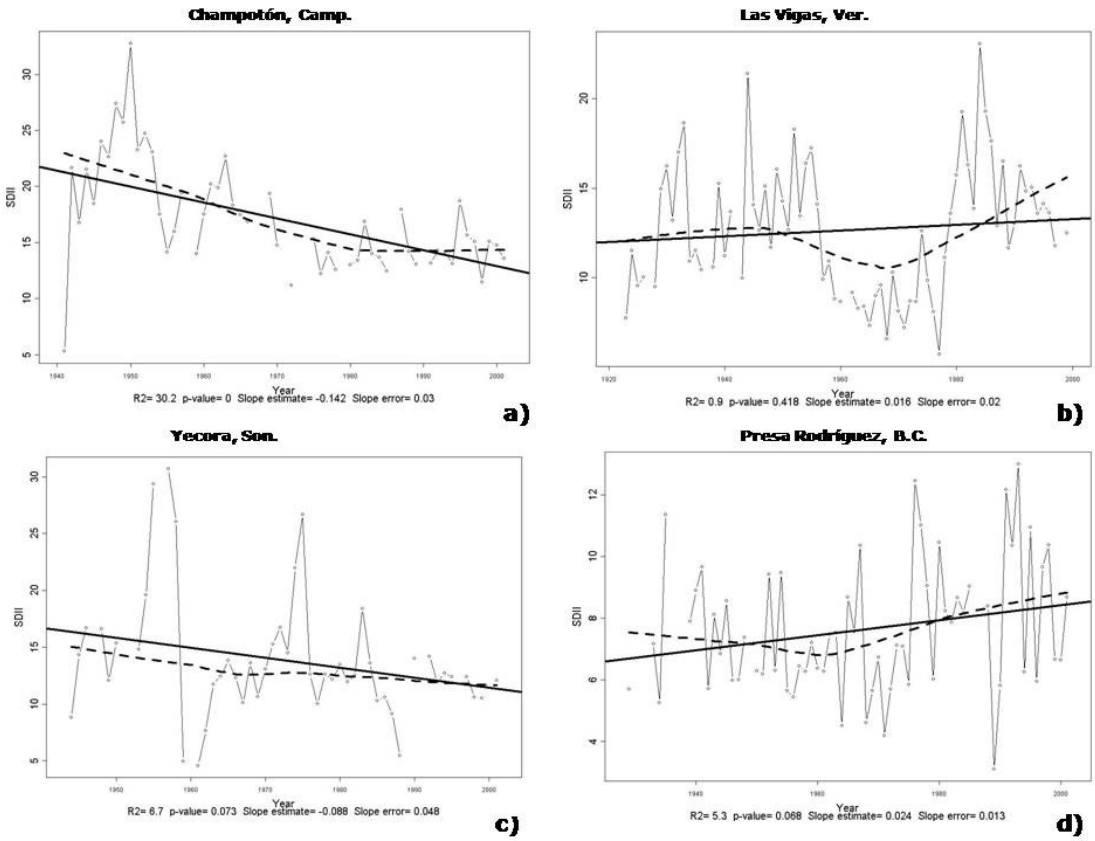

Fig. 5.5. Linear trends calculated using a least-square fitting on the Severity Daily Intensity Index (SDII) index of the stations with the largest number of statistically significant results (see Table 5.1).

Although subtle differences appear when the daily intensity index (SDII) is evaluated, the analysis of trends, for the stations having more statistically significant correlations, has shown consistency across the results. The pattern is clear: increasing trends in the peninsulas and negative trends in the mainland stations. Presa Rodríguez in the peninsula of Baja California, and Champotón in Yucatán are evident examples of how even modest changes in large-atmospheric controls can affect local climates. Within a semi-arid region in Tijuana, the precipitation at the Presa Rodríguez station is strongly affected even with changes in normal atmospheric conditions, like those occurring during El Niño years in this part of the country (Dettinger et al., 2001, Trenberth and Caron, 2000). A different

large-atmospheric control is observed at Champotón station within the Yucatán peninsula. Hurricane associated rainfalls can completely disrupt the local climate in comparison with neighbouring locations. This separation from normality is fully appreciated in the PCA of rainfall (section 4.2.1) when a pattern can only be extracted in the dry season (Nov-Apr), evidently linked to the hurricane-free period in the North Atlantic Ocean basin. Less evident are the physical causes that invoke changes in the precipitation extremes in the stations located in main continental Mexico. Nevertheless, Yecora has consistently shown the largest trends of the four studied stations; but we have to say that Yecora also has the greatest percent of missing data, especially for recent years, and this might be affecting the results. Being at the core of the Mexican Monsoon Region (Region 11 in Table 4.1) and with an altitude of 1500 m.a.s.l., Yecora is directly impacted by the secular changes of the summer rainfall patterns (Cavazos et al., 2002). It is important to point out here the contrasting trends (for the different rainfall extreme indices studied) observed between Yecora in Sonora state and Presa Rodríguez in the northern part of the Baja Californian peninsula; the sea of Cortez can be counted as a possible cause for these different climatic patterns (Stensrud et al., 1997). Finally, as Las Vigas station is located within a region of dense vegetation; deforestation is likely to be the main physical force modulating the trends that lead to drier conditions (Villers-Ruíz and Trejo-Vázquez, 1998). However, as is going to be explored in Chapter 7, the El Niño phenomenon cannot be discarded as another atmospheric control partially modulating its rainfall extremes.

5.3. CONCLUSIONS TO THE CHAPTER.

The occurrence of climate extremes is very rare in terms of their frequency, but large when referred to intensity. Therefore, the study of these sorts of events is of great importance because of the impacts they can have on our socio-economic activities. The knowledge of the patterns and changes over time contribute to understand their nature and causes and indirectly to mitigate their damages.

Total Annual Precipitation (PRCPTOT) shows contrasting conditions for local or regional patterns. Regional precipitation reflects a southern decreased precipitation especially for forested regions possibly suggesting a link to deforestation. However, locally increasing precipitation is observed for those stations located at the head of the Baja California and Yucatan Peninsulas.

In different ways both oceans modulate weather extremes in Mexico. If we only consider statistical significant results, increased precipitation patterns are found in the stations near the Pacific Coast; contrasting with a downward trend observed for those along the Gulf of Mexico. The indices considered to identify this geographic transition are expressed as frequency (number of cases) instead of magnitude and rate.

There is another interesting geographic pattern observed in the (linear) correlations of precipitation extreme indices with time across Mexico. Increasing rainfall trends are found for those stations located at the head of the Peninsulas; in contrast to rainfall stations with a continentality factor that show a reduced precipitation. The partial modulation of the climate by the ocean is suggested here as well.

The analysis performed in this chapter is leading towards some interesting results. When considering statistical significant levels, around 60% of the total accounts for the results significant at 5%, and consequently the remaining near 40% are related to a statistical significance at 1%. Disregarding the sign of the correlations and the statistical significance, the number of cases in the south is greater than in the north of the country.

This latitudinal climatic transition is also repeated when wet weather is contrasted to dry conditions. Once more, the southern part of the country consistently outnumbers the number of cases of significant correlations, than in the north.

Four stations involve about two thirds of the total number of statistically significant results: Presa Rodríguez and Yecora (stations number 2 and 32 in Table 5.1) in the northern part of Mexico; in the south Champotón and Las Vigas (stations number 10 and 35 in Table 5.1). When an analysis of trends is performed for these stations, the results show consistency with the other analyses applied in this chapter: stations in the peninsulas exhibit trends towards wetter conditions, while stations within the continent are pointing towards drier patterns. Those stations at the head of the peninsulas (Champotón and Presa Rodríguez) are directly affected by sudden changes in large-atmospheric controls like Hurricanes or ENSO. Although modulated by more gradual variability (mostly deforestation and the Mexican Monsoon) clear changes on rainfall extremes are found for Las Vigas and Yecora station. There is one clear geographical feature after the analysis of trends: either continental or peninsular, all the stations evaluated are close to the Mexican coasts. Therefore, both the Atlantic and Pacific Oceans play a key role partially controlling the evolution of the rainfall extremes across Mexico.

CHAPTER 6: TEMPERATURE EXTREME INDICES.

6.1. INTRODUCTION.

2005 was the equal warmest (with 1998) global average surface temperature (http://www.nasa.gov/vision/earth/environment/2005_warmest.html). It is important to realise, however, that these extreme conditions in 2005 took place without concomitant El Niño conditions, as was the case in 1998. Temperatures have risen by 0.7°C during the 20th century (IPCC, 2007) that has also been the warmest for the Northern Hemisphere during the last millennium (Osborn and Briffa, 2006). At the continental scale, Europe experienced unusual warmth during the 2003 heatwave; and it was probably the warmest summer since at least 1500 (Luterbacher et al., 2004). Furthermore, this "surprising" climatic pattern closely agrees with some of the scenarios of future climate (2080s) rather than the 1961-1990 normals; and at the local level, averaged June-July-August (JJA) Tmax at Basel, Switzerland exceeded the 29° C threshold for the first time in its long-term instrumental records (Beniston, 2004). At a larger scale, a global study of weather extremes (Alexander et al., 2006) shows a marked upward tendency in daily temperature extremes, particularly towards less cold rather than warmer conditions across the world.

Partly caused by the warm atmospheric conditions of 1998, one of the warmest years on record (a year also associated with the 1997-1998 ENSO phenomenon, one of the strongest ENSOs ever recorded, Magaña, 1999), large areas of North America were under drought conditions during the period between 1998 and 2002 including the Canadian Prairie Provinces, the United States (especially the western states and the Great Plains regions) and northern and western Mexico (Cook et al., 2004). In fact the intensity of the drought ranged from severe to extreme conditions in nearly 30% of the conterminous USA at the beginning of June 2002 (Lawrimore et al., 2002). Due to the intense drought of 1998 (On May 9, 1998, Mexico City recorded 33.9° C, the warmest day on instrumental records, http://www.dbc.uci.edu/~sustain/ENSO.html) the Mexican government needed to intervene financially in order to mitigate the impacts in twelve northern states of the country (Magaña, 1999). Because of these extreme dry conditions

the water supply for agricultural purposes was so scarce along the USA-Mexican border (Cason and Brooks, La Jornada 6/6/2002) that, in Mexico, the federal government and most of the northern Mexican states needed to negotiate in order to comply with the 1944 treaty with the USA that deals with Transboundary water management (Venegas, La Jornada 6/6/02).

The evidence is then accumulating: across different scales of time and space scales, the global climatic conditions are likely moving towards warming. With warming of average temperatures we should expect increases in both the intensity and the frequency of weather extremes (Beniston and Stephenson, 2004). Despite, these diverse efforts to assess weather extremes there is still a necessity for the improvement of daily data archives to undertake these studies especially, in developing countries (New et al., 2006). This chapter aims to deal with the evaluation of extremes events in daily temperatures in Mexico, in order to help to fill a research gap for the region in climatic studies.

Changes in temperature extremes at local scales are analysed using daily temperature records. Here, we discuss the results of calculating non-parametric linear correlations in extreme temperature indices (defined in section 3.3.4) with time from 26 sites with the longest and more complete (data from 1941 to 2001) daily temperature series (Table 6.1; see also table 3.2 and fig. 3.6). All the stations are tabulated (in Table 6.1), whether their positive or negative correlation was statistically significant at the 5 or 1% level and those locations with the greatest number of cases (extreme indices, for their definitions see table 3.1 in chapter 3) evaluated. The purpose is to identify whether the correlations are spatially coherent across the country. Is the pattern of correlations random or is there a spatial structure?

In order to overcome the restriction of working at a local scale, the second analysis of the chapter was undertaken with the extreme temperature indices independently. The parameters were analysed separately in three different groups. The first group deals with the temperature intensity in °C, with the two remaining groups working with records

exceeding set limits: the first kind of limit relates to absolute temperature thresholds in °C, and the second with a percentile (variable from season to season and between stations) limit. The main purpose of these tests was to check spatial consistency in the patterns: local versus larger scales.

With the similar objective of contrasting geographical (latitudinal, longitudinal or elevational) transitions, the next analysis deals with the extreme temperature indices and not solely the individual stations. The statistically significant correlations of the indices with time were counted using two different approaches to evaluation: considering statistical significance levels (positive/negative at the 5 or 1% level) and identifying warmer/colder conditions according to the extreme temperature indices. For both assessments the Tropic of Cancer was established as a geographic limit to separate the southern and northern part of Mexico.

The last analysis of the chapter calculates linear trends using the least-squares approach of the R software explained in section 3.3.4. A pair of stations north and south of the Tropic of Cancer having the largest number of statistically significant results were selected in order to calculate and geographically compare the linear trends among the chosen time-series.

6.2. DISCUSSION.

In order to evaluate which stations with daily data from 1941 to 2001 are experiencing the most drastic changes in the daily temperature records, we have tabulated the stations with extreme temperature indices (defined in table 3.1 of section 3.3.4) that are exceeding the statistical significant levels at the 5 and 1% (Table 6.1). We have decided –as a preliminary stage to further analyses, to consider only those stations that had at least 7 indices with statistically significant results. Two stations have 11 statistically significant results, two more have 8 and a further three have 7. These parameters have been

separated into positive or negative correlations (of the temperature extreme indices with time) in order to facilitate the identification of patterns leading locally towards warming or cooling conditions.

El Paso de Iritu, Baja California (station number 4 in Table 6.1), in the northern part of Mexico, according to the climatic division defined by the Tropic of Cancer; and Ahuacatlán, Nayarit (station number 25 in Table 6.1); south of the Tropic of Cancer are the stations that have more statistically significant results than the rest, both of them independently counting 11 extreme weather indices. The Baja Californian station (El Paso de Iritu) shows that indices related to minimum temperature (TN90p, TN10p, TNn, TNx, TXn, TX10p, CSDI) are the most important in terms of changing climatic patterns. Clearly, at this station, we can observe positive correlations (warming trends) for the night time temperatures (TN90p, TN10p, TNn and TNx). As for the southern station (Ahuacatlán) eight out of the eleven indices (SU25, TN90p, TNn, TNx, TR20, TX90p, TXx and WSDI) with statistically significance at 1% level emphasise negative correlations (cooling trends). Contrasting the results of Ahuacatlán with those of el Paso de Iritu, it can be stated that the extreme climate indices of maximum temperatures are tending towards cooler temperatures. A warming/cooling latitudinal transition can be observed between these two stations with the most statistically significant indices.

Number*	STATION	STATE	Pos. Corr. Statist. Signif. at 5%	Pos. Corr. Statist. Signif. at 1%	Neg. Corr. Statist. Signif. at 5%	Neg. Corr. Statist. Signif. at 1%
1	PABELLON DE ARTEAGA	AGS			SU25, TXx, WSDI	TX90p
2	PRESA RODRIGUEZ	BC	TXx	SU25, TX90p		TX10p
3	COMONDú	BCS	DTR, SU25	TNn, TXn		TNx, TX10p
4	EL PASO DE IRITU (11)	BCS	TN90p, Tx90p, TXn, TXx	CSDI, DTR, TN10p		TNn, TNx, TR20, TX10p
5	LA PURÍSIMA	BCS				
6	SAN BARTOLO	BCS		TNn		TN10p
8	SANTA GERTRUDIS (8)	BCS		TNn	SU25, TXx	TN90p, TNx, TR20, TX90p, WSDI
9	SANTIAGO (7)	BCS	TXn	DTR, TX90p, TXx	FD0	TN90p, TX10p
14	EL PALMITO	DUR	TXn	TNn, TX90p	TNx	FD0, TN10p
15	SANTIAGO PAPASQUIARO	DUR		TNn, TXn	TN10p	FD0
17	IRAPUATO	GTO		CSDI, TX10p		SU25, TN90p, TXn
18	PERICOS	GTO		TNn, TNx	DTR	FD0, TN10p, TX10p
19	SALAMANCA (8)	GTO	TNn	TX10p	SU25, TN10p	DTR, TX90p, TXx, WSDI
21	CUITZEO DEL PORVENIR	MICH	TXx	TNn	CSDI, DTR	FD0, TN10p
22	HUINGO	MICH	CSDI		DTR	TN90p
23	CIUDAD HIDALGO	MICH				TN90p, TNx
24	ZACAPU (7)	MICH	CSDI, TX10p		TXx	DTR, SU25, TX90p, WSDI
25	AHUACATLAN (11)	NAY	CSDI	TX10p	TN10p	SU25, TN90p, TNn, TnX, TR20, TX90p, TXx, WSDI
26	LAMPAZOS	NL			TNx, TXx	
28	MATIAS ROMERO (7)	OAX	TX90p	TNx, TR20, TXx, WSDI	TN10p	DTR
29	SANTO DOMINGO TEHUANTEPEC	OAX		TXn, TXx	TR20	TNx
30	MATEHUALA	SLP		TXx		
31	BADIRAGUATO	SIN	TR20			
33	SAN FERNANDO	TAM			WSDI	
34	ATZALAN	VER	TNn, WSDI	TX90p, TXx		Tn10p
35	LAS VIGAS	VER		TXn	CSDI, SU25, WSDI	TN90p, TX10p

Table 6.1. List of temperature stations (with data from 1941 to 2001) show correlations (Kendall's tau) between the temperature extreme indices with time, that are statistically significant at 5 and 1% level. The stations with the most statistically significant correlations are marked with (11), (8), and (7) depending on the number. * Stations numbers are in correspondence with Table 3.2 and Fig. 3.6.

	STATION	STATE	Non Significant Correlations
1	PABELLON DE ARTEAGA	AGS	FD0, ID, TR20, GSL, CSDI, TNx, TXn, TNn, DTR, TN10p, TX10p, TN90p
2	PRESA RODRIGUEZ	BCN	FD0, ID, TR20, GSL, WSDI, CSDI, TNx, TXn, TNn, DTR, TN10p, TN90p
3	COMONDú	BCS	FD0, ID, TR20, GSL, WSDI, CSDI, TXx, TN10p, TN90p, TX90p
4	EL PASO DE IRITU	BCS	FD, SU25, ID, GSL, WSDI
5	LA PURíSIMA	BCS	FD0, SU25, ID, TR20, GSL, WSDI, CSDI, TXx, TNx, TXn, TNn, DTR, TN10p, TX10p, TN90p, TX90
6	SAN BARTOLO	BCS	FD0, SU25, ID, TR20, GSL, WSDI, CSDI, TXx, TNx, TXn, DTR, TX10p, TN90p, TX90p
7	SANTA GERTRUDIS	BCS	FD0, ID, GSL, CSDI, TXn, DTR, TN10p, TX10p
8	SANTIAGO	BCS	SU25, ID, TR20, GSL, WSDI, CSDI, TXx, TNx, TNn, TN10p
9	EL PALMITO	DUR	SU25, ID, TR20, GSL, WSDI, CSDI, TXx, DTR, TX10p, TN90p
10	SANTIAGO PAPASQUIARO	DUR	SU25, ID, TR20, GSL, WSDI, CSDI, TXx, TNx, DTR, TX10p, TN90p, TX90p
11	IRAPUATO	GTO	FD0, ID, TR20, GSL, WSDI, TXx, TNx, TNn, DTR, TN10p, TX90p
12	PERICOS	GTO	SU25, ID, TR20, GSL, WSDI, CSDI, TXx, TXn, TN90p, TX90p
13	SALAMANCA	GTO	FD0, ID, TR20, GSL, CSDI, TNx, TXn, TN90p
14	CUITZEO DEL PORVENIR	MICH	SU25, ID, TR20, GSL, WSDI, TNx, TXn, TX10p, TN90p, TX90p
15	HUINGO	MICH	FD0, SU25, ID, TR20, GSL, WSDI, TXx, TNx, TXn, TNn, TN10p, TX10p, TX90p
16	CIUDAD HIDALGO	MICH	FD0, SU25, ID, TR20, GSL, WSDI, CSDI, TXx, TXn, TNn, DTR, TN10p, TX10p, TX90p
17	ZACAPU	MICH	FD0, ID, TR20, GSL, TNx, TXn, TNn, TN10p, TN90p
18	AHUACATLAN	NAY	FD0, ID, GSL, TXn, DTR
19	LAMPAZOS	NL	FD0, SU25, ID, TR20, GSL, WSDI, CSDI, TXn, TNn, DTR, TN10p, TX10p, TN90p, TX90p
20	MATIAS ROMERO	OAX	FD0, SU25, ID, GSL, CSDI, TXn, TNn, TX10p, TN90p
21	SANTO DOMINGO TEHUANTEPEC	OAX	FD0, SU25, ID, GSL, WSDI, CSDI, TNn, DTR, TN10p, TX10p, TN90p, TX90p
22	MATEHUALA	SLP	FD0, SU25, ID, TR20, GSL, WSDI, CSDI, TNx, TXn, TNn, DTR, TN10p, TX10p, TN90p, TX90p
23	BADIRAGUATO	SIN	FD0, SU25, ID, GSL, WSDI, CSDI, TXx, TNx, TXn, TNn, DTR, TN10p, TX10p, TN90p, TX90p
24	SAN FERNANDO	TAM	FD0, SU25, ID, TR20, GSL, CSDI, TXx, TNx, TXn, TNn, DTR, TN10p, TX10p, TN90p, TX90p
25	ATZALAN	VER	FD0, SU25, ID, TR20, GSL, CSDI, TNx, TXn, DTR, TN10p, TX10p, TN90p
26	LAS VIGAS	VER	FD0, ID, TR20, GSL, TXx, TNx, TNn, DTR, TN10p, TX90p

Table 6.2. List of temperature stations (with data from 1941 to 2001) show correlations (Kendall's tau) between the precipitation extreme indices with time, that are not statistically significant. * Stations numbers are in correspondence with Table 3.2 and Fig. 3.6.

Two stations independently account for 8 statistically significant indices. Santa Gertrudis –in the southern part of the Baja Californian peninsula- is located just north of the Tropic of Cancer (station number 8 in Table 6.1). Four out of eight correlations of the temperature extreme indices that are statistically significant at the 1% level lead to a clear cooling trend at this location. This is especially true for night-time temperature indices (TNn, TN90p, TNx and TR20) at Santa Gertrudis. Salamanca in the State of Guanajuato (station number 19 in Table 6.1) is the southern station for the analysis. Just as in the former case, four extreme indices show correlations leading to cooler conditions; the

results are statistically significant at the 1% level, and basically related to changes in day-time temperatures (TX10p, TX90p, TXx, and WSDI). Prevailing cooling trends affect Santa Gertudris and Salamanca stations, one in the northern part and the other in central Mexico.

Finally, when those stations with 7 statistically significant indices are considered, three different locations are evaluated: Santiago, Zacapu, and Matías Romero (stations number 9, 24 and 28 in Table 6.1, respectively). Santiago is at the southern tip of the Baja Californian Peninsula, located just north of the Tropic of Cancer. Although correlations of the indices for Santiago are mixed between positive and negative ones, clear variations towards warming conditions can be observed, as the more statistically significant changes are principally occurring for the day-time temperatures (TX90p, TXx and TX10p). The first of the two southern stations to be analysed is Zacapu in Michoacán State. Four out of the seven indices with statistically significant results are for the most significant, 1% level (DTR, SU25, TX90p and WSDI). The changes taking place at the Zacapu occur in the day-time temperature indices, leading to clear cooling conditions. Matías Romero (in the State of Oaxaca) is the only station, located well south of the Tropic of Cancer near the Pacific Ocean, with statistically significant correlations. These changes are concentrated (four out of seven) all at the positive 1% level (TNx, TR20, TXx and WSDI), and are also slightly biased towards variations in night-time temperatures. Overall, at Matías Romero a clear trend towards warmer conditions can be observed.

6.2.1. EXTREME TEMPERATURE INDICES.

In this section, we can simplify the description of the results. The extreme temperature indices (defined in section 3.3.4) can be classified into three groups: one group measures the temperature change (°C) (TNn, TNx, TXn, TXx, and DTR) the second calculates the frequency (number of cases or days) the index is exceeding a defined threshold (WSDI, SU25, TR20, CSDI, and FD0), and the last group also defines the percentage of time an index is exceeding a percentile limit (TN10p, TN90p, TX10p and TX90p). It is expected

that this separation of magnitude, frequency, and percentage can lead us to a better understanding of the specific details of the extreme temperatures in Mexico.

The first group to be considered in the evaluation of temperature extremes deals with the changes in the absolute values (°C) of temperature. The warmest day [TXx, fig. 6.1 a)] is the first index to be assessed. Positive correlations (warmer conditions) are located along both Atlantic and Pacific Coasts, but those statistically significant at the 1% level are concentrated within the southern part of the country. In contrast, negative correlations (cooler conditions) are, basically concentrated in Central Mexico.

Another (day-time) temperature to be evaluated is the TXn index or coolest day [fig. 6.1 c)]. An almost national pattern of positive correlations (between the temperature extreme indices with time) can be observed for this index; this is especially true if we consider that most of the sites have statistically significant results. Geographically these positive trends are located along both Mexican coasts. Of all the indices that are statistically significant, only Irapuato (station number 17 in Table 6.1) is experiencing a negative correlation and this site is located in Central Mexico (Mexican Highlands). Another interesting characteristic to point out about this index is that most of the statistically significant results are concentrated in the northern part of the country.

Night-time temperature variations are described by two indices: Coolest night [TNn; fig. 6.1 d)] and Hottest night [TNx; fig. 6.1 b)]. TNn shows predominantly positive correlations at the 1% statistically significant level, especially along the Pacific Coast. This coastal pattern is not present along the Atlantic coast except for Las Vigas station in Veracruz State (station number 35 in Table 6.1). In the evaluation of this index we have only found two decreasing (both statistically significant at 1% level) correlations (with time): Ahuacatlán in Nayarit state (station number 25 in Table 6.1), and El Paso de Iritu in southern Baja California (station number 4 in Table 6.1). The Hottest night [TNx; fig. 6.1 b)] shows mostly negative correlations among the sites that have statistically significant results. Among those with clear negative patterns (statistically significant at 1% level), they are geographically concentrated along the North Pacific Coast at the tip

of the peninsula of Baja California, except for Ahuacatlán, Nayarit and Ciudad Hidalgo in Michoacán state (stations number 25 and 23 in Table 6.1, respectively). Ciudad Hidalgo makes a contrasting negative/positive transition with the station Pericos in Guanajuato State (station number 18 in Table 6.1), the same contrasting pattern is found in Oaxaca state of the South Pacific Coast (station number 28 and 29 in Table 6.1, respectively). Considering only statistically significant results, we can roughly observe a negative (cooling/north) and positive (warming/south) climatic transition.

Finally, the DTR (Daily Range Temperature) index [fig. 6.1 e)] shows a marked tendency towards increasing values across Mexico. Among all the results, the few negative correlations (the difference between maximum and minimum temperatures is decreasing) with time are located in the southern part of the country. Again, contrasting (negative/positive) correlations are observed in the Guanajuato/Michoacán states region and the coast of Oaxaca state in the South Pacific Area. Also there are slightly more indices with significant results in the southern part compared to the north part of Mexico for the DTR index.

Warmer conditions are mainly observed along the Pacific coast of Mexico, when the temperature extreme indices measuring changes in °C are evaluated.

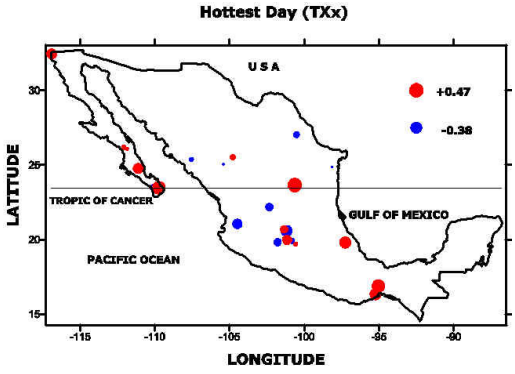

a) Monthly Highest Day Temperature.
Units in Centigrades.

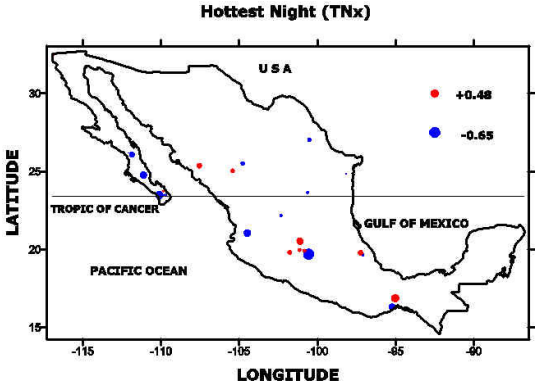

b) Monthly Highest Night Temperature.
Units in Centigrades.

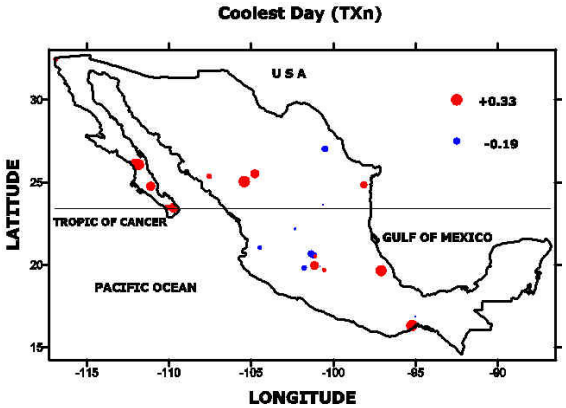

c) Monthly Lowest Day Temperature.
Units in Centigrades.

Fig. 6.1. Extreme temperature indices maps, intensity in °C. A Kendall's tau-b (linear) correlation analysis has been applied between the temperature extreme indices and time. Circles in red are representing a positive and in blue a negative correlation.

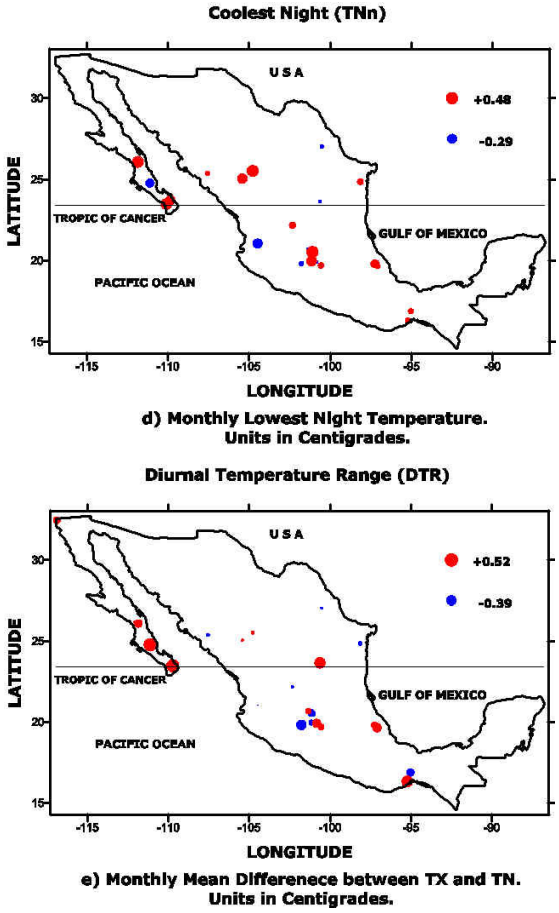

Fig. 6.1. Extreme temperature indices maps, intensity in °C. A Kendall's tau-b (linear) correlation analysis has been applied between the temperature extreme indices and time. Circles in red are representing a positive and in blue a negative correlation.

The second group of indices (fig. 6.2) to be assessed are those that count the frequency of exceeding a set limit; the first index to be considered is FD0 (Frost Days) [fig. 6.2 a)]; this index counts the number of times the daily minimum temperature is below the 0° C threshold. Negative correlations (with time) are observed at the southern tip of the Baja Californian peninsula with a statistical significance of 5% that points to warmer conditions in the region. Similar results are found in northern and central Mexico:

Durango, in the north; Guanajuato and Michoacán in the south. All the results in this part of continental Mexico are statistically significant at the 1% level. Probably the most interesting feature is that in Central Mexico, both stations (Pericos, Guanajuato; and Cuitzeo, Michoacan; stations number 18 and 21 in Table 6.1) are varying in correspondence, opposite to what has already been observed (contrasting patterns) in the earlier analysed indices in this chapter. From central to northern Mexico (including the Peninsula of Baja California) statistically significant counts (warming trends) are observed for the FD0 index.

Another index that measures the changes in the number of warm day-time temperatures is the SU25 (Hot Days) index [fig. 6.2 b)], in this case the upper limit to be exceeded is 25° C. Positive secular correlations with statistical significance below the 1% level are found in the Baja Californian peninsula. There is also a corridor of positive correlations in the eastern part of Mexico. A contrasting pattern of negative correlations with statistically significant results (at the 1% level) can be observed across central Mexico, and especially on the Mexican Plateau. Two regions show contrasting positive/negative patterns on this index: the southern tip of Baja Californian Peninsula and the Tuxtlas region near the Gulf of Mexico. A clear tendency of positive correlations (warmer conditions) with statistically significant results is evident in the north of Mexico.

Night-time temperatures are also evaluated in this group; one of the indices that deals with this kind of variations is the Warm Nights (TR20) index [fig. 6.2 c)]. It defines the annual count of daily minimum temperatures that are above the 20° C threshold. The southern tip of the peninsula of Baja California according to the results is experiencing negative correlations with statistical significance below the 1% level. In contrast, just across the Gulf of California in the North American Monsoon Region (NAMR), also called Mexican Monsoon Region (see section 4.2.1), we can observe positive correlations at the 1% statistical significance level. One of the stations with the most consistent results is Ahuacatlán in Nayarit (station number 25 in Table 6.1); this location is again showing a decreasing correlation (with time) of the night temperatures, and is statistically significant at the 1% level. However, the stations within the South Pacific region in the

state of Oaxaca show contrasting negative/positive patterns. Overall, there is not a clear geographical pattern for this temperature extreme index.

Warm Spell Duration (WSDI) Index [fig. 6.2 d)] is an index that annually counts the number of cases when for at least 6 consecutive days the day temperature (TX) exceeded the 90th percentile of 1961-1990. There are more statistically significant results at the 1% level in central Mexico, and they share negative correlations (with time) in general. Only one positive correlation with statistical significance at 1% is located in the southern part of the country (Matías Romero, Oaxaca; station number 28 in Table 6.1). Contrasting results (positive/negative correlations) are observed within the Tuxtlas region in the state of Veracruz. Significant results with negative correlations at the 1% level are mainly concentrated in western Mexico. Negative correlations are observed in the west, central and northern Mexico.

Lastly in this group, the Cold Spell Duration (CSDI) Index [fig. 6.2 e)] counts annually the number of at least 6 consecutive days when the night temperatures (TN) are below the 10th percentile of 1961-1990. Just north of the tropic of cancer within the peninsula of Baja California a positive correlation with statistical significance at the 1% level can be observed at El Paso de Iritu station (station number 4 in Table 6.1), leading to a cooling trend at this location. Ahuacatlán (station number 25 in Table 6.1), once more, like in the indices already assessed in this section shows a positive correlation statistically significant at the 5% level, leading towards colder conditions. Contrasting patterns of negative/positive correlations are evident across central Mexico within the Michoacán/Guanajuato states region. Warming conditions are observed at Las Vigas station (station number 35 in Table 6.1) near the Gulf of Mexico, this negative correlation with time is statistically significant at the 5% level. A clear pattern towards colder conditions for northern Mexico can be observed; less evident is the climatic divide from colder (north) to warmer (south) conditions for the entire country.

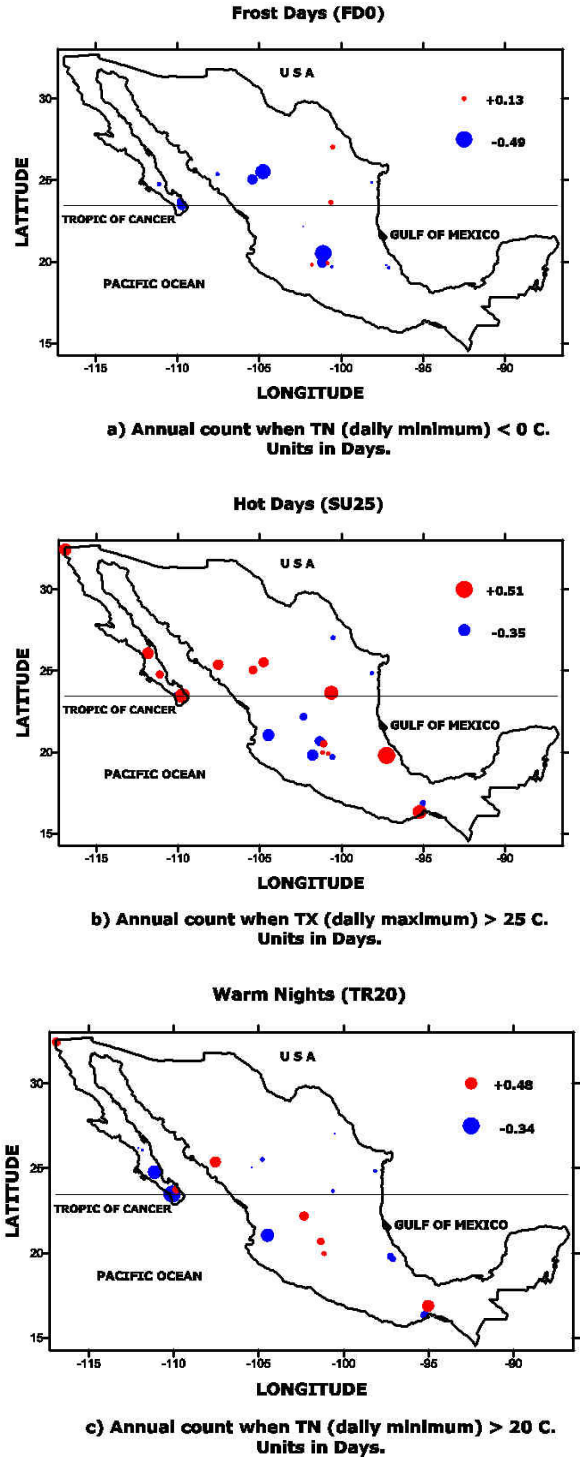

Fig. 6.2. Extreme temperature indices maps, frequency measured in days. A Kendall's tau-b (linear) correlation analysis has been applied between the temperature extreme indices and time. Circles in red are representing a positive and in blue a negative correlation.

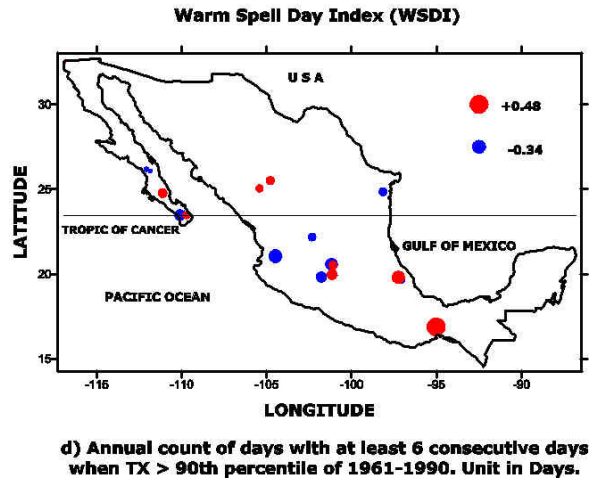

Fig. 6.2. Extreme temperature indices maps, frequency measured in days. A Kendall's tau-b (linear) correlation analysis has been applied between the temperature extreme indices and time. Circles in red are representing a positive and in blue a negative correlation.

Except for a national pattern of warmer conditions for the Hot days index (SU25), no other clear geographic characteristic is seen among the group of indices that exceed a limit in ° C.

The last group of indices deals with the percentage of time a record exceeds a percentile limit. The cool night frequency (TN10p) is the first index [fig. 6.3 a)] to be evaluated. Contrasting correlations of TN10P with time are observed at the southern tip of the Baja Californian peninsula; both results (positive and negative correlations) are statistically significant at the 1% level. In Durango state (northern part of Mexico) negative correlations are found, the stations in this area (varying coherently) show a clear warming climate pattern. A positive correlation which is statistically significant at the 5% level is observed near the Central Pacific Coast at Ahuacatlán, Nayarit (station number 25 in Table 6.1); the records suggest a slight change to cooler conditions. For the Guanajuato/Michoacán states within the Mexican Highlands region, the results show contrasting temperature patterns, most of them are significant at the 1% level. However, near the Gulf of Mexico, clear negative correlations are found for Las Vigas station (station number 35 in Table 6.1), with statistical significance at the 1% level, leading locally to warmer conditions. Slightly warmer conditions can be observed at the South Pacific coast; the station at Matías Romero in the state of Oaxaca (station number 28 in Table 6.1) has experienced a negative correlation with a significance of 5% level. There is no clear climatic pattern for the TN10p index across the country, although warming conditions are dominant in the southern part of Mexico.

Another parameter to be analysed in this group is the Cool Day frequency index or TX10p [fig. 6.3 b)]. A widespread pattern of negative correlations (of TX10P with time) is affecting the peninsula of Baja California; furthermore all these results are statistically significant at the 1% level pointing to widely warmer conditions. A clear trend to colder conditions is present at Ahuacatlán station in Nayarit state (station number 25 in Table 6.1), as a positive correlation with a statistical significance below the 1% level is locally observed here. A positive trend is also found within the Guanajuato/Michoacán region, as here correlations are statistically significant at both the 5 and 1% level are present.

Therefore, we can conclude colder conditions have been experienced in the area. Warmer conditions at Las Vigas station (station number 35 in Table 6.1) within the Tuxtlas region are indicated by negative correlations with a statistical significance below the 1% observed in TX10p [fig. 6.3 b)] with time. No clear climatic picture is found in the evaluation of the cool day frequency index (TX10p). Nevertheless, roughly contrasting continental/coastal patterns are present. Negative correlations and, in consequence, warmer conditions are observed along both the Atlantic and Pacific coasts. Colder conditions (as a result of positive correlations) are prevailing within the continental and highland parts of Mexico.

A trend towards warmer conditions can be assessed by two different parameters: Hot Night frequency (TN90p) and the Hot Day frequency (TX90p) indices. TN90p [fig. 6.3 c)] shows negative secular correlations with statistical significance below the 1% level at the southern tip of the peninsula of Baja California. However, contrasting correlations are found within the Guanajuato/Michoacán states, both are statistically significant at the 1% level. In Ahuacatlán, Nayarit (station number 25 in Table 6.1); a clear decreasing correlation is observed heading towards locally cooler conditions; this result is statistically significant at the 1% level. In Los Tuxtlas region in Veracruz, regional contrasting patterns can be observed, although only at Las Vigas (station number 35 in Table 6.1) is the decreasing trend statistically significant at the 1% level, meaning clear cooling conditions here. Finally, statistically significant at the 5% level, positive correlations are found for Matías Romero, Oaxaca (station number 28 in Table 6.1); slightly warming patterns are prevailing in this part of the southern Pacific. Overall, the TN90p index shows no clear coherent climatic patterns in Mexico. Mostly contrasting correlations are found across the country.

The Hot Day frequency (TX90p) is the last index [fig. 6.3 d)] of this group to be considered. Prevailing climatic patterns in the Baja Californian peninsula show positive correlations (statistically significant at both the 5 and 1% level) with time from the southern tip northwards to the Mexico-USA border at the Presa Rodríguez –Tijuana-

(station number 2 in Table 6.1), pointing towards warmer conditions in this north-western region. In north continental Mexico at El Palmito station (station number 14 in Table 6.1), a positive correlation with statistical significance of 1% level means warmer conditions locally. Central Mexico shares a regional pattern to colder conditions; indeed a widespread area shows negative correlations with statistical significance below the 1% level. Finally, positive correlations (warmer conditions) are observed at Las Vigas (station number 35 in Table 6.1) in the Gulf of Mexico and Matías Romero (station number 28 in Table 6.1) in the Southern Pacific region. But only at Las Vigas does the correlation reach the 1% level of statistical significance. Although a climatic divide can be seen in the results, showing patterns to warmer conditions in the north to colder conditions in Central Mexico, the positive correlations in Las Vigas and Matías Romero in southern Mexico leave the TX90P with no simple climatic pattern. No clear geographic pattern is seen in the group of indices that exceed a percentile limit.

The mean annual range of temperature shows a visible latitudinal transition (see fig. 6.4), just as it is observed in the case of precipitation (fig. 2.1). In the case of the range of temperature more contrasting conditions (between the maximum and minimum temperatures) are observed in northern Mexico, and the differences become smaller as we move towards the far south of the country (Mosiño and García, 1974).

In order to evaluate the changes of the temperature extremes (from a geographical perspective) it was decided to count the number of cases in which the variation of the indices at both the 5 and the 1% of statistical significance (see table 6.2). As considered in the case of rainfall extremes (see section 5.2) we are testing a latitudinal transition in the results. For the purposes of this analysis, the Tropic of Cancer is defined as an artificial geographical divide. For this assessment to be independent it was decided to work with the extreme indices directly instead of the stations. Counting these indices in such a manner can give us an additional insight into how the extreme parameters are (or not) concentrated geographically. Therefore, using the Tropic of Cancer as a limit we are going to be able to appreciate the changes of the temperature extreme indices, and

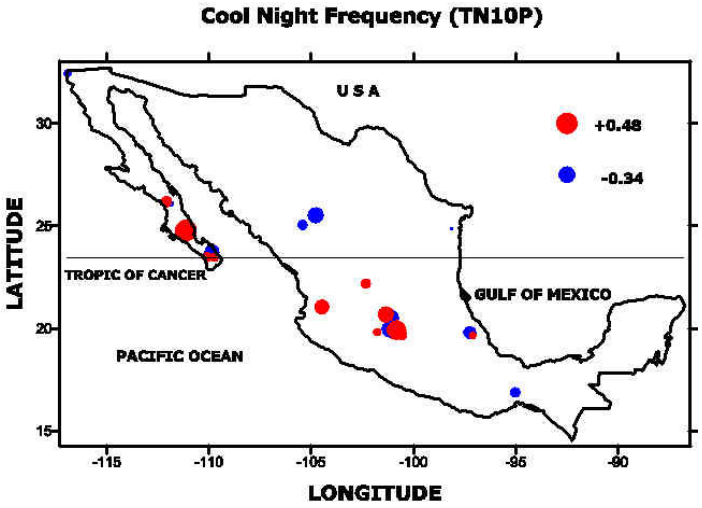

a) Porcentage of days when TN < 10th percentile of 1961-1990. Units in %.

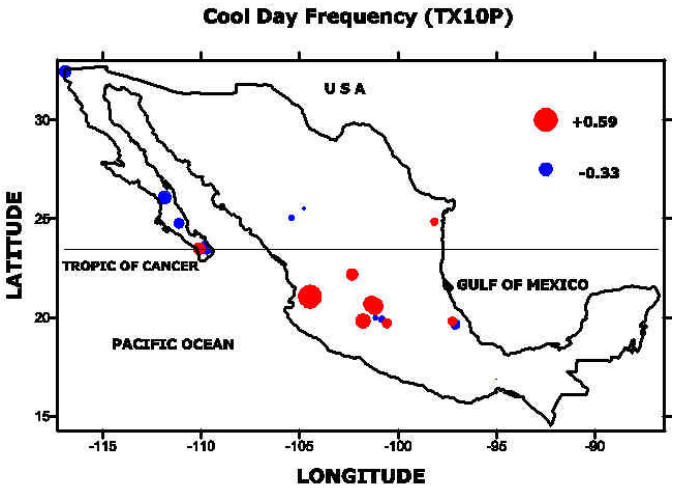

b) Porcentage of days when TX < 10th percentile of 1961-1990. Units in %.

Fig. 6.3. Extreme temperature indices maps, frequency measured in days. A Kendall's tau-b (linear) correlation analysis has been applied between the temperature extreme indices and time. Circles in red represent a positive and in blue a negative correlation.

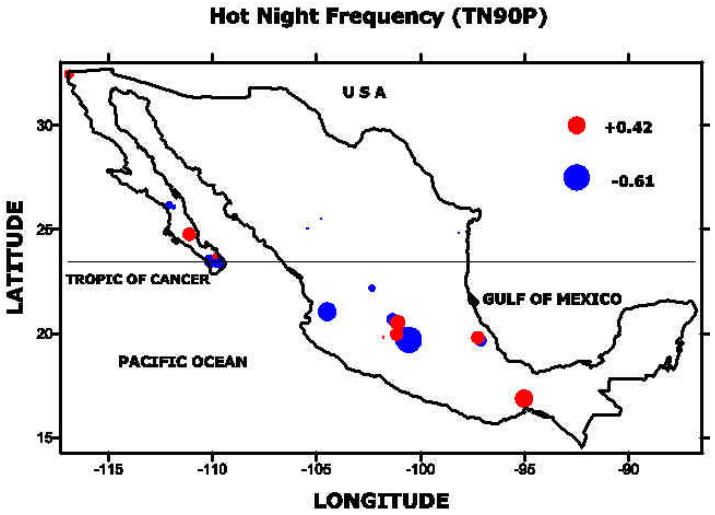

c) Porcentage of days when TN > 90th percentile of 1961-1990. Units in %.

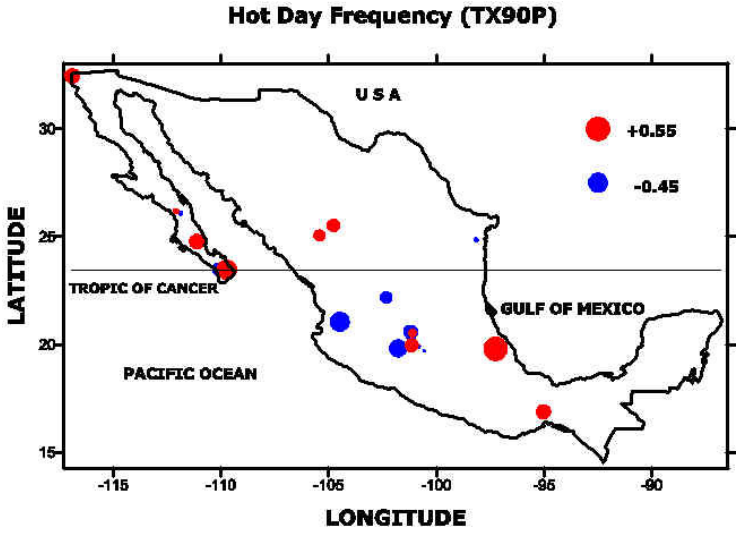

d) Porcentage of days when TX > 90th percentile of 1961-1990. Units in %.

Fig. 6.3. Extreme temperature indices maps, frequency measured in days. A Kendall's tau-b (linear) correlation analysis has been applied between the temperature extreme indices and time. Circles in red represent a positive and in blue a negative correlation.

determine if there are subtle differences between the variations in the north or south of the county or the indices are fluctuating accordingly.

In order to compare different (possibly contrasting) climatic patterns, a counting of extreme indices (regardless of where they are, except north or south) with statistically significant secular correlations was made. Defining the number of cases, using indices instead of stations, can give us the possibility of observing dynamically the variations of the extreme temperatures. For this purpose, we classify these variations into two different modes: one deals with the levels of statistical significance (Table 6.2.) and the other with trends to warmer or cooler conditions (Table 6.3.), both with the already defined North/South transition. That is, for example, the counting of the indices with negative correlations below the 5% level of statistical significance in the northern part of the country accounts for eight cases (Table 6.2); it could be that one station accounts for more than one statistically significant temperature extreme index.

	North	**South**	**Total**
Pos. Corr. (5%)	10	9	19
Pos. Corr. (1%)	16	17	33
Neg. Corr. (5%)	8	16	24
Neg. Corr. (1%)	18	33	51
Total	52	75	127

Table 6.3. Geographical patterns of positive/negative correlations (temperature extreme indices with time using Kendall's tau) with statistical significant levels at 5 and 1%. The number of cases is classified defining the Tropic of Cancer as the limit to separate the northern/southern regions.

We are going to assess important variations in indices below statistically significant levels. A separation was then made into positive and negative correlations with statistical significant levels at 5 and 1% levels. Regardless of the statistical levels, the number of negative cases is, in general, greater than the positive ones. This is fully appreciated when we observe that the sum of number of negative correlations is 75 (24+51) is greater than the positive ones that are only 52 (19+33).

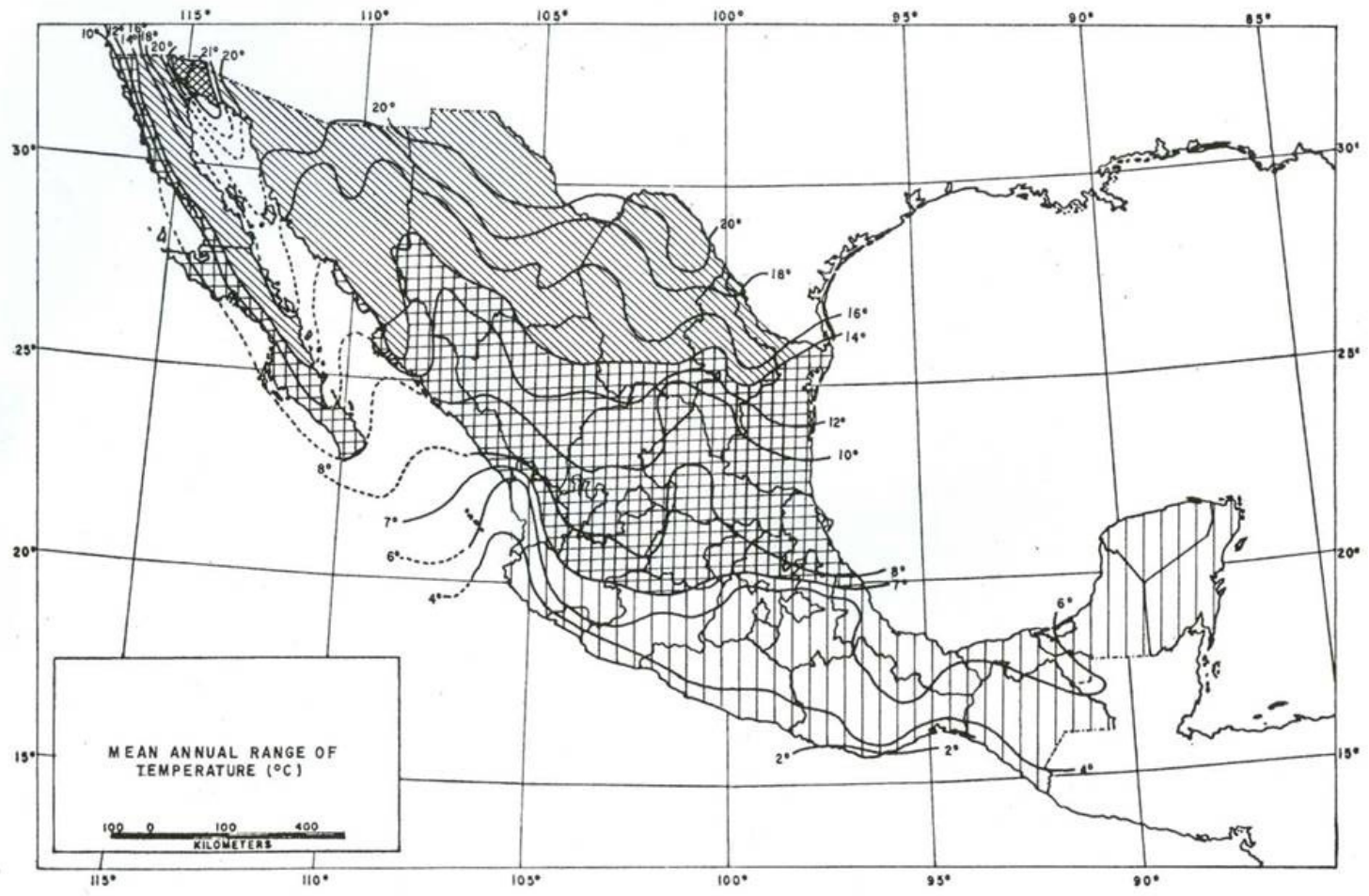

Fig. 6.4. Mean Annual Range of Temperature; according to Mosiño and García (1974).

The second option to test the latitudinal transition in temperature (see Fig. 6.4) is to deal with warm or cold conditions across Mexico, the results are shown in table 6.3. The number of cases heading to cold conditions is greater than for warm conditions, as well as more indices are concentrated in the southern part of the country than in the north. Another interesting feature that can be observed is: with the exception of cold conditions in the south, the number of cases is very similar for the rest of the conditions considered in this table.

	North	**South**	**Total**
Warm	33	27	60
Cold	27	40	67
Total	60	67	127

Table 6.4. Geographical patterns of positive/negative correlations (temperature extreme indices with time using Kendall's tau) with statistical significant levels at 5 and 1%. The number of cases is classified defining the Tropic of Cancer as the limit to separate the northern/southern regions.

6.2.2. LINEAR TREND ANALYSIS.

Linear trends using least-squares approaches is the last analysis applied in this chapter to two stations in the northern and two stations in the southern part of the country. These sites have the largest number of statistically significant (non-parametric) correlations with time, according with the former calculations of this chapter utilising Kendall tau-b (see section 3.3.5). As mentioned in section 5.2.2 the presence of a positive autocorrelation can influence the estimation of a significant trend. Serial correlations for all the extreme indices are computed SPSS 14.0 prior to the linear trend analysis.

Firstly, linear trends are analysed in the most frequent indices (with statistically significant results) that measure changes in the maximum temperatures, i.e., TX10p (Cool Day Frequency) and TXx (Hottest Day). Linear trends in minimum temperature indices [Cool Night frequency (TN10p), and Coolest Night (TNn)] that have more statistically significant results among the selected stations are assessed next. Lastly in

order to observe one index that combines the variations of maximum and minimum temperatures, the trends in the Diurnal Temperature Range (DTR) are evaluated.

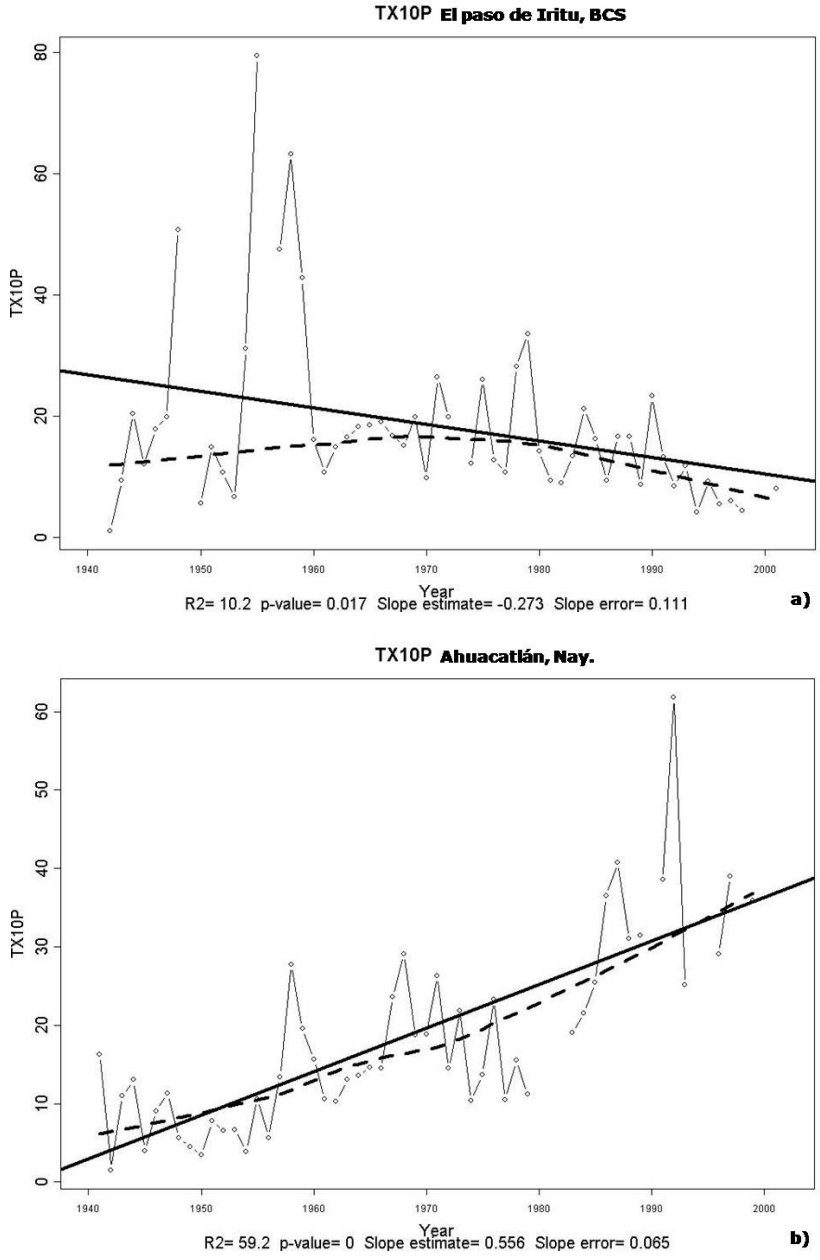

Fig. 6.5. Linear trend analysis applied to the Cool Day frequency (TX10p) using the least-square approach of the R software (see section 3.3.4). Two stations in northern Mexico are considered [El Paso de Iritu, a); Ahuacatlán b)] and two in the southern part of the country [Salamanca, c); Matías Romero d)].

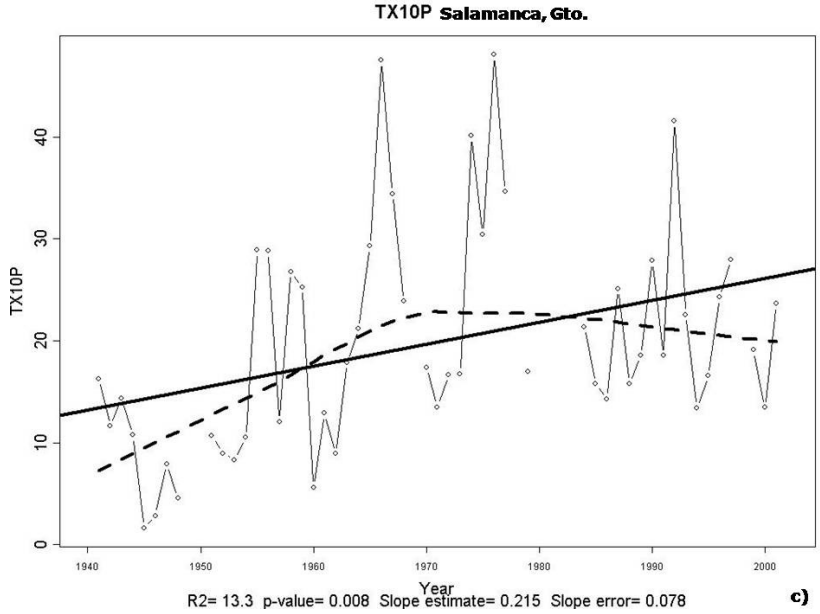

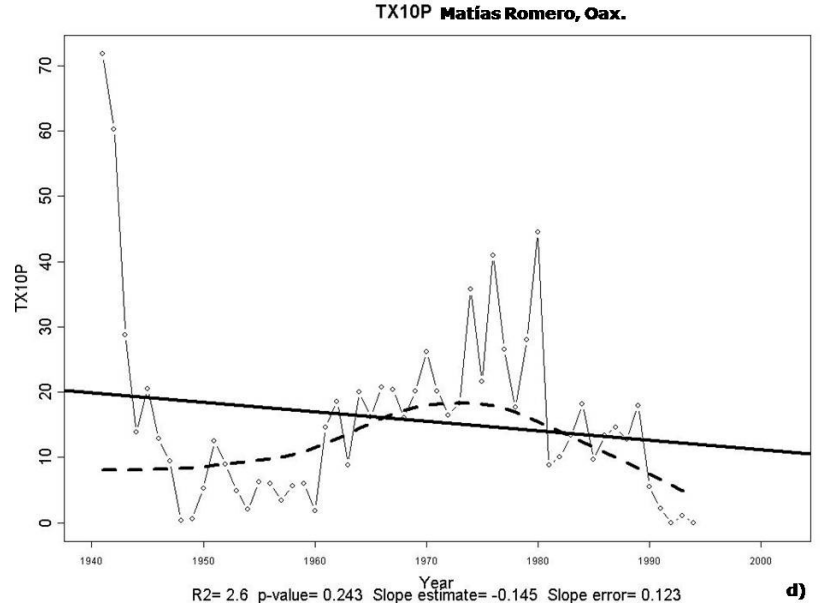

Fig. 6.5. Linear trend analysis applied to the Cool Day frequency (TX10p) using the least-square approach of the R software (see section 3.3.4). Two stations in northern Mexico are considered [El Paso de Iritu, a); Ahuacatlán b)] and two in the southern part of the country [Salamanca, c); Matías Romero d)].

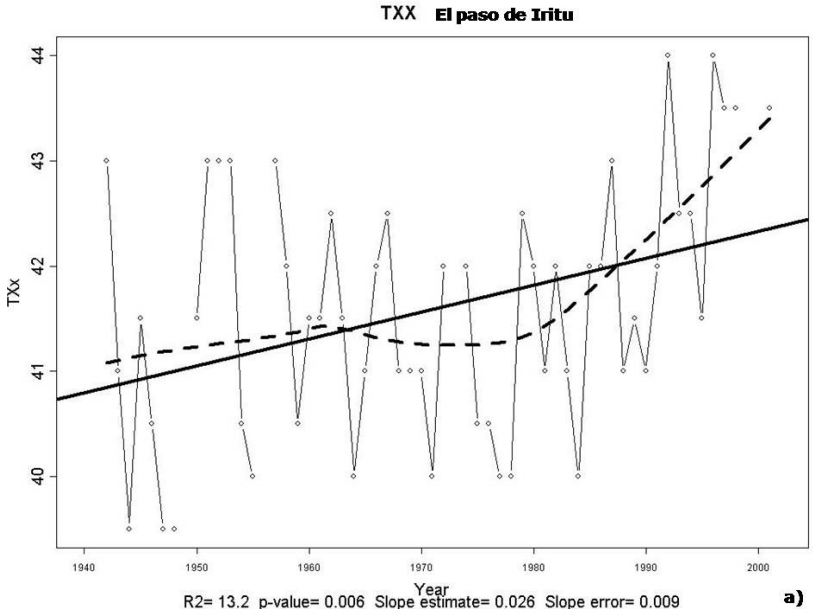

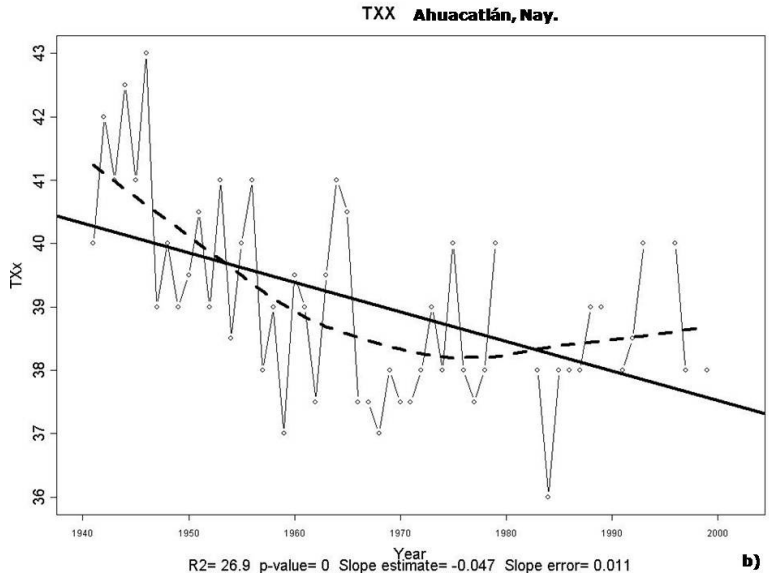

Fig. 6.6. Linear trend analysis applied to the Hottest Day (TXx) using the least-square approach of the R software (see section 3.3.4). Two stations in northern Mexico are considered [El Paso de Iritu, a); Ahuacatlán b)] and two in the southern part of the country [Salamanca, c); Matías Romero d)].

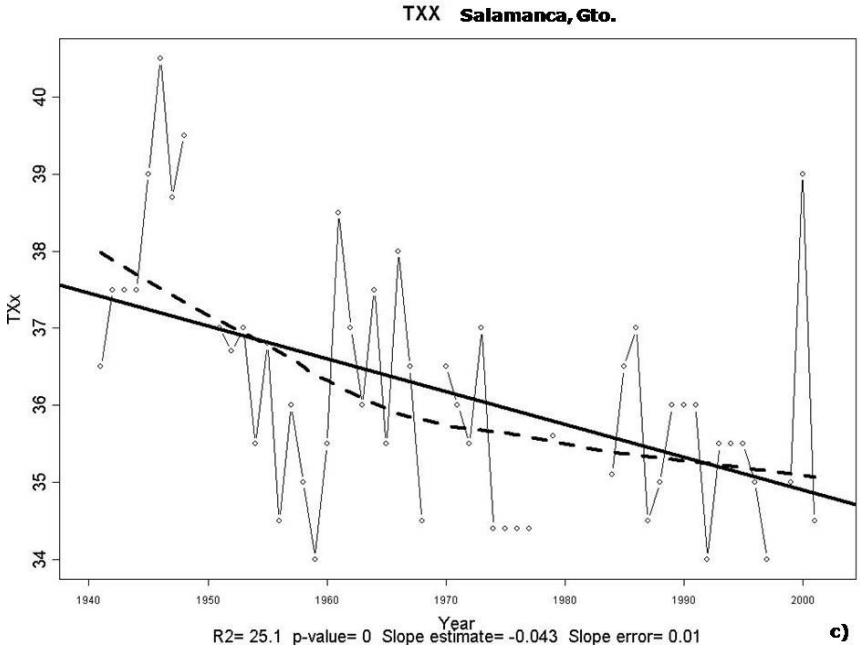

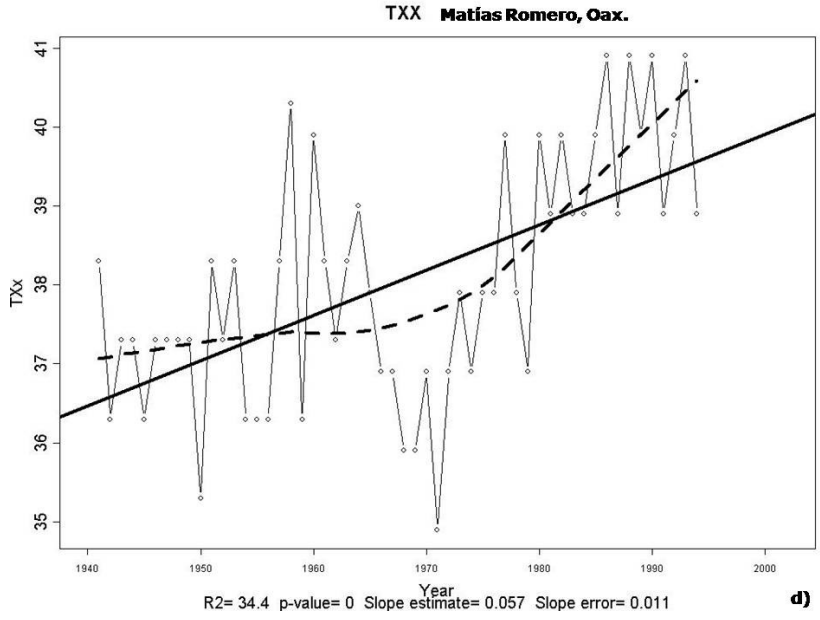

Fig. 6.6. Linear trend analysis applied to the Hottest Day (TXx) using the least-square approach of the R software (see section 3.3.4). Two stations in northern Mexico are considered [El Paso de Iritu, a); Ahuacatlán b)] and two in the southern part of the country [Salamanca, c); Matías Romero d)].

Contrasting patterns are observed in the northern part of Mexico for El Paso de Iritu [fig. 6.5 a)] in south Baja california, and Ahuacatlán [fig. 6.5 b)] in the State of Nayarit for the TX10p (Cool day frequency, see table 3.1) index; both stations are located close to the Pacific Ocean. Differences in the sign of the trends can be seen for both stations: the largest slope is positive (+5.6 % / decade) and is present at Ahuacatlán leading to cooling conditions; while El Paso de Iritu station has a negative trend of -2.7 % / decade, that points to warmer conditions at this site.

The largest observed trends for TXx are located south of the Tropic of Cancer. Matías Romero [fig. 6.6 d)] in Oaxaca (south Pacific coast) shows a secular variation of approximately +0.6 °C / decade; while a negative trend of -0.5 °C / decade for the Ahuacatlán and Salamanca stations [figs. 6.6 b) and c)]. Therefore, contrasting trends are observed between central and southern Mexico among the selected stations.

The first index to be assessed among the minimum temperature indices is TN10p (Cool night frequency, see table 3.1). The largest trends of the results are found in the northern part of Mexico, close to the Pacific Ocean. Both positive trends at El Paso de Iritu and Ahuacatlán [figs. 6.7 a) and b)] lead to colder conditions, and are also of similar magnitude: +6.6 % / decade.

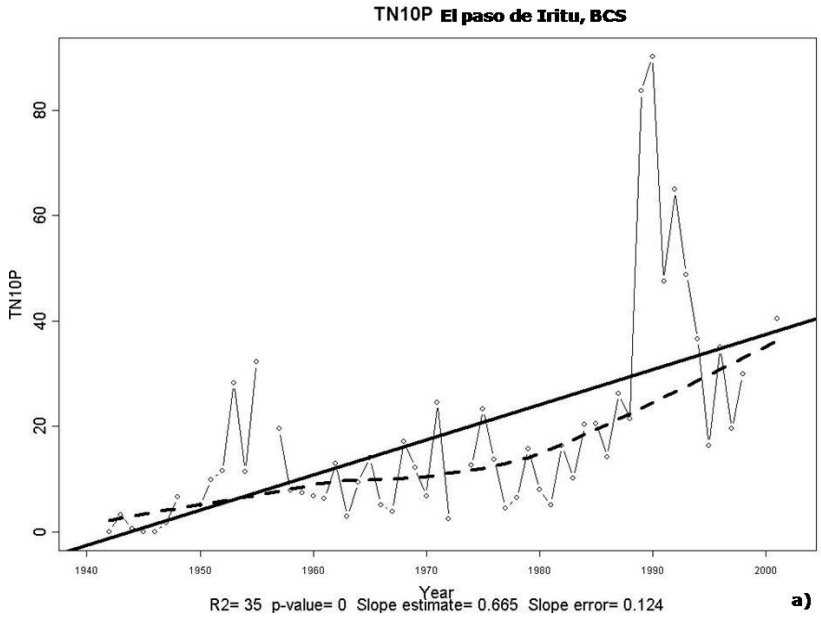

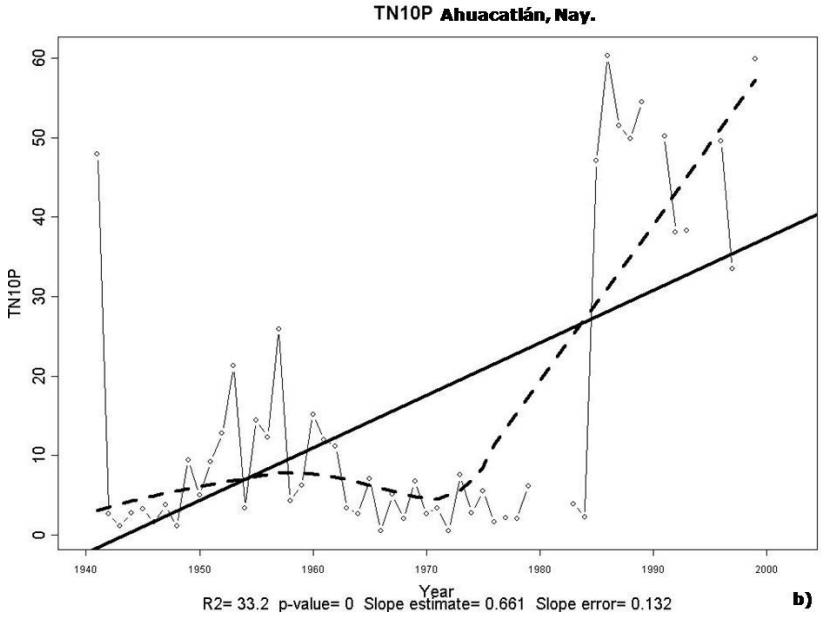

Fig. 6.7. Linear trend analysis applied to the Cool Night frequency (TN10p) using the least-square approach of the R software (see section 3.3.4). Two stations in northern Mexico are considered [El Paso de Iritu, a); Ahuacatlán b)] and two in the southern part of the country [Salamanca, c); Matías Romero d)].

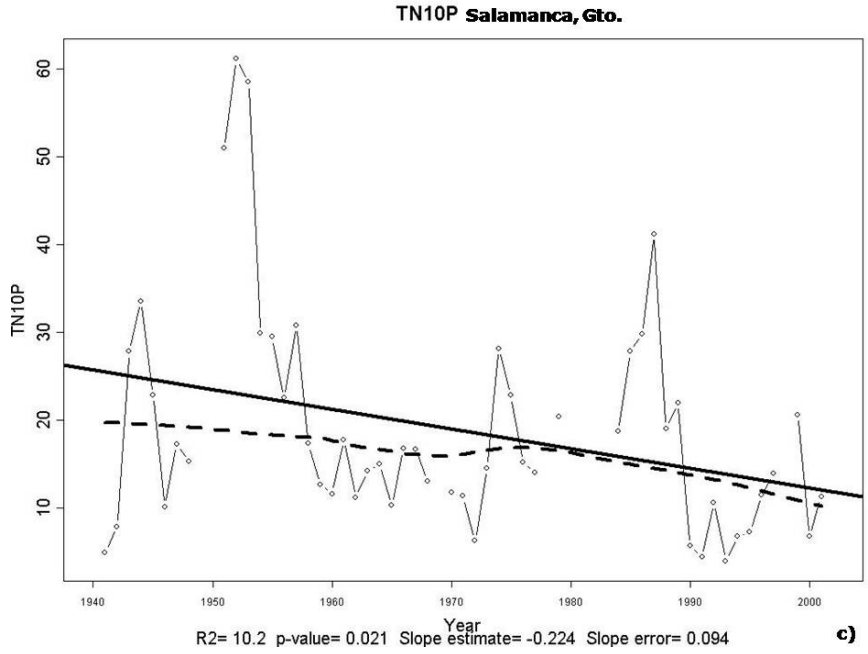

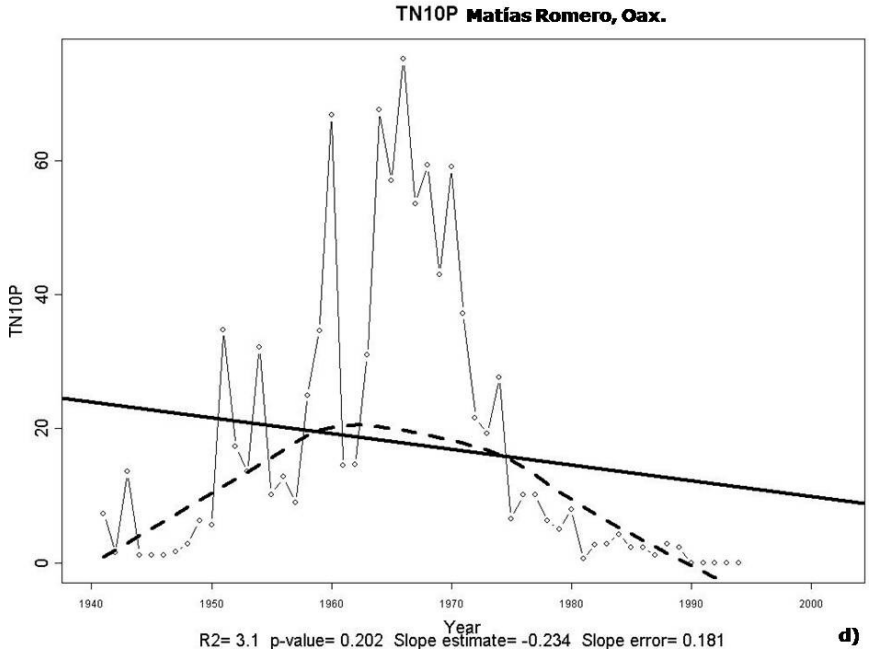

Fig. 6.7. Linear trend analysis applied to the Cool Night frequency (TN10p) using the least-square approach of the R software (see section 3.3.4). Two stations in northern Mexico are considered [El Paso de Iritu, a); Ahuacatlán b)] and two in the southern part of the country [Salamanca, c); Matías Romero d)].

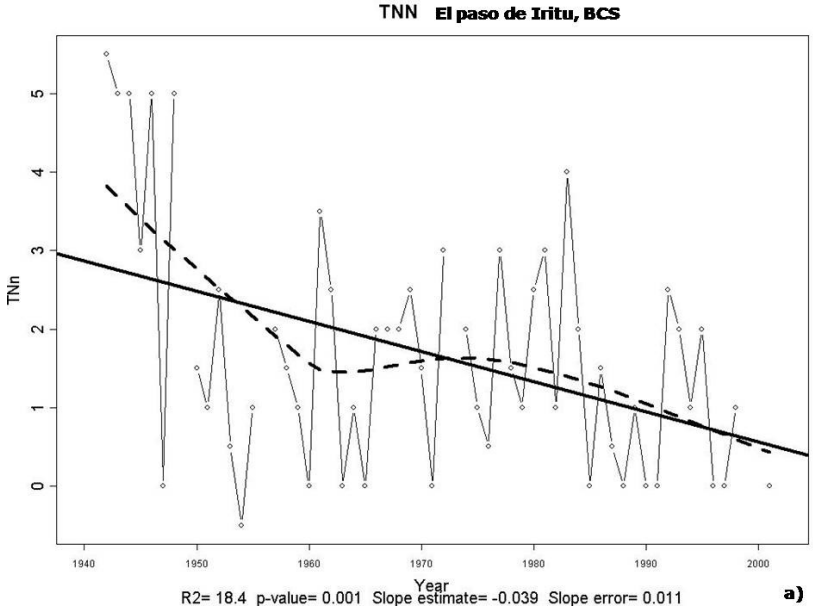

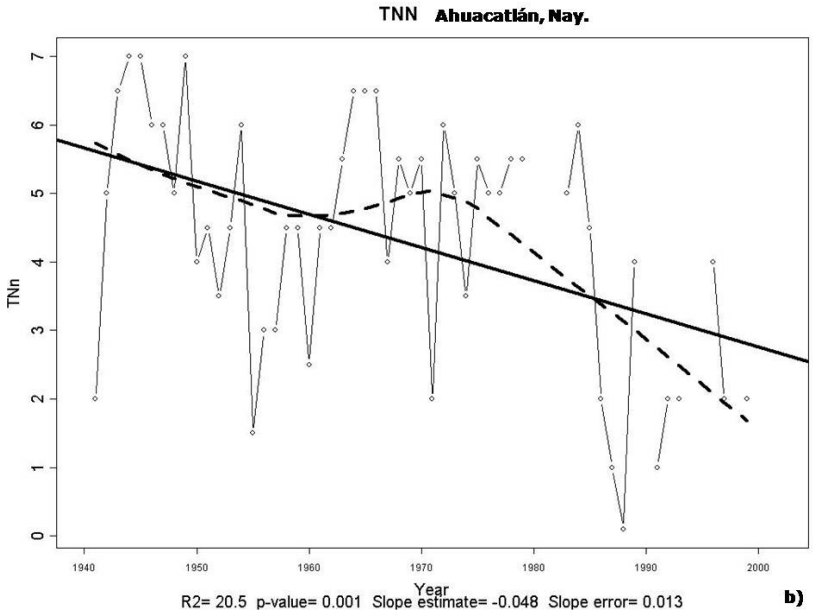

Fig. 6.8. Linear trend analysis applied to the Coolest Night (TNn) using the least-square approach of the R software (see section 3.3.4). Two stations in northern Mexico are considered [El Paso de Iritu, a); Ahuacatlán b)] and two in the southern part of the country [Salamanca, c); Matías Romero d)].

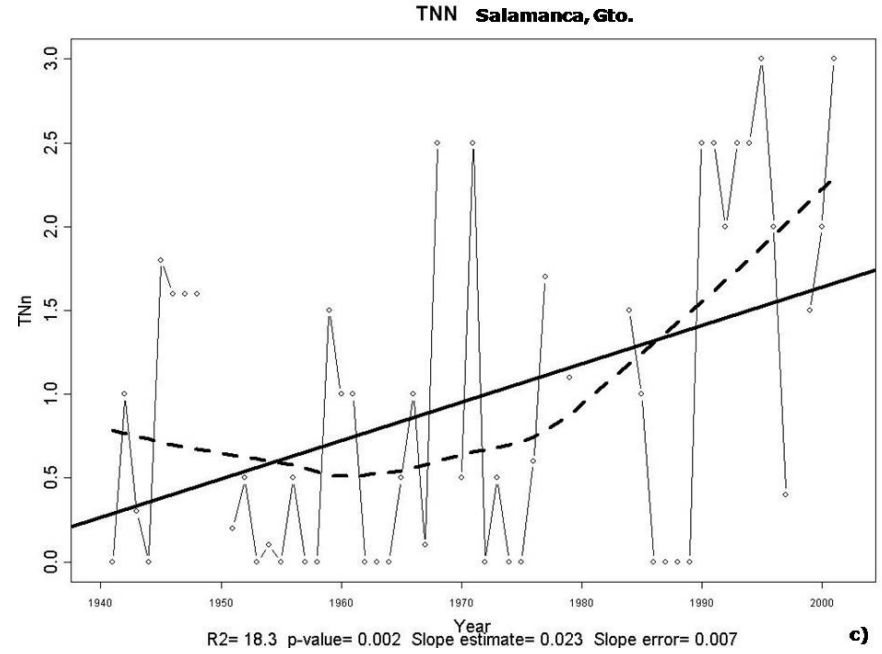

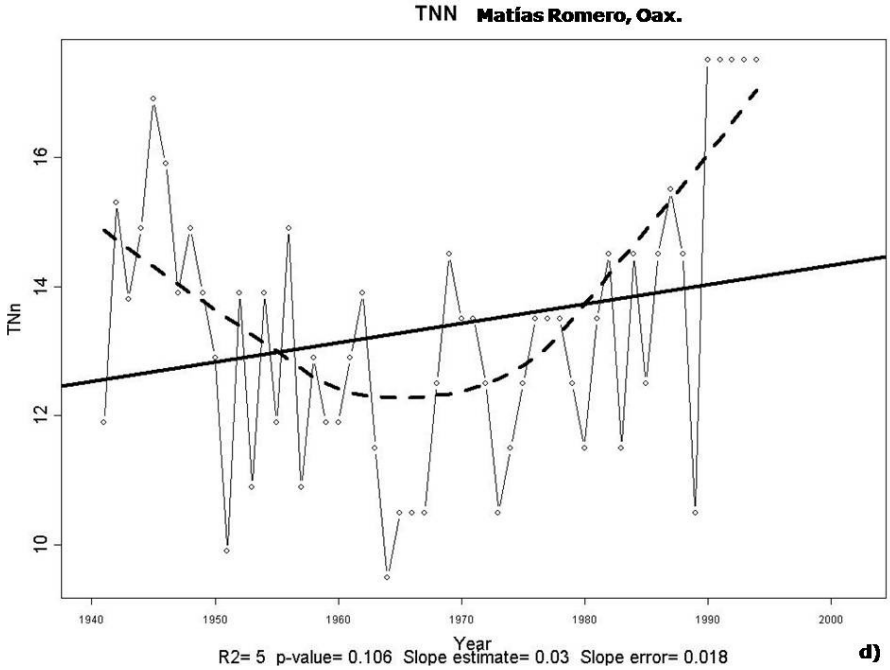

Fig. 6.8. Linear trend analysis applied to the Coolest Night (TNn) using the least-square approach of the R software (see section 3.3.4). Two stations in northern Mexico are considered [El Paso de Iritu, a); Ahuacatlán b)] and two in the southern part of the country [Salamanca, c); Matías Romero d)].

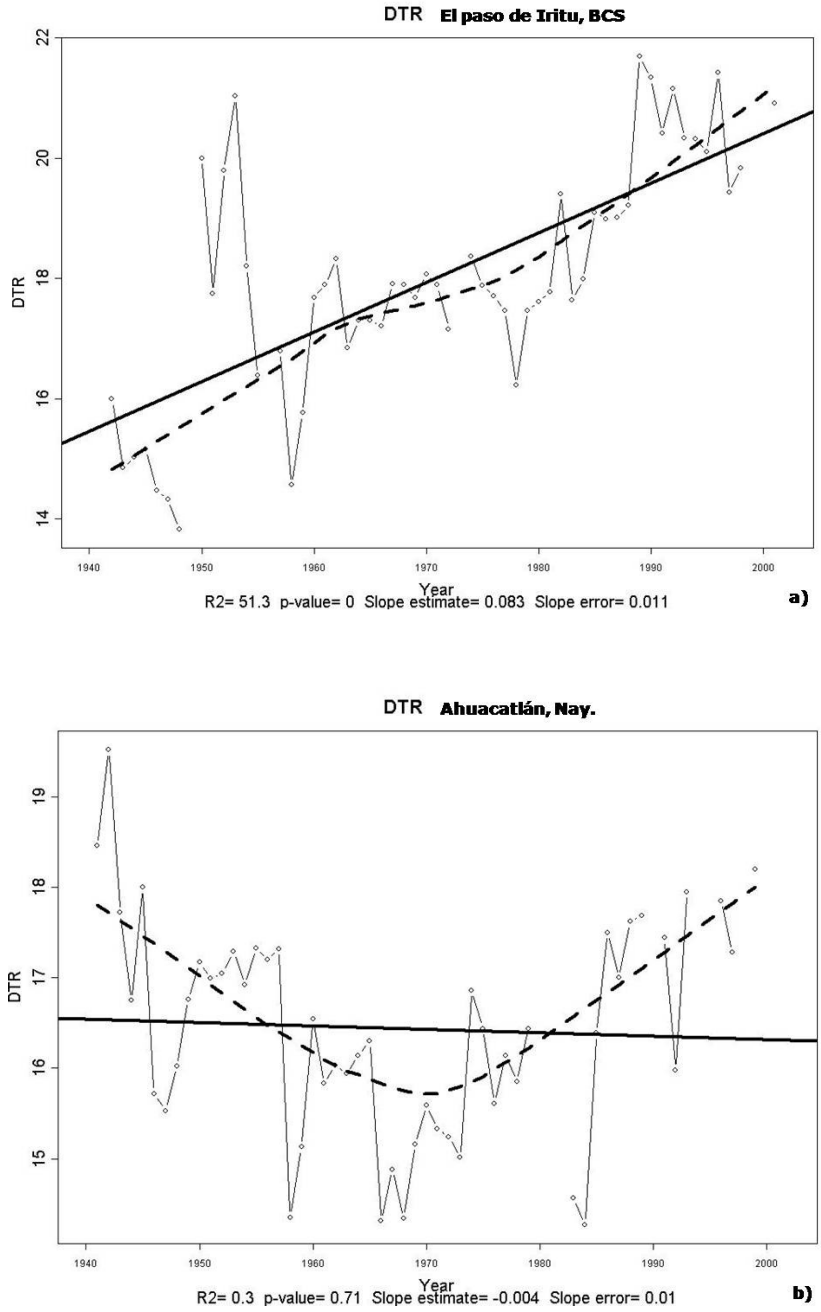

Fig. 6.9. Linear trend analysis applied to the Daily Temperature Range (DTR) using the least-square approach of the R software (see section 3.3.4). Two stations in northern Mexico are considered [El Paso de Iritu, a); Ahuacatlán b)] and two in the southern part of the country [Salamanca, c); Matías Romero d)].

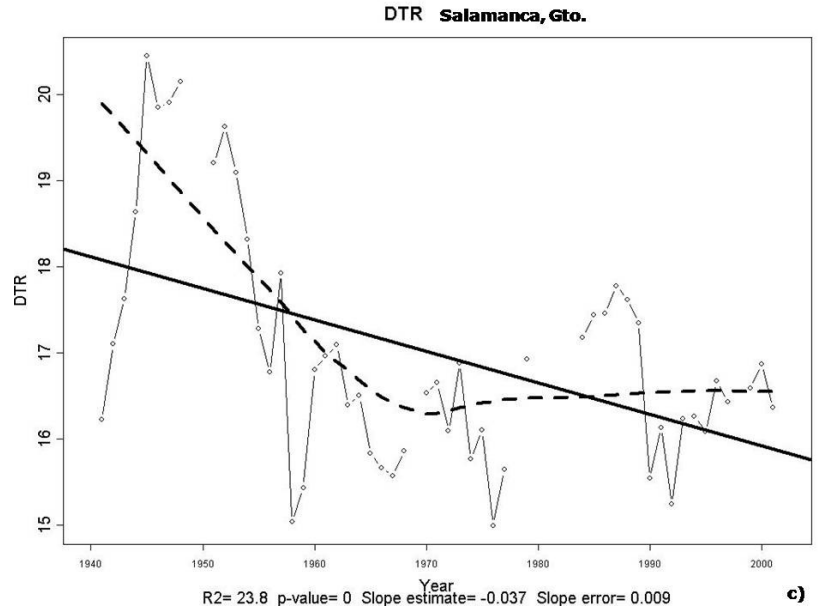

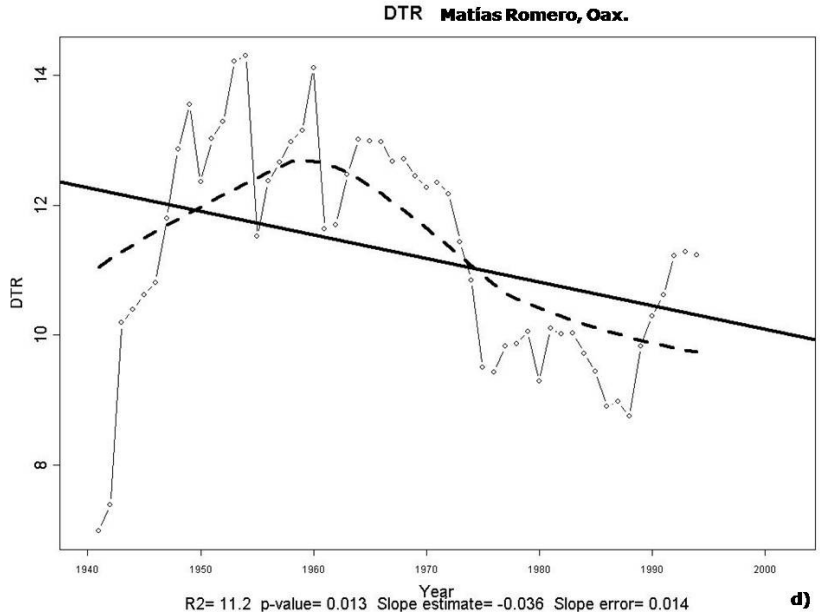

Fig. 6.9. Linear trend analysis applied to the Daily Temperature Range (DTR) using the least-square approach of the R software (see section 3.3.4). Two stations in northern Mexico are considered [El Paso de Iritu, a); Ahuacatlán b)] and two in the southern part of the country [Salamanca, c); Matías Romero d)].

When we analyse the Coolest night (TNn), the northern stations: El Paso de Iritu [fig. 6.8 a)] and Ahuacatlán [fig. 6.8 b)] show the largest trends -0.4 and -0.5 °C / decade respectively. Both stations in the northern Pacific coast are heading towards cooler conditions.

Lastly, the Daily Temperature Range (DTR) was selected in order to evaluate the combined effect of changes in maximum and minimum temperatures (see table 3.1). The largest trend is positive and observed at El Paso de Iritu (+0.8 °C / decade) [fig. 6.9 a) and b)]; Salamanca and Matías Romero [figs. 6.9 a) and b)] have similar magnitudes of trends (-0.4 °C / decade). For the chosen stations an incresing trend is observed in the north and a decreasing trend in southern Mexico.

Studying the linear trends, we can appreciate that two stations have the largest trends for four out of the five selected indices. El Paso de Iritu [fig. 6.9 a)] mainly show changes in minimum temperatures, while at Ahuacatlán [fig. 6.9 b)] variations can be equally seen in the maximum and minimum temperatures indices but not in the DTR index. Geographically, one of these stations is located just north (El Paso de Iritu) and the other south of the Tropic of Cancer (Ahuacatlán). Nevertheless, both sites are close to the Pacific Ocean. It seems that the results are independent of the stations latitude coordinates and the Pacific Ocean is the main regulator of the temperature extremes indices assessed; but it is difficult to conclude it with only two stations. If the Pacific Ocean is the key, among the physical causes we can mention are: the Sea Surface Temperatures (SSTs), the Pacific Decadal Oscillation (PDO) and the ENSO phenomenon. The ENSO hypothesis is going to be explored in deep in chapter 7.

6.3. CONCLUSIONS TO THIS CHAPTER.

In order to have a broader picture of climate change it is necessary to not only study the variations in mean temperature but also the fluctuations of variability, which include extremes. It is precisely these kinds of climatic events that have a great impact on public perception (outside the scientific community) about a changing climate (Beniston and Stephenson, 2004). It is widely accepted that the necessity to expand our understanding on weather extremes is important. The lack of studies in developing countries does not always allow the correct prevention (or mitigation) of the impacts of these extraordinary climatic events. This chapter has aimed to contribute to the subject, by covering this research deficiency in Mexico.

At different scales of space and time, and with dissimilar rates, extreme temperatures are changing in Mexico. At local levels, there are two stations that clearly show these significant fluctuating (taking the climatological mean as a reference) climatic patterns. In the southern tip of the Baja Californian Peninsula, El Paso de Iritu station is getting warmer (for instance, TN90p, TX90p, TXn, and TXx; all with positive correlations with time, statistically significant at the 5% level). On the contrary, cooler conditions are being observed at Ahuacatlán station near the central Pacific coast (For instance, SU25, TN90p, TNn, TNx, TR20, TX90p, TXx, and WSDI; all with negative correlations statistically significant at the 1% level). These results are confirmed when an analysis of trends is applied to four stations (El Paso de Iritu, Ahuacatlán, Salamanca and Matías Romero), that have the largest number of temperature extreme indices with statistically significant results. The clearest pattern to cooling conditions (according to the trends of the temperature extreme indices) is observed at the Ahuacatlán station, in the state of Nayarit in central Mexico, near the Pacific coast. Although these are examples at a local scale a climatic divide can be perceived between warming trends in the north to cooling trends in the south of the country.

The extreme temperature indices were separated into three different groups. According to the results, the groups measuring absolute temperature change (°C) and the one that

calculates the frequency (number of cases or days) of the index exceeding a predefined threshold can be directly compared. These groups are coincident showing clear increasing trends for minimum temperatures. The differences are: in the group that measures absolute temperature change, there is a climatic divide (considering the Tropic of Cancer as a latitudinal limit) with warming conditions in northern Mexico and cooling in the southern part of the country. When the frequency above a threshold is calculated another group of stations has a national pattern of warming conditions. However, there are more cases of indices with significant results when considering the annual counts above thresholds (SU25, TR20 and FD0) than when the annual count is extended into spells (WSDI and CSDI). The last group that defines the percentage of time an index is exceeding a percentile limit (TN90p and TX90p) does not show clear climatic patterns.

An analysis with two different approaches gave us an additional insight about the fluctuations of the extreme temperatures in Mexico. In order to simplify the explanation of the results, the extreme temperature indices were classified per statistical significance (5% or 1% levels of statistical significance) or trends of warming or cooling conditions.

Significant changes in extreme temperatures are observed across Mexico. Three separate analyses show that climatic variations in extreme temperatures are occurring at different spatial scales. A geographical transition has been found as a roughly latitudinal divide between warming trends in the northern part of the country to cooling conditions in the south. Clearly, greater increasing trend can be observed in minimum rather than in maximum temperatures.

CHAPTER 7: THE ENSO MODULATION OF THE CLIMATE OF MEXICO.

7.1. INTRODUCTION.

Previous chapters have shown that different climatic regimes exist in Mexico, and that clear changes are occurring in the most important meteorological variables. Several large-scale atmospheric controls modulate the climate of the country; among these teleconnections, the El Niño-Southern Oscillation exerts an important influence over the fluctuations of precipitation and temperature throughout the country (Magaña and Gay, 2001). Identification of the spatial and temporal patterns of these climatic fluctuations over Mexico is the aim of the chapter seven.

It is very well known that the climate of Mexico is highly seasonal (see section 2.3). In order to find linear correlations between rainfall and temperature with El Niño – Southern Oscillation (ENSO) Kendall's tau-b statistic (see section 3.3.5) will be applied. Annual, wet (May-Oct) and dry (Nov-Apr) season standardised versions of the extreme weather and ENSO indices are used. As the length of the time-series of Niño 3.4 and MEI starts in 1950 instead of 1931 for precipitation and 1941 for temperature, we have to deal with the fact that we cannot use the full capacity of these meteorological variables (see section 3.2.3). Based on the results of the regionalisation using Principal Component Analysis (see chapter 4), only regional precipitation averages are available and not regional temperature time-series.

Climatic responses to large-scale atmospheric controls are frequently delayed in time. For this reason, cross correlation is applied to find the optimal time-shifts that maximise the correlations between the meteorological variables and the ENSO indices; but also to check the spatial consistency when compared with the results of the direct linear correlations. For this purpose, monthly time-series of regional rainfall averages and

extreme weather (precipitation and temperature) indices are (lag) correlated with the ENSO indices.

Linear and lag correlations are calculated in this chapter between the meteorological variables and the different ENSO indices. Section 7.2 describes the relationships between the SOI index and the meteorological variables. Linear correlations involving regional precipitation averages and the extreme weather indices are described in section 7.2.1, while the relationships of the same variables and SOI using lag correlation are explored in section 7.2.2. Analyses using the Niño 3.4 standardised index follow the same pattern: linear correlations with regional precipitation averages are assessed first and with extreme weather indices in section 7.3.1. Section 7.3.2 evaluates the lag correlations of El Niño 3.4 later with the same variables. Finally, sections 7.4.1 and 7.4.2 explore the linear and lag correlations respectively of MEI with regional precipitation averages and extreme weather indices.

The analysis of similarities and differences among the different results are evaluated in the concluding section 7.5. Spatial and temporal climatic patterns among the results from relationships with the ENSO indices are also analysed in this section.

7.2. THE SOI (SOUTHERN OSCILLATION INDEX) INFLUENCE.

The first analysis to be performed in this chapter is the linear correlation between standardised regional averages and SOI indices using Kendall tau-b (see section 3.3.5). The main purpose of the next sections is to correlate (linearly) the regional time series constructed using the results obtained with PCA and three different ENSO indices. The regional time series are classified into three different seasons: Annual, Wet (May-Oct) and Dry (Nov-Apr) seasons. For the rest of the chapter, the three ENSO indices considered in the correlations are: the Southern Oscillation Index (SOI), El Niño 3.4 index and the Multivariate El Niño Index (MEI).

Every time series are in their standardised versions in order to *explicitly avoid* (as much as possible) external influences in the analysis, like altitude (see section 4.2.1). The regional series of precipitation extend from 1931 to 2001 (sections 3.2.1 and 3.2.2), i.e., they use 71 years of instrumental data. Meanwhile, the three ENSO indices have different periods of record: SOI starts on 1866 and finishes in 2004, the Niño 3.4 index and MEI periods are shorter and extend from 1950 to 2004 (see section 3.2.3). Therefore, for this study, they differ in their starting year but coincide, in 2001 as the final year of instrumental temperature and precipitation data. The main objective when using three different standardised indices of ENSO is to test the consistency of the results (linear or lag correlations) with the regional precipitation series.

Basically, there is a correspondence (synchronised in time) between the time series of ENSO indices and regional precipitation when the (linear) correlations analysis are applied, except for the cases in which dry (the November and December months of the year before are computed) are correlated to wet seasons. For instance, wet season standardised versions of regional precipitation averages and SOI indices of 1932 can be correlated, but when we correlate the wet season regional precipitation averages with the

Dry Season SOI of 1932, we use the November and December 1931 indices of SOI also to calculate the November to April index of SOI. In these cases a lag response (frequently seen) is expected in the results, between large-scale atmospheric controls and the meteorological variables. A more precise example of this kind of lagged response will be presented in section 7.2.2 using monthly data.

7.2.1. LINEAR CORRELATION.

Regional Precipitation Averages.

The first analysis to be applied is a linear correlation (Kendall tau-b) between regional precipitation and the different seasonal versions of the standardised SOI index. As described in section 7.2., the SOI is the only index with the possibility of correlating with the regional precipitation series using the full potential of the dataset (1931 to 2001). Firstly, we will start with a description of the regions with the most significant (statistically speaking) results (Fig. 7.1), and at the same time extract the most important climatic patterns associated to these correlations. We have classified the results from positive/negative correlations and separated their levels of statistical significance at either the 5 or 1% level. The seasonal influence will be briefly mentioned here, as later on in this section a more specific analysis is made when the results are contrasted with the extreme weather indices.

One of the regions with the most consistent climatic patterns (being partly modulated) by the El Niño phenomenon is the northern area of the Baja Californian Peninsula (Magaña et al., 2003). In this region, regardless of season, all the statistically significant correlations are negative (for negative anomalies of SOI the regional precipitation is positive, i.e., above normal precipitation during El Niño years). Most of the correlations are statistically significant at the 1% level. This climatic pattern is consistent across all the seasonal (annual, wet and dry) time series for regional precipitation averages. Negative correlations are also observed within the North American Monsoon – also called the Mexican Monsoon – Region (NAMR). All these correlations are better than the 1% level of statistically significance, and the seasonality shows that they are mainly present during the dry season (Nov-Apr). It is worth pointing out that in the

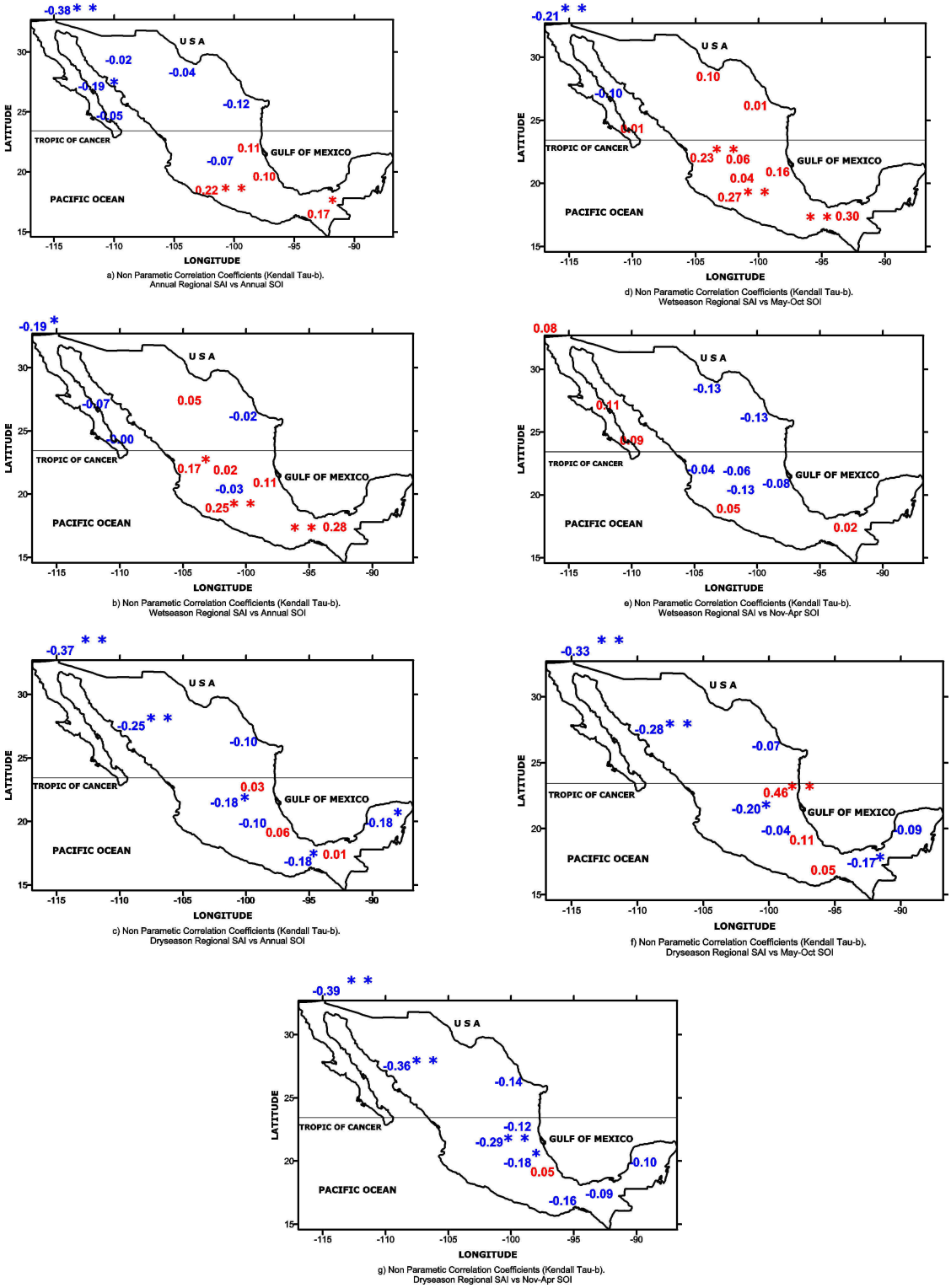

Fig. 7.1. Linear correlations (Kendall tau-b) between the standardised versions of the precipitation regional averages and the Southern Oscillation Index (SOI). Red numbers represent positive and blue numbers negative correlations. * means statistical significant at 5% level and ** at 1% level.

north-western part of Mexico; winter precipitation has a large influence (in percentage terms) on the annual rainfall totals (see section 4.1.2.2).

Some of the correlations between the regional precipitation and the annual SOI are better than the 1% level of statistical significance: positive correlations are observed during the rainfall wet season in the southern Pacific, particularly the south-eastern rainforest and the Michoacán state regions (negative annual SOI or El Niño-like conditions are associated to less than normal precipitation). The same climatic pattern of positive correlations (also statistically significant at the 1% level) is replicated during the May-Oct (wet) season for the south-eastern rainforest region [Fig. 7.1 b) and d)].

A consistent climatic pattern is observed across all the regions having the greatest correlations and statistically significant results: there is a clear latitudinal transition from north to south across Mexico (Cavazos and Hastenrath, 1990). It is interesting to note that this climatic pattern of the most statistically significant correlations is slightly concentrated geographically along the Pacific coast of Mexico. The North Pacific regions within the northern Baja California peninsula and the NAMR respond during the dry season with above normal precipitation during El Niño-like conditions, and dry regimes are seen for the same regions during La Niña [Figs. 7.1 c) and f)]. Meanwhile, the regions along the southern Pacific coast are associated with positive correlations, i.e., deficit rainfall (referred to their long-term means) during the El Niño phase.

Among all the statistically significant results, the greatest correlation (+0.46, better than the 1% of statistical significance) is seen in the La Huasteca (see Table 4.1) region [Fig. 7.1 f)]. This is the only significant result for this region, and is observed when the rainfall dry season is correlated to the wet season of SOI. Therefore, dry conditions are to be expected under El Niño-like conditions for La Huasteca region. Negative correlations (precipitation above normal, during El Niño) at better than the 1% of statistical significance are observed within the north-western part of Mexico, especially for the rainfall dry season combinations [Fig. 7.1 c), f) and g)]. It is well documented (Mosiño

and García, 1974) that boreal winter precipitation (closely in correspondence to what is called the dry season of precipitation for the rest of the country) is very important in terms of the annual totals. This climatic pattern can be clearly noted in both the Mexican Monsoon and the northern Baja Californian regions during the November to April (dry season) period.

The Trans Mexican Volcanic Belt (TMVB or Neovolcanic axis) region is also affected during the dry rainfall season. Most of the stations, in this region, are located at high altitudes. Therefore, as mentioned in section 2.2, the precipitation within this region is strongly influenced – among other geographical factors - by polar fronts (Jauregui, 1997) during the Northern Hemisphere winter. Negative correlations (precipitation below normal) are observed, in this region of high altitude stations, relating the dry rainfall season to both the annual and wet seasons of SOI. All these results are statistically significant at the 5% level.

Earlier in this section, when analysing the stations with the most significant correlations, it was mentioned that, for the annual totals and wet season for precipitation (see Fig. 7.1), a latitudinal response of the climate of Mexico can be observed during El Niño conditions: wetter patterns for the northern part of the country and drier conditions in the south, and that they are mainly geographically concentrated along the Pacific coast (Englehart and Douglas, 2001). The clearest latitudinal climatic transition is found when the Annual SAI (precipitation regional averages) is correlated to the Annual SOI [figure 7.1 a)]. Quite similar, but less clear is the climatic picture when we observe the relationships between wet (May-Oct) SAI (Standardised Anomaly Index) and the annual SOI [figure 7.1 b)].

A similar analysis to the latitudinal climatic features can be applied searching for coastal or continental climatic patterns related to the most (statistically) significant results. Seasonality also plays an important role in the relationships, with annual and wet seasons for the SOI having the clearest results. The greatest correlations are strongly linked to the annual SOI [Figs. 7.1 a), b) and c)]. Utilising either the annual or wet (season) versions of

the SAI, the results exhibit a clear coastal pattern, especially along the Pacific coast, probably with SST as a modulator (Giannini et al., 2001). These are the same combinations that have the best results for the latitudinal climatic transition. However, the largest correlations are found for the annual compared to the wet season SOI. Two regions appear consistently with statistically significant correlations: the Northern part of the Baja Californian peninsula and the south-eastern regions. No continental/coastal climatic pattern is found when using the dry season (Nov-Apr) SOI for correlations [Fig. 7.1 e) and g)].

Of all the seven possible combinations (see fig 7.1), it is the annual SOI [Figs. 7.1 a), b) and c)] that best modulates the rainfall in Mexico, i.e., showing the largest and statistically significant correlations. It can be easily observed in the maps that relate the annual SOI with both the annual and wet season (May-Oct) SAI; a latitudinal climatic transition is clearly seen, especially when the annual SOI is correlated to annual SAI, with greater correlations than when combining with wet season (May-Oct) SAI. The responses of the dry season (Nov-Apr) SAI (regional precipitation) to the annual SOI show a nationally widespread pattern of negative correlations (wetter conditions during El Niño-like years). The Yucatan Peninsula region (RD7 in Table 4.3) is the most interesting result here, although it does not have the largest correlation. It seems that the highly variable amount of rainfall during the hurricane season has an important influence for the rest of the other seasons of SOI (see also section 4.1.2). Wet (May-Oct) and dry (Nov-Apr) seasons SAI have two very different responses to the wet season (May-Oct) SOI. An almost nationally widespread pattern of positive correlations (drier conditions during El Niño phase) can be observed for the wet season (May-Oct) SOI, except for some regions along the Gulf of Mexico, especially for the La Huasteca region (RA7 in Table 4.1), that has the largest correlation (with annual SOI) of all the seasonal combinations. Lastly, when the impact of the dry season (Nov-Apr) SOI is considered, an almost national coverage of negative correlations (wetter conditions during El Niño) can be perceived, the strongest relationships are present within the north-western part of the country especially the North American Monsoon and the North Baja California regions.

Meanwhile, no clear climatic pattern is observed when the dry season (Nov-Apr) SAI and wet season (May-Oct) SOI are correlated [Fig. 7.1 f)].

Extreme Weather Indices.

Precipitation.

For this research, besides the regional precipitation averages, we have correlated the Southern Oscillation Index with the extreme weather indices. Precipitation and extreme temperature indices were extracted using the R software (see chapters 5 and 6). To calculate the extreme indices, daily data of temperature and rainfall extending from 1941 to 2001 have been used (chapter 5), while for the regional average analysis, monthly data (1931-2001) was used (chapter 6). In addition, we are changing the analysis from regional (PCA regions averages, see section 3.3.3) to local (sites) time series; therefore, the results of this analysis can be contrasted with those of the regional series. Both data sets are correlated with three different seasonal (annual, wet –May-Oct- and dry –Nov-Apr-) SOI indices in their standardised versions.

The first analysis performed in this section is to correlate linearly the standardised annual SOI and the extreme precipitation indices (refer to section 3.3.4 for extreme weather indices definitions). As mentioned in the former section, the SOI index allows the use of the full length of the extremes time-series. It is important to note here the practical impossibility, for most of the indices, of dealing (as monthly indices are not available in the results, but only the extreme annual rainfall indices) with seasonal versions of the indices of extremes.

The set of precipitation extreme indices when correlated with the annual SOI show clear results and climatic patterns for two of the indices: Consecutive Dry Days (CDD) and the annual maximum 1-day precipitation (RX1day). These indices are presenting two different aspects of the rainfall extremes evaluation with drier conditions for the former and wetter conditions for the latter. The CDD index map [Fig. 7.2 a)] depicts a clear national pattern of positive correlations, mainly concentrated in the northern part of the country, where four out of the five most statistically significant correlations are found.

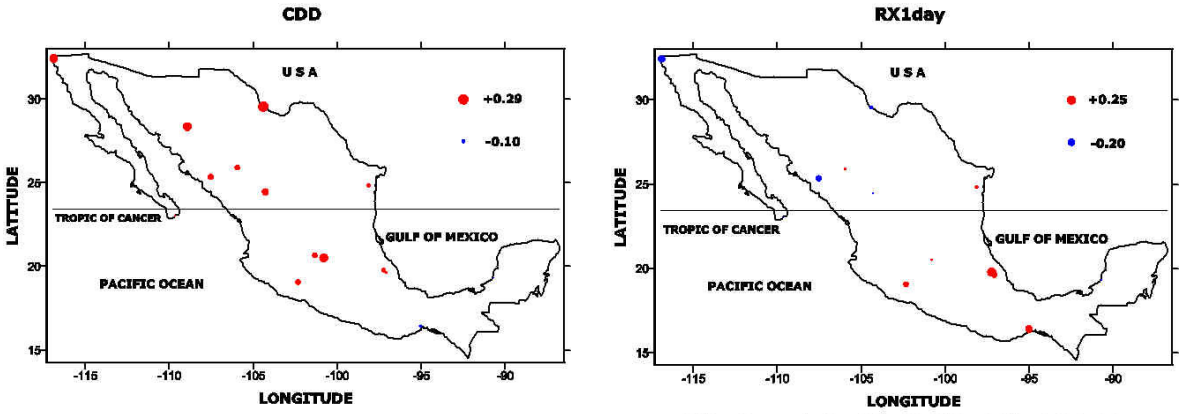

a) Non Parametic Correlation Coefficients (Kendall Tau-b).
Consecutive Dry Days (CDD) vs Annual SOI

b) Non Parametic Correlation Coefficients (Kendall Tau-b).
Maximum 1-day precipitation (RX1day) vs Annual SOI

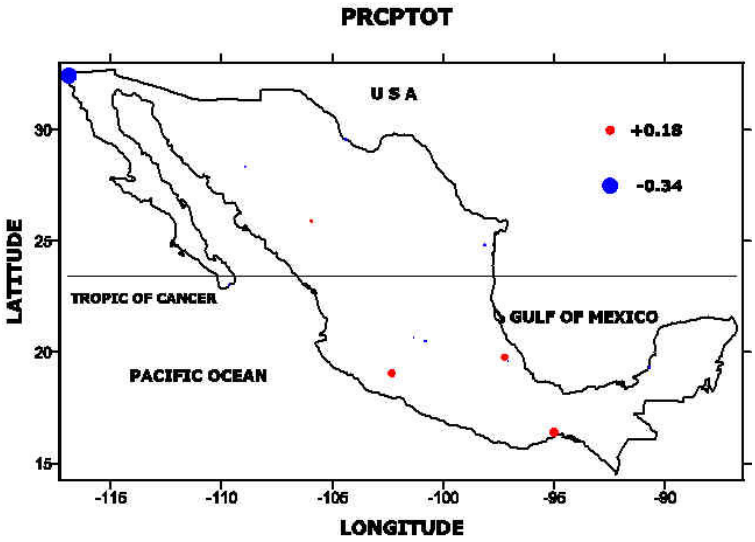

c) Non Parametic Correlation Coefficients (Kendall Tau-b).
Annual Total Precipitation (PRCPTOT) vs Annual SOI

Fig. 7.2. Linear correlations (Kendall tau-b) between the Extreme Precipitation Indices and the Annual Southern Oscillation Index (SOI). Circles in red are representing a positive and in blue negative correlations.

Then, during El Niño (Niña) atmospheric conditions below (above) normal precipitation is experienced especially in the northern (southern) Mexico. In the meantime, RX1day [Fig. 7.2 b)] is linked to a latitudinal climatic transition: positive correlations south the Tropic of Cancer (considering this as a geographic limit) and negative in the northern part of the country. But, there is also a longitudinal transition: southern (positive) correlations are related to the Atlantic Ocean (Gulf of Mexico), while the negative (northern)

correlations are linked to the Pacific Ocean: three out of the four statistically significant correlations are located at the stations along the Pacific Ocean.

There are two stations having the most statistically significant results, for CDD and RX1day: Presa Rodríguez, BC, in the Baja Californian peninsula; and Atzalán, Ver. in the Gulf of Mexico (station numbers 2 and 34 in Table 5.1). Negative correlations are prevalent in the extreme indices of the Presa Rodríguez station, i.e., during El Niño-like conditions above normal precipitation is observed here; geographically speaking, this station is located in the most north-western part of the country, north of the *Tropic of Cancer*. Below normal precipitation is observed in Atzalán, Ver.; which is located south of the Tropic of Cancer. Positive correlations (+0.25) for RX1day mean that during El Niño phase, drier conditions are dominant at this location. The largest correlation (-0.34) of all the extreme indices (when correlated with the standardised annual SOI) is found for the total annual precipitation (PRCPTOT) [Fig. 7.2 c)] at La Presa Rodríguez station. The negative correlation indicates that above normal precipitation is linked to El Niño-like conditions (negative SOI).

Similar to the correlations for precipitation extreme indices with the annual SOI, the standardised version of the wet season (May-Oct) SOI was used to calculate linear correlations. As mentioned in section 2.2.1 the wet season accounts for at least 70% of the total annual precipitation across much of the country. Therefore, it is expected that some similarities arise between the correlations utilising annual SOI and wet season SOI.

We can start reviewing the maps of extreme indices (Fig. 7.3) with the best correlations, as already done using the annual SOI. The precipitation extreme indices that show the clearest climatic patterns are: CDD, R95P, R99P, RX1day and PRCPTOT (for their definitions refer to section 3.3.4). With the exception of CDD [Fig. 7.3 a)], the rest of the rainfall indices are linked to wetter conditions. In fact, three out of five of these indices are related to a heavy rainfall threshold (R95P, R99P and RX1day), and as their units are millimetres, they can be directly compared with precipitation totals or the normal amount.

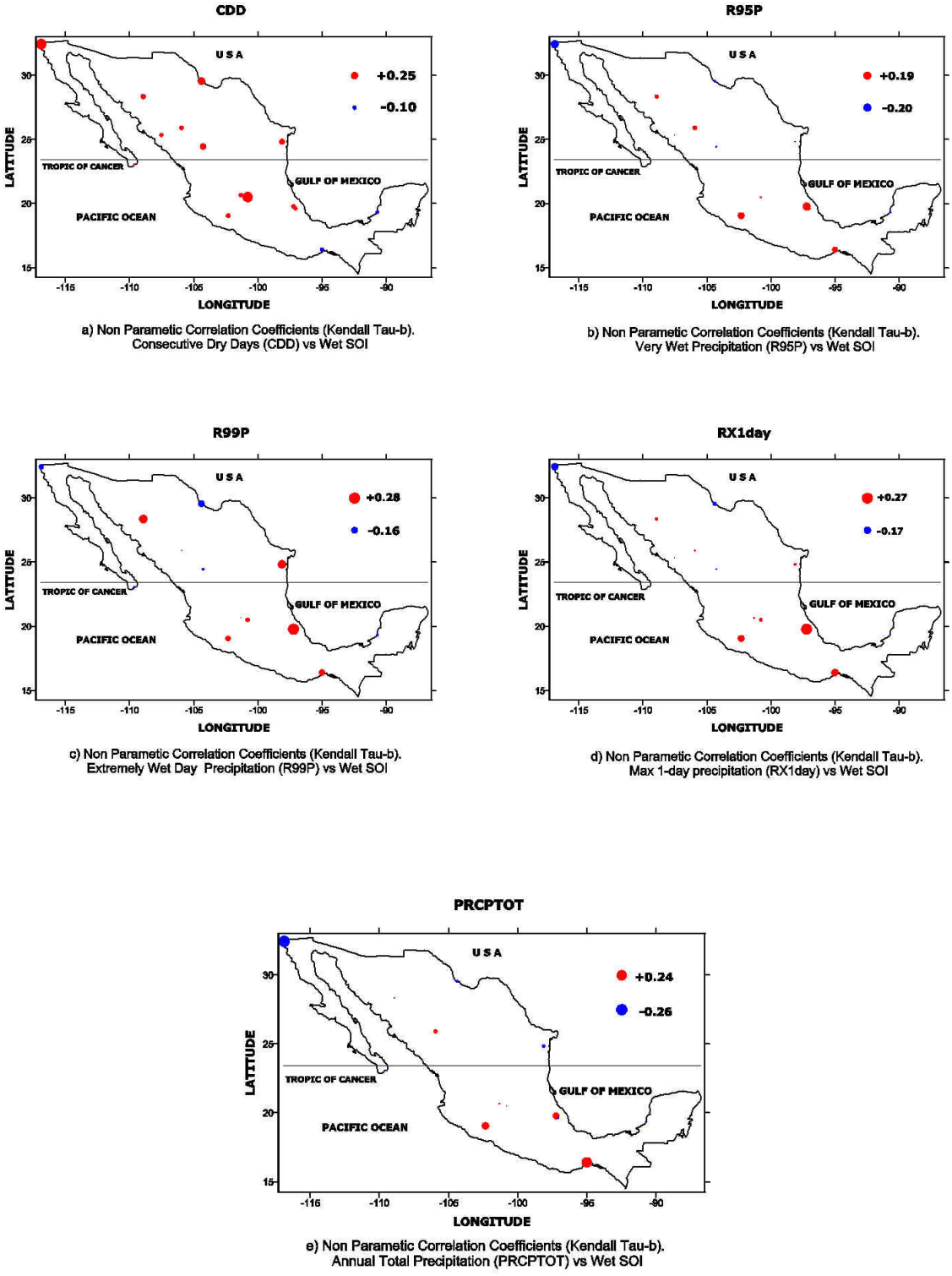

Fig. 7.3. Linear correlations (Kendall tau-b) between the Extreme Precipitation Indices and the May-Oct (wet season) Southern Oscillation Index (SOI). Circles in red are representing a positive and in blue negative correlations.

Among the results with the clearest patterns, the only index that directly measures drier conditions is CDD. Positive correlations are widespread nationally for this index. According to these linear relationships between the wet season SOI and CDD [Fig. 7.3 a)], wetter conditions are mainly observed during El Niño-like conditions. Nevertheless, amongst all the stations only two have statistically significant results: Celaya in Central Mexico, and Presa Rodríguez in the most north-western part of the country (station numbers 16 and 2 in Table 5.1) . More days exceeding the 95th percentile (R95P) are seen in a nearly nationally widespread pattern of positive correlations [Fig. 7.3 b)]. This means that during El Niño conditions fewer rainy days surpass the 95th percentile. For the R95P index, Atzalán and Presa Rodríguez (station numbers 34 and 2 in Table 5.1) are the only stations with statistically significant results: positive for Atzalán and negative correlation for Presa Rodríguez. Although, no clear climatic pattern is observed for the index that measures days exceeding the 99th percentile [(R99P, Fig. 7.3 c)], it can be mentioned that the most important results are located along both coasts. It is worth noting that two out of the three stations with statistically significant correlations, are found along the Gulf of Mexico. There is no latitudinal climatic transition in these correlations, but two of these stations with statistically significant results are located north of the tropic of Cancer: Yecora within the Mexican or North American Monsoon Region –NAMR- (RA11 in Table 4.1) and San Fernando in the North-eastern part of the country (station numbers 32 and 33 in Table 5.1). Meanwhile, Atzalán (located in the Los Tuxtlas region; station number 34 in Table 5.1) is the only station with a correlation better than the 1% statistical significant level. Similar correlation patterns to those of R95P are found for the RX1day index [Fig. 7.3 d)]. Positive correlations are dominant across the country, however only Atzalán station, which is located on the Gulf of Mexico, has a positive correlation that is better than the 1% level of statistical significance. Finally, the PRCPTOT [Fig. 7.3 e)] index shows a climatic pattern similar to that of R95P with almost a national pattern of positive correlations, except the Presa Rodríguez station in the most north-western part of Mexico (station number 2 in Table 5.1) with a negative correlation, and statistically significant at the 1% level. The other largest correlation is located at Juchitán (station number 27 in Table 5.1) within the Southern Pacific coastal region.

The regional climatic features of the ENSO modulation during the May to October period were explored earlier in section 7.2.1. Now, we will evaluate local responses of the extreme climate indices to the wet season SOI, and some interesting climatic features arise. The stations that appear more frequently with statistically significant results are: Presa Rodríguez (north-western Mexico; station number 2 in Table 5.1), Atzalán (Central Gulf of México; station number 34 in Table 5.1) and Juchitán (Southern Pacific coastal region; station number 27 in Table 5.1). The Presa Rodríguez station has statistically significant results for the SDII, CDD, CWD, R20mm and PRCPTOT. A closer study of those correlations shows that, in general, during El Niño conditions, above normal precipitation is prevalent at this location. The station at Atzalán, Ver. shows statistically significant positive correlations in the rainfall extreme indices SDII, R95P, R99P and RX1day. Interpreting the relationships of these indices with the wet season SOI it can be concluded that, during prevalent El Niño conditions, mainly below normal precipitation is observed at Atzalán station. Juchitán in Oaxaca State shows significant correlations for the R20mm, RX5day and PRCPTOT indices. At this station, all the correlations relate to drier conditions during El Niño phase (Cavazos and Hastenrath, 1990). Probably, more stations with statistically significant results are required to strongly support this conclusion, but it can be said that above normal precipitation is observed north of the Tropic of Cancer and drier conditions south of this defined geographic limit during with El Niño-like years.

The last analyses of linear correlation (Kendall tau-b) are now to be applied between the dry season SOI (November to April) and the rainfall extreme indices. As mentioned in section 4.1, for most of Mexico, the dry season does not account for much of the precipitation totals, except in the north-western part of the country (winter precipitation prevails in this latter region, Magaña et al., 2003). For this reason, it is expected that the dry season SOI climatic patterns differ in some sense from those of the other seasons [annual and wet (May-Oct) season].

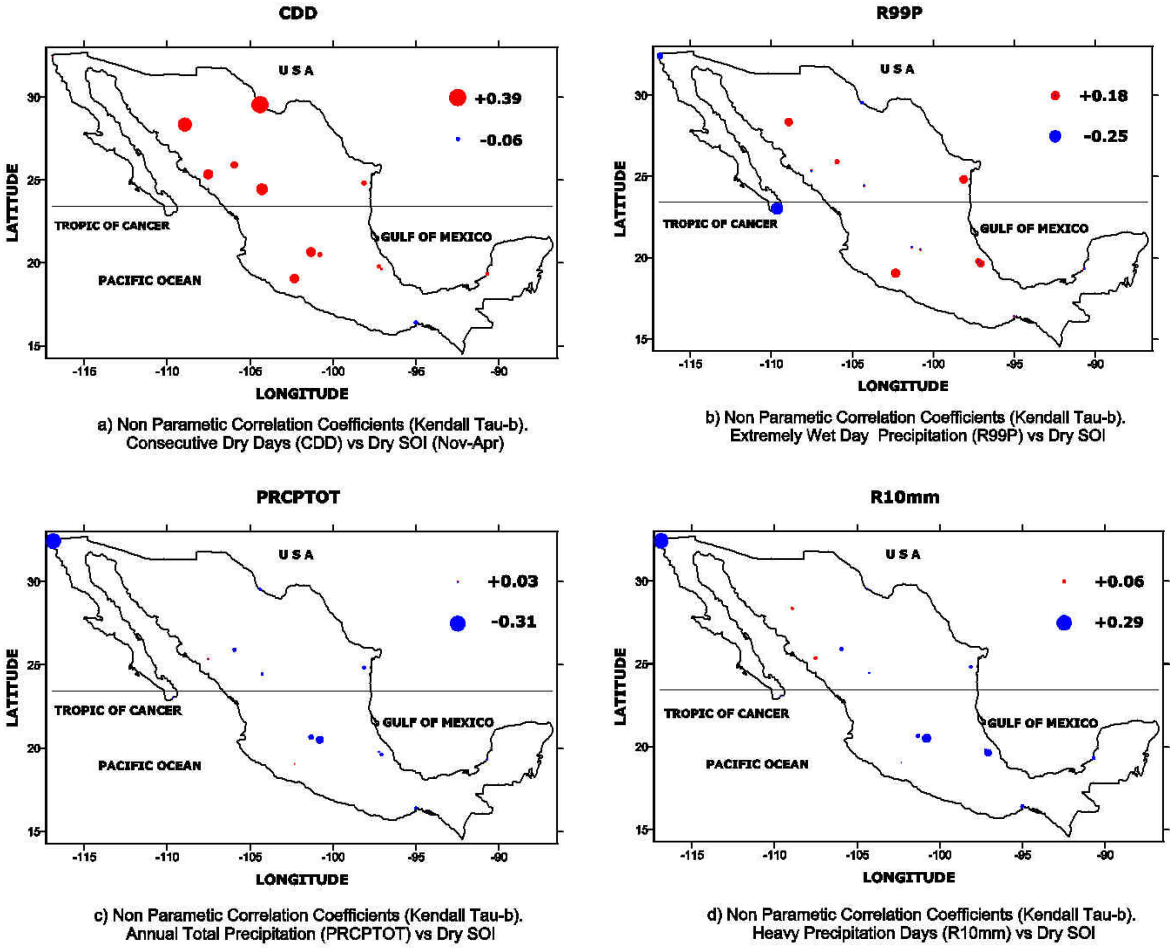

Fig. 7.4. Linear correlations (Kendall tau-b) between the Extreme Precipitation Indices and the Nov-Apr (dry season) Southern Oscillation Index (SOI). Circles in red are representing a positive and in blue negative correlations.

Among the correlations between the extreme rainfall indices and the dry season SOI, the most (statistically) significant results are seen for the CDD, PRCPTOT and R99P indices. The CDD [Fig. 7.4 a)] shows that the most statistically significant results are located along the Pacific Ocean coast especially within the North American Monsoon (or Mexican Monsoon) Region (NAMR; RA11 in Table 4.1). This is an area in which winter precipitation has an important role in the annual rainfall totals, as mentioned in section 2.2.1. Strong EL Niño (La Niña) conditions reinforces the oceanic and atmospheric conditions that lead to wetter (drier) patterns along the Pacific Ocean coast in Mexico. The scale of the results is larger than regional: a nationally widespread pattern of positive

correlations with the dry season is observed. This means that, during El Niño, wetter conditions or fewer Consecutive Dry Days are prevalent nationally. Above normal precipitation is also observed for the PRCPTOT index [Fig. 7.4 c)] during El Niño conditions. A national pattern of negative correlations for PRCPTOT show wetter conditions during the negative phase of SOI. However, only two of these stations have statistically significant correlations: Celaya in Central Mexico, and Presa Rodríguez in Tijuana (station numbers 16 and 2 in Table 5.1), whose correlation is better than the 1% level of statistical significance. The next two indices with the clearest results are related to a set limit, one expressed in mm and the other in percentage terms. Nevertheless, these indices show two very different responses for dry season SOI: negative for R10mm and positive correlations for R99P. Negative correlations are dominant across the country for the R10mm index [Fig. 7.4 d)] for Mexico this means more rainy days exceeding the 10mm threshold. Among all these results only three of them are statistically significant, but only La Presa Rodríguez (station number 2 in Table 5.1) has a correlation better than 1% statistical significance. In the meantime, a continental pattern of positive correlations is seen for R99P [Fig. 7.4 b)], although none of these results are statistically significant, while a completely different pattern of negative correlations are seen across the Baja Californian peninsula, where the station at San José del Cabo has the largest correlation that is statistically significant at the 1% level.

Amongst all the results using the dry season SOI, Ojinaga and Yecora within NAMR (RA11 in Table 4.1) have the largest correlations throughout all the rainfall extreme indices. Both stations have the best correlations for the CDD index, and better than the 1% statistical significance level. These results strongly support what has been already established in section 4.2.1 about the importance of the winter precipitation in the Mexican Monsoon region (Ropelewski et al., 2004). Therefore, at regional and local levels, the CDD correlations are climatically coherent. It can be said that, across México, less Consecutive Dry Days (and possibly precipitation above normal) can be expected during El Niño conditions.

Temperature.

Another aspect of extreme weather likely related to SOI is the daily temperature. At two different levels, the correlations from this study can be compared with the former results: at the local level with the correlations from the extreme rainfall indices, and at the regional scale with the results from the regional precipitation averages. The temperature extreme indices will be correlated, consecutively with annual, wet (May-Oct) and dry (Nov-Apr) season standardised versions of the SOI; just as undertaken for regional precipitation averages and rainfall extremes indices in the previous section.

Annual SOI.

Maps of temperature extreme indices correlated with the annual SOI that have the clearest results include: TR20, TN10p, TN90p, TX90p, DTR and TXx (for definitions refer to section 3.3.4). For an easy interpretation, these indices will be analysed in groups according to the units by which they are measured (days, %, and °C). The results for the TR20 index [Fig. 7.5 a)] show a nearly national climatic pattern of negative correlations. Despite this, statistically significant results are geographically concentrated along the Pacific Coast, north of the Tropic of Cancer, within the NAMR and the Baja California peninsula. These correlations are pointing to a slight increase in warmer (tropical) nights during El Niño conditions. The next three indices evaluated are associated with percentile thresholds: TN10p, TN90p and TX90p, and they are expressed as a percentage of days per year. The first two indices are related to night and the last to day temperatures. An almost national climatic pattern of positive correlations is observed for the TN10p index [Fig. 7.5 b)]. Climatically, this means that the percentage of days the temperature is below the 10th percentile is reduced, i.e., during the negative phase of the Southern Oscillation (El Niño) a warming on minimum temperatures is experienced. Statistically significant results are concentrated along the Pacific Coast, especially in the Baja California peninsula. Correlations better than the 1% level of statistical significance are found north of the Tropic of Cancer. A widespread warming signal is also seen across

Mexico during El Niño-like years for TN90p [Fig. 7.5 c)]. There is a slight concentration of statistically significant (negative) correlations in the southern part of the country. The largest correlations are found at Atzalán (-0.25) and Matías Romero (-0.23) stations, the former located along the Gulf of Mexico coast, and the latter on the southern Pacific coast. Significant results are also found in central Mexico and the Baja California Peninsula. The TX90p index [Fig. 7.5 d)] shows a similar climatic pattern to that of TN90p. Negative correlations are present almost nationally. Just as with TN90p [Fig. 7.5 c)], all the largest correlations are significant at the 5% level of statistical significance, except Atzalán (station number 34 in Table 6.1) that is significant at the 1% level. According to these results, cooler temperatures are dominant during El Niño conditions for TX90p. The DTR index [Fig. 7.5 e)] is also showing an almost national pattern of positive correlations, except for one of the southernmost stations (Santo Domingo Tehuantepec) on the South Pacific coast with a statistically significant result. Therefore, during El Niño conditions DTR decreases. According to the results, this decrease of the DTR index is likely caused by a net increase in minimum temperatures. Finally, for the TXx (Hottest Day) index , a clear pattern of negative correlations is seen along the Mexican Pacific coast, but it is only the station at Matías Romero in Oaxaca (station number 28 in Table 6.1) that has a correlation (-0.31) better than the 1% level of statistical significance. Meanwhile, positive correlations are observed in continental central and northern Mexico, but only the correlation at San Fernando (station number 33 in Table 6.1) is statistically significant. The results for the TXx lead to warmer maximum temperatures during El Niño phases.

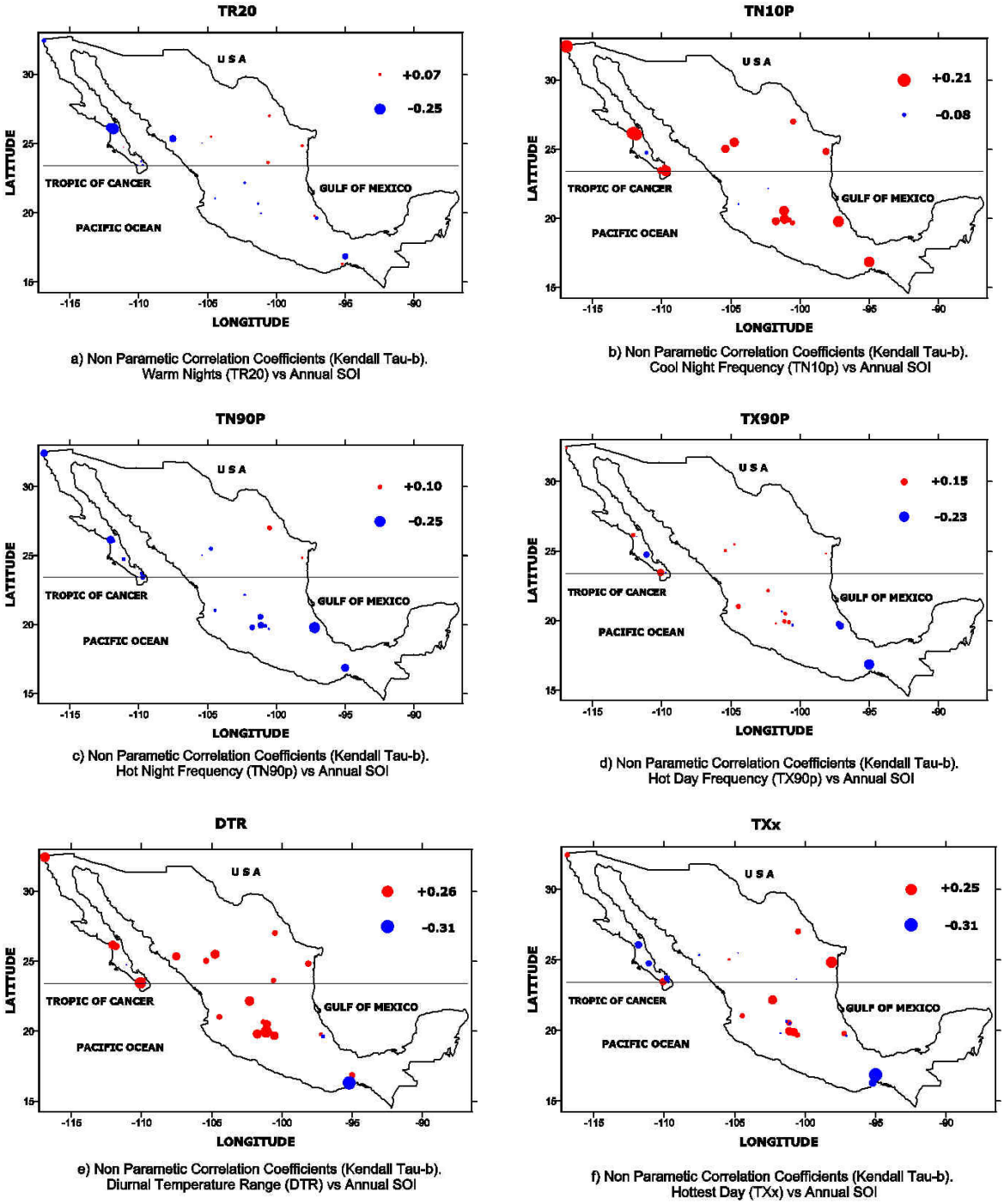

Fig. 7.5. Linear correlations (Kendall tau-b) between the Extreme Temperature Indices and the Annual Southern Oscillation Index (Annual SOI). Circles in red are representing a positive and in blue negative correlations.

Observing the stations with the largest (linear) correlations among the temperature extreme indices, we found that Matías Romero (station number 28 in Table 6.1) is the station that has the most statistically significant results (TX10p, TX90p and WSDI). According to its correlations, during the El Niño phase, warmer conditions are found at this site in the southern Pacific coastal region. In order to compare with a station north of the Tropic of Cancer that also has the largest number of statistically significant results, we have selected San Fernando (station number 33 in Table 6.1), in the north-western part of the country, near the Gulf of Mexico. This location has statistically significant results for SU25 and WSDI. The indices correlations for San Fernando show cooling conditions during El Niño phase. In general, an evident pattern of warmer temperatures during El Niño conditions (utilising the standardised annual SOI index) is seen among the different extreme temperature indices. This is especially true for the minimum temperatures that show consistently increased values in their associated indices during El Niño.

Wet Season SOI.

In order to directly compare with their counterparts from the regional rainfall series and precipitation extreme indices, wet season SOI is used in this section for correlation with the temperature extreme indices. Linear correlations are applied between the wet season (May-Oct) SOI and the temperature extreme indices. The indices with the clearest results and their corresponding maps are going to be analysed dividing them into three different groups according to their measurement units. The first indices to be analysed are FD0 and SU25 (days). TN10p and TN90p are the indices with a percentage limit to be interpreted after. Finally, measured in degrees Celsius (TNn and TXx) are the last indices to be considered.

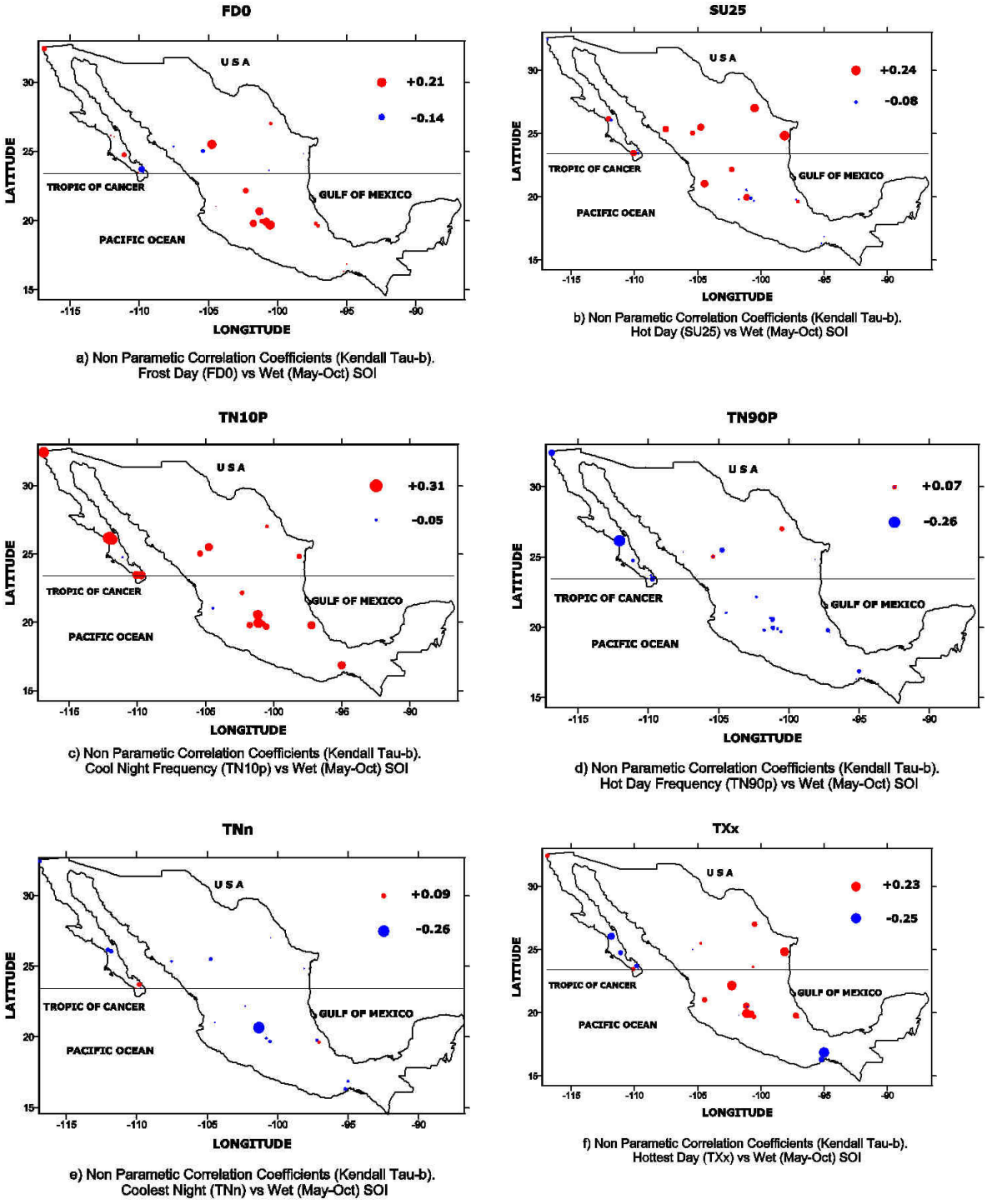

Fig. 7.6. Linear correlations (Kendall tau-b) between the Extreme Temperature Indices and the wet season Southern Oscillation Index (wet season SOI). Circles in red are representing a positive and in blue negative correlations.

The first extreme index to be analysed with May-Oct (wet season) SOI is FD0 (Frost Days, TN< 0°C). A national climatic pattern of positive correlations could easily be observed in [Fig. 7.6 a)]. Only two stations at high altitude (Ciudad Hidalgo and El Palmito; station numbers 23 and 14 in Table 6.1) have statistically significant results: they are located in the Meseta Central (Central Mexican Highlands). Their positive correlations are better than the 5% level of statistical significance. The largest correlations are also geographically concentrated in the western half of the country. A slightly similar pattern is observed for the SU25 (summer days above 25 °C) index. Positive correlations are geographically widespread especially from Central to Northern Mexico [Fig. 7.6 b)]. San Fernando (station number 33 in Table 6.1) in the north-eastern part of Mexico has the largest positive correlation (+0.24), which is statistically significant at the 5% level. The correlations imply a net decrease in both indices (FD0 and SU25) during El Niño conditions. The extreme indices that exceed a set limit (TN10p and TN90p) show a clear pattern towards warmer temperatures during El Niño conditions, especially within the Baja California Peninsula. A national pattern of positive correlations could be clearly observed in the TN10p map [Fig. 7.6 c)]. The largest correlations are found at La Purisima and La Presa Rodriguez (station numbers 5 and 2 in Table 6.1), statistically significant at the 1 and 5% levels respectively. A national climatic pattern of mostly negative correlations is seen in the TN90p index [Fig. 7.6 d)]. The same stations as in TN10p have the largest correlations for TN90p, however, this time their correlations are better than the 1% level of statistical significance. The last group of indices (TNn and TXx) have °C as their measurement units. A clear national pattern of negative correlations is observed for the TNn index. Nevertheless only Irapuato (-0.26) in Central Mexico (station number 17 in Table 6.1) has a statistical significant (better than the 1% level) result. In general, absolute minimum temperatures (TNn) increase during El Niño conditions. The Hottest day (TXx) index shows a rough coastal/continental climatic pattern. Negative correlations are observed along the Pacific Coast, while positive correlations are seen over the interior, with the exception of the San Fernando (station number 33 in Table 6.1) in the north-western part of the country. All these correlations are statistically significant at the 5% level; and geographically concentrated in the

central/northern part of the country. For the TXx index, warmer (colder) temperatures are observed during El Niño (La Niña) conditions.

La Purísima (station number 5 in Table 6.1) is the station that has most indices (CSDI, TN10p, TN90p and TR20) with statistically significant results. All these extreme temperature indices are pointing towards warmer conditions. The index with the greatest positive correlation is CSDI (0.36), and the largest negative correlation is observed in the TN90p index (-0.26); both correlations are statistically significant at the 1% level.

Dry Season SOI.

The final stage in analysing the relationships between the extreme temperature indices and the Southern Oscillation Index is to correlate the dry season version (November to April period) of the standardised SOI and the temperature extreme indices. The maps with the clearest climatic patterns are going to be described, and compared with the previous results (the linear correlations using the standardised annual and wet season). The extreme indices were grouped according to their measurement units are: days (DTR and SU25), percentage (TN10p and TN90p) and °C (TNn and TNx). Considering the local scale, the stations with most statistically significant correlations (indices) are analysed. Finally the greatest correlations among all the indices are contrasted in order to find consistency among the resulting climatic patterns.

Temperature extreme indices that measure the number of days a temperature exceeds a set limit are considered first. Positive correlations are observed over most of the Mexican territory for the DTR index [Fig. 7.7 a)]. Statistically significant results are basically concentrated in Central and Southern Mexico, only Santa Gertrudis station, within the Baja California Peninsula (station number 8 in Table 6.1) is located slightly north of the Tropic of Cancer; and the only negative correlation is found at Santo Domingo Tehuantepec in the southern Pacific (station number 29 in table 6.1). In general, during El Niño conditions decreasing DTRs are seen across Mexico. Meanwhile, positive

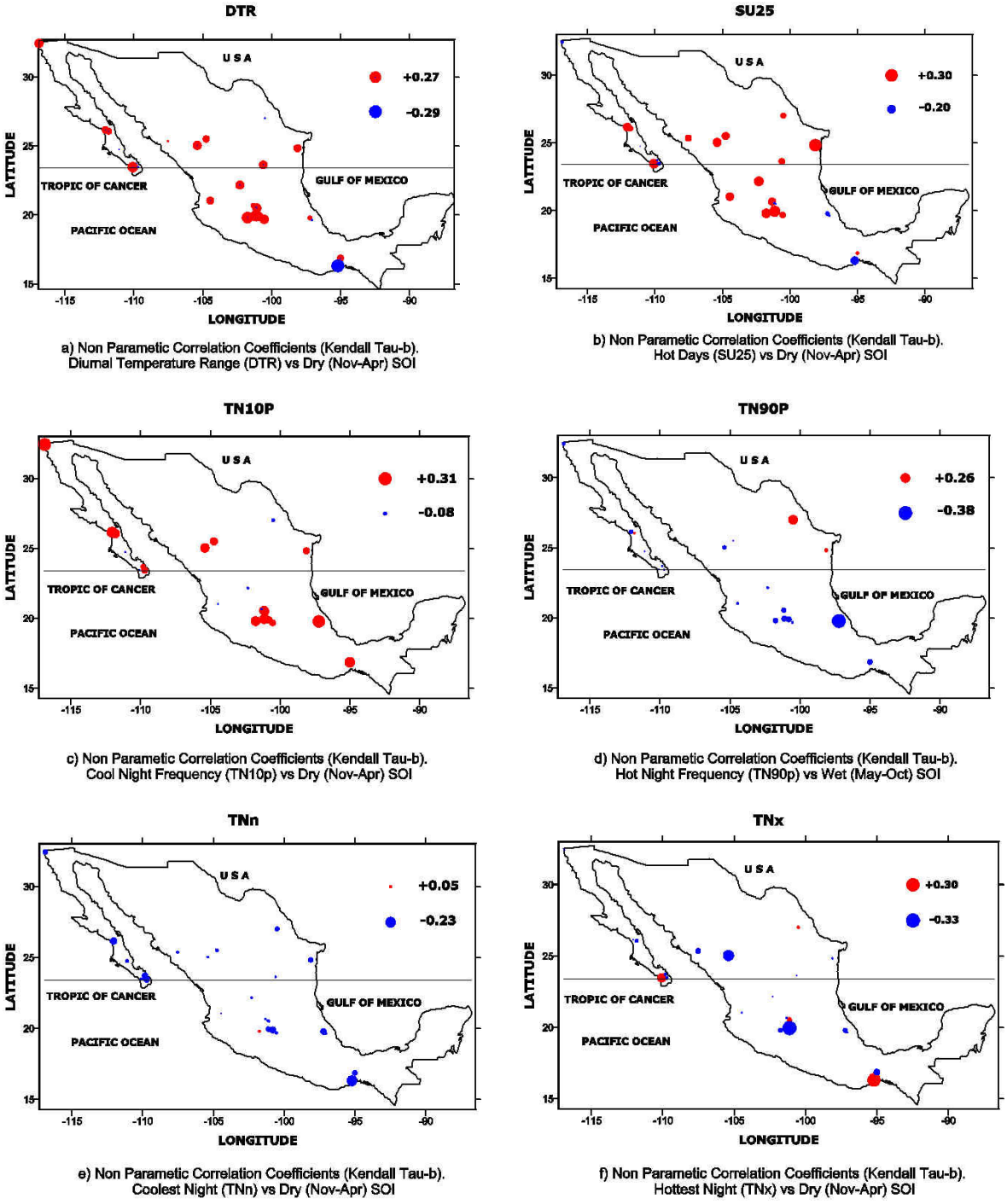

Fig. 7.7. Linear correlations (Kendall tau-b) between the Extreme Temperature Indices and the Dry Season Southern Oscillation Index (dry season SOI). Circles in red are representing a positive and in blue negative correlations.

correlations are almost nationally widespread for the SU25 index [Fig. 7.7 b)]. However, the largest correlations are concentrated in Central and Northern Mexico, precisely the area strongly affected by polar fronts during the boreal winter (see section 2.2.2). San Fernando and Cuitzeo del Porvenir are the only two stations with significant correlations (station numbers 33 and 21 in Table 6.1), these results are statistically significant at better than the 1 and 5% levels respectively. According to these results, colder temperatures are generally observed for the SU25 index during El Niño.

The TN10p and TN90p indices show warmer temperatures during El Niño conditions. A national climatic pattern of positive and negative correlations is observed for TN10p and TN90p respectively. Nevertheless there are subtle differences between these indices. The TN10p map [Fig. 7.7 c)] shows that statistically significant positive correlations are geographically concentrated along both the Atlantic and Pacific coasts. For this index, the stations with the largest correlations (statistically significant at the 1% level) are: La Presa Rodriguez in the northern Baja California Peninsula (station number 2 in Table 6.1) and Atzalán in the Central Gulf of Mexico (station number 34 in Table 6.1). Meanwhile, negative correlations are the most significant results for the TN90p index [Fig. 7.7 d)]. The largest correlation (-0.38) is seen once more at Atzalán. Geographically speaking, the greatest correlations are mainly located within the southern part of Mexico; only La Purísima station in the peninsula of Baja California (station number 5 in table 6.1) is slightly north of the Tropic of Cancer. The only positive correlation (+0.27) among the results for TN90p is found at the Lampazos station in the north-western part of Mexico (station number 26 in Table 6.1) that breaks the simplicity of this climatic pattern.

Finally, let us evaluate two night-time temperature indices that are measured in °C units. An almost national pattern of negative correlations is observed for TNn, and TNx. Statistically significant results are concentrated along the Pacific Coast for the TNn index [Fig. 7.7 e)]. Although national, the climatic pattern for TNx [Fig. 7.7 f)]; the most significant results for this index are found at the Santiago Papasquiaro and Cuitzeo del Porvenir (station numbers 15 and 21 in table 6.1), both are located above 1500 m.a.s.l., and have negative correlations better than the 1% level of statistical significance. Both

extreme indices basically respond with warmer temperatures to atmospheric El Niño conditions.

An almost national climatic pattern (with a component along the Pacific Ocean) of warmer temperatures is seen across Mexico during El Niño-like years. This is especially evident in the case of minimum temperatures that lead to decreasing DTRs across most of the country.

7.2.2. LAG CORRELATION (SOI).

Precipitation Regional Averages.

Local climate responses to ENSO are sometimes difficult to prove, because most of the time these climatic variations take a variable period of time to be evident. For this reason, lag-cross correlation was selected as an alternative to find connections between the climate of Mexico and ENSO. The aim of this technique is to find the lag that maximises the correlation between the variables. Therefore, our objective here is to determine how long it takes, for a certain location, to fully respond to ENSO. This response can be expressed as a small or large fluctuation from the normal climatic conditions.

The lag-cross correlation (using the public software SPSS for Windows, Release 11.0.1, that applies the Pearson correlation coefficient) is used in this section to establish the relationships between the monthly time-series of the standardised Southern Oscillation Index (SOI) and the regional precipitation averages. Theoretically, positive or negative lags are possible in the process of finding the optimal correlations, but spatial consistency is also expected when contrasting the different responses of the regional precipitation to the ENSO influence.

REGION	CENTRAL LOCATION		SOI			NIÑO 3.4			MEI		
	LONGITUDE	LATITUDE	CORR +	CORR -	LAG	CORR +	CORR -	LAG	CORR +	CORR -	LAG
R1	-101.19	20.77	1.00E-99	-0.114	0	0.12	1.00E-99	-3	0.106	1.00E-99	-3
R2	-97.14	19.62	0.086	1.00E-99	1	1.00E-99	-0.092	1	1.00E-99	-0.068	0
R3	-99.85	25.28	0.138	1.00E-99	20	0.13	1.00E-99	-2	0.145	1.00E-99	-3
R4	-104.35	27.39	1E-99	-0.145	-1	0.212	1.00E-99	-2	0.218	1.00E-99	-3
R5	-110.25	23.77	1E-99	-0.097	1	0.12	1.00E-99	-4	0.14	1.00E-99	1
R6	-114.73	32.55	1E-99	-0.12	7	0.191	1.00E-99	2	0.204	1.00E-99	3
R7	-98.78	22.72	1E-99	-0.145	2	0.185	1.00E-99	3	0.208	1.00E-99	1
R8	-111.76	26.23	0.115	1.00E-99	1	1.00E-99	-0.126	1	1.00E-99	-0.134	-1
R9	-92.77	17.38	1E-99	-0.074	-11	0.077	1.00E-99	-3	0.081	1.00E-99	-3
R10	-102.93	18.48	0.066	1.00E-99	20	0.075	1.00E-99	-14	0.057	1.00E-99	4
R11	-109.65	28.42	1E-99	-0.128	0	0.105	1.00E-99	0	0.135	1.00E-99	0

Table 7.1. Lag cross-correlations between the standardised versions of Regional Precipitation Averages and the different ENSO indices: the Southern Oscillation Index (SOI), El Niño 3.4 index, and the Multivariate El Niño Index (MEI). The linear correlation is calculated using the Pearson function. Lags (leads) are expressed in months and related to the maximum correlation found after trying several lags and leads. Regions displayed here are defined in Table 4.1.

In order to evaluate the level of coherence, the lag cross-correlation is applied in this section between standardised SOI and Regional Precipitation Averages. The greatest negative correlations are observed in Regions four, seven, and eleven (RA4, RA7 and RA11 respectively, regions defined in Table 4.1). Correlations and time shifts are similar in magnitude between them -0.15(-1), -0.15(+2), and -0.13(0). The largest positive correlation is found in RA3 (+0.14), but the timing (+20 months) is quite different when compared with the other correlations of the same sign. The clearest geographical teleconnection of ENSO is located in the north-western part of Mexico: the Northern Baja California Peninsula and the Mexican Monsoon regions share similar correlations and timing responses to ENSO modulation. Three of the regions with the largest correlations are located north of the Tropic of Cancer, although their meteorological responses are quite different: wetter conditions are found in the north-western region of Mexico, while the northeast experiences drier conditions. In general it can be said that during El Niño, wetter conditions prevail for northern Mexico, and close to the peak of El Niño-like conditions. This is consistent with the results of the correlation analysis using Kendall tau-b.

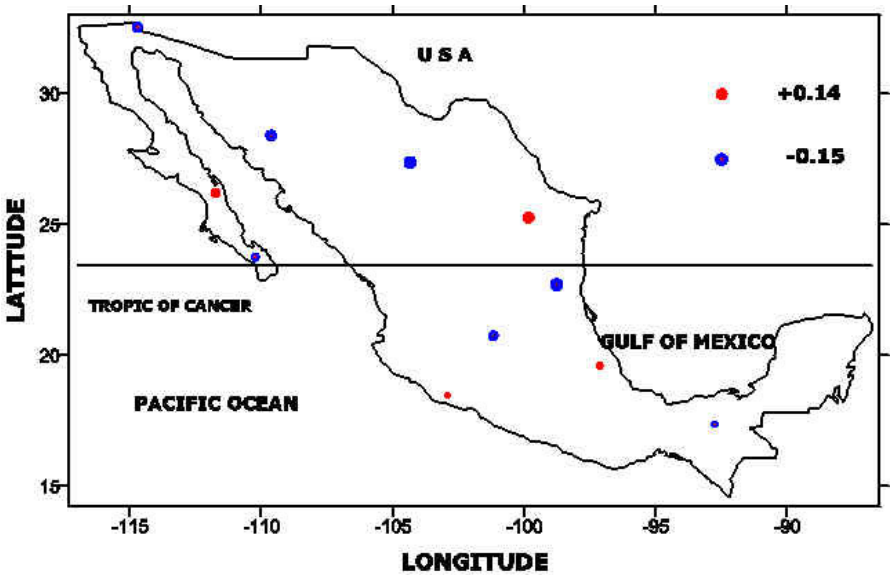

Fig. 7.8. Lag cross-correlations between the standardised versions of Regional Precipitation Averages and the Southern Oscillation Index (SOI). Red circles represent positive and blue circles negative correlations.

Extreme Weather Indices.

Extreme Rainfall Indices

The maximum 1-day precipitation (RX1day) shows a roughly differential climatic pattern of peninsular and continental variations (Table 7.2 and Fig. 7.9). For instance, in the north-western part of Mexico, the northern Baja Californian peninsula (Presa Rodríguez, station number 2 in Table 5.1) has a different response (negative correlation) and timing when compared to stations within the Mexican monsoon region. Yecora in the State of Sonora (station number 32 in Table 5.1) is at the core of this North American Monsoon (or Mexican Monsoon) region, with an altitude reaching 1500 m.a.s.l. Yecora is responding with a net decrease in precipitation amounts (+0.13) during La Niña conditions. Meanwhile, the Presa Rodríguez station is showing negative correlations (-0.11); it is the clearest climatic pattern with wetter conditions during El Niño-like years. The impact in the south-eastern area within the Yucatán Peninsula is nearly negligible.

The north-western part of Mexico shows (with exception of the station at Yecora) a coherent climatic pattern of wetter conditions during El Niño phase (Dettinger et al., 2001), and the (lag) time of response is around the peak of this phenomenon (see Fig. 7.9).

	STATION	LONGITUDE	LATITUDE	SOI		NINO 3.4		MEI	
				CORR	LAG	CORR	LAG	CORR	LAG
1	CELAYA	-100.82	20.53	-0.091	11	0.081	7	0.057	4
2	IRAPUATO	-101.35	20.68	-0.063	-12	0.052	-17	0.040	-21
3	ATZALAN	-97.25	19.80	0.084	1	-0.156	1	-0.097	1
4	LAS VIGAS	-97.10	19.65	-0.060	11	-0.091	-5	-0.089	-3
5	SAN FERNANDO	-98.15	24.85	-0.060	7	0.061	6	-0.051	20
6	GUANACEVI	-105.97	25.93	-0.090	0	0.094	-3	0.101	-3
7	SAN JOSE DEL CABO	-109.67	23.05	-0.071	13	0.096	7	0.094	6
8	PRESA RODRIGUEZ	-116.90	32.45	-0.114	0	0.172	2	0.174	0
9	BADIRAGUATO	-107.55	25.37	-0.092	-1	0.085	4	0.093	1
10	CHAMPOTON	-90.72	19.35	-0.099	-21	0.067	6	0.097	-22
11	JUCHITAN	-95.03	16.43	-0.084	17	0.130	18	0.132	16
12	APATZINGAN	-102.35	19.08	0.058	-12	-0.054	-11	-0.033	3
13	FCO. I MADERO	-104.30	24.47	-0.068	-3	0.097	5	-0.056	-14
14	OJINAGA	-104.42	29.57	-0.087	-2	0.074	-4	0.060	-4
15	YECORA	-108.95	28.37	0.129	19	-0.129	15	-0.145	14

Table 7.2. Lag cross-correlations between the RX1day (Max 1-day Precipitation) Index and the different standardised versions of the ENSO indices: the Southern Oscillation Index (SOI), El Niño 3.4 index, and the Multivariate El Niño Index (MEI). The linear correlation is calculated using the Pearson function. Lags (leads) are expressed in months and related to the maximum correlation found after trying several lags and leads.

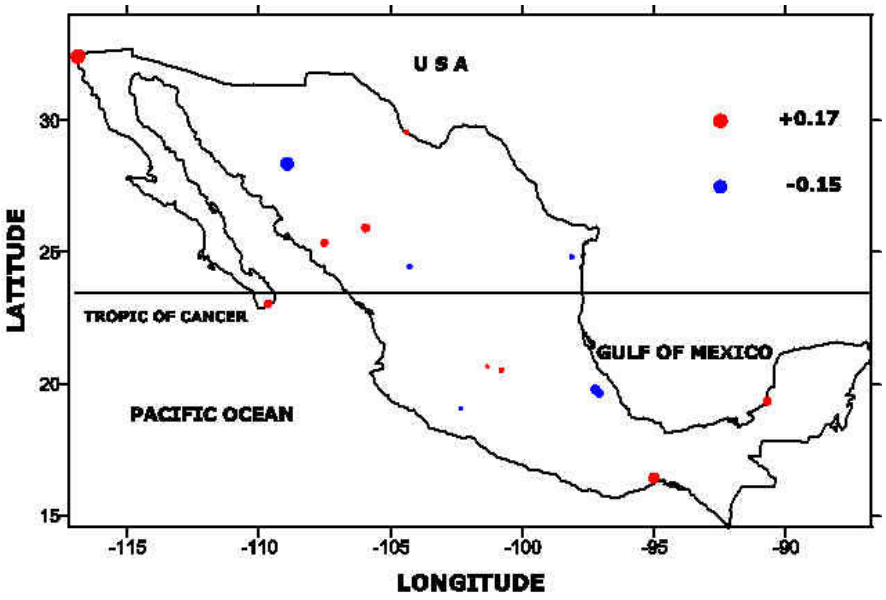

Fig. 7.9. Lag cross-correlations between the RX1day (Max 1-day Precipitation) Index and the standardised version of the Southern Oscillation Index (SOI). Red circles represent positive and blue circles negative correlations.

A climatic feature has been repeating consistently throughout the extreme indices: wetter conditions during El Niño phase, for the Presa Rodríguez station (-0.14 correlation, 0 months lag) in North Baja California Peninsula (station number 2 in Table 5.1). This climatic feature is also true for the RX5day index (Table 7.3 and Fig. 7.10). At the core of the Mexican Monsoon (or North American Monsoon) Region, the climatic response to ENSO takes time to be fully developed. The high-altitude Yecora station in Sonora (station number 32 in Table 5.1), this location experiences drier conditions (+0.22 correlation) during the negative phase of SOI (El Niño). Precipitation below normal is also observed at the South Pacific coast (Juchitán) in Oaxaca (station number 27 in Table 5.1) during El Niño-like conditions near the peak of this phenomenon. A Pacific Ocean component is involved in the ENSO modulation for the 5-day maximum precipitation, although the timing response is similar for the stations at Presa Rodríguez and the Juchitán in Oaxaca, the climatic responses are quite different. Correlations between SOI and RX5day are consistent with the climatic picture already observed for RX1day and the same ENSO index.

	STATION	LONGITUDE	LATITUDE	SOI		NINO 3.4		MEI	
				CORR	LAG	CORR	LAG	CORR	LAG
1	CELAYA	-100.82	20.53	-0.092	11	0.098	7	0.077	7
2	IRAPUATO	-101.35	20.68	-0.059	11	0.051	7	-0.055	-7
3	ATZALAN	-97.25	19.80	0.069	4	-0.144	1	-0.108	2
4	LAS VIGAS	-97.10	19.65	0.073	-5	-0.098	1	-0.095	3
5	SAN FERNANDO	-98.15	24.85	0.055	21	0.042	7	0.060	-10
6	GUANACEVI	-105.97	25.93	-0.079	0	0.084	-3	0.093	2
7	SAN JOSE DEL CABO	-109.67	23.05	-0.067	22	0.088	6	0.083	6
8	PRESA RODRIGUEZ	-116.90	32.45	-0.138	0	0.166	2	0.163	0
9	BADIRAGUATO	-107.55	25.37	-0.092	-1	0.085	4	0.093	1
10	CHAMPOTON	-90.72	19.35	-0.102	-21	0.072	-20	0.104	-22
11	JUCHITAN	-95.03	16.43	0.103	0	0.125	18	0.130	16
12	APATZINGAN	-102.35	19.08	0.049	-4	-0.054	24	-0.029	-14
13	FCO. I MADERO	-104.30	24.47	-0.045	-3	0.098	6	0.063	7
14	OJINAGA	-104.42	29.57	-0.063	-9	0.060	17	0.040	-23
15	YECORA	-108.95	28.37	0.129	19	-0.129	15	-0.145	15

Table 7.3. Lag cross-correlations between the RX5day (Max 5-day Precipitation) and the different ENSO indices: the Southern Oscillation Index (SOI), El Niño 3.4 index, and the Multivariate El Niño Index (MEI). The linear correlation is calculated using the Pearson function. Lags (leads) are expressed in months and related to the maximum correlation found after trying several lags and leads.

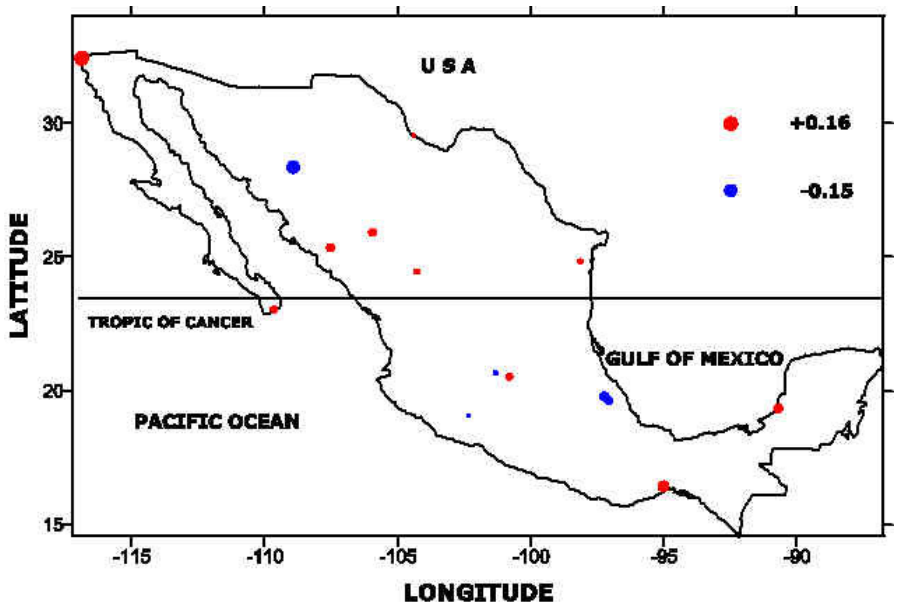

Fig. 7.10. Lag cross-correlations between the RX5day (Max 5-day Precipitation) Index and the standardised version of the Southern Oscillation Index (SOI). Red circles represent positive and blue circles negative correlations.

Extreme Temperature Indices.

DTR

No clear lag pattern is seen correlating DTR and the SOI indices (table 7.4 and fig. 7.11). Highest correlations are slightly concentrated over the southern part of Mexico near the Pacific Ocean. Neither positive nor negative correlations show a clear climatic pattern. There is no clear pattern for the time-lags of response of the different stations to the ENSO phenomenon.

	STATION	LONGITUDE	LATITUDE	SOI		NINO 3.4		MEI	
				CORR	LAG	CORR	LAG	CORR	LAG
1	PABELLON DE ARTEAGA	-102.33	22.18	0.087	5	-0.072	-7	-0.099	-10
2	PRESA RODRIGUEZ	-116.9	32.45	0.150	4	-0.138	2	0.074	-11
3	COMONDú	-111.85	26.08	0.081	7	-0.103	7	-0.102	3
4	EL PASO DE IRITU	-111.12	24.77	-0.169	-12	0.112	-8	0.167	21
5	LA PURíSIMA	-112.08	26.18	0.129	6	-0.156	-24	-0.237	-23
6	SAN BARTOLO	-109.85	23.73	0.109	-20	0.082	16	-0.148	-22
7	SANTA GERTRUDIS	-110.1	23.48	0.181	-4	-0.137	19	-0.219	-2
8	SANTIAGO	-109.73	23.47	0.084	5	0.081	13	0.095	10
9	EL PALMITO	-104.78	25.52	-0.080	-24	-0.053	-3	0.083	-24
10	SANTIAGO PAPASQUIARO	-105.42	25.05	-0.127	24	0.181	24	0.132	24
11	IRAPUATO	-101.35	20.68	-0.084	20	-0.045	6	0.102	18
12	PERICOS	-101.1	20.52	0.068	-20	-0.059	17	-0.077	-10
13	SALAMANCA	-101.18	20.57	-0.071	9	-0.077	-7	-0.082	-10
14	CUITZEO DEL PORVENIR	-101.15	19.97	0.154	16	-0.157	-7	-0.235	-9
15	HUINGO	-100.83	19.92	-0.061	11	-0.066	-7	0.078	10
16	CIUDAD HIDALGO	-100.57	19.7			0.108	23	0.097	21
17	ZACAPU	-101.78	19.82	0.116	-19	-0.095	-19	-0.130	-22
18	AHUACATLAN	-104.48	21.05	-0.069	21	0.078	-21	0.075	-21
19	LAMPAZOS	-100.52	27.03	0.134	-3	-0.138	-3	-0.175	-3
20	MATIAS ROMERO	-95.03	16.88	0.150	-24	-0.147	-24	-0.338	-24
21	SANTO DOMINGO TEHUANTEPEC	-95.23	16.33	-0.191	-2	0.148	1	0.265	-5
22	MATEHUALA	-100.63	23.65	0.094	7	-0.105	7	-0.116	6
23	BADIRAGUATO	-107.55	25.37	0.104	3	-0.102	-1	-0.166	1
24	SAN FERNANDO	-98.15	24.85	0.061	7	0.043	13	-0.065	24
25	ATZALAN	-97.25	19.8	-0.129	20	0.109	18	0.117	18
26	LAS VIGAS	-97.1	19.65	-0.187	20	0.109	18	0.247	19

Table 7.4. Lag cross-correlations between the DTR (Daily Temperature Range) and the different ENSO indices: the Southern Oscillation Index (SOI), El Niño 3.4 index, and the Multivariate El Niño Index (MEI). The linear correlation is calculated using the Pearson function. Lags (leads) are expressed in months and related to the maximum correlation found after trying several lags and leads.

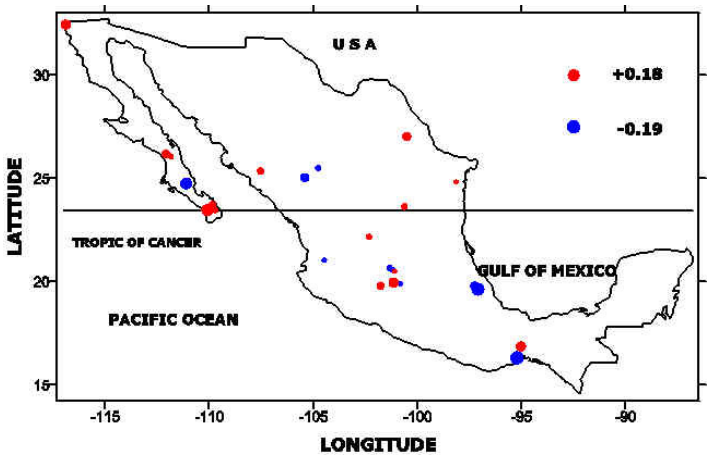

Fig. 7.11 Lag cross-correlations between the DTR (Daily Temperature Range) and the Southern Oscillation Index (SOI). Red circles express positive correlations, and blue circles show negative correlations.

TN10P

Prevailing positive correlations are observed for the TN10P index, although their corresponding lags are not quite homogeneous (Table 7.5). In addition, positive correlations are greater in magnitude than negative correlations. These positive relationships are geographically concentrated in the Baja California Peninsula, but they are also present in the Gulf of Mexico and Michoacán State (Fig. 7.12). The two largest correlations are in the central part of the Baja California Peninsula: La Purísima (station number 5 in Table 6.1) with a correlation of +0.21 and a lag of +2, then Comondú with a lag of -2 and a positive correlation of +0.16. Both are just examples of the dominant tendency towards warmer temperatures during an El Niño phase.

	STATION	LONGITUDE	LATITUDE	SOI		NIÑO 3.4		MEI	
				CORR	LAG	CORR	LAG	CORR	LAG
1	PABELLON DE ARTEAGA	-102.33	22.18	0.082	22	0.099	0	-0.101	-16
2	PRESA RODRIGUEZ	-116.9	32.45	0.203	-2	-0.182	4	-0.260	3
3	COMONDú	-111.85	26.08	0.164	-2	-0.156	0	-0.174	0
4	EL PASO DE IRITU	-111.12	24.77	-0.135	-7	0.140	-9	0.147	-9
5	LA PURíSIMA	-112.08	26.18	0.210	2	-0.212	2	-0.264	2
6	SAN BARTOLO	-109.85	23.73	-0.058	-11	0.083	-16	-0.131	9
7	SANTA GERTRUDIS	-110.1	23.48	0.096	-24	-0.078	21	0.067	10
8	SANTIAGO	-109.73	23.47	0.135	0	-0.134	6	-0.114	-3
9	EL PALMITO	-104.78	25.52	0.091	13	-0.104	11	-0.137	10
10	SANTIAGO PAPASQUIARO	-105.42	25.05	0.088	3	0.139	-10	-0.126	11
11	IRAPUATO	-101.35	20.68	-0.125	1	0.122	-1	0.168	-2
12	PERICOS	-101.1	20.52	0.121	11	-0.077	14	-0.182	12
13	SALAMANCA	-101.18	20.57	0.087	-15	-0.094	-16		
14	CUITZEO DEL PORVENIR	-101.15	19.97	0.169	19	-0.174	16	-0.230	15
15	HUINGO	-100.83	19.92	-0.120	1	0.094	0	0.150	0
16	CIUDAD HIDALGO	-100.57	19.7	0.110	5	0.130	20	0.124	22
17	ZACAPU	-101.78	19.82	0.094	-23	-0.152	-10	0.145	23
18	AHUACATLAN	-104.48	21.05	-0.136	1	0.104	2	0.181	1
19	LAMPAZOS	-100.52	27.03	0.087	0	-0.083	-1	-0.128	2
20	MATIAS ROMERO	-95.03	16.88	0.125	2	-0.097	-16	-0.200	-16
21	SAN FERNANDO	-98.15	24.85	-0.113	19	0.085	20	0.125	3
22	ATZALAN	-97.25	19.8	0.184	6	-0.145	7	-0.203	7
23	LAS VIGAS	-97.1	19.65	-0.123	20	-0.097	6	0.120	24

Table 7.5. Lag cross-correlations between the TN10P (Cool Night Frequency) and the different ENSO indices: the Southern Oscillation Index (SOI), El Niño 3.4 index, and the Multivariate El Niño Index (MEI). The linear correlation is calculated using the Pearson function. Lags (leads) are expressed in months and related to the maximum correlation found after trying several lags and leads.

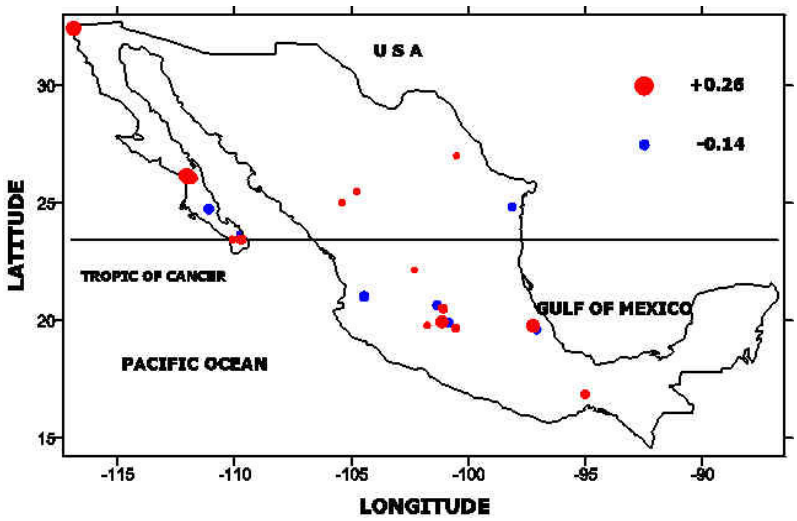

Fig. 7.12. Lag cross-correlations between the TN10P (Cool Night Frequency) and the Southern Oscillation Index (SOI). The linear correlation is calculated using the Pearson function. Red circles express positive correlations, and blue circles show negative correlations.

TN90P

There is no clear geographical pattern when we correlate the SOI and the TN90P index (Table 7.6 and Fig. 7.13). Nevertheless, an interesting feature has arisen here: both correlations (positive and negative) and the lags are descending from south to north in a geographic way following the same pattern of descending correlations (Table 7.6). Negative correlations are greater at a number of stations, and more consistent in their results. These relationships show a preference for the central and northern stations, and a northwards descending pattern in the magnitude of correlations and lags. The continental stations have a dominant characteristic being mostly at high altitude. In climatic terms, the dominant negative correlations observed in Fig 7.13 lead to colder night-temperatures under El Niño conditions. Results of applying lag correlations to TN90P are in accordance with those of linear correlations (Figs. 7.5, 7.6 and 7.7) when the negative correlations are considered, these are leading to more frequent warmer (colder) night-temperatures close to the strongest El Niño (La Niña) conditions, while the positive correlations show an average lag of about 20 months behind the frequency reach its peak, suggesting odd results of the statistical method in trying to match the largest correlations.

	STATION	LONGITUDE	LATITUDE	SOI		NIÑO 3.4		MEI	
				CORR	LAG	CORR	LAG	CORR	LAG
1	PABELLON DE ARTEAGA	-102.33	22.18	0.086	-24	-0.061	5	0.104	-6
2	PRESA RODRIGUEZ	-116.9	32.45	-0.152	5	0.181	0	0.241	1
3	COMONDú	-111.85	26.08	-0.097	-5	0.088	-2	0.071	10
4	EL PASO DE IRITU	-111.12	24.77	0.110	-18	0.117	3	-0.081	-15
5	LA PURíSIMA	-112.08	26.18	0.124	-15	0.168	-24	0.154	-24
6	SAN BARTOLO	-109.85	23.73	-0.123	-19	0.096	-20	0.151	-24
7	SANTA GERTRUDIS	-110.1	23.48	0.079	-20	-0.056	-16	-0.079	-19
8	SANTIAGO	-109.73	23.47	0.105	-16	-0.117	22	0.088	2
9	EL PALMITO	-104.78	25.52	0.092	-18	0.089	11	-0.100	-20
10	SANTIAGO PAPASQUIARO	-105.42	25.05	0.115	-15	0.079	24	-0.120	-16
11	IRAPUATO	-101.35	20.68	0.214	-18	-0.195	-20	-0.306	-20
12	PERICOS	-101.1	20.52	-0.097	5	0.103	5	0.151	4
13	SALAMANCA	-101.18	20.57	0.144	-18	0.164	5	0.131	5
14	CUITZEO DEL PORVENIR	-101.15	19.97	-0.161	7	0.140	14	0.214	5
15	HUINGO	-100.83	19.92	-0.171	7	0.252	6	0.221	5
16	CIUDAD HIDALGO	-100.57	19.7	0.109	20	-0.172	22	-0.189	22
17	ZACAPU	-101.78	19.82			0.106	-23	0.168	4
18	AHUACATLAN	-104.48	21.05	-0.133	6	0.210	5	0.171	5
19	LAMPAZOS	-100.52	27.03	0.110	-2	-0.138	0	-0.124	-2
20	MATIAS ROMERO	-95.03	16.88	-0.117	5	0.098	-14	0.185	-13
21	SAN FERNANDO	-98.15	24.85	-0.083	13	-0.069	0	0.111	12
22	ATZALAN	-97.25	19.8	-0.208	8	0.162	6	0.213	7
23	LAS VIGAS	-97.1	19.65	0.149	-19	-0.155	-20	-0.237	-21

Table 7.6. Lag cross-correlations between the TN90P (Hot Night Frequency) and the different ENSO indices: the Southern Oscillation Index (SOI), El Niño 3.4 index, and the Multivariate El Niño Index (MEI). The linear correlation is calculated using the Pearson function. Lags (leads) are expressed in months and related to the maximum correlation found after trying several lags and leads.

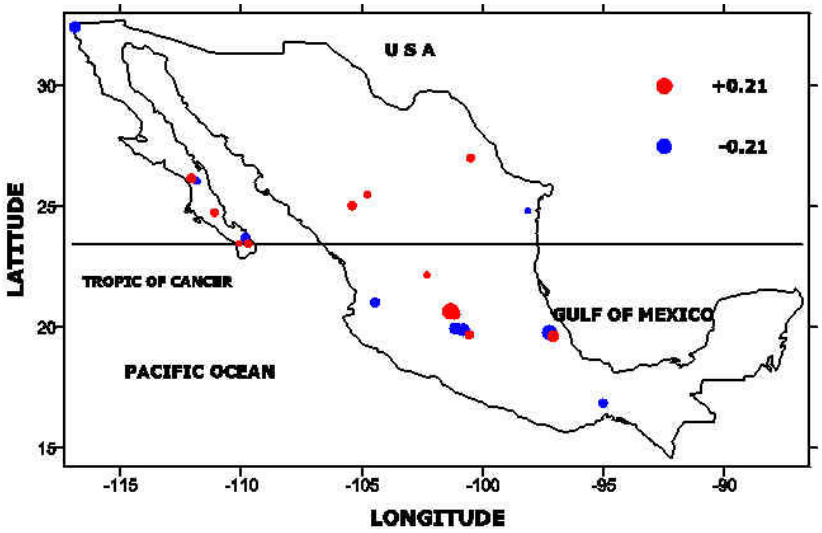

Fig. 7.13 Lag cross-correlations between the TN90P (Hot Night Frequency) and the Southern Oscillation Index (SOI). The linear correlation is calculated using the Pearson function. Red circles express positive correlations, and blue circles show negative correlations.

TNn

Warmer absolute minimum temperatures are observed in southern Mexico under El Niño conditions. Negative correlations are found when we (lag) correlate the TNn index (coolest night) and the SOI (Table 7.7). Largest correlations are found mostly south of the Tropic of Cancer. Although the greatest negative correlation is observed at Matías Romero station (station number 28 in Table 6.1) in the Southern Pacific coast, three of the four largest correlations are located in Michoacán State, and all of them are above the 1000 m.a.s.l. limit, so clearly altitude is exerting its influence in these results (Fig. 7.14). Nevertheless, it also important to point out that the time shifts are not homogeneous among these stations. It can be said that during El Niño phase the TNn index show a pattern towards warmer conditions for the southern part of Mexico.

	STATION	LONGITUDE	LATITUDE	SOI		NINO 3.4		MEI	
				CORR	LAG	CORR	LAG	CORR	LAG
1	PABELLON DE ARTEAGA	-102.33	22.18	-0.052	-8	-0.053	-1	-0.026	-3
2	PRESA RODRIGUEZ	-116.9	32.45	0.080	-17	-0.048	-24	-0.087	18
3	COMONDú	-111.85	26.08	-0.058	2	0.053	5	0.082	1
4	EL PASO DE IRITU	-111.12	24.77	0.078	-13	-0.068	-13	-0.071	-14
5	LA PURíSIMA	-112.08	26.18	0.061	-16	0.074	5	0.074	-23
6	SAN BARTOLO	-109.85	23.73	0.058	20	-0.063	20	0.077	-24
7	SANTA GERTRUDIS	-110.1	23.48	-0.058	-23	0.066	19	0.079	-24
8	SANTIAGO	-109.73	23.47	0.057	-15	0.052	6	0.056	2
9	EL PALMITO	-104.78	25.52	-0.044	17	0.057	17	0.054	13
10	SANTIAGO PAPASQUIARO	-105.42	25.05	-0.070	16	0.067	16	0.075	13
11	IRAPUATO	-101.35	20.68	0.080	-17	-0.048	-24	-0.087	18
12	PERICOS	-101.1	20.52			0.046	17	0.074	-9
13	SALAMANCA	-101.18	20.57	-0.050	-9	0.037	-19	0.055	-10
14	CUITZEO DEL PORVENIR	-101.15	19.97	-0.137	16	0.128	16	0.161	14
15	HUINGO	-100.83	19.92	-0.058	5	0.048	6	-0.044	-4
16	CIUDAD HIDALGO	-100.57	19.7	-0.098	5	0.077	6	0.071	10
17	ZACAPU	-101.78	19.82	-0.121	-8	0.150	-10	0.130	-10
18	AHUACATLAN	-104.48	21.05	0.063	21	-0.059	-21	-0.073	-20
19	LAMPAZOS	-100.52	27.03	0.063	21	-0.043	23	-0.042	17
20	MATIAS ROMERO	-95.03	16.88	-0.174	-19	0.158	-16	0.262	-19
21	SANTO DOMINGO TEHUANTEPEC	-95.23	16.33	-0.060	3	0.104	-4	0.074	-3
22	MATEHUALA	-100.63	23.65	-0.057	24	0.061	-9	0.075	23
23	BADIRAGUATO	-107.55	25.37	-0.067	3	0.041	-15	0.089	-11
24	SAN FERNANDO	-98.15	24.85	-0.042	4	-0.044	23	-0.042	18
25	ATZALAN	-97.25	19.8	-0.083	5	0.066	8	0.095	-1
26	LAS VIGAS	-97.1	19.65	0.084	19	0.077	-9	-0.097	16

Table 7.7. Lag cross-correlations between the TNn (Coolest night) and the different ENSO indices: the Southern Oscillation Index (SOI), El Niño 3.4 index, and the Multivariate El Niño Index (MEI). The linear correlation is calculated using the Pearson function. Lags (leads) are expressed in months and related to the maximum correlation found after trying several lags and leads.

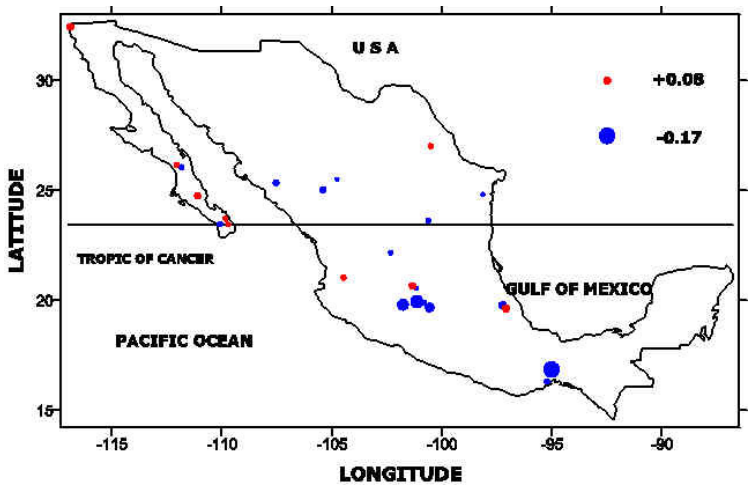

Fig. 7.14. Lag cross-correlations between the TNn (Coolest night) and the Southern Oscillation Index (SOI). The linear correlation is calculated using the Pearson function. Red circles express positive correlations, and blue circles show negative correlations.

TNx

Regarding the sign of the results, most of the stations with the largest correlations are located south of the Tropic of Cancer. A clear pattern of positive correlations can be easily observed nationwide, but the largest ones are clearly concentrated south of the Tropic of Cancer (Fig. 7.15). Only El Paso de Iritu station (+0.10 correlation and a lag of -15 months) slightly north of this geographic limit is the exception. Time shifts are quite similar for both the positive and negative correlations (see Table 7.8). Negative correlations are showing mainly also negative lags, meanwhile the positive correlations are showing a preference towards positive time shifts. Although positive correlations are geographically prevalent, negative correlations are larger in magnitude. In general, the maximum night temperatures increase during El Niño conditions.

	STATION	LONGITUDE	LATITUDE	SOI		NINO 3.4		MEI	
				CORR	LAG	CORR	LAG	CORR	LAG
1	PABELLON DE ARTEAGA	-102.33	22.18	0.078	-14	-0.082	-13	-0.042	-17
2	PRESA RODRIGUEZ	-116.9	32.45	-0.081	-5	0.086	-5	0.082	3
3	COMONDú	-111.85	26.08	-0.094	18	0.071	20	0.080	12
4	EL PASO DE IRITU	-111.12	24.77	0.102	-15	-0.068	-11	-0.081	-15
5	LA PURíSIMA	-112.08	26.18	-0.101	5	0.092	3	0.136	2
6	SAN BARTOLO	-109.85	23.73	-0.052	-23	-0.060	18	0.061	2
7	SANTA GERTRUDIS	-110.1	23.48	0.057	-14	0.040	-3	-0.058	-17
8	SANTIAGO	-109.73	23.47	0.054	-15	0.065	-6	0.063	-10
9	EL PALMITO	-104.78	25.52	0.052	-17	-0.045	-1	-0.049	-16
10	SANTIAGO PAPASQUIARO	-105.42	25.05	0.074	-15	-0.104	-13	-0.089	-16
11	IRAPUATO	-101.35	20.68	0.102	-16	-0.050	22	-0.131	-17
12	PERICOS	-101.1	20.52	-0.072	2			0.080	1
13	SALAMANCA	-101.18	20.57	0.063	-16	0.074	3	0.068	2
14	CUITZEO DEL PORVENIR	-101.15	19.97	-0.128	3	0.101	4	0.165	2
15	HUINGO	-100.83	19.92	0.111	-15	0.124	5		
16	CIUDAD HIDALGO	-100.57	19.7	0.103	21	-0.108	22	-0.012	19
17	ZACAPU	-101.78	19.82	-0.090	6	0.132	5	0.120	2
18	AHUACATLAN	-104.48	21.05	0.106	21	-0.095	-13	-0.126	19
19	LAMPAZOS	-100.52	27.03	0.080	-2	-0.066	-1	-0.042	-3
20	MATIAS ROMERO	-95.03	16.88	-0.161	3	0.123	-20	0.270	-20
21	SANTO DOMINGO TEHUANTEPEC	-95.23	16.33	0.137	-14	-0.103	24	-0.181	16
22	MATEHUALA	-100.63	23.65	0.097	-16	0.077	7	0.064	7
23	BADIRAGUATO	-107.55	25.37	-0.087	3	0.061	-3	0.093	1
24	SAN FERNANDO	-98.15	24.85	0.098	-2	-0.072	-1	-0.073	-4
25	ATZALAN	-97.25	19.8	-0.130	5	0.103	7	0.146	10
26	LAS VIGAS	-97.1	19.65	0.117	-21	-0.109	-6	-0.188	-7

Table 7.8. Lag cross-correlations between the TNx (Hottest night) and the different ENSO indices: the Southern Oscillation Index (SOI), El Niño 3.4 index, and the Multivariate El Niño Index (MEI). The linear correlation is calculated using the Pearson function. Lags (leads) are expressed in months and related to the maximum correlation found after trying several lags and leads.

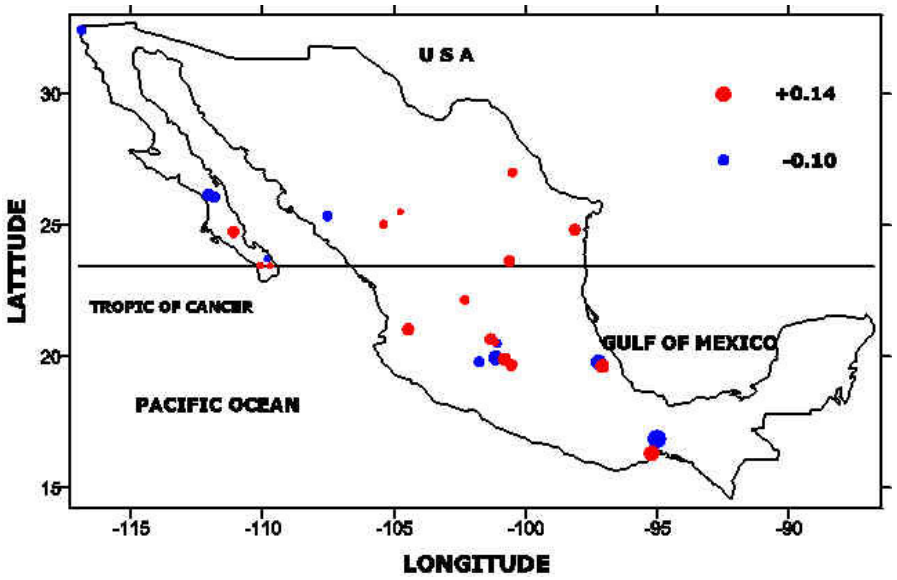

Fig. 7.15. Lag cross-correlations between the TNx (Hottest night) and the Southern Oscillation Index (SOI). The linear correlation is calculated using the Pearson function. Red circles express positive correlations, and blue circles show negative correlations.

TX10P

Colder day temperatures are observed for the TX10P index during El Niño conditions. Negative correlations are widespread in the country, although they are geographically concentrated in the central-western part (Fig. 7.16). These negative relationships dominate both in magnitude and number compared to the positive correlations. For both positive and negative correlations lags are quite similar (Table 7.9). The greatest correlation is found at Cuitzeo del Porvenir in Michoacán state (station number 21 in Table 6.1) with a negative correlation of -0.19 and a time shift of -2 months. According to the geographical distribution it seems that the Pacific Ocean is partly modulating the frequency of hot days in the western part of Mexico.

	STATION	LONGITUDE	LATITUDE	SOI		NINO 3.4		MEI	
				CORR	LAG	CORR	LAG	CORR	LAG
1	PABELLON DE ARTEAGA	-102.33	22.18	-0.161	-1	0.127	-1	0.181	-11
2	PRESA RODRIGUEZ	-116.9	32.45	0.143	14	-0.167	15	-0.220	12
3	COMONDú	-111.85	26.08	-0.171	-6	-0.125	0	-0.142	-2
4	EL PASO DE IRITU	-111.12	24.77	0.151	-12	-0.093	10	-0.155	10
5	LA PURíSIMA	-112.08	26.18	-0.107	-22	0.169	-16	0.226	-22
6	SAN BARTOLO	-109.85	23.73	-0.065	-16	-0.107	8	0.100	-17
7	SANTA GERTRUDIS	-110.1	23.48	-0.184	1	0.140	7	0.207	-3
8	SANTIAGO	-109.73	23.47	0.101	-5	-0.142	9	-0.144	9
9	EL PALMITO	-104.78	25.52	0.109	9	0.150	-2	0.129	-3
10	SANTIAGO PAPASQUIARO	-105.42	25.05	-0.124	23	0.082	0	0.093	0
11	IRAPUATO	-101.35	20.68	-0.113	-2	0.077	-1	0.115	-21
12	PERICOS	-101.1	20.52	-0.083	0	0.077	-1	-0.067	13
13	SALAMANCA	-101.18	20.57	-0.078	0	0.091	13	0.109	-22
14	CUITZEO DEL PORVENIR	-101.15	19.97	-0.192	-2	0.258	-2	0.263	-3
15	HUINGO	-100.83	19.92	0.092	10	-0.091	13	-0.152	12
16	CIUDAD HIDALGO	-100.57	19.7	-0.161	-2	0.189	-1	0.172	-1
17	ZACAPU	-101.78	19.82	-0.129	-20	-0.115	-8	0.168	24
18	AHUACATLAN	-104.48	21.05	-0.172	1	0.195	-1	0.228	0
19	LAMPAZOS	-100.52	27.03	-0.070	-2	-0.079	-23	0.074	-11
20	MATIAS ROMERO	-95.03	16.88	0.084	-9	0.113	-5	-0.107	-10
21	SAN FERNANDO	-98.15	24.85	-0.105	-2	0.091	0	0.093	2
22	ATZALAN	-97.25	19.8	0.081	9	-0.085	-9	-0.071	24
23	LAS VIGAS	-97.1	19.65	0.157	-4	-0.129	-11	-0.208	-17

Table 7.9. Lag cross-correlations between the TX10P (Cool day frequency) and the different ENSO indices: the Southern Oscillation Index (SOI), El Niño 3.4 index, and the Multivariate El Niño Index (MEI). The linear correlation is calculated using the Pearson function. Lags (leads) are expressed in months and related to the maximum correlation found after trying several lags and leads.

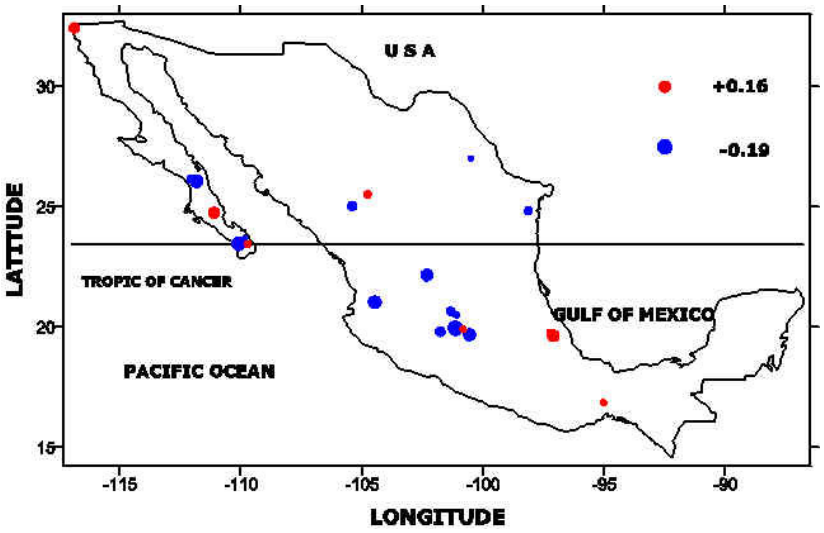

Fig. 7.16. Lag cross-correlations between the TX10P (Cool day frequency) and the Southern Oscillation Index (SOI). The linear correlation is calculated using the Pearson function. Red circles express positive correlations, and blue circles show negative correlations.

TX90P

For the lag correlation between the TX90P and the SOI indices, positive correlations are prevalent from Central to Northern Mexico, especially over the western side of the country (Fig. 7.17). Time shifts for the negative correlations are quite similar, and except for the Presa Rodriguez (station number 2 in table 6.1) they are concentrated in the range between -3 to +5 months, but that is not the case for the positive ones that show a great variation between -14 to +16 months of lag making it difficult to find the optimal relationship (Table 7.10). Positive correlations mean that during El Niño phase the percentage of hot days exceeding the upper 90 percentile increases, i.e., warmer day temperatures. It can also be said, like in the case of the TX10P, that the Pacific Ocean exerts a partial influence over the Hot Day frequency.

	STATION	LONGITUDE	LATITUDE	SOI		NIÑO 3.4		MEI	
				CORR	LAG	CORR	LAG	CORR	LAG
1	PABELLON DE ARTEAGA	-102.33	22.18	0.110	1	-0.136	-15	-0.173	-15
2	PRESA RODRIGUEZ	-116.9	32.45	-0.126	22	0.066	-6	0.107	-24
3	COMONDú	-111.85	26.08	-0.126	-5	-0.077	7	0.106	-7
4	EL PASO DE IRITU	-111.12	24.77	-0.089	21	-0.076	-21	0.121	12
5	LA PURíSIMA	-112.08	26.18	0.113	-4	0.092	11	-0.087	-13
6	SAN BARTOLO	-109.85	23.73	0.103	-11	-0.139	-13	-0.125	-14
7	SANTA GERTRUDIS	-110.1	23.48	0.127	-3	-0.089	1	-0.156	-5
8	SANTIAGO	-109.73	23.47	-0.074	18	0.156	13	0.150	10
9	EL PALMITO	-104.78	25.52	-0.143	-5	0.119	-5	0.142	-7
10	SANTIAGO PAPASQUIARO	-105.42	25.05	0.147	-24	-0.105	-11	-0.159	-21
11	IRAPUATO	-101.35	20.68	0.130	-19	-0.153	-16	-0.195	-18
12	PERICOS	-101.1	20.52	-0.102	3	-0.131	15	0.170	2
13	SALAMANCA	-101.18	20.57	-0.093	4	0.156	3	0.168	2
14	CUITZEO DEL PORVENIR	-101.15	19.97	0.101	-22	-0.120	-22	-0.119	-22
15	HUINGO	-100.83	19.92	0.135	-12	0.203	3	0.212	2
16	CIUDAD HIDALGO	-100.57	19.7	0.081	-22	0.138	24	0.152	24
17	ZACAPU	-101.78	19.82	0.205	14	-0.196	15	-0.239	16
18	AHUACATLAN	-104.48	21.05	0.075	0	-0.115	18	-0.118	17
19	LAMPAZOS	-100.52	27.03	0.167	-3	-0.203	-1	-0.258	-2
20	MATIAS ROMERO	-95.03	16.88	-0.191	3	0.140	4	0.230	1
21	SAN FERNANDO	-98.15	24.85	0.094	-1	0.081	13	-0.071	-21
22	ATZALAN	-97.25	19.8	0.194	16	0.167	17	0.247	0
23	LAS VIGAS	-97.1	19.65	-0.170	3	0.164	6	0.233	6

Table 7.10. Lag cross-correlations between the TX90P (Hot day frequency) and the different ENSO indices: the Southern Oscillation Index (SOI), El Niño 3.4 index, and the Multivariate El Niño Index (MEI). The linear correlation is calculated using the Pearson function. Lags (leads) are expressed in months and related to the maximum correlation found after trying several lags and leads.

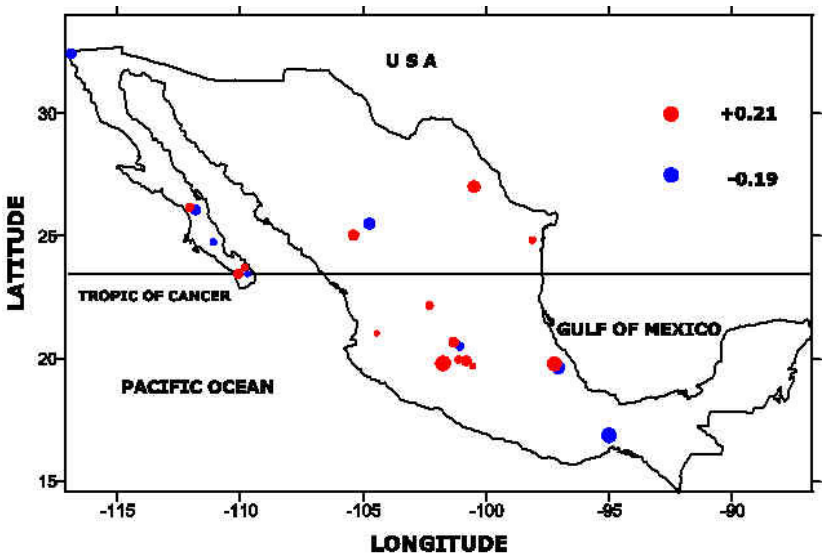

Fig. 7.17. Lag cross-correlations between the TX90P (Hot day frequency) and the Southern Oscillation Index (SOI). The linear correlation is calculated using the Pearson function. Red circles express positive correlations, and blue circles show negative correlations.

TXn

Two different climatic patterns are found for the TXn index. Positive correlations prevail in Central and Northern Mexico, while in the Southern part of the country negative correlations show a few significant results (Table 7.11). This climatic transition from negative in the south to positive correlations in the central and northern part of the country is nearly evident, but not a clear geographical pattern. Although the clusters of positive correlations are clearer for northern Mexico, negative correlations are greater in magnitude (Fig. 7.18). Time shifts are dissimilar for both positive and negative correlations. According to these results, coolest days increase in temperature during El Niño conditions in the western part of Mexico for the central and northern part of the country.

	STATION	LONGITUDE	LATITUDE	SOI		NIÑO 3.4		MEI	
				CORR	LAG	CORR	LAG	CORR	LAG
1	PABELLON DE ARTEAGA	-102.33	22.18	0.132	-2	-0.113	-1	-0.133	-3
2	PRESA RODRIGUEZ	-116.9	32.45	-0.064	18	0.069	16	0.066	12
3	COMONDú	-111.85	26.08	0.141	1	-0.126	-2	-0.136	0
4	EL PASO DE IRITU	-111.12	24.77	-0.069	-8	-0.062	-24	0.082	12
5	LA PURíSIMA	-112.08	26.18	0.074	-15	-0.057	-13	-0.082	-17
6	SAN BARTOLO	-109.85	23.73	0.048	20	0.065	9	-0.078	19
7	SANTA GERTRUDIS	-110.1	23.48	0.120	1	-0.102	0	-0.159	-5
8	SANTIAGO	-109.73	23.47	0.062	2	0.085	13	0.080	12
9	EL PALMITO	-104.78	25.52	-0.086	18	0.101	17	0.087	16
10	SANTIAGO PAPASQUIARO	-105.42	25.05	0.112	-2	-0.105	-24	-0.103	-22
11	IRAPUATO	-101.35	20.68	0.107	-1	-0.107	-1	-0.101	-3
12	PERICOS	-101.1	20.52	0.073	-2	-0.099	-2	0.059	14
13	SALAMANCA	-101.18	20.57	-0.108	13	0.092	13	-0.083	-21
14	CUITZEO DEL PORVENIR	-101.15	19.97	0.110	-2	-0.122	-2	-0.097	-5
15	HUINGO	-100.83	19.92	-0.107	13	0.106	13	0.126	13
16	CIUDAD HIDALGO	-100.57	19.7	0.080	-2	-0.093	-1	-0.071	4
17	ZACAPU	-101.78	19.82	0.113	-19	0.086	-10	-0.100	-24
18	AHUACATLAN	-104.48	21.05	0.096	-2	-0.129	0	-0.133	2
19	LAMPAZOS	-100.52	27.03	0.059	-2	-0.053	23	-0.053	17
20	MATIAS ROMERO	-95.03	16.88	-0.142	2	0.127	-8	0.117	-10
21	SANTO DOMINGO TEHUANTEPEC	-95.23	16.33	-0.194	-7	0.217	-4	0.283	-5
22	MATEHUALA	-100.63	23.65	-0.059	18	-0.069	-15	-0.055	5
23	BADIRAGUATO	-107.55	25.37	-0.086	12	0.121	13	-0.135	-3
24	SAN FERNANDO	-98.15	24.85	0.058	-3	-0.056	-13	-0.047	-6
25	ATZALAN	-97.25	19.8	-0.034	-9	-0.056	12	-0.063	4
26	LAS VIGAS	-97.1	19.65	-0.152	-10	0.156	-6	0.207	-13

Table 7.11. Lag cross-correlations between the TXn (Coolest day) and the different ENSO indices: the Southern Oscillation Index (SOI), El Niño 3.4 index, and the Multivariate El Niño Index (MEI). The linear correlation is calculated using the Pearson function. Lags (leads) are expressed in months and related to the maximum correlation found after trying several lags and leads.

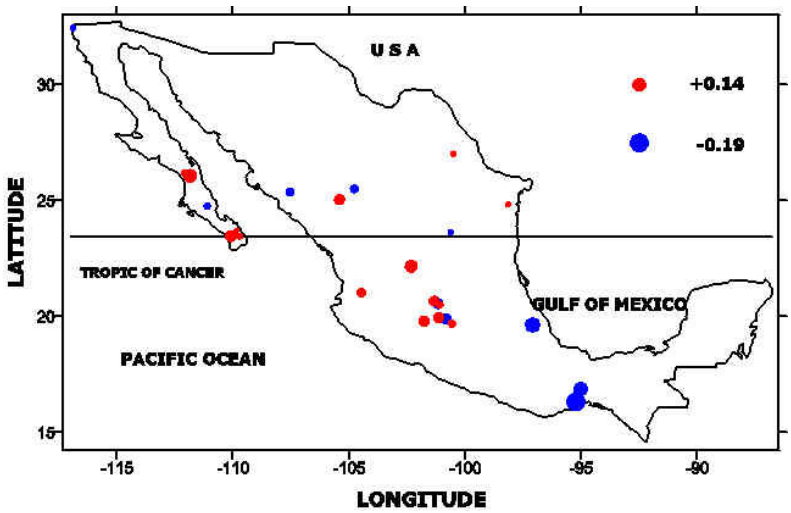

Fig. 7.18. Lag cross-correlations between the TXn (Coolest day) and the Southern Oscillation Index (SOI). The linear correlation is calculated using the Pearson function. Red circles express positive correlations, and blue circles show negative correlations.

TXx

A rough latitudinal climatic transition is observed for the (lag) correlation of the Hottest day (TXx) and the SOI index. Positive correlations dominate in the central and northern part of Mexico, and negative correlations prevail over southern Mexico (Fig. 7.19). Among the largest correlations negative relationships are greater in magnitude than the positive ones (Table 7.12). This climatic feature is especially observed in the Santo Domingo Tehuantepec station in Oaxaca with a negative correlation of -0.21 and a lag of -5; while among the positive, the greatest correlation is observed in the Santa Gertrudis in the southern tip of the Baja Californian peninsula (station number 8 in Table 6.1), with a correlation of +0.14 and a lag of -2. Nevertheless, no matter the sign of the correlations, lags do not show a clear pattern. For central and northern Mexico colder temperatures are found for the TXx during El Niño conditions.

	STATION	LONGITUDE	LATITUDE	SOI		NINO 3.4		MEI	
				CORR	LAG	CORR	LAG	CORR	LAG
1	PABELLON DE ARTEAGA	-102.33	22.18	0.093	-2	-0.101	-15	-0.099	-18
2	PRESA RODRIGUEZ	-116.9	32.45	0.096	0	0.089	-18	0.091	-21
3	COMONDú	-111.85	26.08	-0.088	-7	0.850	-6	0.093	12
4	EL PASO DE IRITU	-111.12	24.77			0.052	-6	0.096	12
5	LA PURíSIMA	-112.08	26.18	0.062	-16	0.069	9	-0.114	-17
6	SAN BARTOLO	-109.85	23.73	0.063	-20	0.065	9	-0.096	-17
7	SANTA GERTRUDIS	-110.1	23.48	0.137	-2	-0.125	24	-0.184	6
8	SANTIAGO	-109.73	23.47	-0.049	13	0.065	15	0.075	12
9	EL PALMITO	-104.78	25.52	0.059	-15	-0.046	-15	0.047	11
10	SANTIAGO PAPASQUIARO	-105.42	25.05	0.119	-16	-0.109	-13	-0.137	-16
11	IRAPUATO	-101.35	20.68	0.089	-17			-0.135	-19
12	PERICOS	-101.1	20.52	-0.056	3	-0.065	21	0.078	1
13	SALAMANCA	-101.18	20.57	-0.094	2	0.097	3	0.088	2
14	CUITZEO DEL PORVENIR	-101.15	19.97	-0.048	12	-0.099	-3	-0.069	-5
15	HUINGO	-100.83	19.92	0.079	-11	-0.090	-13	0.080	10
16	CIUDAD HIDALGO	-100.57	19.7	-0.092	15	-0.090	-1	0.092	23
17	ZACAPU	-101.78	19.82	0.136	17	-0.121	19	-0.159	16
18	AHUACATLAN	-104.48	21.05	0.075	-1	-0.103	-2	-0.095	-3
19	LAMPAZOS	-100.52	27.03	0.100	-2	-0.079	-1	-0.088	-6
20	MATIAS ROMERO	-95.03	16.88	-0.123	-9	0.121	5	0.182	0
21	SANTO DOMINGO TEHUANTEPEC	-95.23	16.33	-0.212	-5	0.234	-3	0.304	-4
22	MATEHUALA	-100.63	23.65	-0.057	21	0.076	15	0.054	22
23	BADIRAGUATO	-107.55	25.37	-0.072	11	0.098	12	-0.111	3
24	SAN FERNANDO	-98.15	24.85	0.145	1	0.127	23	0.085	24
25	ATZALAN	-97.25	19.8	-0.120	14	0.117	17	0.176	5
26	LAS VIGAS	-97.1	19.65	-0.163	2	0.139	3	0.194	6

Table 7.12. Lag cross-correlations between the TXx (Hottest day) and the different ENSO indices: the Southern Oscillation Index (SOI), El Niño 3.4 index, and the Multivariate El Niño Index (MEI). The linear correlation is calculated using the Pearson function. Lags (leads) are expressed in months and related to the maximum correlation found after trying several lags and leads.

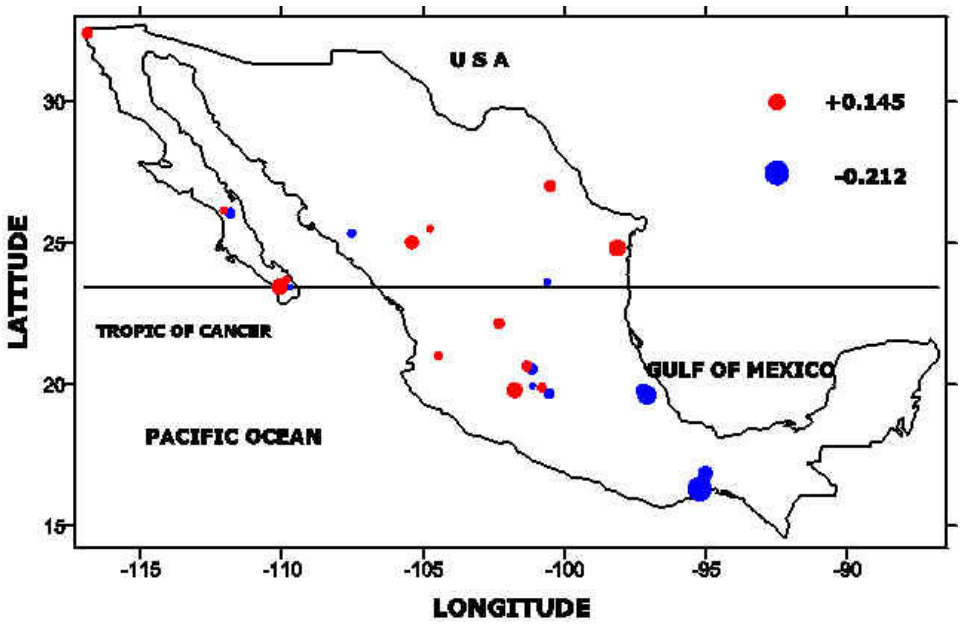

Fig. 7.19. Lag cross-correlations between the TXx (Hottest day) and the Southern Oscillation Index (SOI). The linear correlation is calculated using the Pearson function. Red circles express positive correlations, and blue circles show negative correlations.

There are two clear climatic patterns when we correlate extreme temperature indices and the SOI. Minimum (night) temperatures increase during El Niño conditions, and maximum (day) temperatures are cooler during the same phase. Changes in minimum temperatures related indices have a geographical preference towards southern Mexico and high altitude stations, while maximum temperature results are spatially concentrated in the western half of the country.

Summary of the results (SOI).

Regardless of the geographical scale (regional precipitation averages or local sites), a latitudinal transition (using the Tropic of Cancer as a geographic limit) is observed in the response (using the Kendall tau-b linear correlation method) of rainfall to the annual and wet season (May-Oct) versions of the Southern Oscillation Index (SOI). During El Niño years wetter conditions are prevalent in northern Mexico and drier conditions in the south of the country. Meanwhile, homogeneous national conditions are dominant when the rainfall (regional averages and extreme indices) are linearly correlated with the dry season (Nov-Apr) SOI. The largest impacts (correlations) are observed in the north-western part of the country (the North American Monsoon or Mexican Monsoon Region –RA11 in Table 4.1- and north part of the peninsula of Baja California). Nevertheless, because of the limited number of stations in the case of daily rainfall data (extreme indices), a careful interpretation must be applied to the results of the analysis of linear correlations between extreme rainfall indices and SOI. In the case of the analysis of linear correlation between the extreme temperature indices and SOI, a clear national pattern of increasing minimum temperatures is observed regardless of whether the annual, wet season (May-Oct) or dry season (Nov-Apr) is used. As when we considered rainfall, the conclusions of this analysis can be affected by the limited number of stations with daily temperature data.

The analysis of lag correlation between the Southern Oscillation Index (SOI) and the rainfall and temperature data are consistent with the results of the linear correlation using Kendall tau-b. Lag-cross correlations of SOI with the precipitation regional averages show a latitudinal climatic transition in the results (considering the Tropic of Cancer as a geographic limit). The most affected region by the ENSO phenomenon is the north-western part of Mexico: the North American Monsoon (or Mexican Monsoon) Region (NAMR, RA11 in Table 4.1) and the northern part of the peninsula of Baja California. Wetter conditions are prevalent in northern Mexico during El Niño years (negative SOI), and the largest correlations are mostly observed near of the peak of the ENSO conditions. At local (sites) scale the correlation of the rainfall extreme indices with SOI show that the most important results occur in the north-western part of the country, near the peak of the El Niño (La Niña) conditions. Regardless the geographical scale, according to the results, the Pacific Ocean appears as an important modulator of the precipitation. Moreover, the analysis of lag correlation between the extreme temperature indices and SOI show a national pattern of increasing minimum temperatures near the strongest conditions of the ENSO phenomenon.

7.3. (EL) NIÑO 3.4 (INDEX) INFLUENCE.

7.3.1. LINEAR CORRELATION.

Regional Precipitation Averages.

The first analysis in this section aims to correlate linearly (using Kendall-tau b) the Niño 3.4 index with regional precipitation averages. Seasonal (annual, wet and dry seasons) versions of both time-series are used in order to test the possibility of having a local response of the rainfall to the large-scale phenomenon. The length of the Niño 3.4 index is shorter (1950-2001) than the time-series of the regional precipitation (1931-2001), reducing the potentiality of generating a more complete picture of variability as with the case of the Southern Oscillation Index (SOI). Nevertheless, in order to avoid external influences like altitude, standardised versions of these time series will be used for the analysis.

With the exception of those correlations close to zero, a clear latitudinal climatic pattern can be appreciated when correlating the annual version of the regional precipitation averages and the annual Niño 3.4 [Fig. 7.20 a)]. Negative correlations are found south of the selected geographic limit (Tropic of Cancer), and all these results are statistically significant at the 5% level. Positive correlations are observed north of this divide; and they are statistically significant at the 1% level. Therefore, drier conditions are dominant during El-Niño like years in the southern part of Mexico, and annual precipitation totals above normal are found in the northern part of the country, geographically concentrated within the Baja California peninsula.

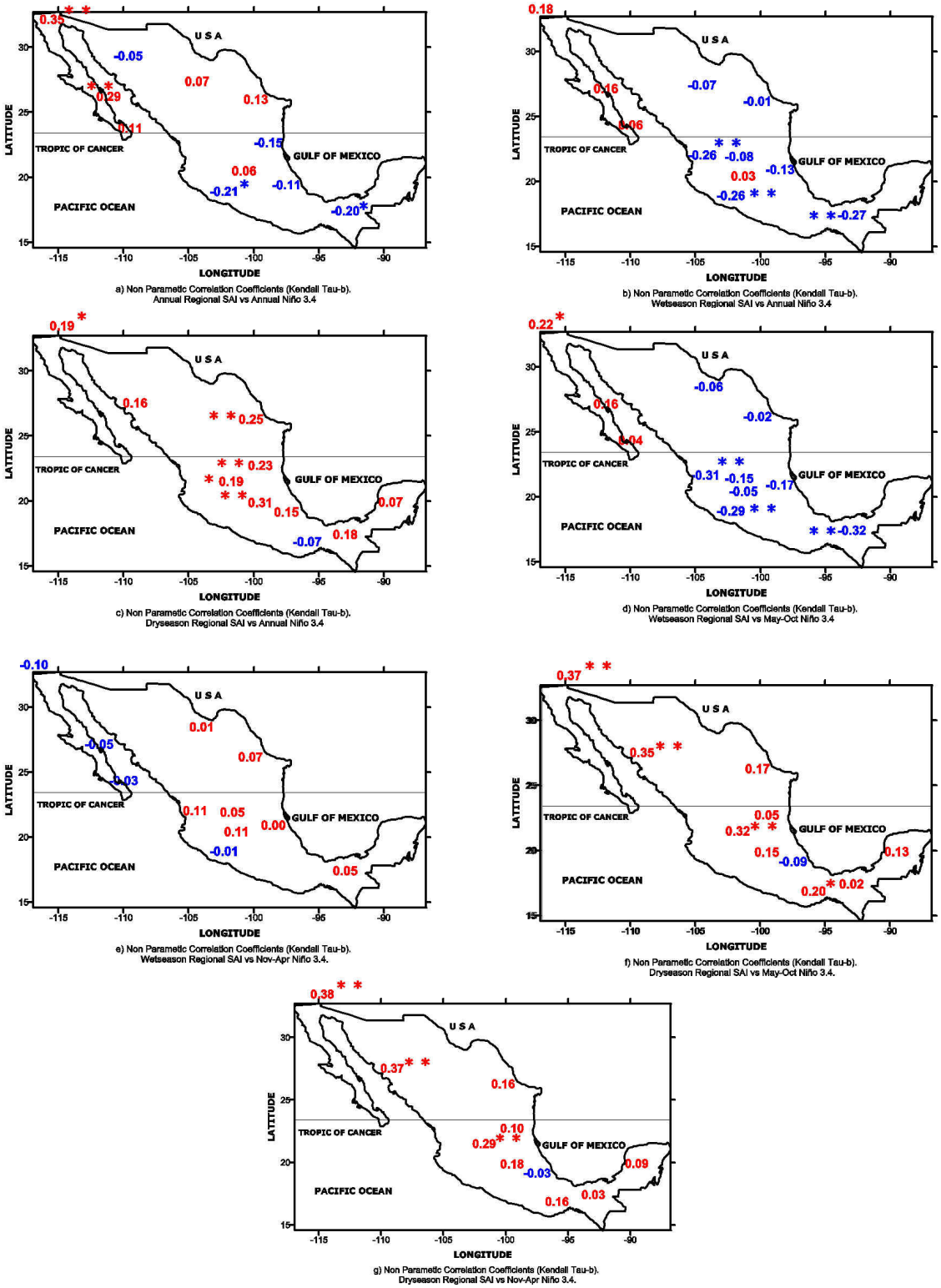

Fig. 7.20. Linear correlations (Kendall tau-b) between the standardised versions of the regional precipitation averages and the Niño 3.4 index. Red numbers represent positive and blue numbers negative correlations. * means statistical significant at 5% level and ** at 1% level.

With the exception of the neovolcanic belt region (refer to section 4.2.2) that breaks the climatic picture [Fig. 7.20 b)], a combined pattern of continental/peninsula and latitudinal transitions can be observed for the wet season rainfall averages. In the first case, negative correlations are found over the Mexican mainland; all the statistically significant correlations are concentrated south of the Tropic of Cancer. Positive correlations are located within the Baja California peninsula, but no significant results are observed here. Disregarding the close to zero correlations a latitudinal climatic transition is found when correlating wet season regional precipitation (Standardised Anomaly Index, SAI) and annual Niño 3.4 [Fig. 7.20 b)]. Drier conditions dominate south of the Tropic of Cancer for El Niño-like years.

An almost national widespread pattern of positive correlation is found when correlating dry season SAI of rainfall and the annual version of Niño 3.4. Statistically significant results are concentrated from central to northern Mexico [Fig. 7.20 c)]. It is interesting to observe that, the north-eastern part of the country is clearly responding during the winter to the annual Niño 3.4 modulation that was not seen for the annual and wet seasons. Perhaps the fact that polar fronts could extend as far as southern Mexico is affecting the rainfall amount during this season (Giddings et al., 2005). Nevertheless, the largest correlation is found in the Neovolcanic Axis region, an area of high altitude sites that is certainly influencing the results. A clear climatic pattern of wetter conditions during the El Niño phase is observed almost nationally.

A continental factor is evident when we correlate wet season (May-Oct) regional SAIs and the wet season version of Niño 3.4 indices. A homogeneous picture of negative correlations is found across mainland Mexico [Fig. 7.20 d)], while positive correlations are prevalent within the Baja California peninsula. A pattern of southwards increasing negative correlations is found for the continental part of the country. Meanwhile, the positive correlations increase northwards, reaching the highest correlation in the northern part of the Baja California Peninsula. Nevertheless, the largest correlations are negative and located south of the Tropic of Cancer; therefore, drier conditions are dominant during (wet season) El Niño years for the southern part of Mexico.

The main characteristic when correlating the wet season (May-Oct) version of the regional precipitation averages and the dry season (Nov-Apr) Niño 3.4 is that no statistically significant results are found [(Fig. 7.20 e)]. It can be said, however, that drier conditions are observed in mainland Mexico, while above normal precipitation totals are found within the Baja California peninsula during El Niño-like years.

A national climatic pattern is clear when correlating the dry season (Nov-Apr) version of the regional precipitation series and the wet season (May-Oct) Niño 3.4 index [Fig. 7.20 f)]. Disregarding the negative correlation (nearly zero correlation is observed in this region) in the Los Tuxtlas region, positive correlations are prevalent across most of Mexico. So, wetter conditions are observed during El Niño-like years, for this combination. The largest correlations among all the results are found in the north-western part of Mexico, the area where winter precipitation has a strong influence on the annual totals (Mosiño and García, 1974). However, the Mexican central highlands, a region with stations of high altitude is the only region showing a statistically significant result at the 1% level like in the northern counterparts. Only the Oaxaca region on the South Pacific coast has another significant correlation south of the Tropic of Cancer. It seems that there is a wet season (May-Oct) Pacific Ocean modulation of the winter precipitation during El Niño conditions.

Positive correlations are observed in most of the country, when correlating the dry season (Nov-Apr) SAI (Standardised anomaly indices) of regional precipitation and the dry season version of El Niño 3.4 index [Fig. 7.20 g)]. As in the other combinations the highest correlations are consistently observed in the north-western part of the country: the North American Monsoon (Mexican Monsoon) and the northern Baja California peninsula regions. Although not statistical significant the Yucatan Peninsula region appears with a clear correlation, in the hurricane-free (Nov-Apr or dry) season, pointing to the importance of the disruption of the normal climatic patterns that have for some of the times extraordinary precipitation totals associated with tropical cyclones (Englehart and Douglas, 2002). Another important climatic feature is that most of the stations with significant correlations are linked with the Pacific Coast. Wetter conditions are to be

expected for the regional precipitation averages during El Niño phase for the dry season (Nov-Apr). The most evident characteristic of the application of linear correlation (Kendall's tau-b) between the standardised versions of the regional precipitation averages and El Niño 3.4 index is the strong influence of seasonality in the results. The most statistically significant correlations are observed during the annual and the wet (May-Oct) precipitation seasons: drier conditions are observed during the El Niño phase for the southern (considering the Tropic of Cancer as a geographic limit) part of Mexico, when correlating with the annual and wet season (May-Oct) Niño 3.4 indices. This latitudinal climatic transition is also accompanied with a continental/peninsula pattern; defining continental as the mainland (the non-coastal territory), and the peninsula of Baja California. Wetter conditions for the north (peninsula) and the clear climatic picture of drier conditions for the southern part (continental) of Mexico are observed. Regional rainfall averages for the dry season (Nov-Apr) show precipitation above normal across almost the entire country.

Changing the spatial scale to regional levels, we can clearly see some consistency across the results. Among the positive correlations (wetter conditions), two regions appear frequently: North Baja California (near the Mexico-USA border), and the Mexican Monsoon Region (or North American Monsoon, RA11 in table 4.1); both in the north-western part of Mexico, areas strongly influenced by a winter pattern of precipitation and the Pacific Ocean. Meanwhile, the South-eastern rainforest, the Southern Pacific and the Nayarit Coast regions show the highest consistency among the negative correlations, leading to precipitation below normal during the El Niño phase.

Extreme Weather Indices.

Precipitation.

Extracted from daily data of rainfall and temperature, weather extreme indices are correlated with the Niño 3.4 index. The length of the extreme indices is defined from 1941 to 2001, but 1951 is the starting year of the Niño 3.4 index. Therefore, it was not possible to use the full potential of the meteorological data. The maps with the clearest results – largest correlation values with statistically significant results – are selected to extract the most important climatic patterns of the extreme weather indices modulated by ENSO (through El Niño 3.4.). Seasonal analyses are proposed to evaluate the subtle differences on the climate of Mexico. Annual, wet season (May-Oct) and dry season (Nov-Apr) are used in both the extreme weather (precipitation and temperature) and the Niño 3.4 indices. The analysis is expected to test the latitudinal climatic transition of the Mexican climate allowing a comparison against the results of the correlations of the extreme indices and SOI.

Linear correlation (using Kendall's tau-b) between precipitation extremes and the annual Niño 3.4 indices is the first combination to be addressed in this section. With the exception of the RX5day, all other indices (CDD, RX1day and PRCPTOT) were also analysed using SOI (see section 7.2.1). The Consecutive Dry Days (CDD) index [Fig. 7.21 a)] shows negative correlations at three stations from central to northern Mexico, two of them can be considered to be within the area of influence of the Mexican Monsoon system: Yecora (-0.23, linear correlation) and Ojinaga (-0.30), while Celaya (-0.29) is located in central Mexico [station numbers 32, 11 and 16 in Table 5.1 and Fig. 3.6 a)]. In geographical terms, the most significant results (Celaya and Ojinaga; statistically significant at the 1% level) are in a central line from a longitudinal perspective. Only southern stations with statistically significant results are found for RX1day [Fig. 7.21 b)]. Negative correlations are prevalent south of the Tropic of Cancer, pointing to drier conditions at these sites during El Niño conditions. Two of these

stations: Atzalán (-0.39) and Las Vigas (-0.21) are within the Los Tuxtlas region [stations number 34, and 35 in Table 5.1 and Fig. 3.6 a)]. Juchitán, near the South Pacific coast [station number 27 in Table 5.1 and Fig. 3.6 a)] has a correlation of -0.26 and a statistical significance better than the 1% level. Similar results are observed for the RX5day index [Fig. 7.21 c)]: negative correlations are dominant south of the geographical limit defined by the Tropic of Cancer. The maximum 5-day precipitation shows statistically significant results at Atzalán (-0.28) and Juchitán (-0.25) stations, heading to drier conditions during El Niño. These stations are also present with the largest correlations and statistical significance for the RX1day index. Finally, the annual total precipitation (PRCPTOT) [Fig. 7.21 d)] shows some similarity to the results of the already analysed indices (CDD, RX1day and RX5day). The most significant correlations show a latitudinal climatic pattern. In the northern part of Mexico, the Presa Rodríguez [station number 2 in Table 5.1 and Fig. 3.6 a)] show a positive correlation (+0.28) that is statistically significant at the 1% level, that leads to precipitation above the normal for this location. Meanwhile, south of the Tropic of Cancer, Atzalán (-0.23) and Juchitán (-0.23) stations show statistically significant (better than the 5% level) negative correlations. Therefore, drier conditions are dominant for these sites in the southern part of the country.

A clear latitudinal transition is observed for the extreme precipitation indices when correlated with the Niño 3.4 index. Northern stations show a pattern towards above normal precipitation; especially a decreasing trend in the Consecutive Dry Days (CDD) index. However, the most consistent climatic picture is among the indices that measure changes in wet days (RX1day, RX5day and PRCPTOT). During El Niño, drier conditions are prevalent for the stations south of the Tropic of Cancer. This statement is particularly true for the Atzalán and Juchitán [station numbers 34 and 27 in Table 5.1 and Fig. 3.6 a)], near the narrower land mass of the Tehuantepec isthmus in southern Mexico.

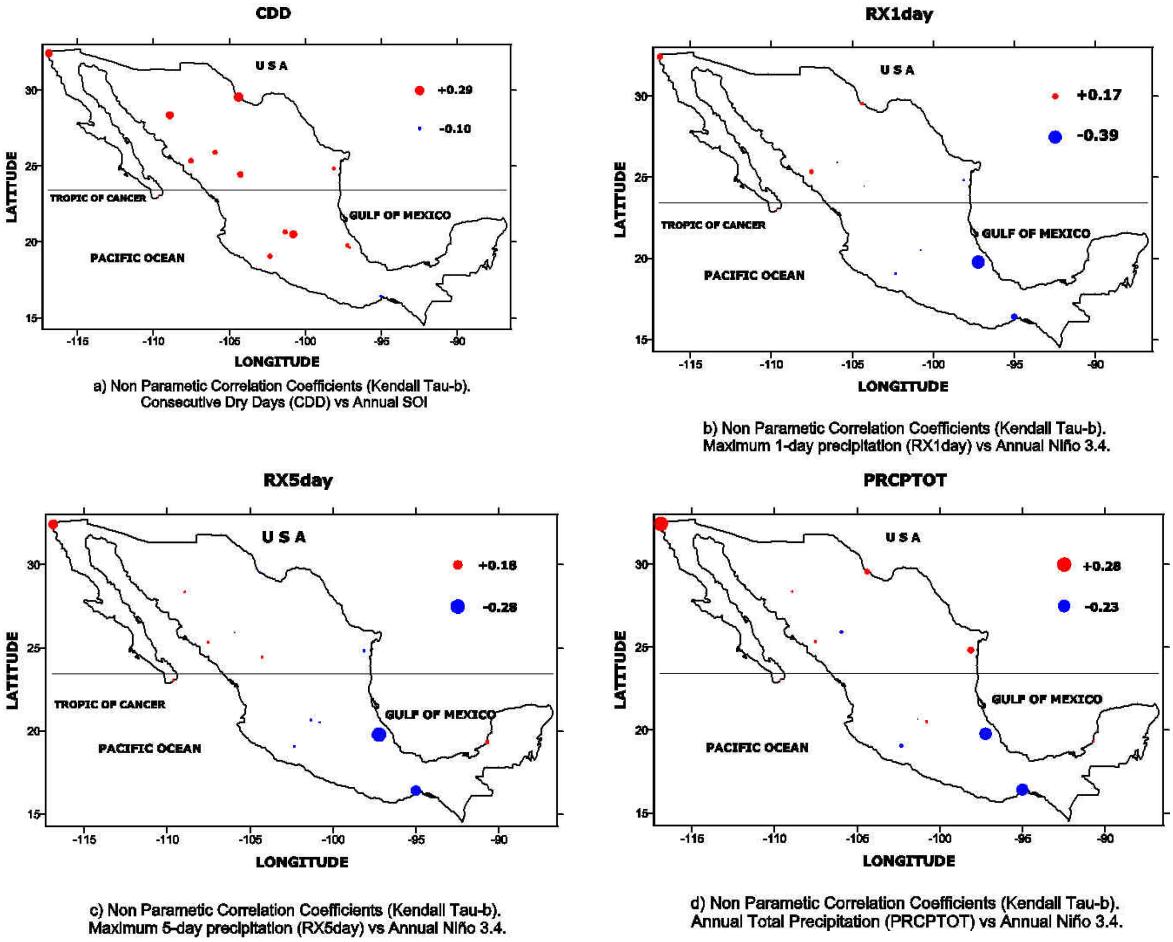

Fig. 7.21. Linear correlations (Kendall tau-b) between the Extreme Precipitation Indices and the Annual Niño 3.4 Index. Circles in red are representing a positive and in blue negative correlations.

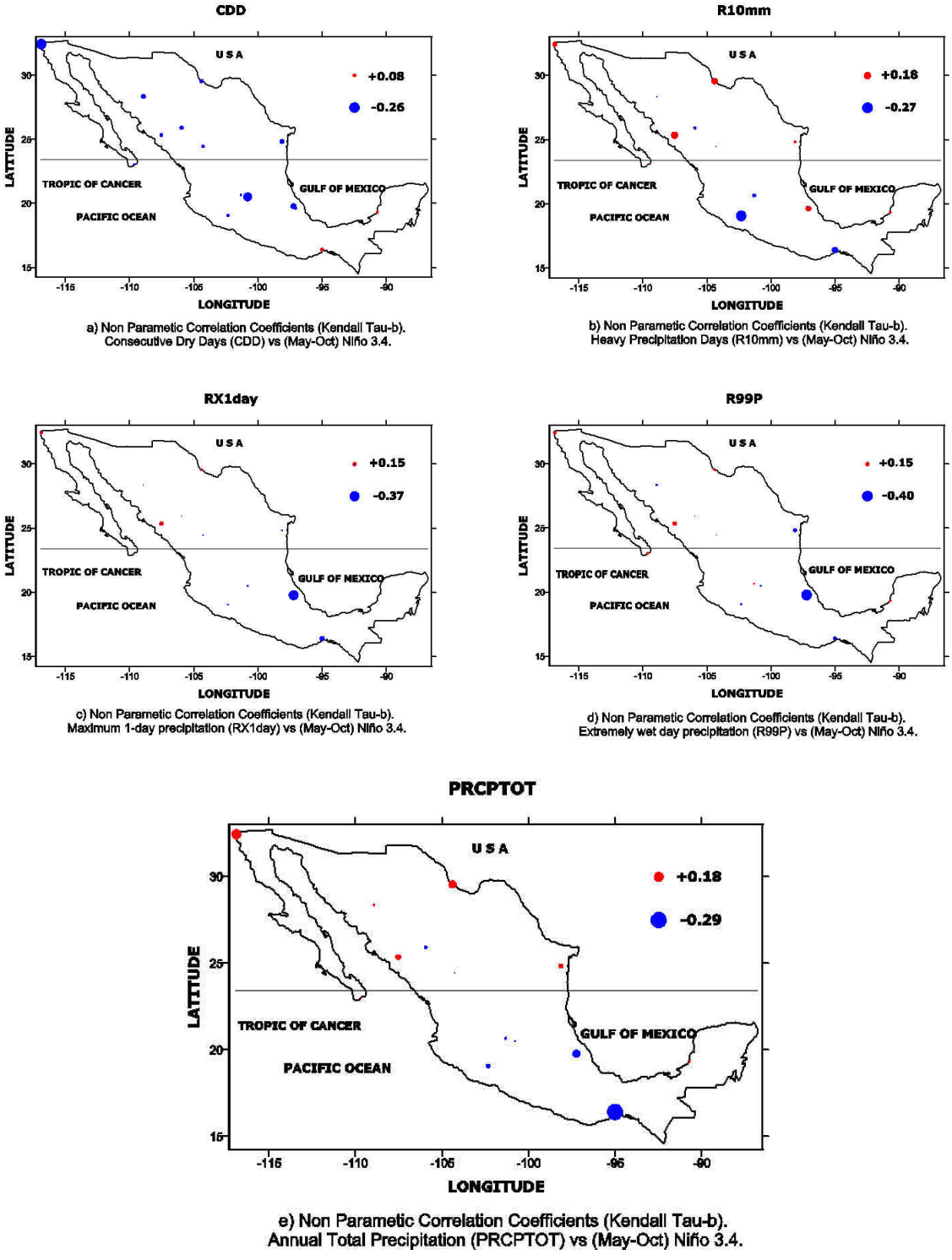

Fig. 7.22. Linear correlations (Kendall tau-b) between the Extreme Precipitation Indices and the Wet Season (May-Oct) Niño 3.4 Index. Circles in red are representing a positive and in blue negative correlations.

Wet Season

The relationships between the extreme precipitation indices and May-Oct (wet season) Niño 3.4 index are the next assessment in this section. May to October is the period (wet season) when most of the annual total precipitation occurs (see section 2.2 in chapter 2). Therefore, it is expected that the results will be close to those of the annual Niño 3.4 index. The precipitation extreme indices to be analysed with Niño 3.4 are: CDD, R10mm, RX1day, R99P and PRCPTOT, because they have the clearest and most important results amongst the potential rainfall indices evaluated. When compared with those evaluated using the annual El Niño 3.4, R10mm and R99P indices have been included this time.

The first precipitation extreme index to be analysed is the Consecutive Dry Days (CDD). An almost national pattern of negative correlations (less consecutive dry days during El Niño years, i.e., wetter conditions) is observed for CDD [Fig. 7.22 a)] when correlated with the May-Oct Niño 3.4 index. Although not statistically significant there is a clear concentration of the largest correlations in the western part of Mexico, especially within the Mexican Monsoon Region. The highest result is observed at Presa Rodriguez station in North-western Mexico [station number 2 in Table 5.1 and Fig. 3.6 a)], right on the border Mexico-USA border, its correlation (-0.26) is better than the 1% of statistical significance. In central Mexico, Celaya and Atzalán [station numbers 16 and 34 in table 5. 1 and fig. 3.6 a)] have correlations (-0.25 and -0.21 respectively) statistically significant at the 5% level; it is also important to mention that both stations are located above the 1500 m.a.s.l. The heavy precipitation days index (R10mm) shows a prevalence of negative correlations across the country [Fig. 7.22 b)], but the climatic pattern is not as clear as for CDD. The largest relationships are found for Apatzingán and Juchitán [station numbers 20 and 27 in Table 5. 1 and Fig. 3.6 a)] with correlations of -0.27 and -0.22 respectively; both above the 5% of statistical significance. Geographically speaking, it can be said that there is a strong Southern Pacific connection with the results, pointing to a clear ENSO modulation of this extreme index. Evaluated in the same measuring units (as mm) R10mm, the RX1day index or max 1-day precipitation show a clear southern climatic pattern [Fig. 7.22 c)]. The most significant correlations are located at Atzalán (-

0.37), Juchitán (-0.26), and Las Vigas (-0.22) [station numbers 34, 27, and 35 in Table 5.1 and Fig. 3.6 a)]. They are located near the Tehuantepec isthmus, the narrower continental land mass of Mexico. The correlations at two of these stations (Atzalán and Juchitán) are better than the 1% level of statistical significance. No significant results are found in the northern part of Mexico. Most significant correlations for the R99P index [Fig. 7.22 d)] are observed along the eastern part of Mexico, near the Gulf of Mexico coast. The largest results are observed at Atzalán, Las Vigas and San Fernando [station numbers 34, 35 and 33 in Table 5.1 and Fig. 3.6 a)]. The last two have statistically significant correlations (-0.23 correlation in both cases) better than the 5% level. However, the largest correlation (-0.40) is found within the Los Tuxtlas region at Atzalán, and the relationship is significant at the 1% of significant level. It is possible (as these three stations with statistically significant results are along the coast of the Gulf of Mexico) that the hurricane season could be affecting the results of this index. Finally, annual total precipitation only shows significant results south of the Tropic of Cancer, close to the results already observed for the RX1day index. The stations with the largest correlations are geographically located near the Tehuantepec Isthmus. Highest correlations are found at Juchitán (-0.29) and Atzalán (-0.21) better than the 1 and 5% of statistical significance respectively [station numbers 27 and 34 in Table 5.1 and Fig. 3.6 a)]. PRCPTOT results [Fig. 7.22 e)] lead to a climatic pattern of precipitation below normal in the southern part of Mexico, while no clear pattern evident over the northern part of the country.

The results when precipitation extreme indices and the (May-Oct) Niño 3.4 index are correlated show that the most significant changes occur south of the Tropic of Cancer. Negative correlations prevail in most of the extreme indices analysed pointing to drier conditions during El Niño, especially for the southern part of the country. Only the Presa Rodriguez and San Fernando stations, both located in northern Mexico [station numbers 2 and 33 in Table 5.1 and Fig. 3.6 a)] break with this climatic picture. Two interesting features also appear when analysing these combinations: most of the significant results are geographically concentrated in southern Mexico near the Tehuantepec Isthmus and although explicitly avoided (using the standardised version of the Niño 3.4), it seems that

high altitudes play an important role in the climatic responses of the extreme rainfall indices to ENSO.

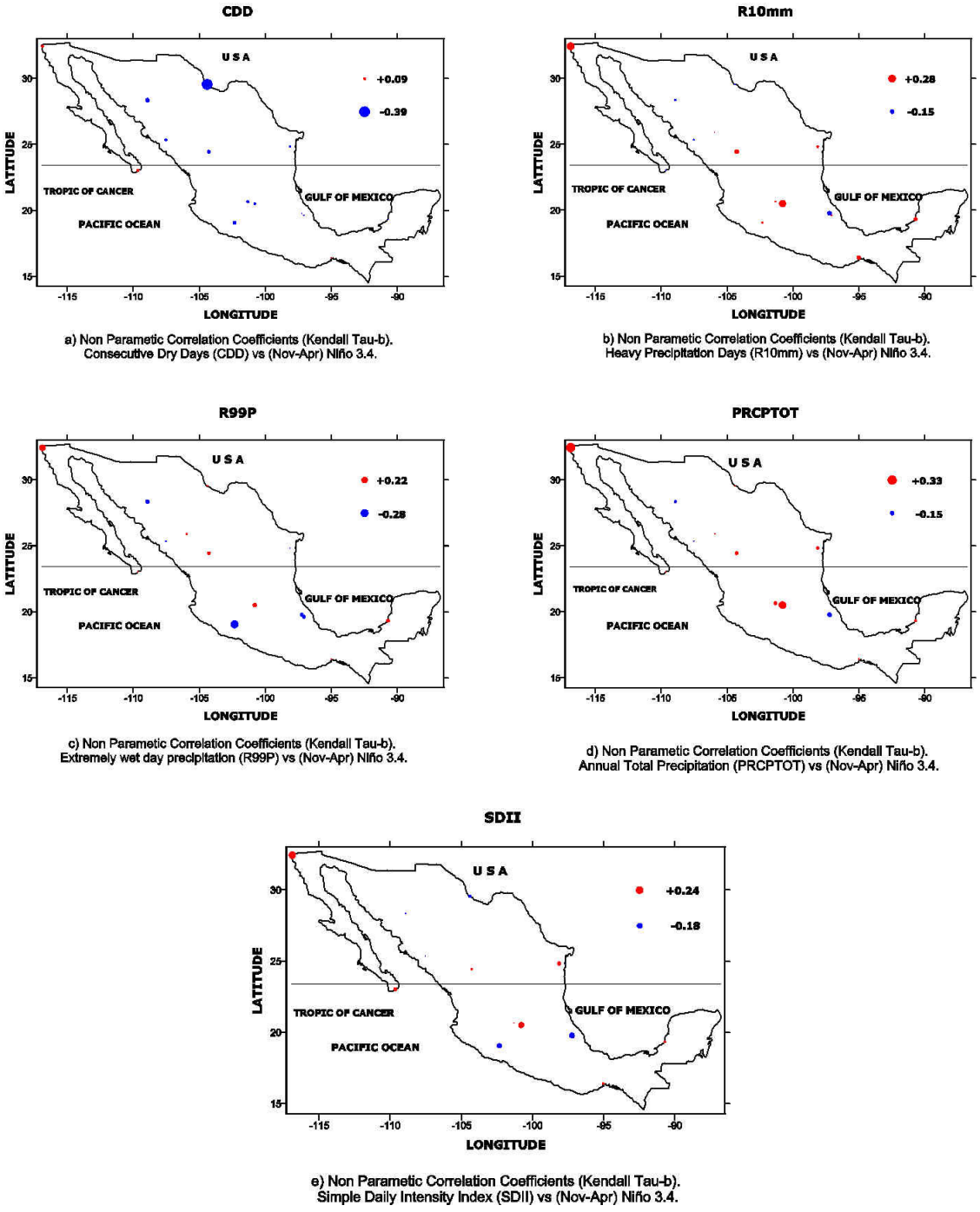

Fig. 7.23. Linear correlations (Kendall tau-b) between the Extreme Precipitation Indices and the Dry Season (Nov-Apr) Niño 3.4 Index. Circles in red are representing a positive and in blue negative correlations.

Dry Season

The last analysis among the extreme precipitation indices is to correlate them with the dry season (Nov-Apr) Niño 3.4 index (Fig. 7.23). The November to April period is the dry season for much of Mexico, except some northern areas of the country, where winter precipitation makes a large contribution to the annual total rainfall (see section 2.3). This climatic pattern contrasts markedly with much of the rest of the country. The extreme indices to be analysed are: CDD, R10mm, R99P, PRCPTOT and SDII. When compared with the annual and wet seasons RX1day and RX5day do not have significant results, and SDII is evaluated here, but was not assessed in the previous analyses.

For the November to April season, the Consecutive Dry Days (CDD) is the first index to be evaluated. Then, most significant results are found in northern Mexico [Fig. 7.23 a)], especially within the influence of the Mexican Monsoon Region (section 2.2.2). Almost a national picture of negative correlations (fewer consecutive dry days, i.e., wetter conditions) is observed for CDD. Ojinaga (-0.39) and Yecora (-0.24) [station numbers 11 and 32 in Table 5.1 and Fig. 3.6 a)] have the largest correlations among all the stations, and both are statistically significant at the 1% level. Mostly positive correlations are evident in central and northern Mexico for the Heavy Precipitation Days (R10mm), and they are slightly concentrated in the western half of the country [Fig. 7.23 b)]. The Presa Rodriguez in the most north-western part of the country [station number 2 in Table 5.1 and Fig. 3.6 a)], near the border with the USA shows the largest correlation (-0.28), and the result is statistically significant at the 1% level. A latitudinal transition can be seen in the results of the extremely wet day precipitation (R99P) index [Fig. 7.23 c)]. South of the Tropic of Cancer, Juchitán [station numbers 27 in Table 5.1 and Fig. 3.6 a)] has the largest negative correlation (-0.28); in northern Mexico the highest (positive) correlation (+0.22) is observed at the Presa Rodríguez station. Both results are statistically significant at better than the 5% level. Despite this climatic transition, no clear climatic pattern can be found in the R99P index. Wetter conditions are dominant in central and northern Mexico according to the annual precipitation totals (PRCPTOT) results [Fig. 7.23 d)]. No clear climatic pattern can be extracted from the results, but it can be

mentioned that the largest correlation values are observed in the central and northern part of the country, coinciding with the importance of winter precipitation in annual totals. The highest positive correlation (+0.33) is found at the Presa Rodríguez station, at better than 1% of statistical significance. Lastly, only one significant correlation is seen when we evaluate the Simple Daily Intensity Index (SDII). Although not clear, positive correlations can be observed in Central and Northern Mexico; wetter conditions are dominant during the El Niño phase [Fig. 7.23 e)]. A clear example of this picture, is the Presa Rodriguez station that has the only significant correlation (+0.24) among the results, in the north of the Baja California peninsula, the correlation is statistically significant at the 5% level.

In general, above normal precipitation can be observed during the (Nov-Apr) Niño 3.4 index, when it is correlated with the extreme rainfall indices. Geographically speaking, this climatic pattern is concentrated in central and northern Mexico. The Presa Rodriguez [station numbers 2 in Table 5.1 and Fig. 3.6 a)] has consistently shown this pattern of wetter conditions during the "dry" season of El Niño. Meanwhile, only one statistically significant correlation has been observed (across all the indices) for the southern part of Mexico. Therefore, it can be concluded than the dry season (Nov-Apr) Niño 3.4 is modulating the precipitation extreme indices mostly in the northern part of Mexico.

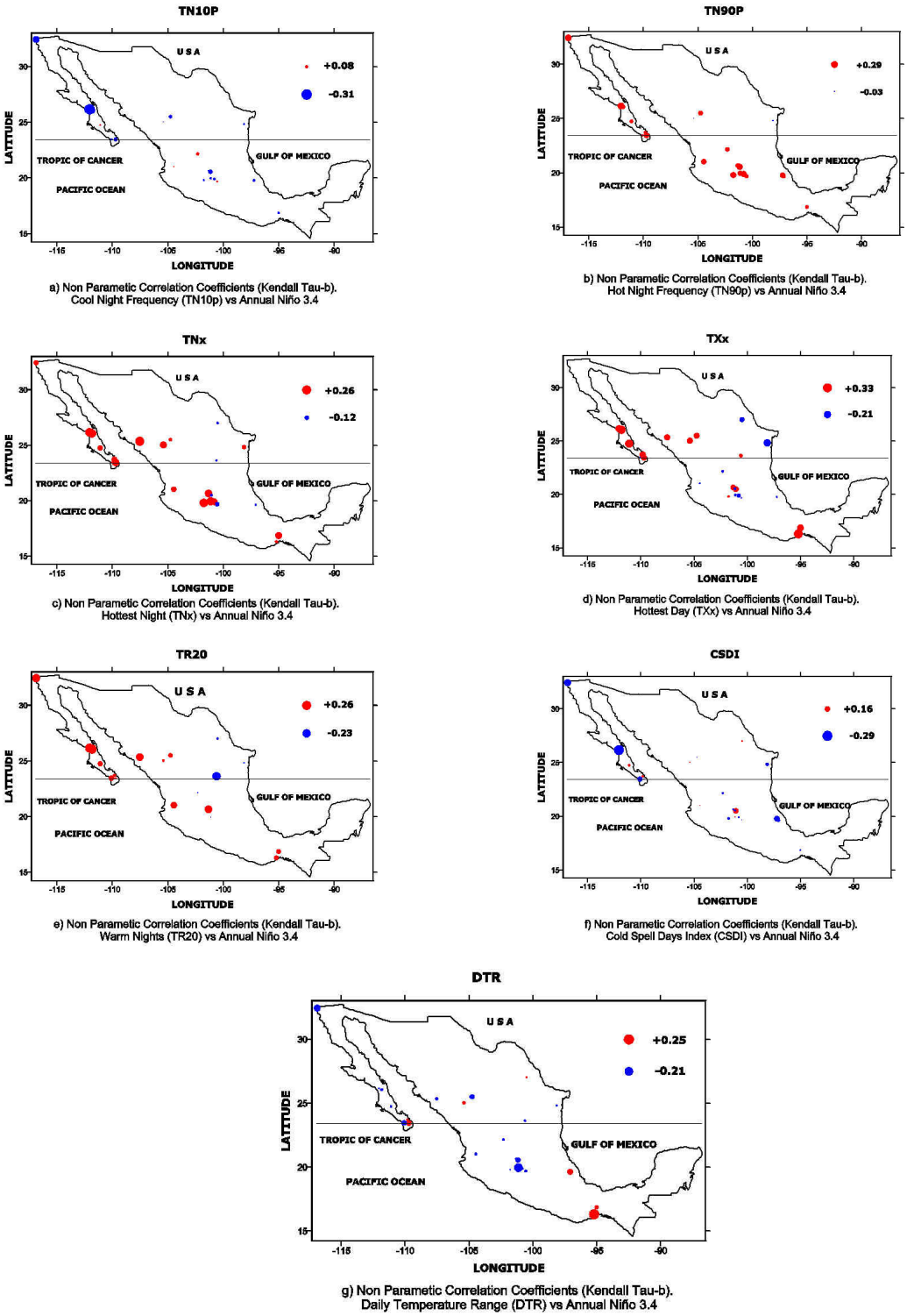

Fig. 7.24. Linear correlations (Kendall tau-b) between the Extreme Temperature Indices and the Annual Niño 3.4 Index (Annual Niño 3.4). Circles in red are representing a positive and in blue negative correlations.

Temperature.

The other aspect of weather extremes to be correlated with the Niño 3.4 index is temperature. The different seasonal versions (annual, May-Oct and Nov-Apr) of Niño 3.4 will in this section be correlated with the extreme temperature indices. The length of the time series is the same as for precipitation (1941-2001). A latitudinal climatic transition is also expected in this analysis; we consider the Tropic of Cancer as a geographical limit to define different regime patterns.

The extreme temperature indices considered, because of their clear results, when correlated with the annual Niño 3.4 index are: TN10P, TN90P, TNx, TXx, TR20, CSDI and DTR. These parameters have been divided, in such a way that minimum and maximum temperatures are evaluated first, and then the DTR that summarise the differences between maximum and minimum temperatures. The Cool Night Frequency (TN10P) shows [Fig. 7.24 a)] mostly a pattern of negative correlations (fewer cool nights, i.e., warmer temperatures). All significant results are located north of the Tropic of Cancer, particularly within the Baja California peninsula. Highest correlations are observed at La Purísima (-0.31) and the Presa Rodríguez (-0.27) [station numbers 5 and 2 in Table 6.1 and Fig. 3.6 b)], both correlations are better than the 1% level of statistical significance. A clear national climatic picture of positive correlations is observed for the Hot Night Frequency (TN90P) index. The most significant results are geographically concentrated in central and northern Mexico [Fig. 7.24 b)]. La Purísima and the Presa Rodríguez stations have the largest correlations both with values of +0.29, and they are statistically significant at the 1% level. The rest of the significant correlations located in Central Mexico are high altitude stations [Salamanca, Zacapu and Huingo; stations number 19, 24 and 22 in Table 6.1 and Fig. 3.6 b)] that exceed 1500 m.a.s.l. Warmer conditions are then expected for the TN90P index during an El Niño phase. A similar pattern as for the TN90P can be seen for the Hottest Night (TNx) index [Fig. 7.24 c)]. Positive correlations are almost nationally widespread. The largest correlations are slightly biased to the western half of the country near or along the Pacific coast. Warmer

temperatures are then expected at night during El Niño phases. Warmer conditions are also dominant during the day time temperatures according to the TXx correlations [Fig. 7.24 d)]. Indeed, positive correlations can be observed over much of the country. Because of the geographical location of many of the significant correlations, it seems that the Pacific Ocean has a strong influence on this index. The correlations at Santo Domingo Tehuantepec and El Paso de Iritu [stations 29 and 4 in Table 6.1 and Fig. 3.6 b)] are all at better than the 1% level of statistical significance. Warm or tropical nights index (TR20) also shows a prevalence towards positive correlations [Fig. 7.24 e)]. The most significant results are concentrated in the peninsula of Baja California and north of the Tropic of Cancer. In accordance with these correlations, more nights above the 20°C threshold are expected during El Niño. Less clear is the climatic profile for the Cold Spell Days Index (CSDI). Negative correlations are observed in the Baja California peninsula and the Los Tuxtlas region [Fig. 7.24 f)]. Fewer spells of 6 consecutive days when TN<10^{th} percentile of 1961-1990 are expected for the Purísima, Comondú and Atzalán [station numbers 5, 3 and 34 in Table 6.1 and Fig. 3.6 b)]. Finally, lower values of the Daily Temperature Range (DTR) are observed during El Niño in Central and Northern Mexico, while they increase in the southern half of the country [Fig. 7.24 g)]. Therefore, we can speak of a latitudinal transition in the response of the DTRs for this index.

A clear increase in these extreme indices associated with minimum temperatures is observed when correlated with the annual version of the Niño 3.4 index. Warming conditions are found in central and northern Mexico, which is especially clear for the stations north of the Tropic of Cancer in the Baja California Peninsula (La Purísima, Presa Rodríguez and Comondú). Although increasing, maximum temperatures do not have a clear pattern like the changes in minimum temperatures.

Wet Season

In this section we correlate extreme temperature indices and the May to October version of the Niño 3.4 index. Due to their significant results the indices to be analysed in this section are: TN10P, TN90P, TNx, TXx, TR20, CSDI and DTR. They have been classified in such a manner that the indices related to minimum and maximum temperatures are analysed first, finishing with DTR that combines the maximum and minimum temperatures in an index.

The first index associated with minimum temperatures evaluated is the Cool Night Frequency (TN10P) [Fig. 7.25 a)]. Mostly negative correlations are seen across the country; the most significant results are observed north the Tropic of Cancer in the peninsula of Baja California. La Purísima, Comondú, and the Presa Rodríguez [station numbers 5, 3, and 2 in Table 6.1 and Fig. 3.6 b)] are the stations with the largest correlations, but only at La Purísima are the results better than the 1% level of statistical significance. According to these results, the frequency of cool nights decreases during the May-Oct (wet season) El Niño phase. An almost nationally widespread pattern of positive correlations is found for the Hot Night Frequency (TN90P) [Fig. 7.25 b)]. Therefore, warmer nights can be expected during the rainfall wet season (May-Oct) under El Niño conditions for TN90P. The highest correlations for this index are seen at La Presa Rodríguez and La Purísima [station numbers 2 and 5 in Table 6.1 and Fig. 3.6 b)], both statistically significant at the 5% level. The Pacific Ocean seems to be a strong influence in the modulation of the extremes associated with minimum temperatures. This is especially true when we evaluate the Hottest Night Index (TNx) [Fig. 7.25 c)]. The largest (positive) correlations are geographically concentrated in the western half of Mexico, but only the result at La Purísima (+0.25) is statistically significant at the 5% level. Nevertheless, warmer nights could expect to be dominant in the western part of Mexico during the May to October period of El Niño phase. A latitudinal climatic transition can also be observed in the results of the Hottest Day Index (TXx) [Fig. 7.25 d)]. Positive correlations are prevalent in the western part of Mexico, especially near the Pacific coast and the Baja California peninsula. In fact, the most significant results are

found here, north of the Tropic of Cancer at Comondú and El Paso de Iritu [station numbers 3 and 4 in Table 6.1 and Fig. 3.6 b)], being both below the 1% level of statistical significance. Warmer day time conditions along the Pacific Coast and cooler temperatures in the northeast part of Mexico are to be observed during May-Oct (wet season) El Niño. Mixed climatic patterns are found for the Tropical Nights (TR20) [Fig. 7.25 e)]. Nevertheless, the largest (positive) correlations are seen in the Mexican Monsoon Region and the Baja Californian peninsula in the northwest part of Mexico. More nights above the 20°C limit are expected for these regions during May-Oct (wet season) El Niño. Negative correlations are evident within the Baja Californian peninsula for the Cold Spell Days Index (CSDI) [Fig. 7.25 f)], i.e., fewer spells are present when a fully developed El Niño is occurring during the May to October period (wet season). Only one statistically significant (at the 5% level) result is found for the Daily Temperature Range (DTR) index. Positive correlations are slightly stronger south of the Tropic of Cancer. But, no clear climatic pattern is observed for DTR [Fig. 7.25 g)].

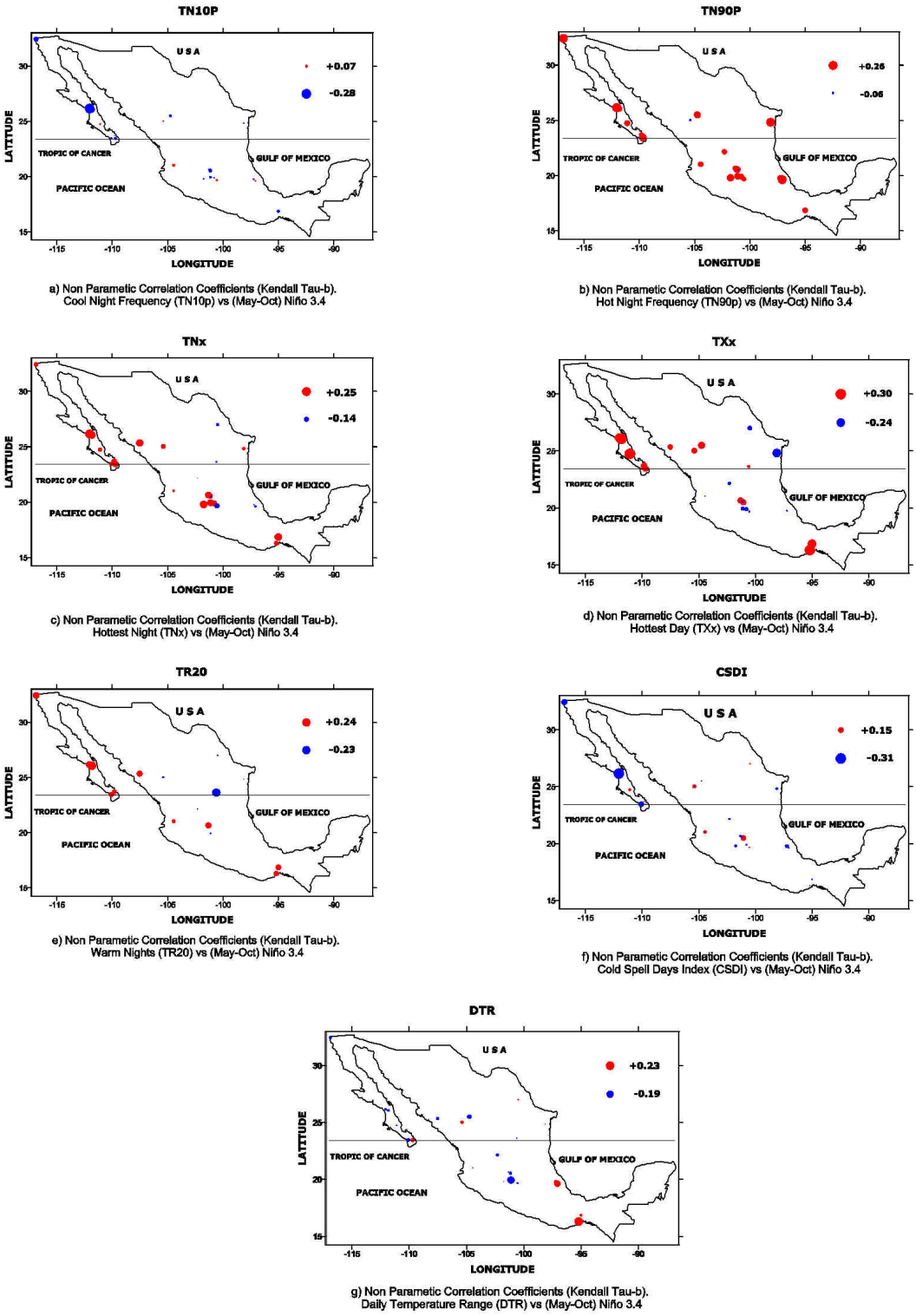

Fig. 7.25. Linear correlations (Kendall tau-b) between the Extreme Temperature Indices and the Wet Season (May-Oct) El Niño 3.4 Index (Wet Niño 3.4). Circles in red are representing a positive and in blue negative correlations.

The temperature extreme indices show an almost general pattern of warmer conditions when (they are) correlated with the May to October (wet season) standardised version of Niño 3.4. Geographically speaking these warming conditions prevail over the Baja California peninsula, but also along the Pacific coast within the Mexican monsoon region (RA11 in table 4.1).

Dry Season

The application of the linear correlation between the temperature extreme indices and the November to April version of Niño 3.4 is the last analysis to be performed. The indices to be analysed in this section are: TN10P, TN90P, TNn, TNx, TX10P, TR20, and CSDI. These indices have been divided aiming to analyse in the first place minimum temperatures but finishing this time with a measure of cold spell days (CSDI).

Although not clear, a national pattern of negative correlations is dominant for the TN10P index [Fig. 7.26 a)]. The only statistically significant correlation (-0.24) is observed at La Presa Rodríguez [station number 2 in Table 6.1 and Fig. 3.6 b)] in the north of Baja California. In general, it can be said that warmer temperatures prevail during Nov-Apr (dry season) El Niño. A national climatic picture of positive correlations is found for the TN90P index [Fig. 7.26 b)]. Most significant results are concentrated in Central Mexico, and south of the Tropic of Cancer. An interesting feature is seen for this index, all the stations are above 1500 m.a.s.l. It can be concluded that the frequency of nights exceeding the 90th percentile increases during El Niño (Nov-Apr). Positive correlations are also nationally widespread for the Coolest Night Index (TNn) [Fig. 7.26 c)], but, the largest correlations with statistically significant results are located within the peninsula of Baja California, north the Tropic of Cancer. Warmer conditions for the TNn index are nationally observed during (Nov-Apr) El Niño. Almost the same national pattern of positive correlations is repeated for the TNx index [Fig. 7.26 d)]. The highest correlations are geographically located in Central and Northern Mexico (within the area of influence

of the Mexican Monsoon). Except for Badiraguato in the north-western part of the country [station number 31 in Table 6.1 and Fig. 3.6 b)], all these stations exceed 1500 m.a.s.l. Warmer nights are then expected during El Niño. The most significant results north of the Tropic of Cancer are also observed for the TX10P [Fig. 7.26 e)]. There is a clear continental/peninsula climatic pattern for this index: most continental land shares positive correlations, while within the peninsula of Baja California negative correlations are dominant. The greatest correlation (better than the 1% level of statistical significance) is found at Santiago (-0.31) [station numbers 9 in Table 6.1 and Fig. 3.6 b)]. The fact that this large correlation is occurring during the Nov-Apr period points to a clear example of the role that winter precipitation plays in the area, especially during El Niño years. According to these results, warmer temperatures are to be expected in the Baja California peninsula during the November to April period of El Niño phase. Mexico is nearly dominated by positive correlations when the TR20 [Fig. 7.26 f)] and the (Nov-Apr) Niño 3.4 indices are correlated. The largest correlations are geographically biased to the western half of the country; all these results are statistically significant at the 5% level. An increasing number of warmer nights (TN>20°C) are observed during (Nov-Apr) El Niño conditions. A mixed pattern of positive and negative correlation is found for the Cold Days Spell Index [Fig. 7.26 g)]. Although most significant results [Comondú and Las Vigas; station numbers 3 and 35 in Table 6.1 and Fig. 3.6 b)] are negative correlations statistically significant at the 5% level, the climatic picture is not geographically clear for this index. Nevertheless, fewer spells of cold days (warmer temperatures) can be expected during the Nov-Apr period of El Niño.

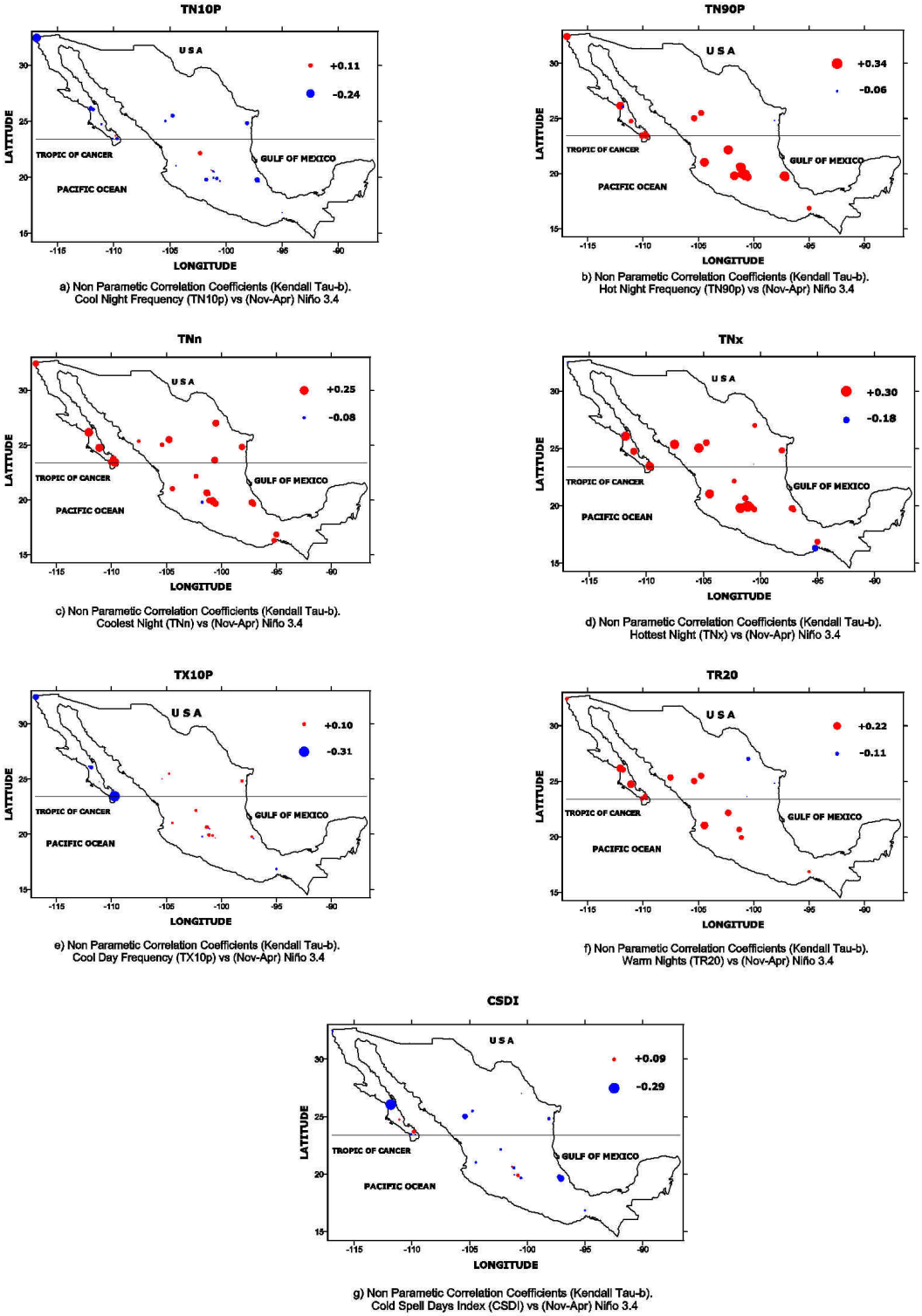

Fig. 7.26. Linear correlations (Kendall tau-b) between the Extreme Temperature Indices and the Dry Season (Nov-Apr) El Niño 3.4 Index (Dry Niño 3.4). Circles in red are representing a positive and in blue negative correlations.

Warmer temperatures during the November to April (the rainfall dry season) period during El Niño events are to be expected across most of Mexico. This is especially true for minimum temperatures indices (TN10P, TNn, TNx and TN90P); results lead to a persistence of warmer conditions during El Niño phase for central and northern Mexico. The same geographical pattern could be said to apply to the maximum temperatures, but it is less clear. Clearer results prevail in the Baja Californian peninsula. However, no clear geographical climatic picture is observed for the CSDI Index; but certainly above normal temperatures are to be expected. Therefore, a nationally widespread pattern of warmer temperatures is very likely to be found during the November to April "season" of El Niño.

7.3.2. LAG CORRELATION.

Regional Precipitation Averages

Positive correlations are a dominant characteristic of the largest correlation values between Regional Precipitation Averages and the Niño 3.4 index (see Table 7.1). Similar time shifts (-2, +2, and +3 months) are observed for regions RA4 (Central Mexican Highlands), RA6 (North Baja California) and RA7 (La Huasteca Region) (see Table 4.1 for the regional definitions and their climatic characteristics). Correlations increase when moving from west to east and south to north (See Fig. 7.27). In this sense, the largest response of the regional precipitation averages to Niño 3.4 is located in the north-western part of Mexico (RA4 and RA6) just as it was observed when they were correlated with SOI, with a delayed time-shift. La Huasteca region (RA7) has a quite similar climatic response in its correlations and lags. In fact, according to these results, it can be said that wetter conditions are found during El Niño phase for northern Mexico near to El Niño peak conditions.

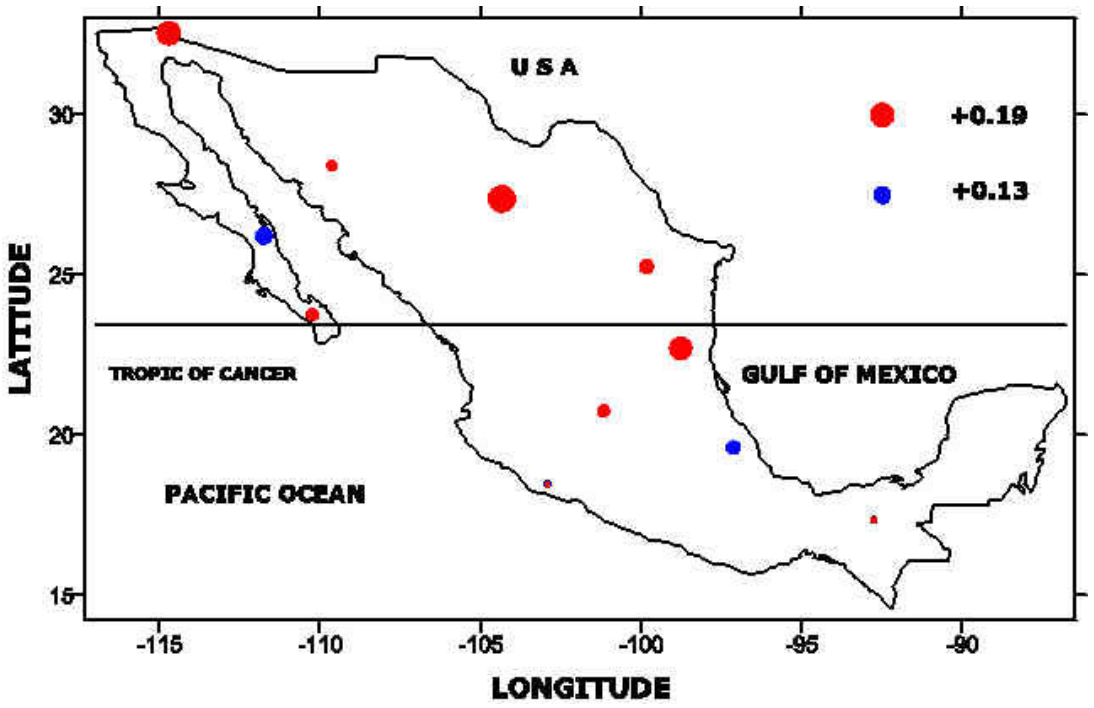

Fig. 7.27. Lag cross-correlations between the standardised versions of Precipitation Regional Averages and the El Niño 3.4 index. Red circles represent positive and blue circles negative correlations.

Extreme Weather Indices.

Extreme Rainfall Indices

Because of their clear statistically significant results, only two rainfall extreme indices will be analysed. Both extreme indices are related to maximum precipitation: the maximum 1-day precipitation (RX1day) and the maximum 5-day precipitation (RX5day).

The strongest response of the maximum 1-day precipitation (RX1day) to El Niño (expressed by the Niño 3.4 index) is observed within the most north-western part of Mexico, at La Presa Rodríguez in the northern Baja Californian Peninsula [station number 2 in Table 5.1 and Fig. 3.6 a)], with a positive correlation of +0.17 and a lag of 2 months (Fig. 7.28). A similar timing of the response occurs for Atzalán near the coast of the Gulf of Mexico [station number 34 in Table 5.1 and Fig. 3.6 a)], its correlation is of negative sign (-0.16) meaning dry conditions during El Niño phase.

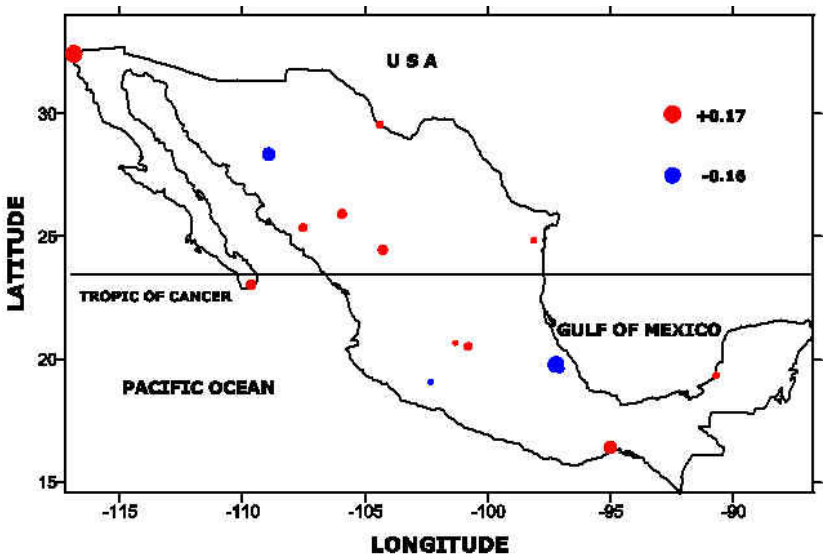

Fig. 7.28. Lag cross-correlations between the RX1day (Max 1-day Precipitation) Index and the standardised version of the El Niño 3.4 Index. Red circles represent positive and blue circles negative correlations.

Less clear are the results in the south Pacific station region for the Juchitán in the state of Oaxaca state [station number 27 in Table 5.1 and Fig. 3.6 a)] that responds with a net increase of the amount of rainfall for 1-day maximum but the correlation is small (+0.13) and with a long delay (+18 months). Similar timing characteristics but a net decrease (-0.13) in the 1-day maximum precipitation is observed at Yecora within the Mexican Monsoon region [station number 32 in Table 5.1 and Fig. 3.6 a)]. The climatic pattern found for RX1day is: wetter conditions are dominant during El Niño for the RX1day index.

The climatic response of the maximum 5-day precipitation to Niño 3.4 index is basically replicating the pattern already seen for the maximum 1-day rainfall (Fig. 7.29). The strongest response is observed at Presa Rodríguez [station number 2 in Table 5.1 and Fig. 3.6 a)], in which RX5-day is positively correlated (+0.17) to the Niño 3.4 index, meaning that the amount of maximum 5 day precipitation increases during El Niño-like years.

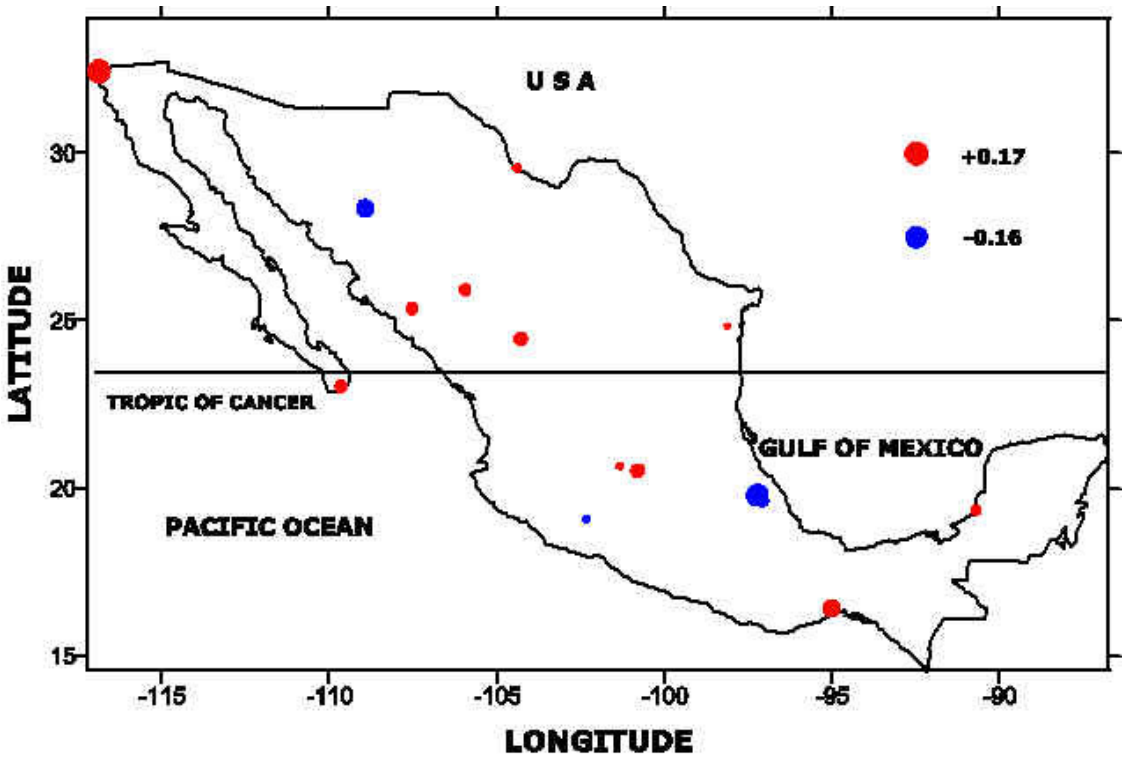

Fig. 7.29. Lag cross-correlations between the RX5day (Max 5-day Precipitation) Index and the standardised version of the El Niño 3.4 Index. Red circles represent positive and blue circles negative correlations.

Drier conditions are observed within the North American Monsoon Region (also called Mexican Monsoon Region; RA11 in table 4.1) with a negative correlation (-0.13) for Yecora [station number 32 in table 5.1 and fig. 3.6 a)], the timing being quite different for both stations (see table 7.2). Nevertheless, stations with positive correlations (wetter conditions) in north-western Mexico share a similar timing (close to the peak) of response to El Niño conditions.

Wetter conditions dominate most of the country when rainfall extreme indices are evaluated (using lag correlations) under El Niño conditions. The most significant results are concentrated along the Pacific Ocean coast, especially in the north-western part of the country, and these climatic responses are observed near to the peak of the El Niño phenomenon.

Extreme Temperature Indices

Patterns of delayed (or simultaneous) climatic responses of temperatures to El Niño (using the Niño 3.4 index) are going to be explored in this section. The extreme indices to be considered are: TN10p, TN90p, TNn, TNx, TX10p, TX90p, TXn, TXx, and DTR. Minimum-related extremes correlations are evaluated first, then maximum-related indices, and finally DTR to assess if the most significant changes are occurring for minimum or maximum extremes.

No clear climatic picture is observed for the TN10P index. A mixed combination of positive and negative correlations (warmer conditions during El Niño years) is observed across the country, particularly in Central Mexico (Fig. 7.30).

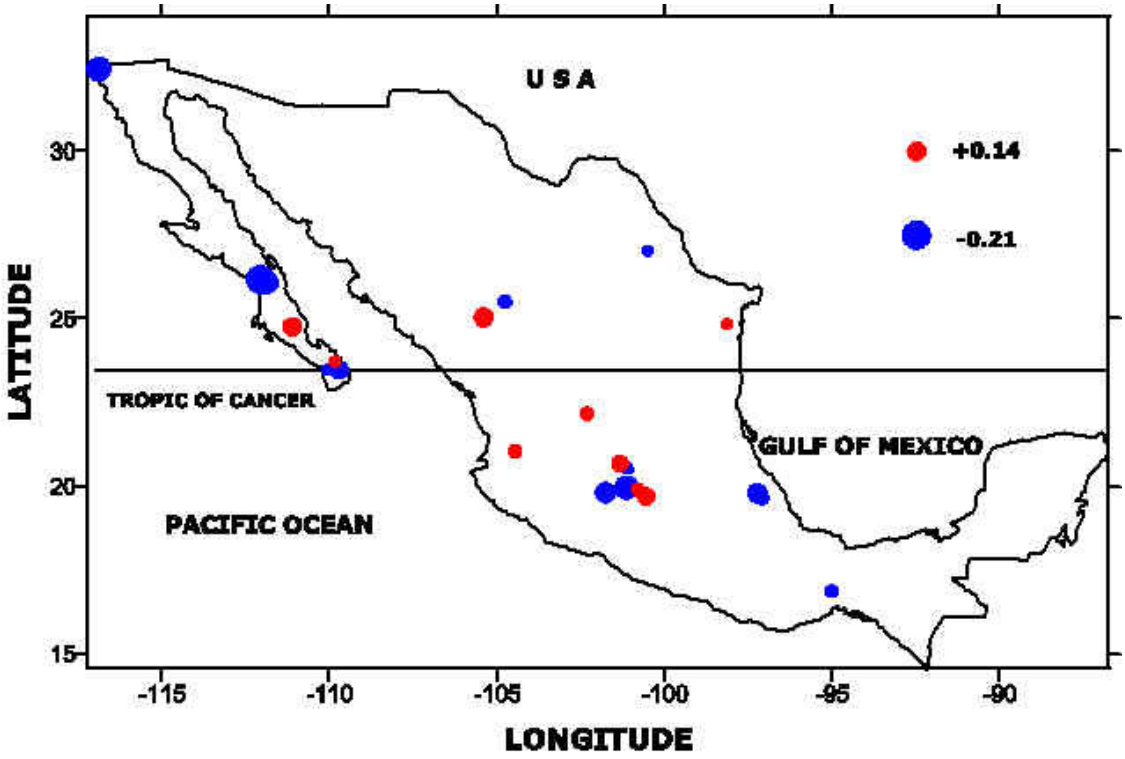

Fig. 7.30 Lag cross-correlations between the TN10P (Cool Night Frequency) and El Niño 3.4 Index. The linear correlation is calculated using the Pearson function. Red circles express positive correlations, and blue circles show negative correlations.

Nevertheless, among these contrasting patterns for TN10P, two regions show clusters of negative correlations: Los Tuxtlas and Oaxaca (near the influence of the Tehuantepec isthmus, where a narrow land area is the bridge between the Atlantic and Pacific oceans) and within the northern part of the Baja Californian peninsula (see Table 7.5). It is precisely, within the Baja Californian peninsula that the time-shifts are similar, the rest of the correlations do not show consistency among their lags.

Positive correlations prevail in Mexico for the TN90P index (Fig. 7.31), especially in the western half of the country. A positive timing of response is also associated to these correlations (Table 7.6). Longer (negative) time-shifts are linked to negative correlations. A clear modulation of El Niño, leading to warmer temperatures is observed in the western half of Mexico (especially along the Pacific coast and the Baja Californian peninsula). The timing pattern seems to incorporate an early response in the south and then moving to the north finishing in the peninsula of Baja California near the border with the USA.

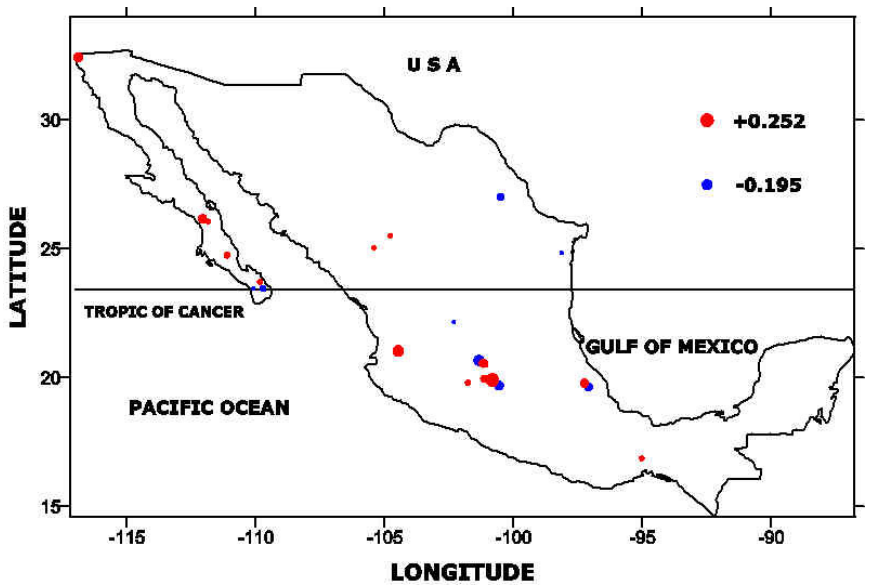

Fig. 7.31 Lag cross-correlations between the TN90P (Hot Night Frequency) and El Niño 3.4 Index. The linear correlation is calculated using the Pearson function. Red circles express positive correlations, and blue circles show negative correlations.

The largest positive correlation values are observed south of the Tropic of Cancer for the Coolest Night Index (TNn). These results are also geographically concentrated in the western half of the country (Fig. 7.32). Meanwhile all negative correlations are close to zero (Table 7.7). Climatically the lags associated with the largest positive correlations are located in the Zacapu and Santo Domingo Tehuantepec in southern Mexico [station numbers 24 and 29 in Table 6.1and Fig. 3.6 b)]; their negative time-shifts are -10 and -16 months respectively. Warmer (colder) conditions dominate the coolest night-temperatures during El Niño (La Niña) phase.

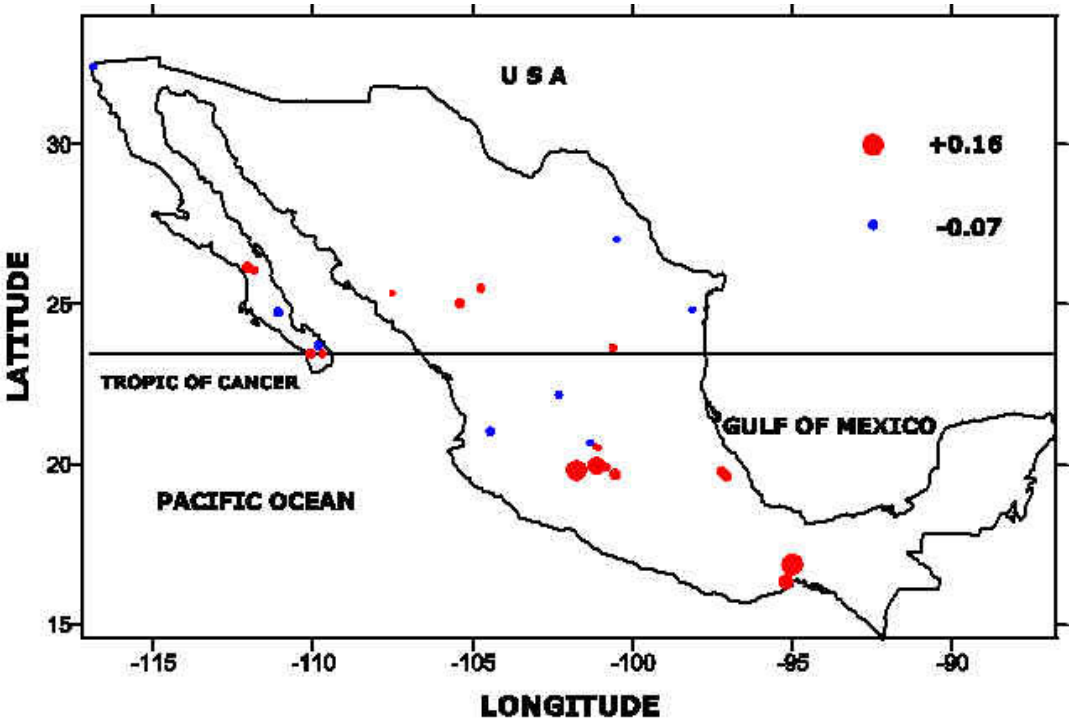

Fig. 7.32 Lag cross-correlations between the TNn (Coolest night) and El Niño 3.4 Index. The linear correlation is calculated using the Pearson function. Red circles express positive correlations, and blue circles show negative correlations.

Warmer temperatures prevail for the Hottest Night Index (TNx) during El Niño conditions (Fig. 7.33). Time lags show that the largest positive correlations imply climatic responses close to the peaks of El Niño phase. Most significant results are found in the southern part of Mexico in Michoacán state [Zacapú, Huingo, and Ciudad Hidalgo; station numbers 24, 22 and 23 in Table 6.1and Fig. 3.6 b)], but it is really with Las Vigas station in Los Tuxtlas region [station number 35 in Table 6.1 and Fig. 3.6 b)] that these stations share similarity, showing variations between -6 and +5 months in the time-shifts (Table 7.8). So, we can speak of dominant warmer night temperatures south of the Tropic of Cancer near to the peak of El Niño-like conditions.

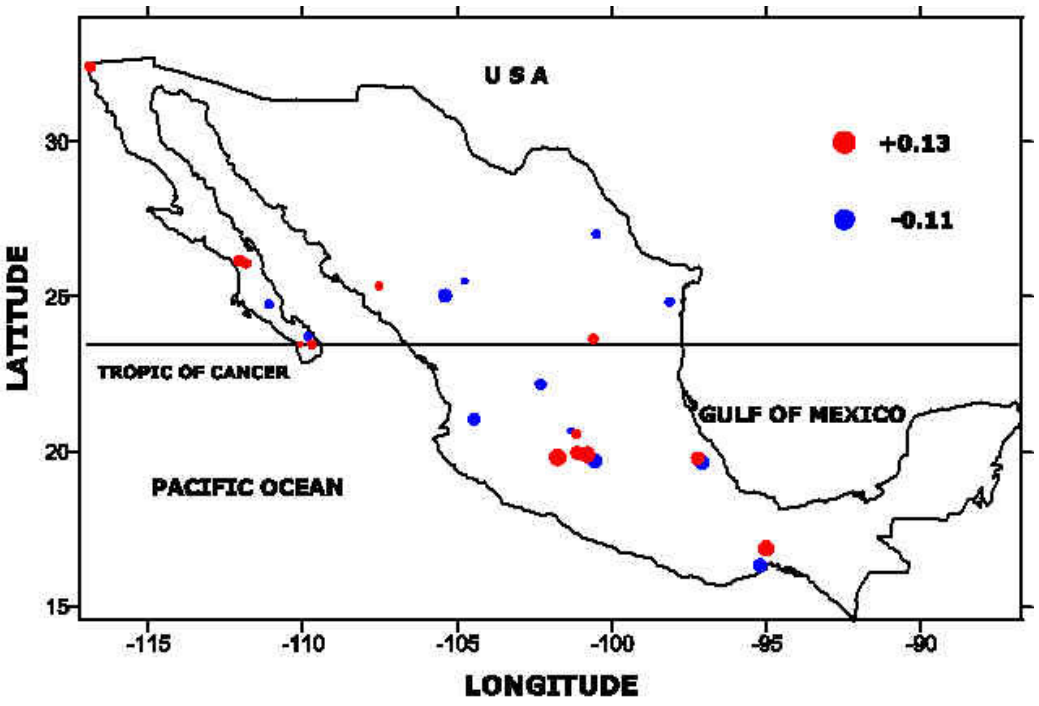

Fig. 7.33 Lag cross-correlations between the TNx (Hottest night) and El Niño 3.4 Index. The linear correlation is calculated using the Pearson function. Red circles express positive correlations, and blue circles show negative correlations.

Close to the strongest El Niño conditions are the correspondent climatic responses of the Cool Night Frequency Index (TX10P). The largest positive correlation values are observed in the western half of Mexico near the Pacific coast (Fig. 7.34). Here, the station time-lag responses are, on average, one month behind the peak of El Niño-like phase (Table 7.9). Less clear are the negative correlations, especially the variability of the time-lags that fluctuate between -11 and +15 months when looking for the best correlation. Geographically speaking these negative correlations are located in the Baja California peninsula, although Las Vigas, near the Gulf of Mexico [station number 35 in Table 6.1 and Fig. 3.6 b)], shows a significant decrease in the TX10P index. But, the clearest climatic picture when applying the lag correlation technique between TX10P and the Niño 3.4 indices shows decreasing frequencies of night temperatures below the 10th percentile, i.e., warmer conditions during El Niño, with variable times of response, especially in the western half of Mexico.

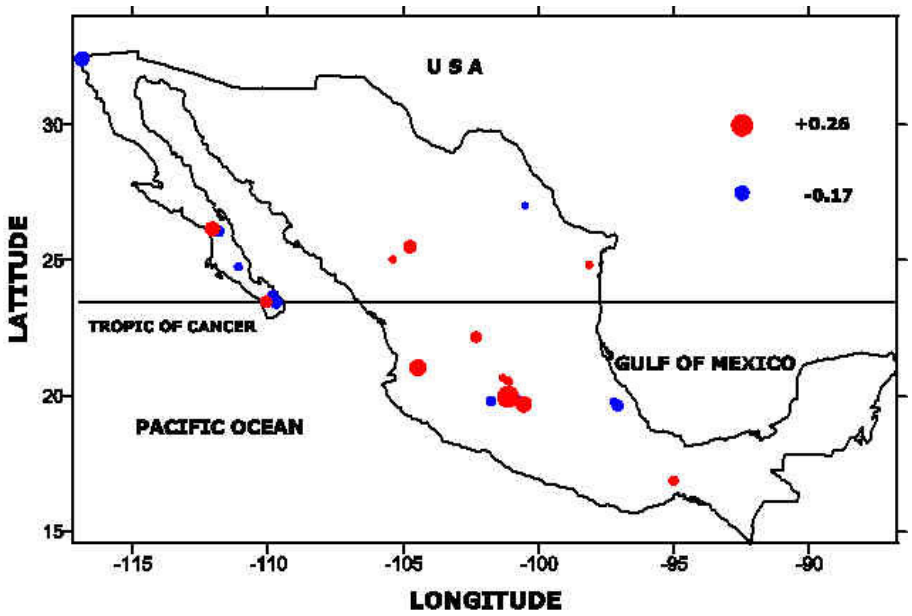

Fig. 7.34 Lag cross-correlations between the TX10P (Cool Day Frequency) and El Niño 3.4. The linear correlation is calculated using the Pearson function. Red circles express positive correlations, and blue circles show negative correlations.

Although a clear climatic pattern is observed for the Hot Day Frequency Index (TX90P); positive correlations are dominant in the southern part of Mexico, especially within the Los Tuxtlas region (Fig. 7.35). Similar also are the timings of response of these southern stations, having the greatest impact on day temperatures near to the peak of El Niño phase (Table 7.10). Warmer day temperatures are observed within the southern part of the country close to the peak of El Niño conditions.

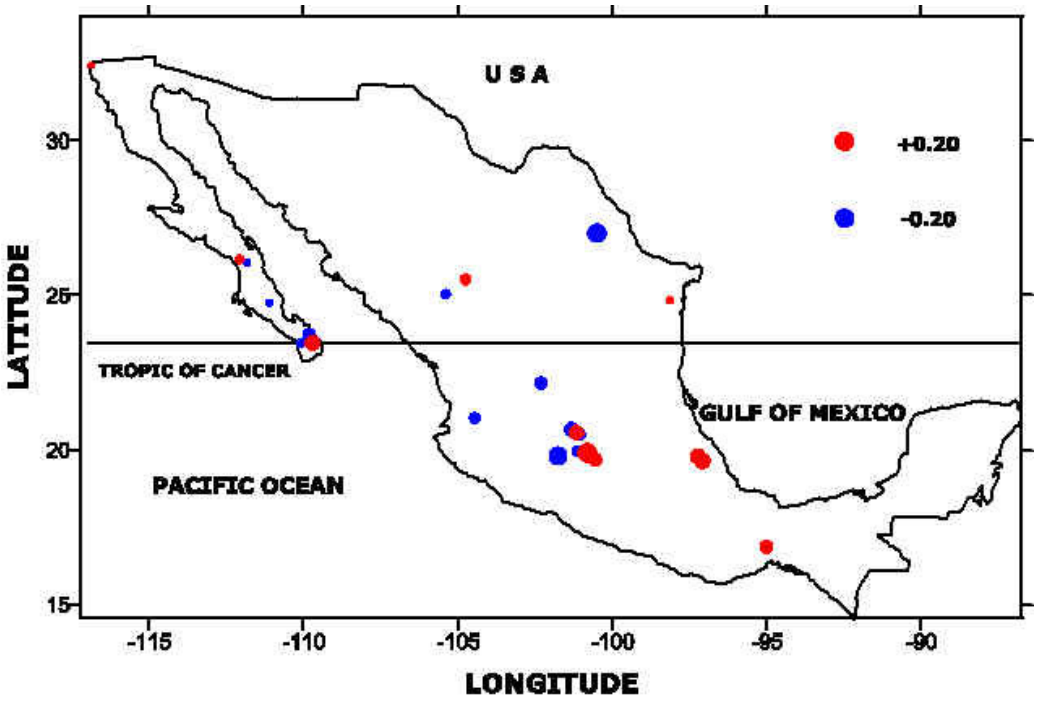

Fig. 7.35 Lag cross-correlations between the TX90P (Hot Day Frequency) and El Niño 3.4 Index. The linear correlation is calculated using the Pearson function. Red circles express positive correlations, and blue circles show negative correlations.

Mixed climatic patterns are found for the TXn index, with no clear spatial distribution of negative correlations (Fig. 7.36). Time-shifts to find the best correlation with El Niño 3.4 index are also quite dissimilar (Table 7.11). Negative correlations are mostly geographically located in the western half of Mexico. However, clearer results are found in the southern part of the country. Consistency (spatially) is observed for positive correlations and time-lags (-6 months average) which are close to the strongest conditions of the El Niño phenomenon. Therefore, according to these results, warmer day temperatures are expected during El Niño phase, close to its peak.

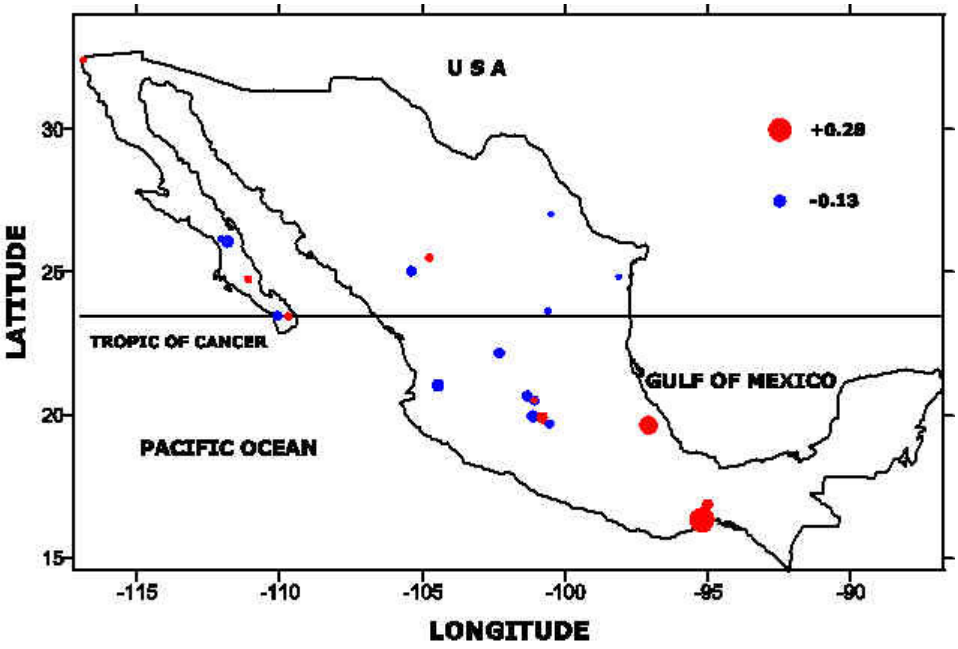

Fig. 7.36 Lag cross-correlations between the TXn (Coolest Day) and El Niño 3.4 Index. The linear correlation is calculated using the Pearson function. Red circles express positive correlations, and blue circles show negative correlations.

A longitudinal climatic transition in continental Mexico could be observed for the Hottest day Index (TXx). Roughly, positive correlations are dominant in the eastern part of Mexico, while negative correlations are prevalent in the western part of the country (Fig. 7.37). Positive correlations are located along the Atlantic Coast, except the most southern station in Oaxaca that, in fact, it has the greatest correlation (+0.23) among all the results. Time lags for these positive correlations are very similar, climatically responding with warmer temperatures close to the peak of El Niño (Table 7.12). Negative correlations are geographically biased to the western half of the country, but time-shifts of climatic impact to El Niño are quite different. North of the Tropic of Cancer in the Baja California peninsula positive correlations prevail. Nevertheless, these correlations in the peninsula are not large enough to be considered significant in terms of correlations and time response consistency. Warmer conditions are found for TXx in the eastern half of Mexico close to the strongest conditions of El Niño.

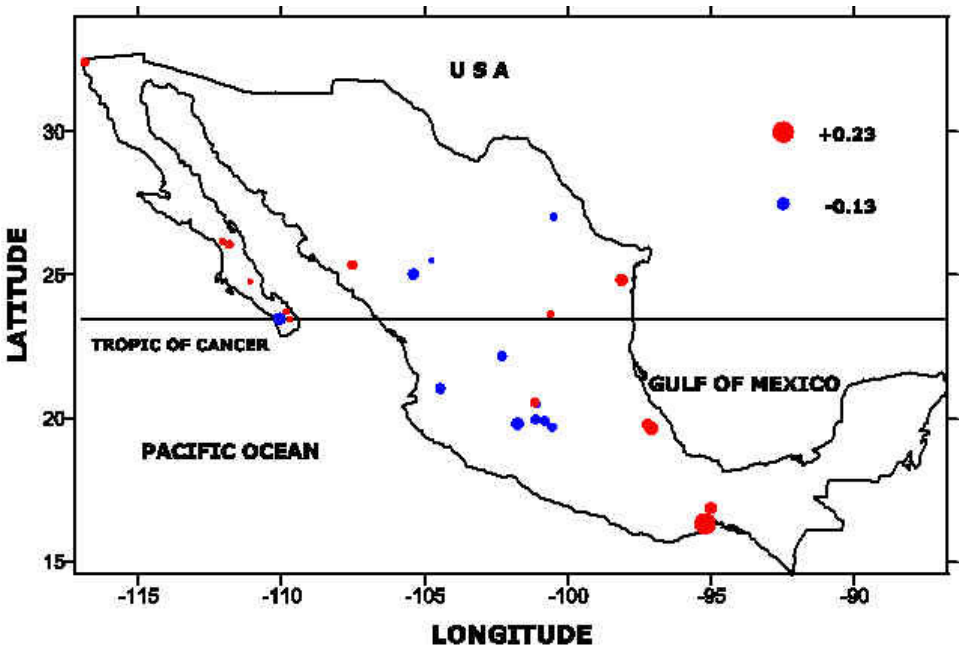

Fig. 7.37 Lag cross-correlations between the TXx (Hottest Day) and El Niño 3.4 Index. The linear correlation is calculated using the Pearson function. Red circles express positive correlations, and blue circles show negative correlations.

Largest (negative) correlations for the DTR index are geographically concentrated in central and northern Mexico (Fig. 7.38 and Table 7.4). As evident in the already analysed extreme indices, changes in minimum temperatures are clearer than in the maximum-related indices, and certainly more strongly are reflected in the decreasing DTRs.

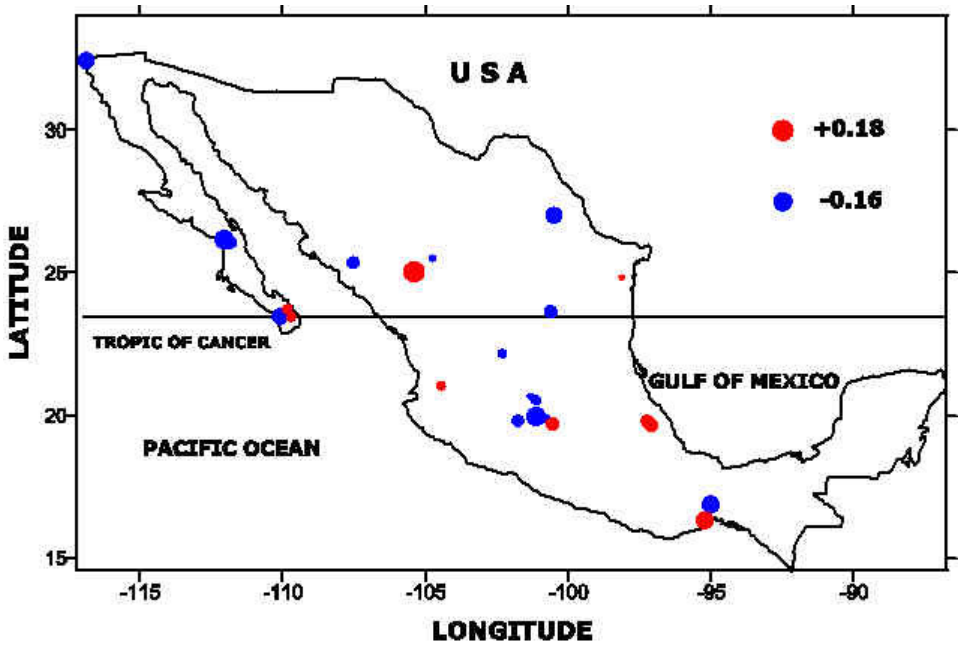

Fig. 7.38 Lag cross-correlations between the DTR (Daily Temperature Range) and El Niño 3.4 Index. The linear correlation is calculated using the Pearson function. Red circles express positive correlations, and blue circles show negative correlations.

A clear climatic pattern towards warmer temperatures is clear when we correlate extreme temperature indices and Niño 3.4. However, we have to point out that maximum temperature related indices have a geographic preference for changes in the southern part

of the country. Meanwhile, minimum temperature indices are basically varying north of the Tropic of Cancer.

Summary of the section (El Niño 3.4 Index).

The results of the (correlations) analysis of influence of the El Niño 3.4 index on temperature and precipitation show strong consistency with those of SOI (section 7.2). This coherence can be fully observed in the latitudinal transition and the seasonal factor of the climatic patterns. No matter the variable analysed (precipitation or temperature) or the scale used (regional or local), the timing response of the best results is close to the peak of El Niño conditions.

A latitudinal climatic transition is observed when the annual and wet season (May to October) Standardised Anomaly Indices (SAI) of precipitation are used. Wetter conditions in northern Mexico (especially the north-western part of the country) and drier conditions in the South prevail during El Niño years. In addition, this climatic transition shows a preference of the largest correlations for the sites along the Pacific coast. An almost national pattern of above (below) normal precipitation during El Niño (La Niña) years is seen for the dry season (November to April) of the rainfall SAIs. These climatic patterns are also replicated for the precipitation extreme indices, but the importance of the dry season rainfall on the north-western part of Mexico is clearer.

Contrasting climatic conditions are also observed for the temperature extreme indices. During El Niño years, changes in maximum temperatures prevail in southern Mexico, while in the North of the country the most important variations are seen in minimum temperatures. Nevertheless, these climatic patterns are mostly concentrated along the Pacific Ocean coast in Mexico. The most important results also show a timing response close to the strongest ENSO conditions.

7.4. THE MEI (MULTIVARIATE ENSO INDEX) INFLUENCE.

7.4.1. LINEAR CORRELATION.

Precipitation Regional Averages.

The last El Niño index to be linearly correlated (using Kendall's tau-b) to the regional precipitation averages is the Multivariate ENSO Index (MEI). As in the previous sections the time-series are divided into annual, wet (May-Oct) and dry (Nov-Apr) seasons for both the regional averages and the MEI indices. The final aim is to find either spatial or temporal climatic patterns of the impacts of El Niño in the regional rainfall averages.

Taking the Tropic of Cancer as a geographical limit, a clear latitudinal transition could be observed when correlating the annual versions of SAI and MEI. Positive correlations are found in northern Mexico, while negative correlations prevail in the southern part of the country [Fig. 7.39 a)]. The highest correlation values are concentrated within the Baja California Peninsula. This climatic pattern has been consistent across the other combinations of regional averages and ENSO indices: the greatest correlations are positive, and can be seen in the northern part of the peninsula. These results are mostly better than the 1% level of statistical significance. Negative correlations are located along the southern Pacific coast. These correlations are statistically significant at the 5% level. Nevertheless, there is an evident geographic pattern (along the Pacific Ocean) of the annual total rainfall in a clear transitional climatic pattern; during El Niño years the annual regional precipitation totals are above their normal for the northern part of the country, especially in the peninsula of Baja California; while drier conditions are observed for the southern Pacific coast.

Closely replicating the former results the correlation between the wet season (May-Oct) SAI and the annual MEI shows a differential climatic pattern: negative correlations south of the Tropic of Cancer and positive north of this geographical limit [Fig. 7.39 b)]. Wetter conditions are experienced during El Niño years for the northern half of Mexico and

below normal precipitation is dominant during the same phase of ENSO for the southern part of the country. It is clear that all the stations with statistically significant correlations (these results are better than the 1% level of statistical significance) are concentrated along the Pacific Ocean coast suggesting a strong modulation of the summer regional precipitation by ENSO. The only region that breaks this clear climatic pattern is the Neovolcanic Belt region, but its correlation is close to zero.

Positive correlations prevail all over the country when correlating dry season (Nov-Apr) SAI and Annual MEI [Fig. 7.39 c)]; this is one of the clearest climatic patterns across all the combinations of the rainfall extreme indices and MEI. Statistically significant correlations are concentrated from central to northern Mexico. Let us recall that, during winter polar fronts heavily influence the temperature and rainfall of the northern part of Mexico (section 2.3). This can be easily seen as the highest correlations are found in the northern Baja California peninsula and the high altitude Neovolcanic Belt region. Above normal precipitation above their normal is observed during the boreal winter in northern Mexico during El Niño years.

Drier conditions are observed in the southern part of Mexico, and wetter climatic regimes for the Baja California peninsula during El Niño phase. Positive correlations are dominant when we correlate the wet season (May-Oct) SAI and wet season MEI north of the Tropic of Cancer [Fig. 7.39 d)], especially in the Baja Californian peninsula where the greatest correlation (better than the 1% level of statistical significance) is found within the northern part of the peninsula. Meanwhile, negative correlations prevail along the southern coast of the Pacific Ocean. Two areas break this precipitation pattern, the Neovolcanic Belt and the central northern part of Mexico, although, both regions show near zero correlations, so they can easily be disregarded as affecting the whole climatic picture described above.

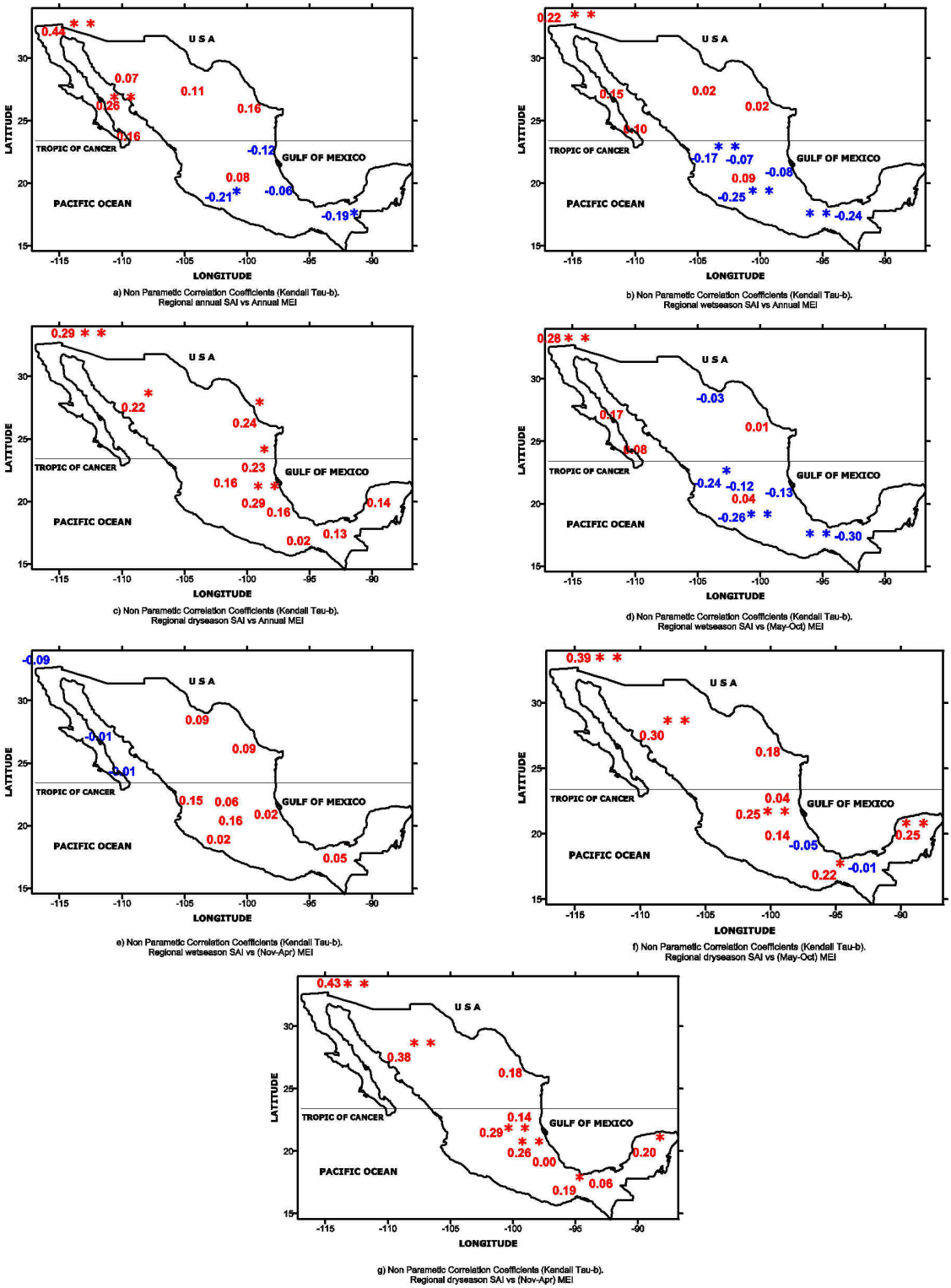

Fig. 7.39. Linear correlations (Kendall tau-b) between the standardised versions of the regional precipitation averages and the Multivariate El Niño Index (MEI). Red numbers represent positive and blue numbers negative correlations. * means statistical significant at 5% level and ** at 1% level.

Although there is a clear differentiation between continental and coastal climatic patterns, no statistically significant correlations are observed when correlating wet season (May-Oct) SAI and dry season (Nov-Apr) MEI. Wetter conditions (positive correlations) are found in mainland Mexico, while below normal precipitation (negative correlations) is evident within the Baja Californian peninsula, during El Niño phase [Fig. 7.39 e)].

The climatic pattern of almost nationally widespread positive correlations when correlating dry season (Nov-Apr) SAI and wet season (May-Oct) MEI [Fig. 7.39 f)] is quite similar to the former relating dry season (Nov-Apr) SAI and annual MEI [Fig. 7.39 c)]. Nevertheless, there are a couple of regions that break this climatic picture: Los Tuxtlas and the southeast rainforest regions. The largest correlations are found in the north-western part of the country, a very well known region affected by winter rainfall patterns. It is also the first time that we have found a statistically significant result for the Yucatán peninsula. Precipitation above normal is dominant across most of Mexico for the dry rainfall season when El Niño phase is present during the wet season (May-Oct).

A clear national pattern of positive correlations is found when dry season (Nov-Apr) SAI and dry season (Nov-Apr) MEI are correlated [Fig. 7.39 g)]. In fact, the greatest correlation (+0.43) is found at the northern Baja Californian peninsula and close to this result is the correlation for the Mexican Monsoon Region (+0.38), both correlations are statistically significant at the 1% level. A strong phase of El Niño phenomenon must reinforce the atmospheric conditions that make the winter precipitation an important part of the annual precipitation totals (see section 2.2.1). It is during this season that we see the regional precipitation fully responding to the dry season (Nov-Apr) ENSO modulation across the Yucatan peninsula. It is possible that the nearly chaotic hurricane-associated rainfall can strongly affect the precipitation patterns during the other seasons (annual and wet seasons), implying that this region is unlikely to be climatically coherent with its neighbouring regions. The Neovolcanic Belt and the Mexican central Highlands regions are clearly modulated by ENSO during the dry season (Nov-Apr). High altitude

stations and polar fronts during winter, can possibly explained the significant correlations in these areas (Metcalfe et al., 2000).

Two different geographical patterns are observed when the temperature extreme and MEI indices are correlated. A latitudinal climatic transition is observed for the annual and wet season (May-Oct) SAIs (Standardised Anomaly Indices). Wetter conditions are found for the northern part of Mexico, with below normal precipitation evident for the southern part of the country. A nationally widespread pattern of wetter conditions dominates the Dry Season (Nov-Apr) SAIs combinations. Both geographical climatic pictures are observed regardless of the season of the MEIs.

Extreme Weather Indices.

Precipitation.

In this section extreme precipitation indices will be correlated (linearly) with the seasonal versions (annual, May-Oct and Nov-Apr) of MEI. The indices with the greatest number of statistically significant results will be analysed. A comparison among the maximum and minimum temperatures related indices is then made, and finally among all the responses of the indices to the seasonal MEIs.

When the significance of the correlations with the annual MEI is considered, the extreme precipitation indices to be analysed are: CDD, CWD, R99P, RX1day, and PRCPTOT (see definitions in section 3.3.3). These give the clearest results when we correlate extreme precipitation indices and the annual MEI.

The climatic pattern for the CDD index [Fig. 7.40 a)] shows the most statistically significant results, geographically concentrated in central and northern Mexico, especially within the region of influence of the North American Monsoon (NAM, see table 4.1) or Mexican Monsoon. The prevalent negative correlations lead to wetter conditions during El Niño phase, mostly north of the Tropic of Cancer. A mixed climatic picture is observed for the CWD index [Fig. 7.40 b)]. A decrease in the number of

Consecutive Wet Days is found along the North Pacific Coast within the NAMR. Meanwhile, the largest positive correlation (statistically significant at the 1% level) is observed at the Presa Rodríguez station (Tijuana) that means wetter conditions under El Niño-like years. A longitudinal climatic pattern is seen for the R99P index [Fig. 7.40 c)]. Negative correlations are dominant along the Atlantic coast, while positive correlations are observed at the northern Pacific coast at Tijuana. Therefore, more days exceeding the 99^{th} percentile are observed in the north of the Baja California peninsula, and drier conditions for those stations along the Gulf of Mexico. Just like in the results of R99P, a coastal pattern can be observed for the RX1day index [Fig. 7.40 d)]. Although only three statistically significant results are found, a latitudinal climatic transition can be observed for RX1day. The 1-day maximum precipitation (in mm) decrease in Los Tuxtlas Region, and increase for Presa Rodríguez station in Tijuana. Correlations which are statistically significant at the 1% level show a strong response to El Niño. No clear climatic pattern is observed for the PRCPTOT index [Fig. 7.40 e)]. The only statistically significant correlation (at the 1% level) is found at the Presa Rodríguez station, i.e., annual total rainfall increases at Tijuana during El Niño-like years.

Consistently wetter conditions are observed for the northern part of the Baja California peninsula. Drier conditions are more variable (geographically speaking), ranging from the North American Monsoon to the Los Tuxtlas region. But, roughly we can conclude that when we correlate extreme rainfall indices with the annual version of MEI, wetter conditions are dominant north of the Tropic of Cancer and drier conditions prevail in southern Mexico. There is also a longitudinal transition: southern (positive) correlations are related to the Atlantic Ocean (Gulf of Mexico), while the negative (northern) correlations are linked to the Pacific Ocean: three out of the four statistically significant correlations are located at stations along the Pacific Ocean.

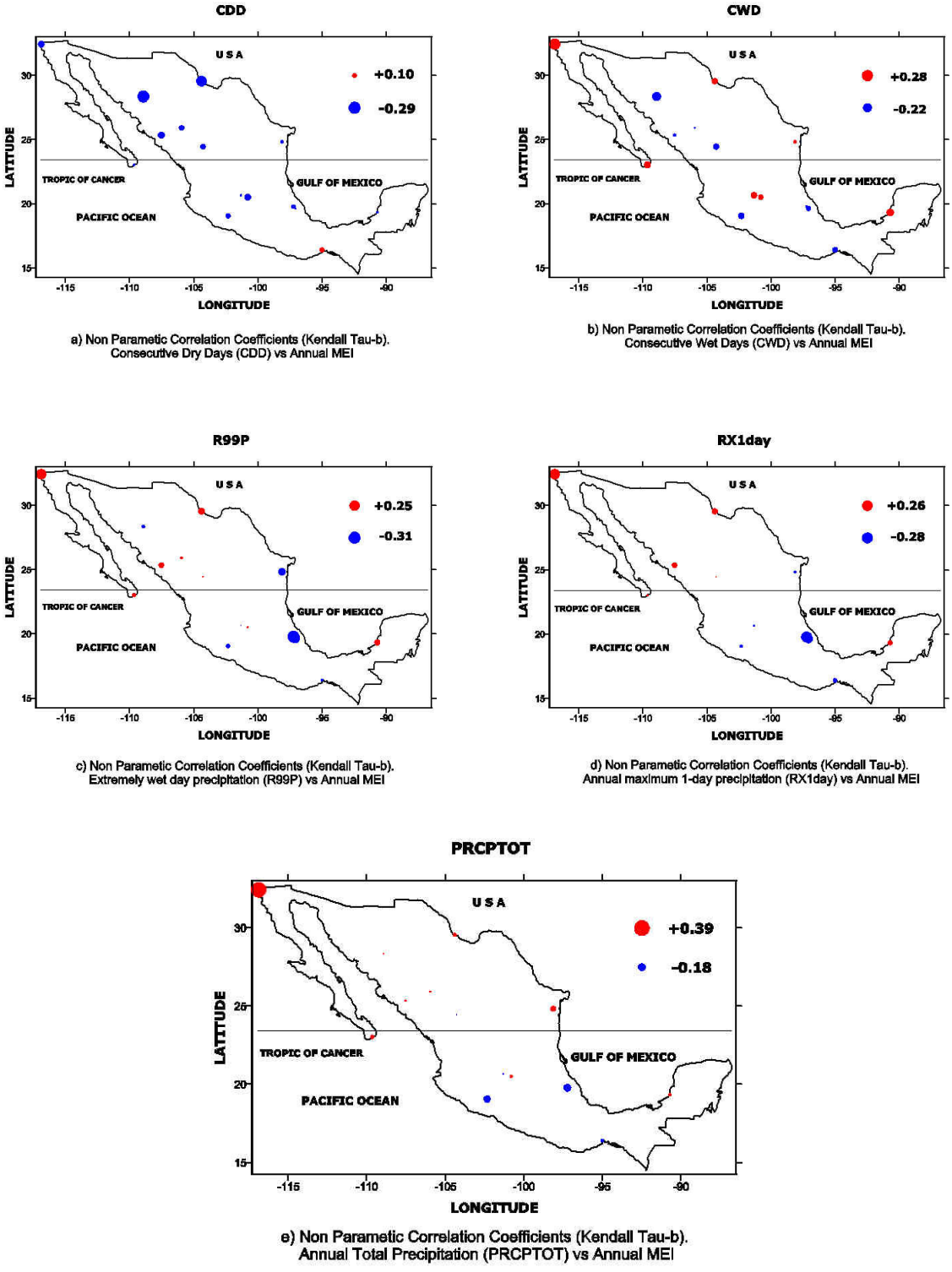

Fig. 7.40. Linear correlations (Kendall tau-b) between the Extreme Precipitation Indices and the Annual Multivariate ENSO Index (MEI). Circles in red are representing a positive and in blue negative correlations.

The application of linear correlations (Kendall's tau-b) between precipitation extreme indices and the May-Oct (wet season) version of MEI is analysed here. Because of their clear results, the indices to be considered are: CDD, CWD, R99P, RX1day and PRCPTOT. These are precisely the same indices analysed with the annual MEI, so a direct comparison is possible with those results.

The extreme indices involving consecutive conditions of dryness (CDD) or wetness (CWD) are analysed first. A national climatic pattern of negative correlations can be seen for CDD [Fig. 7.41 a)], but statistically significant results are concentrated from central to northern Mexico within the western half of the country. Therefore, wetter conditions are dominant for these stations during El Niño phase. A mixed picture of positive and negative correlations is observed across the country for the Consecutive Wet Days (CWD) index [Fig. 7.41 b)]. For those stations with statistically significant results, drier conditions (fewer consecutive wet days) are observed in mainland Mexico, while more Consecutive Wet Days are seen during El Niño-like conditions for Presa Rodríguez in Tijuana. A longitudinal climatic response is observed for the R99P index [Fig. 7.41 c)]. More days of extreme rainfall exceeding the 90^{th} percentile are observed at Presa Rodríguez, and the opposite (less days surpassing that limit) are seen along the Gulf of Mexico coast during El Niño conditions. With the exception of San Fernando in the north-eastern part of Mexico, similar geographic patterns to that of the R99P are found for the RX1day index [Fig. 7.41 d)]. During El Niño phase, the max 1-day precipitation increases at the Presa Rodríguez station in the northern part of the Baja California peninsula, while this index decreases in the Los Tuxtlas region, where the correlation is statistically significant at the 1% level. The annual total precipitation (PRCPTOT) index does not show a clear spatial distribution across Mexico [Fig. 7.41 e)]. The only statistically significant correlation is observed at the Presa Rodríguez station in Tijuana. Wetter conditions are then dominant for this part of northern Baja California during El Niño-like conditions. The only station that shows statistically significant results (wetter conditions) for PRCPTOT is Presa Rodríguez in the northern part of the Baja California

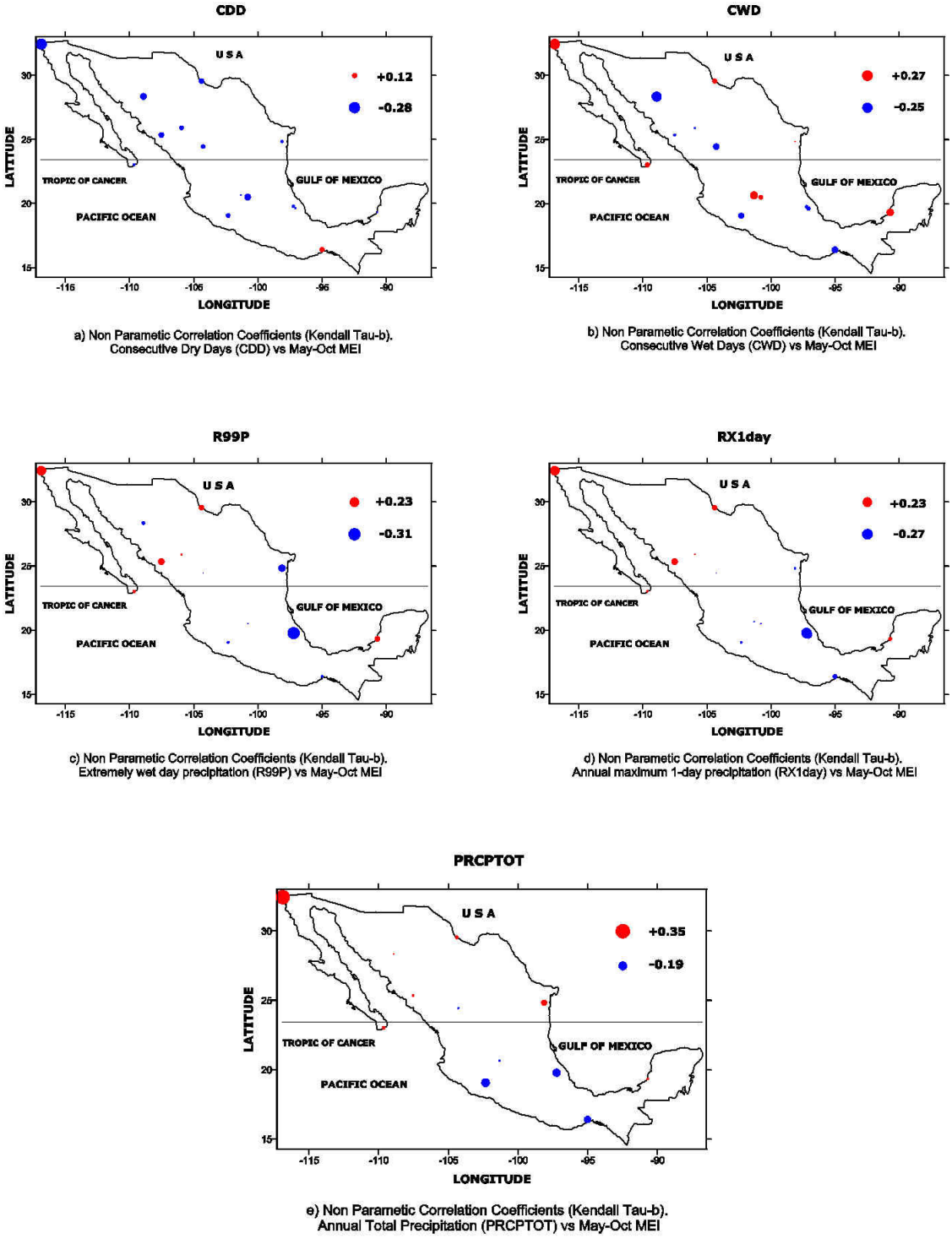

Fig. 7.41. Linear correlations (Kendall tau-b) between the Extreme Precipitation Indices and the wet season (May-Oct) Multivariate ENSO Index (MEI). Circles in red are representing a positive and in blue negative correlations.

peninsula, supporting the conclusions so far observed across this chapter that, this region is strongly affected by El Niño-like conditions.

Wetter conditions are mainly observed in the northern part of the Baja Californian peninsula, and below normal precipitation is found in mainland (the continent) Mexico. It is important to point out here that these results are consistent with the former correlations using annual MEI.

The final analysis for extreme rainfall indices is to correlate linearly these parameters with the Nov-Apr version of the Multivariate Index (MEI). As mentioned in section 3.2.1, November to April is the dry period for most of the country, so we expect different spatial patterns to those resulting from annual and wet season. Having the most significant results, the extreme indices to be analysed in this section are CDD, CWD, RX1day and PRCPTOT.

The spatial distribution of the negative correlations for the CDD index shows predominance in the western half of central and northern (continental) Mexico [Fig. 7.42 a)]. Fewer consecutive dry days are expected during El Niño conditions for these stations; especially those within the influence of the North American Monsoon System. Less clear is the climatic pattern for the Consecutive Wet Days (CWD) [Fig. 7.42 b)]. Although most of the correlations are positive across the country, the only statistically significant result is found at the southern tip of the Baja Californian peninsula, where more consecutive wet days are to be expected during El Niño-like years. One statistically significant correlation is observed for the RX1day index [Fig. 7.42 c)], but this time it is located in the northern part of the Baja California peninsula. The annual maximum 1-day precipitation increases under El Niño conditions. The annual total precipitation (PRCPTOT) tends to be above normal during El Niño for the central and northern regions of Mexico [Fig. 7.42 d)]. The largest correlations are positive and are observed at Celaya (central) and Tijuana (northern) stations, both results are statistically significant at the 1% level.

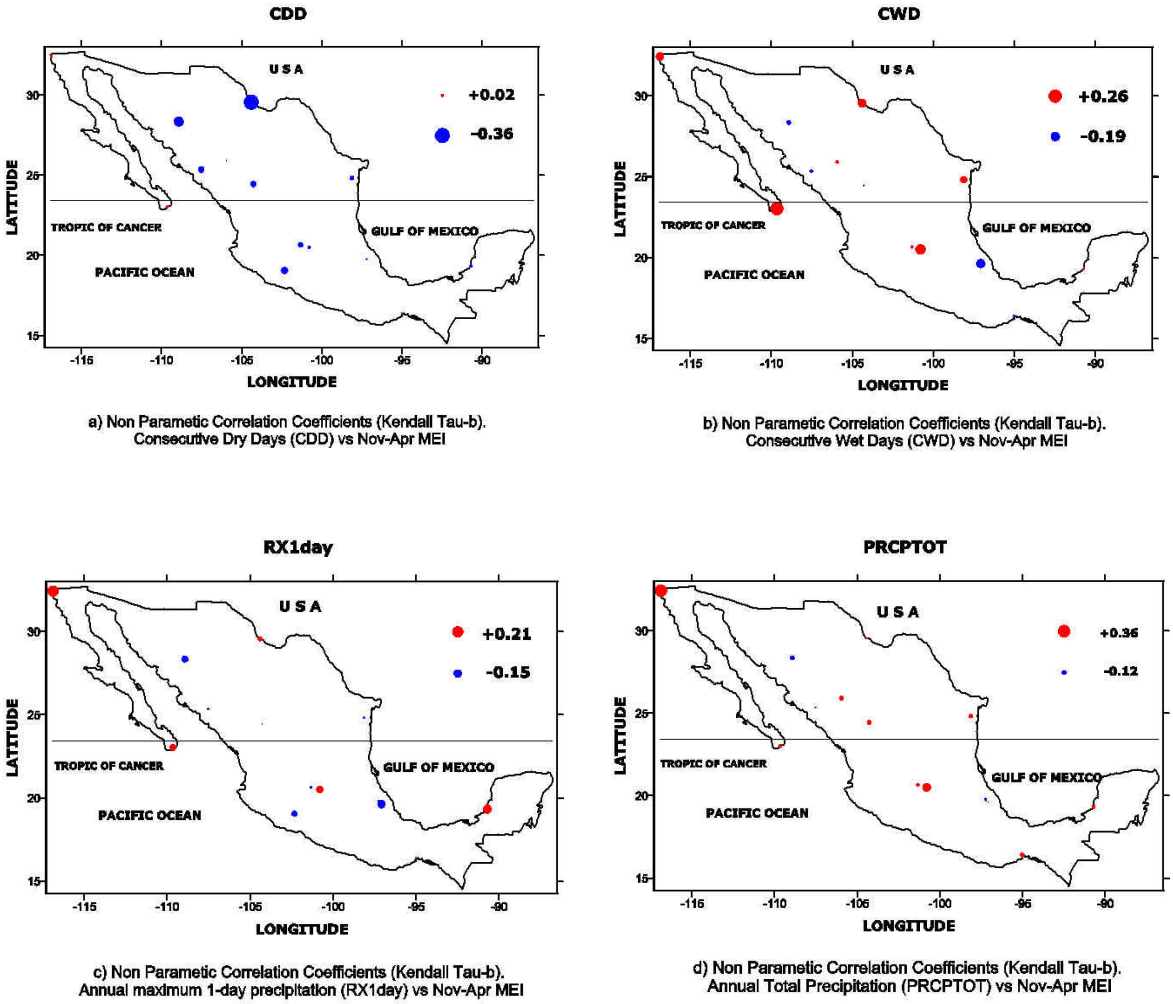

Fig. 7.42. Linear correlations (Kendall tau-b) between the Extreme Precipitation Indices and the dry season (Nov-Apr) Multivariate ENSO Index (MEI). Circles in red are representing a positive and in blue negative correlations.

Extreme precipitation above the normal is expected especially in central and northern Mexico under El-Niño like conditions. This climatic picture is consistently observed across all the rainfall extreme indices when they are correlated with the annual version of MEI. These results support the very well known winter rainfall patterns that are a substantial fraction of the annual total precipitation in those regions of the country.

Temperature.

The last analysis of linear correlation of this chapter combines temperature extreme indices and the seasonal versions (annual, wet and dry) of MEI. As mentioned for the SOI and Niño 3.4 indices, the results from this section can be compared at different temporal and spatial scales with the regional precipitation averages and extreme rainfall indices. The (linear) correlation between the temperature extreme indices and the annual Multivariate Index is the first part of this section. Because of their clearest results the indices to be analysed are TN10P, TN90P, TNn, TNx, TR20, TX10P, TXx and DTR.

A national climatic pattern of negative correlations can be seen for the TN10P index [Fig. 7.43 a)]. Fewer days are occurring in which TN<10^{th} percentile. The largest negative correlations –statistically significant at the 1% level- are geographically concentrated within the Baja California peninsula. Warmer conditions are then expected in Central and the northern Baja California during El Niño phase. A similar spatial distribution (when compared with TN10P) is observed for the TN90P index, but this time the climatic pattern is for positive correlations [Fig. 7.43 b)]. In the central region and north of the Tropic of Cancer in the Baja California peninsula more days when the night temperature exceeds the 90^{th} percent are expected during El Niño conditions. Warmer temperatures are also likely to occur during El Niño for the TNn index [Fig. 7.43 c)]. Although this pattern is geographically widespread across the country, most significant results are concentrated in the western half of the country. With the exception of the variable correlations in central Mexico, most of the country show positive correlations for the TNx index, especially in the western part of the country [Fig. 7.43 d)]. Warmer night temperatures are expected during El Niño phase for most of Mexico. Night temperatures also increase during El Niño similar to the results for the TR20 index [Fig. 7.43 e)]. Most significant results are seen in the north-western part of the country. A rough pattern of positive correlations in the main part of continental Mexico and negative correlations along the Baja California peninsula is observed for the TX10P index [Fig. 7.43 f)]. Most significant results are found in the peninsula of Baja California, where fewer days below the 10^{th} percentile limit are dominant during El Niño conditions. Warmer day

temperatures prevail over most of Mexico during the El Niño phase. Positive correlations are found for the TXx index across the country, but most significant results are located along the Pacific Ocean coast [Fig. 7.43 g)]. One interesting negative correlation in the north-eastern part of Mexico breaks this pattern. In San Fernando colder day temperatures are prevalent during El Niño-like years. A latitudinal transition is observed for the most significant results of the DTR index [Fig. 7.43 h)]. Negative correlations are seen in the central and the southern tip of the Baja California peninsula, while only one positive correlation –statistically significant at the 5% level- is observed in the southern pacific coast in Oaxaca. In general, decreasing DTRs are evident across Mexico during El Niño-like conditions.

Linear relationships between the temperature extreme indices and the annual MEI show a national pattern of increasing minimum temperatures during El Niño-like conditions. This is especially clear north of the Tropic of Cancer. Warming conditions (for the stations close to the northern Pacific Ocean) during El Niño are also expected for the indices related to maximum temperatures. According to the results, a decrease in Daily Temperature Range index show that the greater changes are occurring in minimum temperatures.

Linear correlations of the extreme indices with the May to October (Wet Season) version of MEI will be assessed in this section. The indices with the best results (the largest numbers of significant correlations) are: TN10P, TN90P, TNn, TNx, TR20, TX10P, TX90P, TXx and DTR.

Extreme indices related to minimum temperatures (TN10P, TN90P, TNn and TNx) are the first to be analysed. Negative correlations prevail in most of the country during El Niño conditions for the TN10P index [Fig. 7.44 a)]. The clearest geographical pattern of statistically significant results is found in the Baja California peninsula, north of the Tropic of Cancer. Significant correlations are also observed in central and southern Mexico. Therefore, it can be said that the number of days when TN<10^{th} percentile decreases during El Niño phase, leading to warmer temperatures. Positive correlations are

dominant across Mexico for the TN90P index [Fig. 7.44 b)]. The spatial distribution of the most significant results is very similar to that for the TN10P index. Warmer conditions are dominant during El Niño phase across Mexico, especially within the Baja California peninsula. Positive correlations are also dominating Mexico for the TNn index [Fig. 7.44 c)]. Nevertheless, the most significant correlations are mostly found in the western part of the country from central to northern Mexico. The largest correlations are observed at Presa Rodríguez and El Palmito in the north-western part of the country, a region where winter rainfall is very important to the annual total precipitation. Warmer night temperatures are expected throughout Mexico during El Niño conditions, especially in the western half of the country. Positive correlations are also nationally widespread for the TNx index, except for Ciudad Hidalgo and Atzalán stations in central Mexico [Fig. 7.44 d)]. For the TR20 index [Fig. 7.44 e)], night temperatures increase during El Niño conditions across the country for most of Mexico, with a slight geographical preference to the western half of the country. A mixed climatic pattern is observed, although the largest (statistically significant) correlations are positive. Geographically these positive relationships are biased to the western half of the country along the Pacific Ocean coast, suggesting an important influence of the El Niño years. Warmer tropical nights (TR20) are observed during El Niño years in most of Mexico especially within the north-western part of the country, in the area of influence of the North American Monsoon System (NAMS) or Mexican Monsoon Region (RA11 in Table 4.1). Only a few statistically significant correlations are found within the mixed climatic pattern of the TX10P index [Fig. 7.44 f)]. The largest negative correlations are geographically concentrated in the Baja California peninsula, and north of the Tropic of Cancer. Warmer day temperatures are likely to be seen under El Niño conditions in the northern part of the

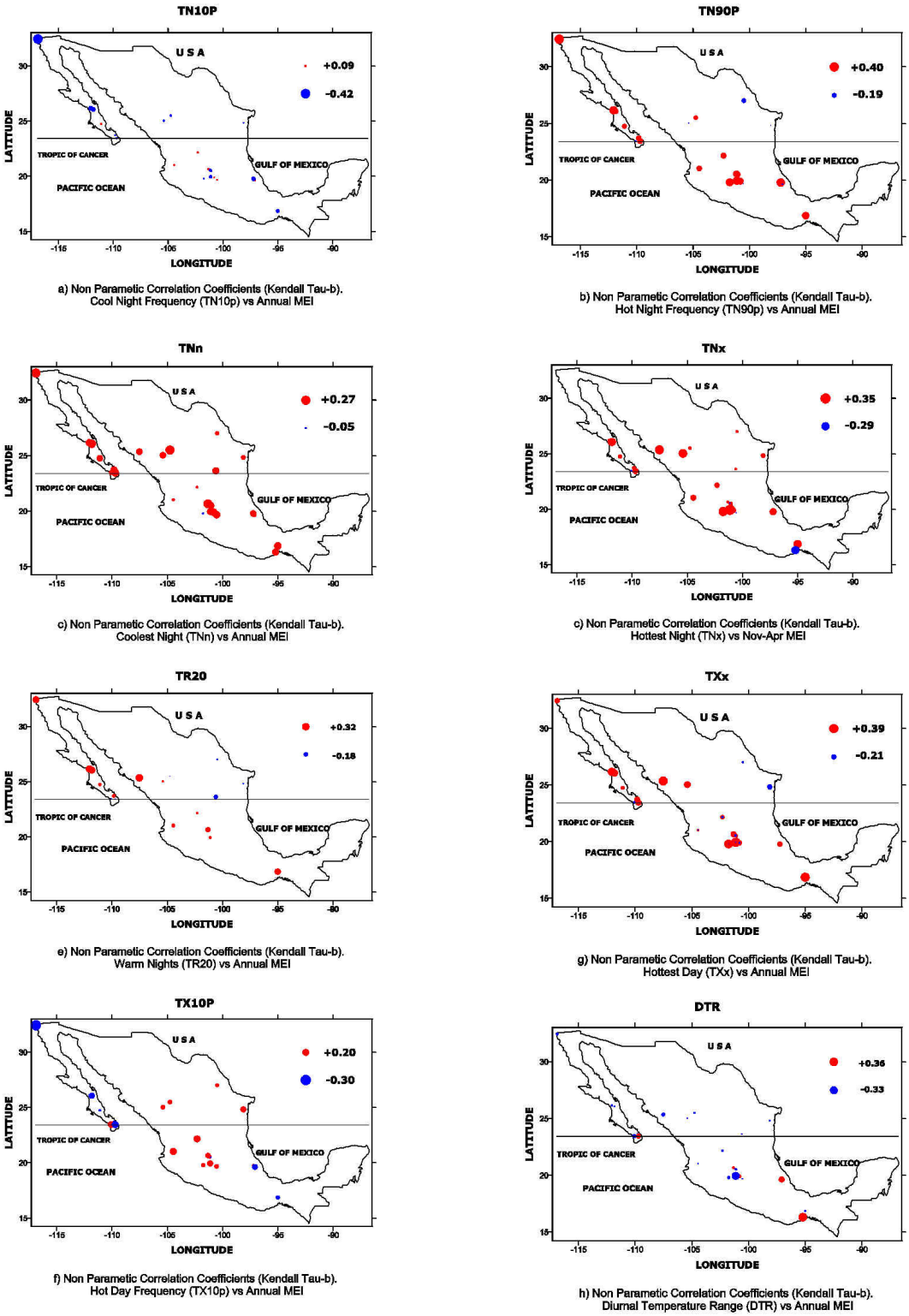

Fig. 7.43. Linear correlations (Kendall tau-b) between the Extreme Temperature Indices and the Annual Multivariate ENSO Index (Annual MEI). Circles in red are representing a positive and in blue negative correlations.

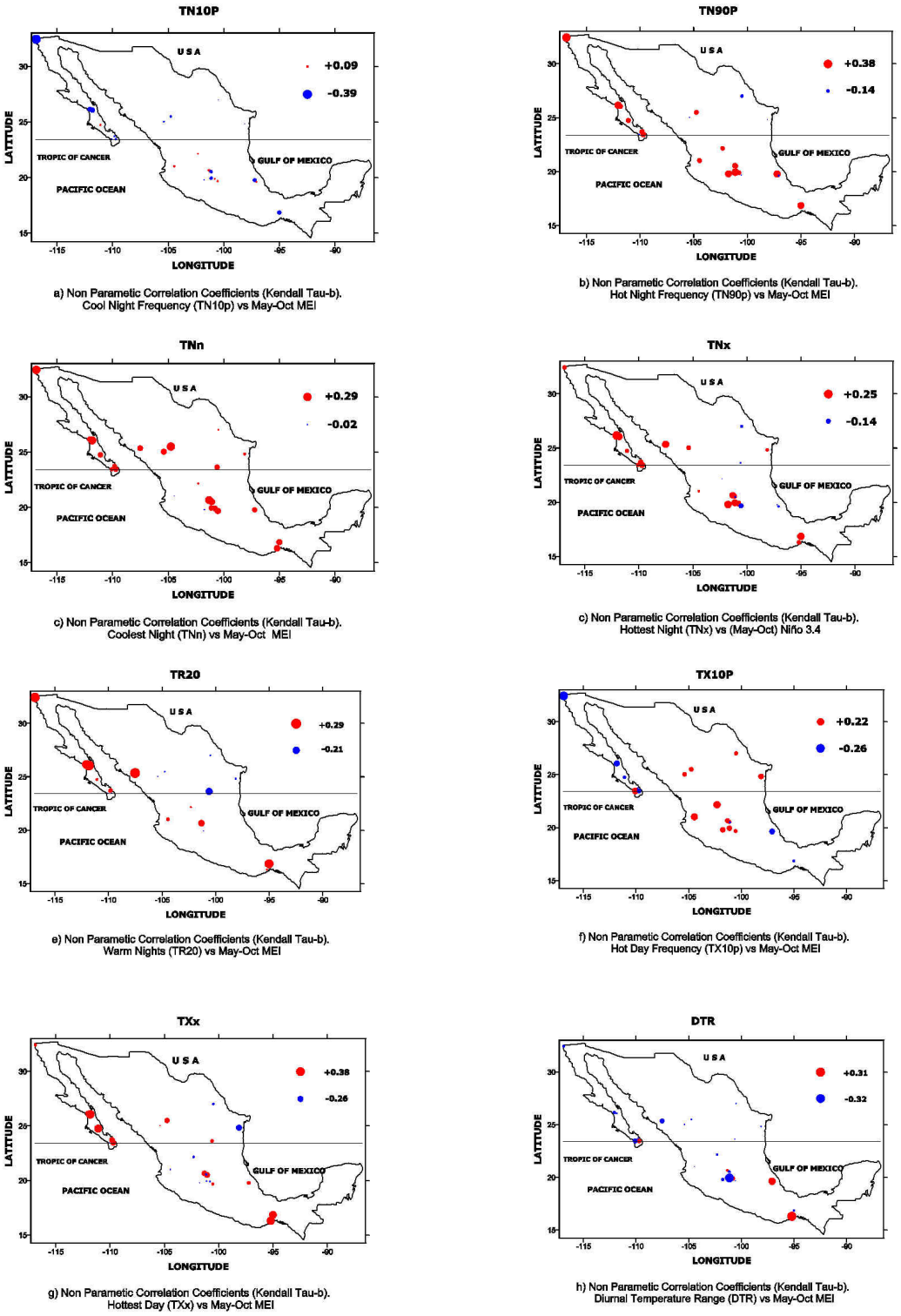

Fig. 7.44. Linear correlations (Kendall tau-b) between the Extreme Temperature Indices and the wet season (May-Oct) Multivariate ENSO Index (Annual MEI). Circles in red are representing a positive and in blue negative correlations.

Baja California peninsula and Los Tuxtlas regions. Positive correlations are almost nationally prevalent across Mexico for the TXx index [Fig. 7.44 g)]. Warmer (day) temperatures are observed almost nationally, especially along the Pacific coast. The most significant exception to this pattern is observed at the San Fernando station in north-eastern Mexico. Finally, (statistically significant) negative correlations are found in central and northern Mexico, and positive correlations in the southern part of the country for the DTR index, especially near the Tehuantepec isthmus [Fig. 7.44 h)].

In accordance with the former results when the extreme indices and the wet season (May-Oct) MEI are linearly correlated, increasing temperatures are observed across Mexico. The most significant changes are mainly found in the minimum temperatures, therefore, directly affecting the Daily Temperature Range values. Geographically, climatic responses of maximum and minimum temperatures are concentrated in the northern part of the country.

The last set of indices to be analysed are those resulting from the correlation of the temperature extremes and the dry season (Nov-Apr) MEI. For their clarity in the results the group of extreme temperature indices to be evaluated are TN90P, TNn, TNx, TR20, TX10P, TX90P and DTR. Minimum temperature indices are assessed first, and then maximum temperature parameters finishing with the DTR index.

The Hot Night Frequency (TN90P) index is evaluated first. An almost national pattern of positive correlations can be observed in [Fig. 7.45 a)]. Statistically significant results are geographically concentrated in Central Mexico for TNn. This is particularly true for the largest correlations that are located within the area of the so called Neovolcanic axis, all these stations (Atzalán, Zacapú and Huingo, see table 3.2) are above the 1500 m.a.s.l [Fig. 7.45 b)]. Indeed, an almost national pattern of positive correlations can be easily seen. Nevertheless, the most significant results are geographically concentrated in Central and Northern Mexico. The largest correlation values (mainly positive) are spatially concentrated in continental Mexico, and especially biased to the western half of the

country, for the TNx index [Fig. 7.45 c)]. During the peak of El Niño conditions there is a net increase in the night maximum temperatures, in northern Mexico. Positive correlations dominate central and northern Mexico when the TR20 index is evaluated [Fig. 7.45 d)]. There is a clear tendency for these statistically significant results to be located in the western half of the country. Warmer tropical nights (TN>20C) are observed during El Niño conditions for northern Mexico. A continental/peninsular climatic pattern is observed for the TX10P index: positive correlations are found in continental Mexico, while within the Baja California peninsula negative correlations are dominant, and these are the only statistically significant results [Fig. 7.45 e)]. Therefore, warmer day temperatures are observed in the Baja California peninsula during El Niño phase. A different kind of transition is observed for the TX90P index [Fig. 7.45 f)]. The statistically significant results are divided in a latitudinal way: positive correlations are geographically concentrated south the Tropic of Cancer, and negative correlations are located north of this limit within the Baja California peninsula. More days when the minimum temperature exceeds the 90^{th} percentile are observed in the southern part of the country during El Niño conditions, while fewer days below this percentile are found under the same climatic conditions. Negative correlations are prevailing across Mexico for the DTR index. Nevertheless, only a few of the results are statistically significant. Those are mostly concentrated in Central Mexico and on the southern tip of the Baja Californian peninsula. The only significant positive correlation is observed at Santo Domingo Tehuantepec on the southern coast of the Pacific Ocean. The DTR climatic pattern is reflecting that most significant changes are occurring in minimum temperatures, especially from central to northern Mexico [Fig. 7.45 g)].

Linear correlations between the temperature extreme indices and the Nov-Apr (dry season) MEI show an almost national climatic pattern of increase in temperatures for El Niño years. However, the most significant results are observed in minimum temperatures indices like TN90P, TNn, TNx, and TR20. Geographically these important changes in night temperatures are mostly concentrated north of the Tropic of Cancer. A net decrease in the DTR index from central to northern Mexico is a direct consequence of these warmer minimum temperatures.

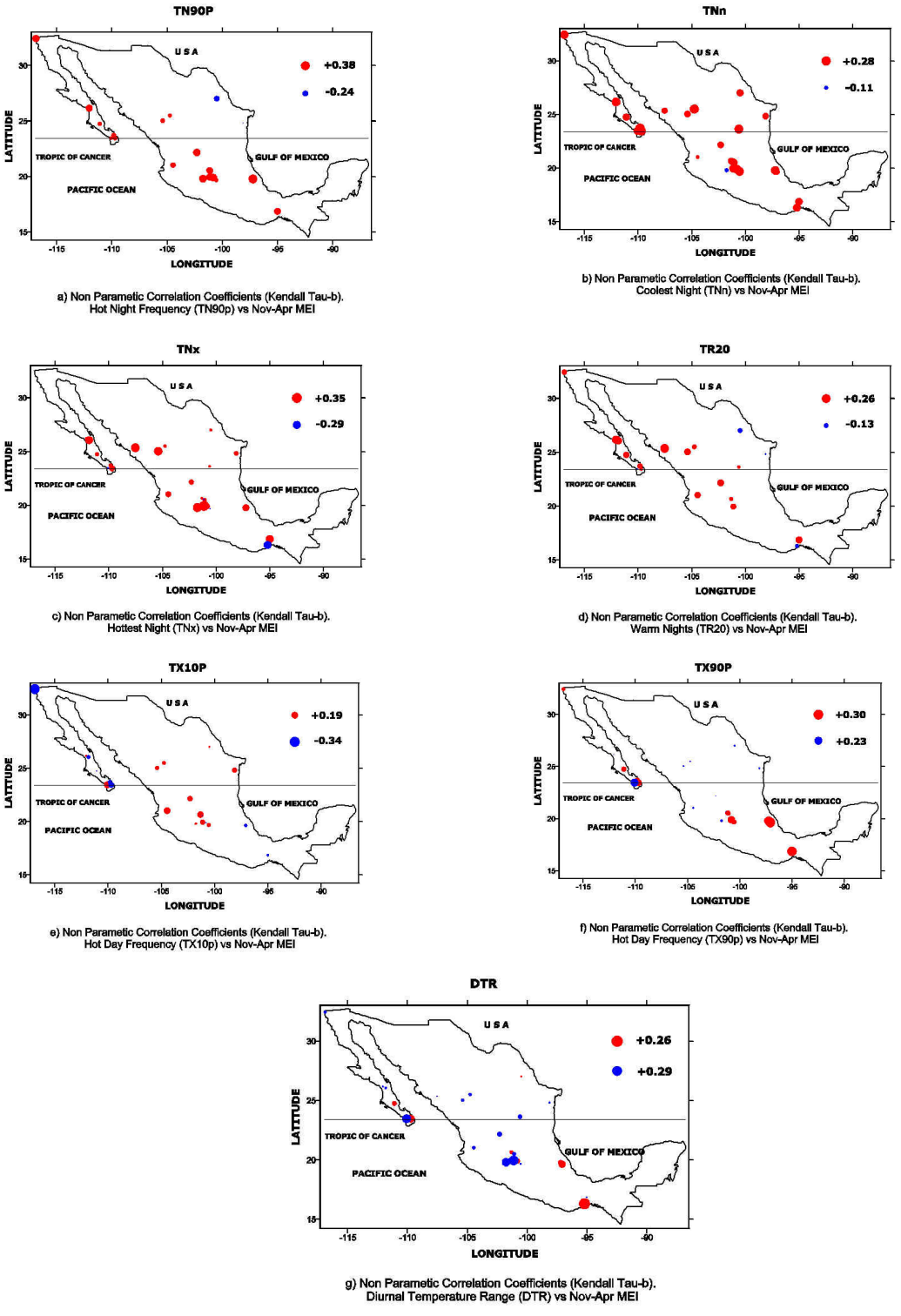

Fig. 7.45. Linear correlations (Kendall tau-b) between the Extreme Temperature Indices and the dry season (Nov-Apr) Multivariate ENSO Index (Annual MEI). Circles in red are representing a positive and in blue negative correlations.

7.4.2. LAG CORRELATION.

Precipitation Regional Averages (MEI).

Consistency is seen among the resultant climatic patterns when the three different ENSO indices (including MEI) and the Regional Precipitation Averages are correlated. Positive correlations are observed in the following regions (definitions and climatic characteristics in Table 4.1): RA4, RA7, RA6 and RA3 (Fig. 7.46). Three of them are geographically located north of the Tropic of Cancer; only La Huasteca at the fringes of this limit does not strictly comply with this condition. Timings are similar and close to the strongest El Niño conditions. According to these results with MEI (and the other ENSO indices used in this chapter) it is evident that during El Niño (close to the peak of its phase) wetter conditions are prevalent in the northern part of Mexico, particularly when we consider the Tropic of Cancer as a geographical limit.

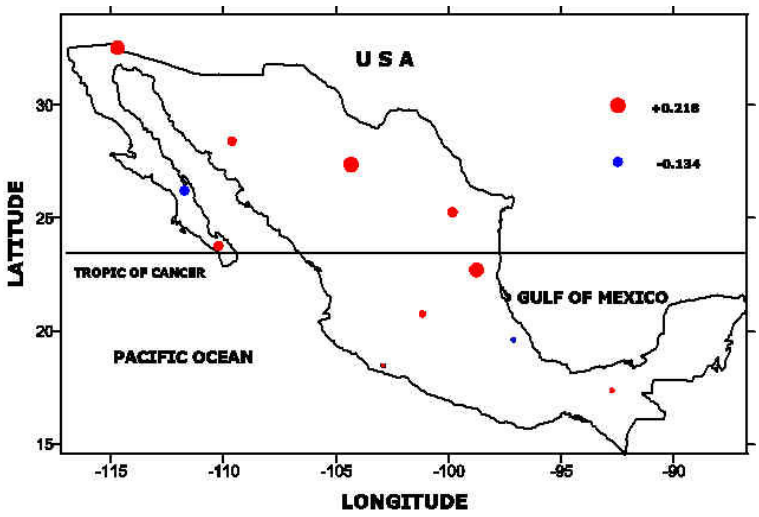

Fig. 7.46. Lag cross-correlations between the standardised versions of Precipitation Regional Averages and the Multivariate El Niño Index (MEI). Red circles represent positive and blue circles negative correlations.

Extreme Weather Indices.

Extreme Precipitation Indices

Consistency is the main characteristic of the extreme rainfall indices when they are correlated with the different El Niño indices, and MEI is not an exception. For the RX1day index (Fig. 7.47), the largest positive correlation (+0.174) is found at La Presa Rodríguez (northern part of the Baja California Peninsula), meaning wetter conditions right at the peak of El Niño phase. A positive correlation (+0.101) is also seen in the Guanaceví station within the Desertic north of Mexico, and a similar time-shift (-3). Therefore, a (small) net increase is seen in the amount of maximum 1-day precipitation associated to El Niño-like years. A delayed (+14 months lag) ENSO-impact is observed at the core of the Mexican Monsoon region. Maximum 1-day rainfall amounts at the Yecora station show a small net decrease (-0.145 correlation) during El Niño conditions, contrasting with its neighbouring stations.

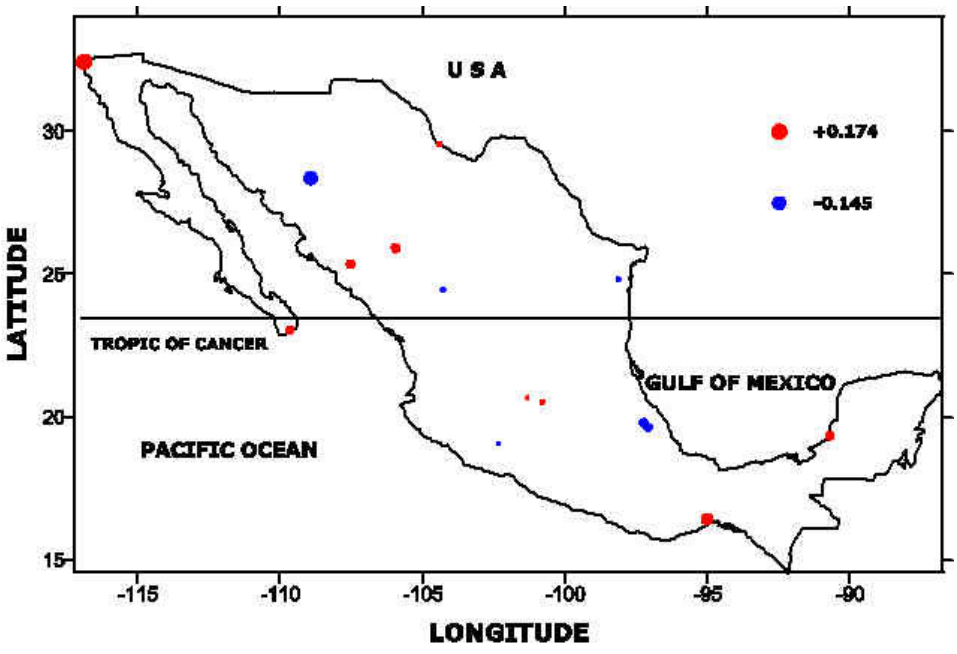

Fig.7.47. Lag cross-correlations between the Maximum 1-day precipitation (RX1day) Index and the Multivariate El Niño Index (MEI). Red circles represent positive and blue circles negative correlations.

Wetter conditions for the Northern part of the Baja Californian Peninsula are the constant feature among the different ENSO indices for the rainfall extreme indices. This climatic feature is also observed when the RX5day is lag-correlated with MEI (Fig. 7.48), although with different responses and timings as the largest correlations are in the north-western part of Mexico, at La Presa Rodriguez within the Baja California peninsula (correlation +0.163 and lag = 0) and within the Mexican Monsoon Region for the Yecora station in Sonora (correlation -0.145, lag=+14). Although with different time-shifts, it is evident that the Pacific Ocean exerts a greater influence (Mechoso et al., 2004) than the Atlantic one, especially at those stations along the northern Pacific coast. Finally, RX5day results are close to those correlations already observed applying the MEI to the RX1day index.

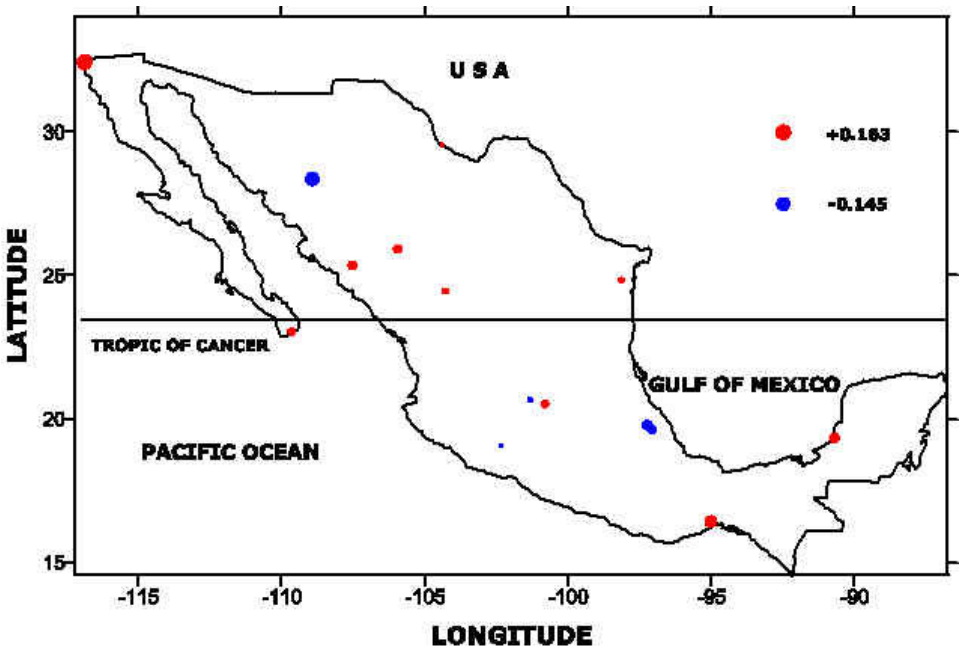

Fig. 7.48. Lag cross-correlations between the Maximum 5-day precipitation (RX5day) Index and the Multivariate El Niño Index (MEI). Red circles represent positive and blue circles negative correlations.

Prevalent wetter conditions are observed in north-western Mexico and the Baja Californian peninsula. These climatic responses are seen close to the peak of El Niño phase for the rainfall extreme indices.

Extreme Temperature Indices

The resulting (lag) correlations between DTR and MEI show a variable response across Mexico (Fig. 7.49). No spatial homogeneity is found among the positive or negative correlations. In fact, the greatest correlations (Santo Domingo Tehuantepec and Matías Romero) are both located within the Tehuantepec Isthmus region (Southern Pacific coast), but their time-shifts (see table 7.4) are quite different (-5 and -24 months respectively). Despite, its variable time lag responses, the most significant below normal precipitation (greatest negative correlations) seems to have a geographic component along the Pacific Ocean coast.

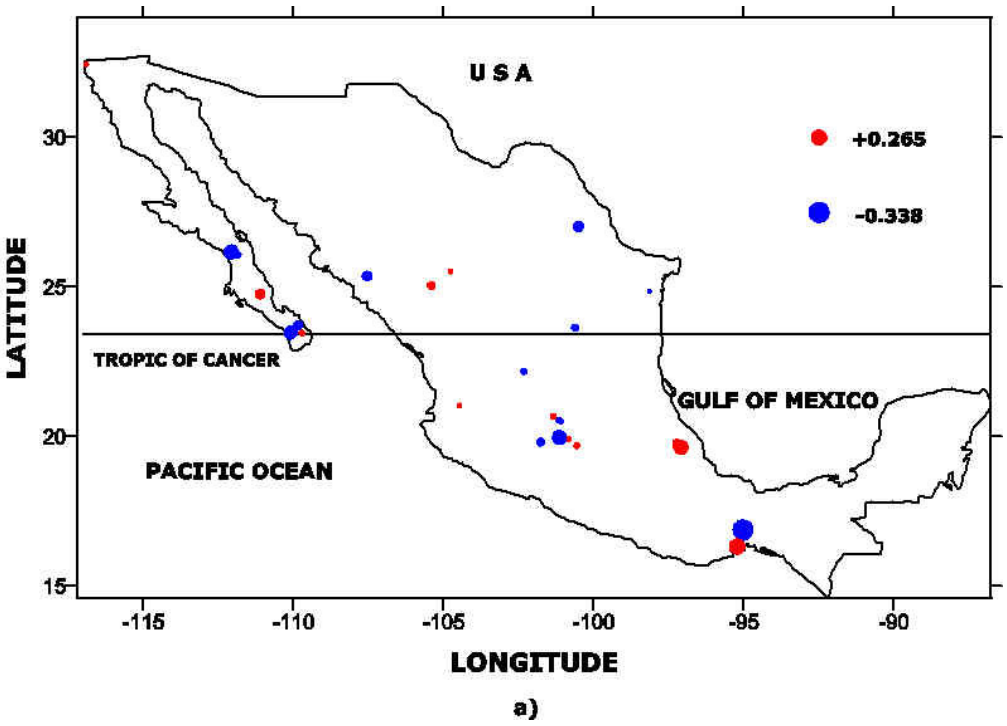

Fig. 7.49 Lag cross-correlations between the DTR (Daily Temperature Range) and the Multivariate El Niño Index (MEI). Red circles express positive correlations, and blue circles show negative correlations.

A mixed spatial distribution of positive and negative correlations is seen across Mexico for the TN10P index (Fig. 7.50). In central Mexico high altitude stations seem to be linked to these positive correlations, only the station at Ahuacatlán (900 m) is below the level of 1500 m.a.s.l. Negative correlations are widespread nationally but with no real clear climatic pattern. Optimal time-shift responses to the modulation of El Niño are similar among the positive correlations, as they are close to the peak of this phenomenon. Therefore, with the exception of a set of high-altitude stations in Central Mexico, a pattern of warmer conditions is observed across Mexico.

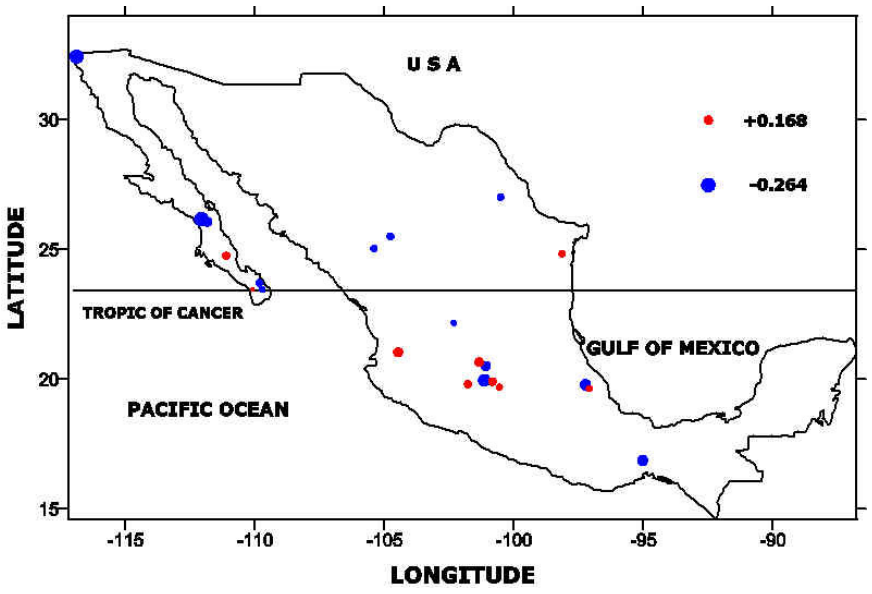

Fig. 7.50. Lag cross-correlations between the TN10P (Cool Night Frequency) and the Multivariate El Niño Index (MEI). Red circles express positive correlations, and blue circles show negative correlations.

A combination of positive and negative correlations -similar to the pattern observed for TN10P- without a clear climatic picture is seen when we evaluate the TN90P Index (Fig. 7.51). In the main continental Mexico, central and southern regions in Mexico are dominated by positive correlations with similar relationships also seen in the peninsula of Baja California. Time lags for the best climatic responses are associated with these correlations close to the peak of El Niño (see table 7.6). In general, more frequent cool nights exceeding the 90th percentile (warmer conditions) are observed close to the strongest El Niño conditions.

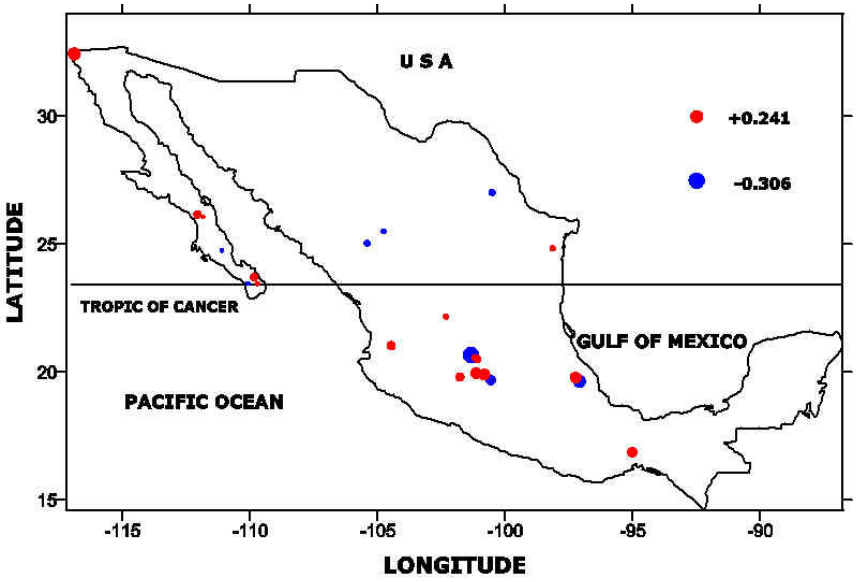

Fig. 7.51. Lag cross-correlations between the TN90P (Hot Night Frequency) and the Multivariate El Niño Index (MEI). Red circles express positive correlations, and blue circles show negative correlations.

Mostly positive correlations are seen across Mexico for the Coolest Night (TNn) Index. Lower negative correlations are spatially dispersed from Central to Northern Mexico (Fig. 7.52). Nevertheless when we compare the different time-shifts of response to the MEI index, for the positive correlations we find variable time responses (ranging from -19 to +10 months of lag to get the best climatic correlation) and more homogeneous time-shifts for the negative correlations (+16 to +18 months of lag). Although with different time-lags of climatic responses, warmer night temperatures are dominant across Mexico during El Niño phase.

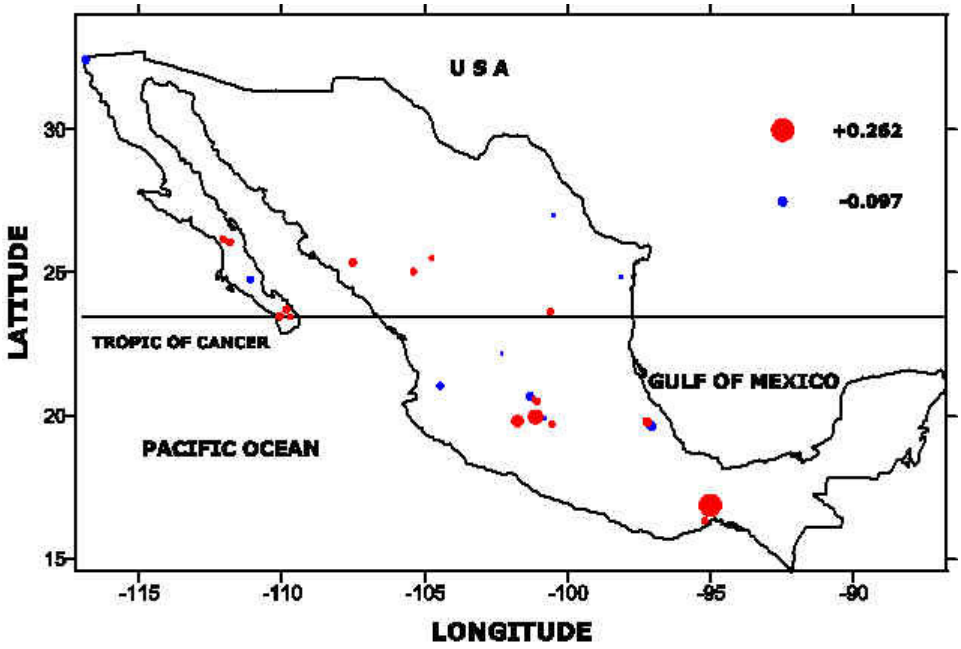

Fig. 7.52. Lag cross-correlations between the TNn Index (Coolest Night) and the Multivariate El Niño Index (MEI). The linear correlation is calculated using the Pearson function. Red circles express positive correlations, and blue circles show negative correlations.

A mixed combination of positive and negative correlations is found for the TNx Index. Positive correlations prevail mostly in the Baja California peninsula, while negative correlations are spatially distributed across continental Mexico (Fig. 7.53). The time response of this index to El Niño modulation is very variable lags found for the negative correlations (-17 to +16 months), while more consistency is observed for the positive correlations (between +2 to +4 months of lag). Warmer conditions (at night time) dominate in Central and South Mexico near to the peak (average of 2 months response) of El Niño phase.

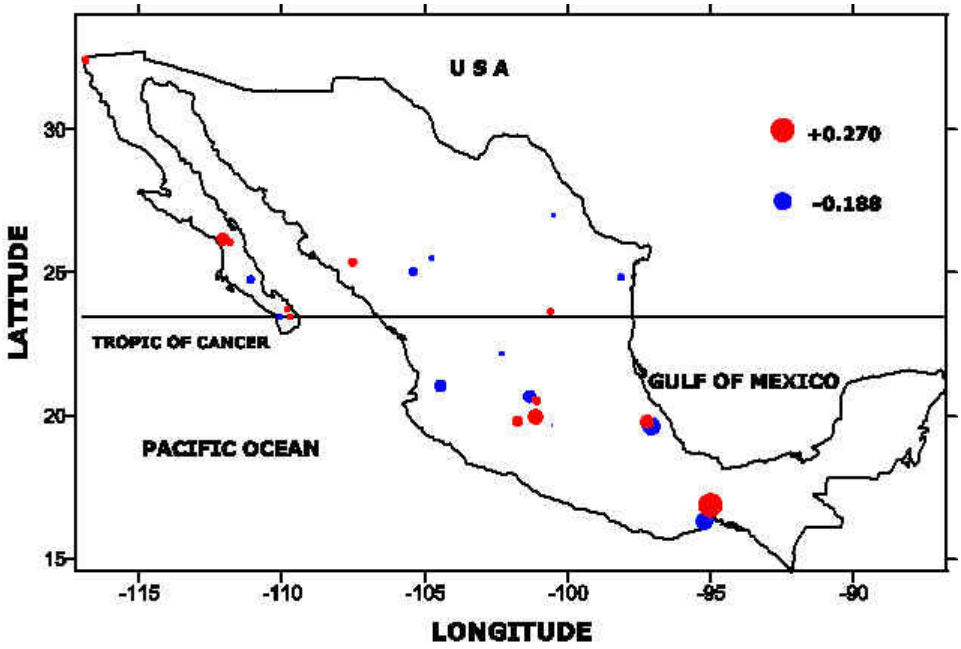

Fig. 7.53. Lag cross-correlations between the TNx Index (Hottest Night) and the Multivariate El Niño Index (MEI). The linear correlation is calculated using the Pearson function. Red circles express positive correlations, and blue circles show negative correlations.

Positive correlations prevail in central and northern Mexico, with variable time-lags (ranging from -22 to 0 months) among the largest positive correlations for the TX10P (see Fig. 7.54 and Table 7.9) index. Negative correlations are found in central and southern Mexico and the northern part of the Baja Californian peninsula, with also a great variability in the lag of response to ENSO modulation. Positive correlations are slightly greater than negative and also in spatial extent. In accordance with these results an increasing frequency of cool days in central and northern Mexico with variable time lags are to be expected during El Niño conditions.

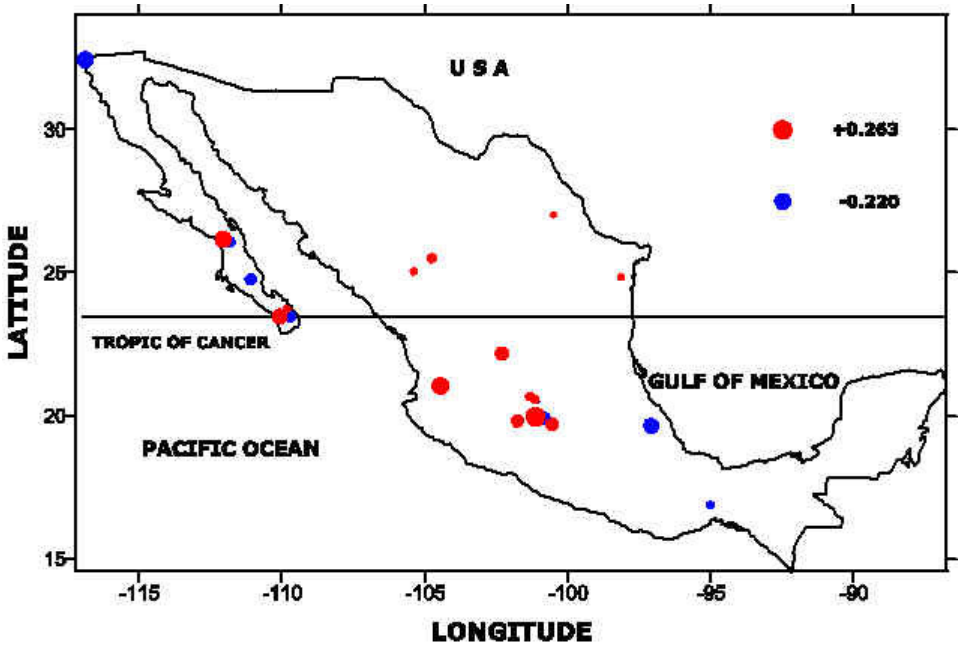

Fig. 7.54. Lag cross-correlations between the TX10P Index (Cool Day Frequency) and the Multivariate El Niño Index (MEI). The linear correlation is calculated using the Pearson function. Red circles express positive correlations, and blue circles show negative correlations.

A latitudinal transition in mainland Mexico is observed for TX90P. Positive correlations prevail in central and southern Mexico, while the negative correlations are dominant from Central to northern Mexico, especially in the western half of the country (Fig. 7.55). This climatic picture is not as clear within the Baja California peninsula, where mixed correlations can be observed. Similar time lags are seen for the positive correlations, that show that the strongest climatic response evident near (+3 months lag of average) the peak of El Niño. According to these results, hot nights are more frequent close to the strongest El Niño conditions in central and southern Mexico. Meanwhile, fewer hot nights are expected for northern Mexico, with variable timings of response.

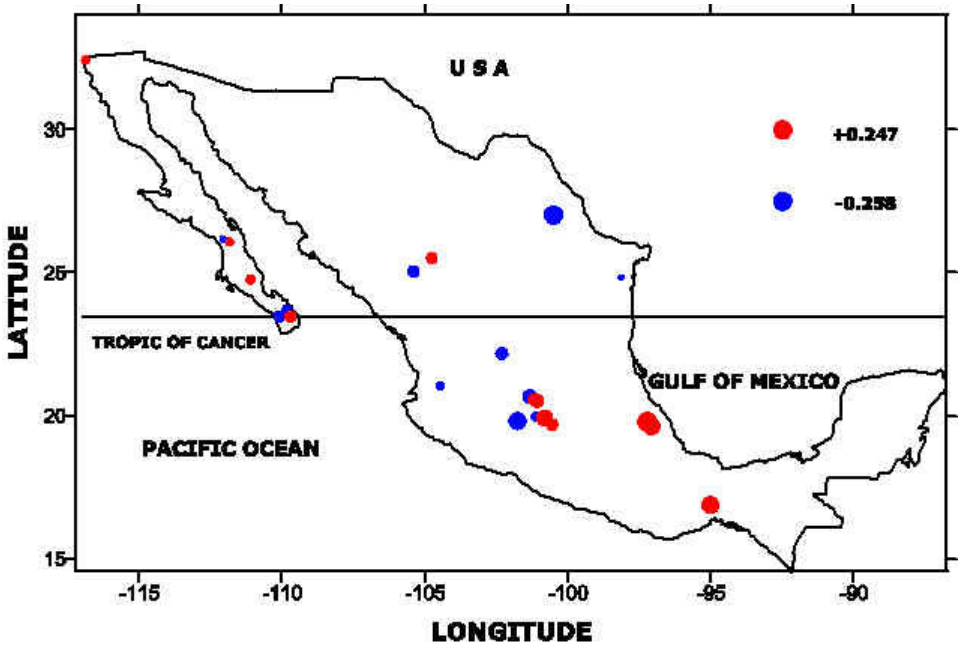

Fig. 7.55. Lag cross-correlations between the TX90P Index (Hot Day Frequency) and the Multivariate El Niño Index (MEI). Red circles express positive correlations, and blue circles show negative correlations.

A longitudinal climatic transition is observed in the results for the Coolest Day Index (TXn). Negative correlations predominate in the western part of Mexico, and the largest positive correlations prevail in southern Mexico near to the Tehuantepec Isthmus (Fig. 7.56). Time-lags are associated with negative correlations range from -5 to 0 months for the greatest correlations. Colder days are likely to be found from Central to Southern Mexico in the western half of the country close to the peak of El Niño-like conditions.

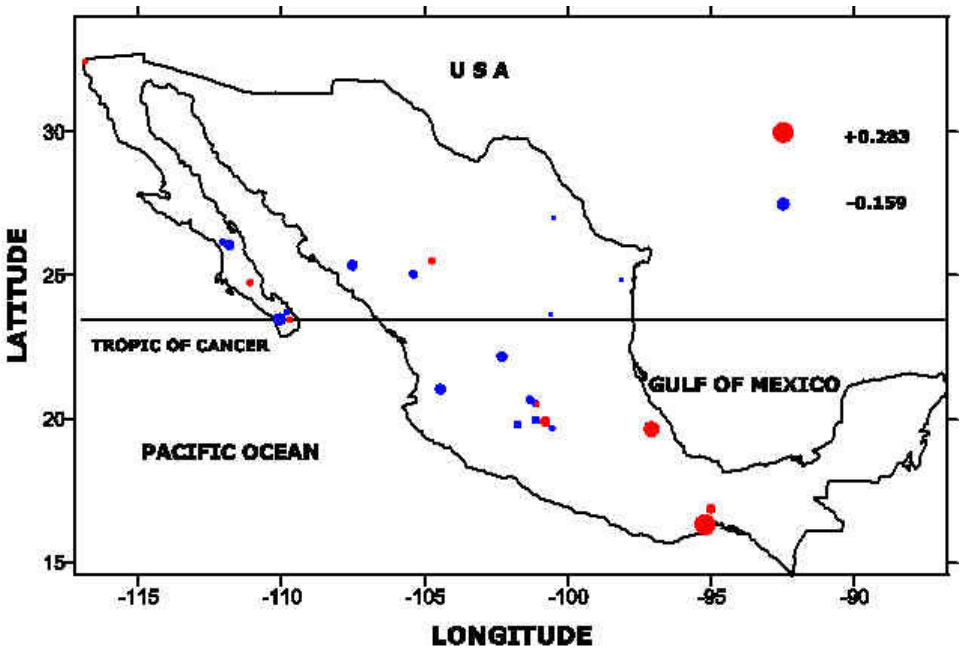

Fig. 7.56. Lag cross-correlations between the TXn Index (Coolest Day) and the Multivariate El Niño Index (MEI). Red circles express positive correlations, and blue circles show negative correlations.

A clearer meridional pattern is found for the TXx when compared with the climatic picture observed for TNx (Fig. 7.57). Positive correlations are observed along the Atlantic coast from the northeast until we reach the Tehuantepec Isthmus in southern Mexico. In contrast, negative correlations dominate the western half of Mexico, except the most north-western station in Tijuana (La Presa Rodríguez). The greatest correlation (+0.304) is found within the South Pacific coast at Santo Domingo Tehuantepec station, having a time-lag of -4 months to fully respond to the El Niño modulation. According to these results, during El Niño conditions warmer day temperatures are observed along the Gulf of Mexico close to the peak of the phenomenon, while colder temperatures are likely to be observed in the western part of the country, with variable time responses.

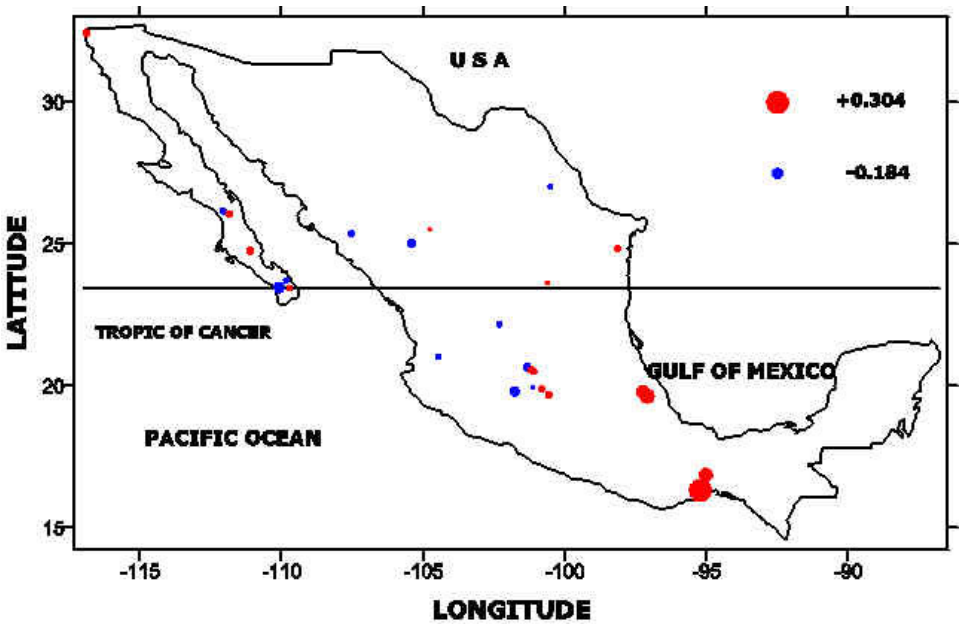

Fig. 7.57. Lag cross-correlations between the TXx Index (Hottest Day) and the Multivariate El Niño Index (MEI). Red circles express positive correlations, and blue circles show negative correlations.

Summary of the section (MEI).

Kendall tau-b (linear) and lag correlations of the precipitation and temperature time-series with the Multivariate El Niño Index (MEI) have shown consistency with the analyses of SOI and Niño 3.4 indices (see sections 7.2 and 7.3).

A clear seasonality factor is observed in the geographical patterns of precipitation that is (partially) modulated by the MEI. When the annual and wet season (May-Oct) of (Regional) Standardised Anomaly Indices (SAI) are considered, a clear latitudinal transition is seen: wetter (drier) conditions are observed North (South) of the Tropic of Cancer during El Niño (La Niña) years. Meanwhile, above (below) normal precipitations are seen nationally for the dry season (Nov-Apr) SAIs under El Niño (La Niña) years. These climatic patterns (latitudinal transition or national wet or dry conditions) are replicated for the local scale (sites) when the extreme precipitation indices are analysed. Nevertheless, the largest correlations are geographically concentrated along the western coast, suggesting an important role of the Pacific Ocean, and particularly the sea surface temperatures (SSTs) in the rainfall totals and extremes. The clearest results are seen in North-western Mexico, especially the Northern part of the peninsula of Baja California. The timing of the largest responses for precipitation are close (a few months lag) to the strongest El Niño conditions.

When correlated with MEI, extreme temperature indices have less clear results. Linear correlations (Kendall tau-b) show a national pattern of increasing minimum temperatures, especially north of the Tropic of Cancer, and the maximum temperature changes are mainly concentrated along the Pacific Ocean coast. Another aspect of the analysis of the ENSO modulation (utilising MEI) is to apply lag correlations on extreme temperature indices. Variable time lags are found with the different extreme indices but the largest correlations are observed close to the peak of El Niño (La Niña) conditions. In geographic terms, there are no clear climatic patterns for either maximum or minimum temperatures, when the lag correlation method is applied. Due to this lack of consistency

in the maximum and minimum temperature indices, no spatial homogeneity is observed for the Daily Temperature Range (DTR).

7.5. CONCLUSIONS TO THE CHAPTER.

This chapter has dealt with the final major analysis of this thesis. The aim has been to determine the characteristics of the large-scale atmospheric control (El Niño-Southern Oscillation phenomenon) of the main meteorological variables (precipitation and temperature) across Mexico. ENSO is the main modulator of the precipitation across the country (Magaña et al., 2003), and also has a great influence in the hurricane activity (Reyes and Troncoso, 1999). Using instrumental data at different temporal and spatial scales, linear (Kendall's tau-b) and lag correlations have been applied to explore the modulation of ENSO on recent climatic changes in Mexico.

Linear correlations of the seasonal SAIs (Standardised Anomaly Index) and the ENSO indices (SOI, Niño 3.4 and MEI) show consistency across the results. A clear latitudinal transition can be observed when the annual and wet season SAIs and annual and (May-Oct) ENSO indices are correlated. Wetter conditions are found north of the Tropic of Cancer, while below normal precipitation is evident in southern regions. More extended geographically are the results when the dry season (Nov-Apr) SAIs and dry season ENSO indices are combined: an almost national climatic pattern of wetter conditions prevails this time. Regardless of these seasonal variations, the regions with the most consistent results (largest correlations) are mainly found in the north-western area: the North American Monsoon (or Mexican Monsoon) region and Northern Baja California peninsula. It is important to point out that these regions are strongly affected by winter rainfall patterns contrasting with the climatic patterns of rest of the country.

Rainfall extreme indices results replicate the seasonal effect that has been already described in the case of regional precipitation. A latitudinal transition is directly

responding to sesonal ENSO modulations. When we combine the annual and wet season (May-Oct) versions of the SAIs and ENSO indices, the correlations show that wetter conditions prevail north of the Tropic of Cancer, and drier conditions dominate the southern part of Mexico. This latitudinal transition of wetter in northern and drier conditions in southern Mexico is also seen for the correlations between dry (Nov-Apr) SAIs and ENSO indices. Nevertheless, the most significant results are found in the northern part of the country, this can be fully appreciated in the climatic response at Presa Rodriguez (north-western) to the ENSO modulation.

At regional and local scales, when lag correlations are applied, precipitation is consistently responding close to the peak of El Niño-like conditions with amounts above their normals mainly in the north-western part of Mexico, especially the Mexican Monsoon and the northern Baja California peninsula. This climatic picture is also coincident with the results obtained applying linear correlation using Kendall tau-b.

Due to the difficulty of developing regional temperature averages (see sections 4.3), temperature is only evaluated at the local scale. Nevertheless, linear and lag correlations were also applied to the extreme temperature indices.

When linear correlations have been applied, the greatest changes in extreme temperatures with ENSO phases are found in the indices related to minimum temperatures. Geographically, warmer temperatures are observed across all the country, but the most significant results are found in the northern part of Mexico. Although no clear pattern could be found when lag correlations were applied between extreme temperature and ENSO indices, it can be concluded that warmer temperatures are observed south of the Tropic of Cancer, close to the peak of El Niño conditions. This climatic picture is especially true for the indices related to minimum temperatures.

The core processes of the El Niño Southern Oscillation (ENSO) phenomenon occur in a latitudinal band along the equatorial Pacific Ocean. As Mexico lies in the (northern) climatic transition between tropical and extratropical conditions, we needed a technique

to explore the time-dependence between the Mexican temperature and precipitation and ENSO; for this purpose the lag-cross correlation method was applied to those meteorological parameters. The largest impacts on local and regional scales are mostly observed close to the peak of El Niño (La Niña) conditions. But, as we have seen in this chapter, the ENSO modulation is also associated to seasonal and geographical characteristics. For example, two regions are largely influenced by El Niño: the Mexican Monsoon region (see Table 4.1) during the wet season (May-Oct) and the North Baja Californian peninsula during the dry season (Nov-Apr). The possibility of (approximately) knowing the time of the greatest response of the precipitation to ENSO could have practical applications in agriculture; for instance, directly in the tomato crops in the Mexican Monsoon region and indirectly in the wine production in the northern region of the peninsula of Baja California.

The climatic responses at regional and local levels of rainfall and temperatures to ENSO are clear. A latitudinal climatic transition (if we define the Tropical of Cancer as a geographical limit) in precipitation can be appreciated with the wet season (May-Oct) and annual versions of the ENSO indices. Wetter conditions are found in northern Mexico; while drier conditions prevail in the southern part of the country. Under extra-tropical conditions, an almost national pattern of wetter conditions are seen when the dry season (Nov-Apr) ENSO conditions are dominant. Nevertheless, the time of response of the precipitation is directly linked to the spatial scale, regional time-series are strongly affected close to the peak of El Niño conditions, and precipitation extremes are more variable in their timing with ENSO modulation. Temperature extremes do not reflect a clear climatic picture. Although significant changes can observed in the extreme indices related to minimum temperatures, the geographical distribution is less clear as is their response timing. Fluctuations toward warming can be appreciated across all Mexico, the largest correlations are found in the northern part of the country especially the Baja California peninsula, but the impacts are first observed in southern Mexico close to the peak of El Niño conditions. Precipitation seems more climatically stable in its response to ENSO than temperature, especially regional rainfall averages.

CHAPTER 8: CONCLUSIONS

8.1. MAIN FINDINGS.

A network of stations with high-quality and long-term instrumental data of precipitation and temperature has been built to study recent climatic changes in Mexico. The monthly database consists of 175 stations of rainfall data spanning from 1931 to 2001; and a set of 52 stations with monthly temperature data has been extracted, whose length extends from 1941 to 2001. A network of 15 precipitation and 26 temperature stations with daily data goes from 1941 to 2001 has also been developed.

The construction of the meteorological network used in the present study has been a difficult and time-consuming task. The extraction of the data was based on the advent of several efforts (since the early 1990s) to digitise the instrumental records of Mexico. Therefore, having more information among the possible meteorological variables to be analysed, daily data of precipitation and temperature was the main objective of the extraction. In order to fulfil this purpose five different sources of data were used, and a process of cross-checking applied among the databases (see section 3.2). Because of the great importance that agriculture has had in the Mexican economy, the precipitation network has better spatial coverage than temperature, and an addtional monthly database was used to complete the daily records of precipitation, that was not possible in the case of temperature (because there was not a monthly database available). Long-term and completeness were the main conditions used to include a time-series in the database. Nevertheless, one of the main goals of the construction of the network was quality control of the data, in order to assure the reliability of the results on the study of the patterns of climate change in the country.

Mexico is a territory with a complex climatic picture. Many factors (natural amd athropogenic) contribute to modulate the climate of the country. Principal Component Analysis (PCA) was chosen to isolate groups of stations that vary coherently across time.

PCA results were also used to compare directly the climatic fluctuations at regional and local scales. This method was applied to monthly rainfall and mean temperature data to define the different climatic regions across the country.

In most of the Mexican territory the largest percent of the annual total precipitation occurs during the May to October period (Mosiño and García, 1974; Hastenrath, 1967). Therefore, the analysis on precipitation was divided into three parts: annual precipitation, wet (May-Oct) and dry (Nov-Apr) seasons. Due to their clearer results PCA rotated solutions were selected over the unrotated solutions (see section 4.2.1). Varimax and Promax (kappa=2) were used to regionalise the precipitation patterns across the country. Both techniques basically lead to the same results, Promax performing slightly better than Varimax.

Successful regionalisations were found using PCA for rainfall regardless of the season considered. Very similar regions were found for the annual total precipitation and the wet season, basically one replicating the results of the other, but a different climatic picture is seen for the dry season (Nov-Apr, see section 4.2). Nevertheless several interesting differences appear amongst the different seasonal resulting PCA regions.

The North American Monsoon -or Mexican Monsoon- Region (NAMR) and La Huasteca are two regions that only appear for the PCA regionalisation of annual total rainfall. Although the greatest component of precipitation falls during the summer months, the NAMR (Ropelewski et al., 2004; Arritt et al., 2000; Barlow et al., 1998; Stensrud et al., 1997; Higgins et al., 1997; Douglas et al., 1993) can only be extracted by applying PCA to the annual precipitation. This limitation can be linked to the greater importance that winter precipitation (Giddings et al., 2005; Mechoso et al., 2004) has for the NAMR, especially in the north-western part of Mexico. The other region that only appears during the annual rainfall regionalisation is La Huasteca. Here, winter precipitation also plays a key role in the annual precipitation; polar fronts can reach these latitudes during the winter, and when combined with the moisture from the Gulf of Mexico, can enhance the precipitation during this season (Cavazos, 1997). This atmospheric (winter) processes

rarely occurs within the large inner area protected by the two mountain ranges barriers of the rest of Mexico.

Two regions are distinctive when applying PCA regionalisation to wet season time series of rainfall. The Nayarit coast region can be considered as the southern limit of the NAMR. Significant amounts of moisture from the Pacific Ocean directly affect the summer precipitation in this area. Nevertheless, it is unlikely that cold fronts can penetrate this far south as is the case for the northern part of the NAMR during the winter season and, therefore, can only be extracted during the wet season. The other group of stations that only appear from the PCA results from the wet season (May-Oct) is the Neovolcanic Belt region (Demant and Robin, 1975). Although explicitly avoided by using standardised time series (Comrie and Glenn, 1998), the influence of altitude plays a key role in this area; capturing the humidity of the convention processes (widely characteristic in Mexico) during the warm Season (Mosiño and García, 1974).

Perhaps, because its rainfall patterns are not affected by the large-scale convection processes characteristic of the summer period, the dry season (Nov-Apr) shows three different regions that do not appear during the annual precipitation or wet season periods. In fact, there can be a fourth region, if we also add the NAMR as a region that is impacted by winter precipitation, as discussed earlier. The NAMR can be climatically linked to the North Baja California Peninsula and defined as a region in which the annual total precipitation is strongly affected by the cold air masses of the winter season. The other two groups of stations only found applying PCA to the dry season (Nov-Apr) time series are the south-eastern and the Yucatán Peninsula regions. Both regions are profoundly affected by hurricanes during the warm season. Therefore, their climatic patterns can be completely disrupted by tropical cyclones, in comparison with their neighbouring stations (Englehart and Douglas, 2002).

Although wet season (May-Oct) rainfall contributes with the largest percent of the annual total precipitation, is the dry season (Nov-Apr) that really helps to identify the large-scale atmospheric processes that are controlling the rainfall patterns in Mexico. For instance,

by contrasting the different results by season, we can conclude that more research is needed in several atmospheric phenomena that are controlling the climate of Mexico, and that have not been extensively explored such as: altitude, hurricanes or polar fronts. These topics of future research will be addressed briefly at the end of this chapter.

Extreme events are a direct measure of the effects of a changing climate. The frequency of the weather extremes is more dependent on the variability than in the means (Katz and Brown, 1992). The Climate extremes are rare in terms of frequency but have large impacts on intensity. Therefore, it is very important to study these sorts of events to fully understand climatic changes. We have calculated and analysed weather extreme indices using the Expert Team (ET) on Climate Change Detection and Indices (ETCCDI) approach, and Kendall tau-b to estimate their linear correlations with possible forcing factors.

At regional levels total precipitation is decreasing in southern Mexico, especially in the forests of Los Tuxtlas (near the Gulf of Mexico), the rainforest of south-eastern Mexico and in Michoacán state. In contrast, at local levels, precipitation is increasing above normal over the Yucatán Peninsula and also the northern part of the Baja California.

We have also counted the number of statistically significant results related to extreme rainfall indices, dividing the country north and south considering the Tropic of Cancer as a geographical limit. According to these conditions, decreasing precipitation is observed for the stations close to the Atlantic Coast (Gulf of Mexico), and an upward trend (wetter conditions) for those stations located near the Pacific Coast. Another spatial pattern observed in the results is one of increasing precipitation in both peninsulas (Yucatán and Baja California) and decreasing rainfall for the continental (mainland Mexico) stations.

Extreme temperature indices were also explored in this study. Their correlations at local scales (by station) show warming conditions in the north of Mexico, while in the southern part of the country a cooling trend is observed. The stations with the most pronounced changes are El Paso de Iritu (in the southern tip of the Baja Californian peninsula) that

shows a trend towards warmer conditions; and the Ahuacatlán station near the Nayarit (central Pacific) coast whose indices are leading to colder conditions, especially those related to night temperatures.

The same method (applied on precipitation) of counting the most statistically significant results was applied to the temperature time-series, in order to establish their changing climatic patterns. According to this process, warming conditions are seen in the northern part of Mexico, and a downward (cooling) trend is observed in the southern part of the country. Throughout all the results observed in the analysis of extreme temperature indices, a clear national pattern of warming conditions is observed in minimum temperatures.

The last analysis of this thesis tried to relate the climatic variations (rainfall and temperature) in Mexico with a large-scale atmospheric control. Because of their planetary scale, we have selected El Niño Southern Oscillation phenomenon as a good option to be explored. For this purpose, we applied non-parametric (Kendall tau-b) and lag correlations to the selected meteorological variables. We have utilised three different standardised ENSO indices (SOI, Niño 3.4 and MEI) to test the consistency of the results.

As in the case of PCA regionalisation and extreme weather indices, we have found clearer results when correlating the ENSO indices with precipitation than with temperature. This is particularly true at regional scales, i.e., regional precipitation averages. Defining again (as we did for extreme weather indices) the Tropic of Cancer as a limit, we observe a clear climatic transition. Regional above normal precipitation is found in northern Mexico and drier conditions in the southern part of the country during El Niño conditions for the May to October (tropical conditions) and annual versions of the regional Standardised Anomaly Indices (SAIs). In contrast, during El Niño, an almost national pattern of wetter conditions is observed when we correlate the November to April (extra-tropical conditions) version of the regional SAIs. The timing of response is also clearer for regional (rainfall averages) than local (extreme indices) scales.

Regional average precipitation responds close to the peak of El Niño conditions, while the timing of the extreme indices is in general more variable.

Although extreme temperature indices clearly show an upward trend towards warming conditions, especially in minimum (night-time) temperatures; less clear is their spatial distribution, as there is little homogeneous climatic patterns due to changing temperature. Nevertheless, the most significant results are found in the northern part of the country, where increases in minimum temperatures are leading to warming conditions, and the largest correlations (and changes) are observed in the Baja California Peninsula. The timing of the climatic response of extreme temperature indices is first seen in the southern part of the country close to the peak of El Niño-like conditions, after which it gradually moves northwards. The clearest pattern found exploring the ENSO modulation is that precipitation seems more climatically stable in its response to ENSO than temperature, especially regional rainfall averages that respond close to the strongest conditions of El Niño.

Based on a newly constructed long-term and high quality database of temperature and precipitation; the network of precipitation has been successful regionalised using Principal Component Analysis (PCA), while poor regionalisation was found for temperature. This might be due to the markedly fewer stations in the dataset and might be related to elevation effects as well. At both regional (precipitation averages) and local (extreme indices) scales, precipitation shows a clear latitudinal climatic transition, that is directly dependent on tropical or extra-tropical conditions. The timing of response is close to the peak of El Niño-like conditions for regional precipitation averages. The analyses of temperature are not as conclusive as for precipitation. Nevertheless, there are clear changes toward warming conditions for minimum (night-time) temperatures, but their timing of response to ENSO is more variable. As shown –in this chapter- when analysing the regional precipitation averages, and also when the most significant correlations were classified, the climatic latitudinal transition is a topic that needs to be explored more extensively.

8.2. FUTURE RESEARCH.

Although a high-quality database has been constructed for this study, the network of stations can be updated together with the addition of as much recent meteorological data as possible, either from other studies or directly from the Mexican Meteorological Office. Currently, some researchers are working on the homogeneity of the network of meteorological data. This is a topic in which the present study can be certainly linked for a better understanding of the climate of Mexico.

Despite the different methods in this thesis were applied to standardised versions of the data aiming to avoid direct influences, elevation plays an important role in the climate of Mexico; the importance of this permanent control was already mentioned in an early study on the climate of Mexico by Mosiño and García (1974). However, this area has not been sufficiently explored yet. The different analyses used in this research show a clear link of the orography with both spatial and temporal scales. Principal Components (Chapter 4) on precipitation has pointed out that two regions: the Mexican Central Highlands and the Neovolcanic Belt (see Table 4.1) are excellent examples of the mechanism in which altitude is an essential physical feature to explain their coherent variations across time. All the stations in the Transverse Neovolcanic Belt exceeds the 1000 m.a.s.l. The elevation factor is also consistent when we consider the ENSO influence on rainfall (Chapter 7).The three ENSO indices (SOI, Niño 3.4, and MEI) show a strong relationship with the Transverse Neovolcanic Belt. At local scales, Yecora station (within the Mexican Monsoon Region) because its altitude (1500 m.a.s.l.; see table 3.2) has been linked to both secular changes on its rainfall extreme indices (Chapter 5), and to the physical modulation of the three different ENSO indices (Chapter 7).

Seasonal regional precipitation is strong related to the orography as well. Extracting groups that varies coherently across time utilising PCA and exploring the ENSO influence, unveil that during the dry season (Nov-Apr) there is an important link between some large-scale atmospheric controls like the Westerlies (see section 2.3) and Polar Fronts and high altitude stations within the Transverse Neovolcanic Belt and the Mexican

Central Highlands. Therefore, the influence of high-altitude in the climate in Mexico is a topic that warrants more detailed study in the future.

Several studies have dealt with the geographical extension and temporal intervals of the North American Monsoon Region (Mechoso et al, 2004; Hu and Feng, 2002; Castro et al., 2001; Higgins et al., 1997). One indirect result of this study has been the identification of the Mexican Monsoon Region (Douglas et al., 1993) as one of the important climatic regions of this country. Although, Englehart and Douglas (2002) have pointed out that the largest amount of rainfall is concentrated during June, July and August, and the winter precipitation is considerable (Griddings et al., 2005; Mechoso et al., 2004), the Mexican Monsoon Region is only extracted for the annual totals (see section 4.2.1). An appraisal of the precipitation within this north-western area utilising also the definitions of wet (May-Oct) and dry (Nov-Apr) seasons is suggested in order to compare the atmospheric processes that modulate the Monsoon in this region. Another additional aspect that could be explored is the southern limit of this region. The NAME is a promising start to address this objective, but this effort needs to be extended in order to increase our climatic understanding of the region.

The intense precipitation and damage caused by Hurricane Stan and Wilma during the 2005 hurricane season in the south-eastern part of Mexico showed the great importance of these phenomena in the country. Their influence can be so large, that they can completely disrupt the precipitation pattern of an entire region when compared with their neighbouring areas. Mexico is strongly affected by tropical cyclones on both coasts during the hurricane season. Currently, climatologists are still debating if climate change is changing the frequency of hurricanes across the globe, and their impacts in coastal areas. Certainly, this is a topic that (because of its great impact) needs to be studied more profoundly in Mexico.

A climatic pattern is clear in some of the southern regions of Mexico. Decreasing precipitation and warming conditions are observed in several of the forests of the country, like Los Tuxtlas near the Atlantic Coast, in Michoacán state or the south-eastern

rainforest. Deforestation can be one of the causes to explain these changes, but the climatic picture is complex; this study has shown that the El Niño Southern Oscillation (ENSO) phenomenon is also affecting the climate of those regions. A further study on this topic can certainly lead to a better understanding of the impact of natural variability or anthropogenic influences on the forests of Mexico.

Although, in most of Mexico, annual precipitation is modulated by large-scale phenomena during the May to October period (tropical conditions); some of the regions in northern Mexico are strongly affected by winter precipitation (extra-tropical conditions). The northern part of the Baja California Peninsula, the North American Monsoon region in north-western Mexico; la Huasteca, near the Atlantic coast, or even far south in the Tehuantepec Isthmus are sometimes strongly affected by polar fronts especially when they bring large amounts of moisture across the country from both the Atlantic and the Pacific Oceans. Furthermore, the impact of cold fronts is strongly linked to altitude, particularly on precipitation. Therefore, it is desirable that cold fronts get more attention within the atmospheric sciences, taking advantage of the recent digital databases of the most important meteorological parameters in Mexico.

The analyses applied in this thesis are geographically limited to the tropical Pacific influence due to the ENSO indices used. A possibility to expand spatially our knowledge of the large-scale ocean and atmosphreric controls on the mexican climate can be explored using the Pacific Decadal Oscillation (Mantua and Hare, 2002; McCabe et al., 2004), as an alternative to the ENSO indices utilised. A reconstruction of the air temperature based on tree rings (along the Pacific ocean) in North America shows the areal extension of the influence of this phenomenon (Minobe, 1997). The climate in the extra-tropics is inter-annually dominated by several tropical influences (like ENSO or the equatorial SSTs), inter-decadal climatic anomalies at sub-tropical latitudes are modulated by a constantly out of equilibrium Pacific Ocean (Trenberth and Hurrell, 1994). The PDO has an important influence on multidecadal winter precipitation in the southwestern USA (Arizona and New Mexico), near the northern Mexican borders (Gutzler, 2002). A latitudinal transition is found in the tropical storm activity in northwestern Mexico: a

stronger Southern Oscillation Index (SOI) influence is observed in the northern part of the area; meanwhile, the southern half is modulated by the PDO (Díaz et al., 2008). Precisely, intraseasonal rainfall is more intense and of longer duration for northwestern Mexico than in the Arizona state in the USA (Englehart and Douglas, 2006).

At temporal scales, recurrent, non-linear and multidecadal droughts in the USA are closely correlated to with the North Atlantic Ocean, but these droughts are modulated by the sign of the PDO (Mc cabe et al., 2004). The frequency between PDO manifestations varies from 20 to 30 years, the last undisputable shift in the PDO phase was originated at 1976-77 affecting the Central and North Pacific basin. Nevertheless, tree ring studies have shown a longer 50-70 years oscillation (Minobe, 1997). An assessment of the frequency relations between the PDO and the meteorological digital data can be made, for a better understanding of the climate of Mexico.

About 30% of the total variance of the extratropical winter temperatures in the northern hemispheric can be explained by the North Atlantic Oscillation (NAO) (Perry, 2000). Therefore, another topic to be addressed for future studies is the influence of the NAO on the climate of Mexico using instrumental data. The sign of the NAO has direct influence on the speed and direction of the westerlies across the north Atlantic ocean (Lamb and Peppler, 1987). As the climate of northern Mexico during the boreal winter is partially modulated by the Westerlies (see section 2.3), the influence of the NAO is a topic that needs to be studied. In addition, Huang et al. (1998) have evaluated the spectral density of the relation between the NAO and ENSO, finding two bands of maximum power at the 5-6 and 2-4 years periods. Hence, it is also important to assess the periodicities of the relations of the climate of Mexico and the NAO.

One last area of study in which the database, built for the present research, can be used in the future is to assess climate models. Although there are several studies that evaluate future climatic scenarios in Mexico (Villeras-Ruiz et al., 1998; Magaña et al., 1997), they lack of a strict analysis of the quality of the data. For its spatial extent, the high-quality

and long-term characteristics, the constructed database for this thesis is suitable to fill the necessity on future studies that aim to evaluate the outputs of the latest General Circulation Models (GCM).

REFERENCES:

ADEM J. 1991. Review of the development and applications of the Adem thermodynamic climate model. *Climate Dynamics* 5: 145-160.

ADEM J., RUIZ A., MENDOZA, V.M., GARDUÑO, R., BARRADAS, V. 1995. Recent experiments on monthly weather prediction with the Adem Thermodynamic Climate Model, with special emphasis in Mexico. *Atmósfera* 8: 23-34.

AGUILAR, E., AUER, I., BRUNET, M., PETERSON, T.C., WIERINGA, J. 2003. Guidance on metadata and homogeneization. *WMO-TD No.1186*, (WCDMP-No. 53). p*p. 51*.

AGUILAR E., PETERSON T.C., OBANDO R.P., FRUTOS R., RETANA J.A., SOLERA M., SOLEY J., GONZALEZ GARCIA I., ARAUJO R.M., ROSA SANTOS A., VALLE V.E., BRUNET M., AGUILAR J., ALVAREZ L., BAUTISTA M., CASTAÑON C., HERRERA L., RUANO E., SINAY J.J., SANCHEZ E., HERNANDEZ OVIEDO G.I., OBED F., SALGADO J.E., VAZQUEZ J.L., BACA M., GUTIERREZ M., CENTELLA M., ESPINOSA J., MARTINEZ D., OLMEDO B., OJEDA ESPINOSA C.E., NUÑEZ R., HAYLOCK M., BENAVIDES H. AND MAYORGA R. 2005. Changes in Precipitation and Temperature in Central America and Northern South America. *Journal of Geophysical Research* 110: D23107, doi:10.1029/2005JDD006119.

AL-KANDARI N.M., JOLLIFFE I.T. 2005. Variable selection and interpretation in correlation principal components. *Environmetrics* 16: 659-672.

ALEXANDER, L. V., ZHANG, X., PETERSON, T.C., CAESAR, J., GLEASON, B., KLEIN TANK, A., HAYLOCK, M., COLLINS, D., TREWIN, B., RAHIMZADEH, F., TAGIPOUR, A., AMBENJE, P., RUPA KUMAR, K., RAVADEKAR, J., GRIFFITHS, G., VINCENT, L., STEPHENSON, D., BURN, J., AGUILAR, E., BRUNET, M., TAYLOR, M., NEW, M., ZHAI, P., RUTICUCCI, M., VAZQUEZ-AGUIRRE, J.L. 2006. Global Observed Changes in Daily Climate Extremes of Temperature and Precipitation. *J. Geophys. Res.*, 111. D05109,doi:10.1029/2005JD006290.

ARRITT R.W., GOERING D.C., ANDERSON, C.J. 2000. The North American monsoon system in the Hadley Centre coupled ocean-atmosphere GCM. *Geophysical Research Letters* 27(4): 565-568.

AUBRY A. 2005. El Soconusco (I-VI). *La Jornada.* http://www.jornada.unam.mx/2005/11/01/022a1pol.php

BARLOW, M., NIGAM, S., BERBERY E.H. 1998. Evolution of the North American Monsoon. *Journal of Climate* 11: 2238-2257.

BARNSTON, A.G., CHELLIAH, M. 1997. Documentation of a Highly ENSO-Related SST Region in the Equatorial Pacific. *Atmosphere-Ocean* 35(3): 367-383.

BENISTON, M., STEPHENSON, D.B. 2004. Extreme climatic events and their evolution under changing climatic conditions. *Global and Planetary Change* 44:1-9.

BOHRA A. K., BASU S., RAJAGOPAL E.N., IYENGAR G.R., DAS GUPTA M., ASHRIT R., ATHIYAMAN B. 2006. Heavy rainfall episode over Mumbai on 26 July 2005: Assessment of NWP guidance. *Current Science* 90(9): 1188-1194.

BRADLEY, R.S., JONES, P.D. (Editors). 1992. *Climate since A.D.1500.* 679pp. Routledge, London.

BURROUGHS W. (Ed.). 2003. Climate: Into the 21st Century. *World Meteorological Organization. Cambridge University Press.*

CASTRO C.L., MCKEE T.B., PIELKE R.A. 2001. The Relationship of the North American Monsoon to Tropical and North Pacific Sea Surface Temperatures as Revealed by Observational Analyses. *Journal of Climate* 14: 4449-4473.

CATTELL R.B. 1966. The Scree Test for the Number of Factors. *Multivariate Behavioral Research* 1(2): 245-276.

CAVAZOS T. 1999. Large-Scale Circulation Anomalies Conductive to Extreme Precipitation Events and Derivation of Daily Rainfall in North-eastern Mexico and South-eastern Texas. *Journal of Climate* 12: 1506-1523.

CAVAZOS T. 1997. Downscaling large-scale circulation to local winter rainfall in north-eastern Mexico. *International Journal of Climatology* 17: 1069-1082.

CAVAZOS T, COMRIE A.C., LIVERMAN D.M. 2002. Intraseasonal Variability Associated with Wet Monsoons in Southeast Arizona. *Journal of Climate* 15: 2477-2490.

CAVAZOS T., HASTENRATH S. 1990. Convection and rainfall over Mexico and their modulation by the Southern Oscillation. *International Journal of Climatology* 10: 377-386.

CHATFIELD, C. 1991. *Problem Solving: A Statiscian's guide*. *Chapman and Hall.* Pp. 261.

CLImat COMputing Project (CLICOM). http://www.wmo.ch/web/wcp/wcdmp/html/clicom.html

COMRIE A.C., GLENN E.C. 1998. Principal components-based regionalization of precipitation regimes across the southwest United States and northern Mexico, with an application to monsoon precipitation variability. *Climate Research* 10: 201-215.

COOK S.F. 1946. The Incidence and Significance of disease among the Aztecs and Related Tribes. *The Hispanic American Historical Review* 26(3): 320-335.

CRICHTON, N.J. 2001. Information point: Kendall's tau. *Journal of Clinical Nursing* 10: 707-715.

CROWLEY T.J. 2000. Causes of Climate Change Over the Past 1000 Years. *Science* 289: 270-277.

DEMANT, A., ROBIN, C. 1975. Las fases del vulcanismo en México; una síntesis en relación con la evolución geodinámica desde el cretácico. *Revista del Instituto de Geología* 75(1): 66-79.

DETTINGER M.D., BATTISTI D.S., GARREAUD R.D., McCABE G.J., BITZ C.M. 2001: Interhemispheric effects of interannual and decadal ENSO-like climate variations on the Americas. *In Interhemispheric climate linkages: Present and Past Climates in the Americas and their Societal Effects.* V. Markgraf (Ed.), Academic Press: 1-16.

DIAZ, H.F., KILADIS G.N. 1992: Atmospheric teleconnections associated with the extreme phases of the Southern Oscillation. *In El Niño: Historical and Paleoclimatic Aspects of the Southern Oscillation. H. F. Diaz and V. Markgraf (Eds.)*, Cambridge University Press: 7-28.

DOUGLAS M.W., MADDOX R.A., HOWARD K. 1993. The Mexican monsoon. *Journal of Climate* 6:1665-1677.

DYER, T.G.J. 1975. The assignment of rainfall stations into homogeneous groups: an application of principal component analysis. *Quarterly Journal of the Royal Meteorological Society* 101(430): 1005-1013.

EASTERLING, D.R., EVANS, J.L., GROISMAN, P.Y., KARL, T.L., KUNKEL, K.E., AMBENJE, P. 2000. Observed variability and trends in extreme climate events: a brief review. *Bulletin of the American Meteorological Society* 81 (3): 417-425.

EASTERLING, D.R., DIAZ, H.R., DOUGLAS, A.V., HOGG, W.D., KUNKEL, K.E., ROGERS, J.C., WILKINSON, J.F. 1999. Long-term observations for monitoring extremes in the Americas. *Climatic Change* 42 (1): 285-308.

EASTERLING, D.R., HORTON, B., JONES, P.D., PETERSON, T.C., KARL, T.R., PARKER, D.E., SALINGER, J.M., RAZUVAYEV, V., PLUMMER, N., JAMASON, P., FOLLAND, C.K. 1997. Maximum and minimum temperature trends for the globe. *Science* 277: 364-367.

ENCISO L.A. Desastres naturales dejan este año pérdidas económicas sin precedente. *La Jornada.* December 8, 2005. http://www.jornada.unam.mx/2005/12/08/050n1soc.php

ENGLEHART P.J., DOUGLAS A.V. 2004. Defining Intraseasonal Rainfall Variability within the North American Monsoon. *Journal of Climate* 19(17): 4243-4253.

ENGLEHART P.J., DOUGLAS A.V. 2004. Characterizing regional-scale variations in monthly and seasonal air temperature over Mexico. *International Journal of Climatology* 24:1897-1909.

ENGLEHART, P.J., DOUGLAS, A.V. 2003. Urbanization and seasonal temperature trends: observational evidence from a data-sparse of North America. *International Journal of Climatology* 23 (10): 1253-1263.

ENGLEHART P.J., DOUGLAS A.V. 2002. Mexico's summer rainfall patterns: an analysis of regional modes and changes in their teleconnectivity. *Atmósfera* 15:147-164.

ENGLEHART P.J., DOUGLAS A.V. 2001. The Role of Eastern North Pacific tropical Storms in the Rainfall Climatology of Western Mexico. *International Journal of Climate* 21:1357-1370.

FIELD, A. 2005. Discovering Statistics using SPSS. *SAGE Publications.* Second Edition.

FRICH, P., ALEXANDER, L.V., DELLA-MARTHA, P., GLEASON, B., HALOCK, M., KLEIN TANK, A.M.G., PETERSON, T. 2002. Observed coherent changes in climatic extremes during the second half of the twentieth century. *Climate Research* 19: 193-212.

GARCIA E. 1988. Modificaciones al sistema de clasificación climática de Köppen. *Instituto de Geografía*, UNAM. 220 pp.

GARCIA E., VIDAL R., HERNANDEZ M.E. 1990. Las Regiones climáticas de México. In García de Fuentes, Ana. Editora. *Atlas Nacional de México.* UNAM, Instituto de Geografía. Vol. 2. Cap. IV. No. 10. Map at 1:12,000,000. México.

GARCIA-OLIVA, F., EZCURRA, E., GALICIA, L. 1991. Pattern of Rainfall Distribution in the Central Pacific Coast of Mexico. *Geografiska Annaler* 73(3-4): 179-186.

GARDUÑO, R. 1999. Aportaciones mexicanas al estudio del clima. *Geofísica* 51: 69-89.

GARZA G. 2002. Frecuencia y duración de sequías en la cuenca de México de fines del siglo XVI a mediados del XIX. *Boletín del Instituto de Geografía*, UNAM 48: 106-115.

GERSHUNOV, A. 1998. Enso influence on intraseasonal extreme rainfall and temperature frequencies in the contiguous United States: Implications for long-range predictability. *Journal of Climate* 11: 3192-3203.

GERSHUNOV, A. and BARNETT, T.P. 1998. Interdecadal Modulation of ENSO Teleconnections. *Bulletin of the American Meteorological Society* 79: 2715-2725.

GIANNINI, A., CHIANG, J.C.H, MARK, M.A., KUSHNIR, Y, SEAGER, R. 2001. The ENSO Teleconnection to the Tropical Atlantic Ocean: Contributions of the Remote and Local SSTs to the Rainfall Variability in the Tropical Americas. *Journal of Climate* 14:4530-4544.

GIDDINGS, L., SOTO, M., RUTHERFORD, B.M., MAAROUF, A. 2005. Standardized Precipitation Index Zones for México. *Atmósfera* 18:33-56.

GONZALEZ Y. 1998. DAT322 (SOFTWARE). *Instituto Mexicano de Tecnología del Agua (IMTA).*

GUTRO R. 2005 Warmest Year in Over a Century. *Goddard Space Flight Center.* January 1, 2006. http://www.nasa.gov/vision/earth/environment/2005_warmest.html

GUTZLER D.S. 2002. Modulation of ENSO-Based Long-Lead Outlooks of Southwestern U.S. Winter Precipitation by the Pacific Decadal Oscillation. *Weather and Forecasting* 17:1163-1172.

HANNACHI, A. 2004. A primer for EOF analysis of Climate Data. http://www.met.rdg.ac.uk/~han/Monitor/eofprimer.pdf

HASTENRATH S.L. 1967. Rainfall Distribution and Regime in Central America. *Arch. Meteorol.Geophys.Biokimatol.* Ser.B 15:201-241.

HAYLOCK, M. 2005. Linear Regression Analysis for STARDEX. http://www.cru.uea.ac.uk/projects/stardex/Linear_regression.pdf

HAYLOCK, M.R., PETERSON, T., ABREU DE SOUSA, J.R., ALVES, L.M., AMBRIZZI, T., BAEZ, J., BARBOSA DE BRITO, J.I., BARROS, V.R., BERLATO, M.A., BIDEGAIN, M., CORONEL, G., CORRADI, V., GRIMM, A.M., JAILDO DOS ANJOS, R., KAROLY, D., MARENGO, J.A., MARINO, M.B., MEIRA, P.R., MIRANDA, G.C., MOLION, L., MUNCUNIL, D.F., NECHET, D., OTANEDA, G., QUINTANA, J., RÁMIREZ, E., REBELLO, E., RUSTICUCCI, M., SANTOS, J.L., VARILLAS, I.T., VILLANUEVA, J.G., VINCENT, L., YUMIKO, M. 2006. Trends in total and extreme South American rainfall 1960-2000 and links with sea surface temperature. *Journal of Climate* 19(8): 1490-1512.

HERNANDEZ-UNZON A., BRAVO C. 2005. Resumen del Huracán "Stan" del Océano Atlántico. Comisión Nacional del Agua (CNA). México.

HERNANDEZ-UNZON A., BRAVO C. 2005. Resumen del Huracán "Wilma" del Océano Atlántico. Comisión Nacional del Agua (CNA). México.

HETWINSON B.C., CRANE R.G. 1992. Large-Scale atmospheric controls on local precipitation in Tropical Mexico. *Geophysical Research Letters* 19:1835-1838.

HIGGINS R.W., YAO Y., WANG X.L. 1997. Influence of the North American Monsoon System on the U.S. Summer Precipitation Regime. *Journal of Climate* 10:2600-2622.

HORN J.L., ENGSTROM R. 1979. Cattell's Scree Test in Relation to Barlett's Chi-Square Test and Other Observations on the Number of Factors Problem. *Multivariate Behavioral Research* 14(3): 283-300.

HOUGHTON J.T., DING Y., GRIGGS D.J., NOGUER M., VAN DER LINDEN P.J., XIAOSU D. 2001. Climate Change: The Scientific Basis. Contribution of Working Group I to the Third Assessment Report of the Intergovernmental Panel on Climate Change (IPCC). *Cambridge University Press*, UK; pp 994.

HU Q., FENG S. 2002. Interannual rainfall variations in the North American Summer Monsoon Region: 1900-98. *Journal of Climate* 15: 1189-1202.

HUANG J., HIGUCHI K., SHABBAR A. 1998. The relationship between the North Atlantic Oscillation and El Niño-Southern Oscillation. *Geophysical Research Letters* 25(14): 2707-2710.

IPCC. 2007. Climate Change: The Physical Science Basis. Summary for Policymakers. IPCC Secretariat, SWITZERLAND pp 18. http://www.ipcc.ch

JAUREGUI E. 2003. Climatology of Landfalling Hurricanes and Tropical Storms in Mexico. Atmósfera 16(4): 193-204.

JAUREGUI E. 1997. Climate changes in Mexico during the historical and instrumented periods. *Quaternary International* 43/44: 7-17.

JAUREGUI, E. 1995. Algunas alteraciones de largo periodo del clima de la ciudad de México debidas a la urbanización. *Investigaciones Geográficas* 31: 9-44.

JAUREGUI E. 1992. Aspects of monitoring local/regional climate change in a tropical region. *Atmósfera* 5: 69-78.

JOLIFFE, I.T. 2002. Principal Component Analysis. *Springer_Verlag*, 2nd Edition, New York.

JONES, P.D., HORTON, E.B., FOLLAND, C.K., HULME, M., PARKER, D.E., BASNETT, T.A. 1999. The use of indices to identify changes in climatic extremes. *Climatic Change* 42 (1): 131-149.

JONES, P.D., HULME, M. 1996. Calculating Regional Climatic Time Series for Temperature and Precipitation: methods and illustrations. *International Journal of Climatology* 16: 361-377.

KARL, T.R., EASTERLING, D.R. 1999. Climate extremes: selected review and future research directions. *Climate Change* 42: 309-325.

KARL, T.R., KNIGHT, R.W., EASTERLING, D.R., QUAYLE, R.G. 1996. Indices of climate change for the United States. *Bulletin of the American Meteorological Society* 77(2): 279-292.

KARL, T.R., JONES, P.D., KNIGHT, R.W., KUKLA, G., PLUMMER, N., RAZUVAYEV, V.N., GALLO, K.P., LINDSEAY, J., CHARLSON, R.J., PETERSON, T.C. 1993. A new perspective on recent global warming: asymmetric trends of daily maximum and minimum temperature. *Bulletin of the American Meteorological Society* 74 (6): 1007-1023.

KARL, T.R., KUKLA, G., RAZUVAYEV, V.N., CHANGERY, M.J., QUAYLE, R.G., HEIM, R.R., EASTERLING, D.R., FU, C.B. 1991. Global warming: evidence for asymmetric diurnal temperature change. *Geographical Research Letters* 18 (12): 2253-2256.

KARL, T.R., DIAZ, H.R., KUKLA, G. 1988. Urbanization: Its detection and effect in the United States climate record. *Journal of Climate* 1: 1099-1123.

KATZ, R.W., BROWN, B.G. 1992. Extreme Events in a Changing Climate: Variability is more important than Averages. *Climatic Change* 21:289-302.

KLEIN TANK, A.M.G., PETERSON, T.C., QUADIR, D.A., DORJI, S., ZOU, X., TANG, H., SANTHOSH, K., JOSHI, U.R., JASWAL, A.K., KOLLI, R.K, , SIKDER, A.B., DESHPANDE, N.R. REVADEKAR, J.V., YELEUOVA, K., VANDASHEVA, S., FALEYEVA, M., GOMBOLUUDEV, P., BUDHATHOKI, K.P., HUSSAIN, A., AFZAAL, M., CHANDRAPALA, L., ANVAR, H., AMANMURAD, D., ASANOVA, V.S., JONES, P.D., NEW, M.G., SPEKTORMAN, T. 2006. Changes in daily temperature and precipitation extremes in central and south Asia. *Journal of Geophysical Research* 111: D16105.

LAMB P.J., PEPPLER R.A. 1987. North Atlantic Oscillation: Concept and Application. *Bulletin of the Meteorological Society* 68(10): 1218-1225.

LAWRIMORE D.L., LEVINSON D., HEIM R., STEPHENS S., WAPLE A., TANKERSLEY, C. 2005. State of the Climate for 2005. National Climatic Data Center, NOAA (http://ams.confex.com/ams/pdfpapers/99981.pdf).

LIVERMAN D.M., O'BRIEN K.L. 1991. Global Warming and Climate Change in Mexico. *Global Environmental Change* 1(5): 351-364.

LUTERBACHER J., DIETRICH D., XOPLAKI E., GROSJEAN M., WANNER H. 2004. European Seasonal and Annual Temperature Variability, Trends, and Extremes since 1500. *Science* 303: 1499-1503.

MAGAÑA V. 1994. An Strategy to determine regional climate change. México ante el cambio climático. *Primer taller de Estudio de País: México.* Cuernavaca, México, pp. 45-51.

MAGAÑA V., AMADOR J.A., MEDINA S. 1999. The midsummer drought over Mexico and Central America. *Journal of Climate* 12: 1577-1588.

MAGAÑA V., CONDE C., SANCHEZ O., GAY, C. 1997. Assessment of current and future regional climate scenarios for Mexico. *Climate Research* 9: 107-114.

MAGAÑA, V., GAY, C. 2001. Vulnerabilidad y Adaptación Regional ante el Cambio Climático y sus Impactos Ambiental, Social y Económicos. *Informe final presentado al Instituto Nacional de Ecología*. México, 31 pp.

MAGAÑA V., VAZQUEZ J.L., PEREZ J.L., PEREZ, J.B. 2003. Impact of El Niño on precipitation in Mexico. *Geofísica Internacional* 42(3): 313-330.

MANTON, M.J., DELLA-MARTA, P.M., HAYLOCK, M.R., HENNESSY, N., NICHOLLS, N., CHAMBERS, L.E., COLLINS, D.A., DAW, G., FINET, A., GUNAWAN, D., INAPE, K., ISOBE, H., KESTIN, T.S., LEFALE, P., LEYU, C.H., LEWIN, T., MAITREPIERRE, N., OUTPRASITWONG, C.M., PAGE, C.M., PAHALAD, J., PLUMMER, N., SALINGER, M.J., SUPPIAH, R., TRAN, V.L., TREWIN, V., TIBIG, I., YEE, D.. 2001. Trends in extreme daily rainfall and temperature in Southeast Asia and the South Pacific. *International Journal of Climatology* 21: 269-284.

MANTUA N.J., HARE S.R. 2002. The Pacific Decadal Oscillation. *Journal of Oceanography* 58: 35-44.

MASERA O.R., ORDOÑEZ M.J., DIRZO R. 1997. Carbon Emissions from Mexican Forests: Current Situation and Long-Term Scenarios. *Climate Change* 35: 265-295.

MATHER P.M. 1976. Computational Methods of Multivariate Analysis in Physical Geography. *John Wiley and sons*, London.

MAYER-ARENDT K.J.. 1991. Hurricane Gilbert: The Storm of the Century. *Geojournal* 23(4): 323-325.

McCABE G.J., PALECKI M.A., BETANCOURT J.L. 2004. Pacific and Atlantic Ocean influences on multidecadal drought frequency in the United States. *Procedings of the National Academy of Sciences of the United States of America* 101 (12): 4136-4141.

MECHOSO C.R., ROBERTSON A.W., ROPELEWSKI C.F., GRIMM A.M. Nov. 2004. The American Monsoon Systems. *System Proceedings, 3rd International Workshop on Monsoons.* Hangzhao, China.

MENDOZA V.M., VILLANUEVA E.B., ADEM J. 1997. Vulnerability of basins and watersheds in Mexico to global climate change. *Climate Research* 9: 139-145.

METCALFE S.E. 1987. Historical data and climatic change in Mexico—A review. *The Geographical Journal* 153: 211-222.

METCALFE, S.E., O'HARA, S.L., CABALLERO, M., DAVIES, S.J. 2000. Records of Late Pleistocene-Holocene climatic change in Mexico – a review. *Quaternary Science Review* 19:699-721.

MINOBE S. 1997. A 50-70 year climatic oscillation over the North Pacific and North America. *Geophysical Research Letters* 24(6): 683-686.

MITCHELL D. L., IVANOVA D., BROWN T.J., REDMOND K. 2002. Gulf of California Sea Surface Temperaturas and the North American Monzón: Mechanistic Implications from Observations. *Journal of Climate* 15(17): 2261-2281.

MOSIÑO P., GARCIA E. 1974. The climate of Mexico. *World Survey of climatology. Climates of North America.* R.A. Bryson and F.K. Hare, Eds. 11: 345-404.

NEW, M., HETWINSON, B., STEPHENSON, D.B., TSIGA, A., KRUGER, A., MANHIQUE, A., GÓMEZ, B., COELHO, C.A., MASISI, D.N., KULULANGA, E., MBAMBALALA, E., ADESINA, F., SALEH, H., KANYANGA, J., ADOSI, J., BULANE, L., FORTUNATA, L., MDOKA, M.L., LAJOIE, R. 2006. Evidence of trends in daily climate extremes over southern and west Africa. *Journal of Geophysical Research* 111 (D14).

NORTH, G.R., BELL, T.L., CALAHAN, R.F., MOENG, F.J. 1982. Sampling errors in the estimation of empirical orthogonal functions. *Monthly Weather Review* 110 (7): 699-706.

O'HARA S.L., METCALFE S.E. 1995. Reconstructing the climate of Mexico from historical records. *The Holocene* 5: 485-490.

ORTEGA, G., VELAZQUEZ, A. 1995. Variabilidad de la precipitación en México. *Revista de Ingeniería* LXV 4/4: 203-205.

OSBORN T. J., BRIFFA K.R. 2006. The Spatial Extent of 20th-Century Warmth in the Contexto f the Past 1200 Years. *Science* 311: 841-844.

PERES-NETO P.R., JACKSON D.A., SOMERS K.M. 2005. How many principal components? stopping rules for determining the number of non-trivial axes revisited. C*omputational Statistics and Data Analysis* 49: 974-997.

PERRY A. 2000. The North Atlantic Oscillation: an enigmatic see-saw. *Progress in Physical Geography* 24(2): 289-294.

PIELKE Jr. R.A., LANDSEA C., MAYFIELD M., LAVER J., PASCH R. 2005. Hurricanes and Global Warming. *Bulletin of the American Meteorological Society* 86(11): 1571-1575.

PIELKE Jr. R.A., RUBIERA J., LANDSEA C., FERNANDEZ L.M., KLEIN L. 2003. Hurricanes Vulnerability in Latin America and the Caribbean: Normalized Damage and Loss Potential. *Natural Hazards Review* 4(3): 101-114.

PRINN R., JACOBY H., SOKOLOV A., WANG C., XIAO X., YANG Z., ECKHAUS P., STONE D., MELILLO J., FITZMAURICE J., KICKLIGHTER D., HOLIAN G., LIU Y. 1999. Integrated Global System Model for Climate Policy Assessment: *Feedbacks and Sensitivity Studies* 41(3): 469-546.

QUINTAS I. 2001. ERIC: Extractor Rápido de Información Climatológica (SOFTWARE). *Instituto Mexicano de Tecnología del Agua (IMTA).*

REYES, S., TRONCOSO, R. 1999. El impacto del fenómeno El Niño-Oscilación del Sur en la generación de ciclones tropicales alrededor de México. *Rev. Ciencia y Mar* 5: 3-22.

RICHMAN, M.B. 1986. Review article: rotation of principal components. *Journal of Climatology* 6: 293-335.

RICHMAN, M.B and LAMB, P.J. 1985. Climatic pattern analysis of 3- and 7-day summer rainfall in the central United States: Some methodological considerations and a regionalisation. *Journal of Climate and Applied Meteorology* 24: 1325-1343.

ROPELEWSKI C.F., GUTZLER D.S., HIGGINS R.W. 2004. The North American Monsoon System. *System Proceedings, 3rd International Workshop on Monsoons.* Hanzhao, China. Review Topic A4: American Monsoon.

ROPELEWSKI, C.F., HALPERT, M.S. 1996. Quantifying Southern Oscillation – Precipitation Relationships. *Journal of Climate* 9: 1043-1059.

ROPELEWSKI, C.F., JONES, P.D. 1987. An extension of the Tahiti-Darwin Southern Oscillation Index. *Monthly Weather Review* 115: 2161-2165.

SCHROPE M. 2005. Meteorology: Winds of change. *Nature* 438: 21-22.

SCHUMWAY, R.H. 1988. Applied Statistical Time Series Analysis. *Prentice Hall*. New York, 379 pp.

SOON, W., BALIUNAS, S., IDSO, C., IDSO, S., LEGATES, D.R. 2003. Reconstructing Climatic and Environmental Changes of the Past 1000 Years: A Reappraisal. *Energy and Environment* 2-3 (14): 233-296.

STENSRUD D.J., GALL R.L., NORDQUIST, M.K. 1997. Surges over the Gulf of California during the Mexican Monsoon. *Monthly Weather Review* 125: 417-437.

TABONY, R.C. 1981. A principal component and spectral analysis of European rainfall. *Journal of Climatology* 1: 283-294.

THERRELL M.D., STAHLE D.W., ACUÑA-SOTO R. 2004. Aztec drought and the curse of one rabbit. *Bulletin of the American Meteorological Society* 85: 1263-1272.

TRENBERTH K. 2005. Uncertainties in Hurricanes and Global Warming. *Science* 308: 1753-1754.

TRENBERTH M.D., CARON J.M. 2000. The Southern Oscillation revisited: Sea level pressures, surface temperatures, and precipitation. *Journal of Climate* 13: 4358-4365.

TRENBERTH K.E., HURRELL J.W. 1994. Decadal atmosphere-ocean variations in the Pacific. *Climate Dynamics* 9: 303-319.

VILLERS-RUIZ L., TREJO-VAZQUEZ I. 1998. Climate change on Mexican forests and natural protected areas. *Global Environmental Change* 8: 141-157.

VIRMANI J.I., WEISBERG R.H. 2006. The 2005 hurricane season: An echo of the past or a harbinger of the future? *Geophysical Research Letters* 33: 1-4.

VOSE, R.S., EASTERLING, D.R., GLEASON, B. 2005. Maximum and minimum temperatures trends for the globe: An update through 2004. *Geographical Reseach Letters* 32: L23822.

WALLEN, C.C. 1955. Some Characteristics of precipitation in Mexico. *Geografiska Annaler.* 37: (1-2) 51-85.

WANG, X.L. 2003. Comments on "Detection of Undocumented Changepoints: A Revision of the Two-Phase Regression Model". *Journal of Climate* (Notes and correspondence): 3383-3385.

WELSH, W.F. 1999. On the reliability of Cross-Correlation Function Lag Determinations in Active Galactic Nuclei. *The Astronomic Society of the Pacific* 111: 1347-1366.

WHITE D., RICHMAN M., YARNAL B. 1991. Climate regionalization and rotation of principal components. *International Journal of Climatology* 11(1): 1-25.

WOLTER, K. 1987. The Southern Oscillation in Surface Circulation and Climate over the Tropical Atlantic, Eastern Pacific and Indian Oceans as captured by Cluster Analysis. *Journal of Climate and Applied Meteorology* 26: 540-558.

WOLTER, K., TIMLIN, M.S. 1993. Monitoring ENSO in COADS with a seasonally adjusted principal component index. *Proc. 17th Climate Diagnostics Workshop*, Norman, OK, NOAA/NMC/CAC, 52-57.

WUENSCH, K.L. 2005. Principal Components Analysis - SPSS. http://core.ecu.edu/psyc/wuenschk/MV/FA/PCA-SPSS.doc

YAN, Z., JONES, P.D., DAVIES, T.D., MOBERG, A., BERGSTRÖM, H., CAMUFFO, D., COCHEO, C., MAUGERI, M., DEMARÉE, G.R., VERHOEVE, T., THOEN, E., BARRIENDOS, M., RODRÍGUEZ, R., MARTÍN-VIDE, J., YANG, C. 2002. Trends of extreme temperatures in Europe and China based on daily observations. *Climatic Change* 53 (1-3): 355-392.

ZHANG, X., AGUILAR, E., SENSOY, S., MELKONYAN, H., TAGIYEVA, U., AHMED, N., RAHIMZADEH, F., TAGHIPOUR, A., HANTOSH, T.H., ALBERT, P., SEMAWI, M., KARAM, A.M., AL-SHABIBI, M.H.S., AL-OULAN, Z., ZATARI, T. KHELET I.A.D., HAMOUD S., SAGIR R., DEMIRCAN M., EKEN M., ADIGUZEL M., ALEXANDER L., PETERSON T.C., WALLIS T. 2005. Trends in Middle East Climate Extreme Indices from 1950 to 2003. *Journal of Geophysical Research* 110.